ROLES OF CALSYNTENIN-3 IN SYNAPSE DEVELOPMENT AND OPTIMIZING CONDITIONAL GENE DELETION

by

Lin Luo

B.Sc., Peking University, 2011

A THESIS SUBMITTED IN PARTIAL FULFILLMENT OF

THE REQUIREMENTS FOR THE DEGREE OF

DOCTOR OF PHILOSOPHY

in

THE FACULTY OF GRADUATE AND POSTDOCTORAL STUDIES

(Neuroscience)

THE UNIVERSITY OF BRITISH COLUMBIA

(Vancouver)

August 2019

© Lin Luo, 2019

The following individuals certify that they have read, and recommend to the Faculty of Graduate and Postdoctoral Studies for acceptance, the dissertation entitled:

Roles of calsyntenin-3 in synapse development and optimizing conditional gene deletion

submitted by Lin Luo in partial fulfillment of the requirements for

the degree of PhD

in Neuroscience

Examining Committee:

Ann Marie Craig
Supervisor

Yu Tian Wang
Supervisory Committee Member

Supervisory Committee Member

Lynn Raymond
University Examiner

James Johnson
University Examiner

Additional Supervisory Committee Members:

Tim O'Connor
Supervisory Committee Member

Shernaz Bamji
Supervisory Committee Member

Abstract

Synaptic adhesion molecules play central roles in synapse organization and neuronal signal transduction machineries. This dissertation first focuses on calsyntenin-3, a crucial synaptic adhesion molecule identified by our lab, based on *in vitro* and *in vivo* biochemistry, immunofluorescence, electron microscopy, and electrophysiological studies.

Chapter 2 shows that calsyntenin-3 interacts with α-neurexins, but not β-neurexins, at nanomolar affinity. Being calcium-dependent and regulated by the heparan sulfate modification of α-neurexins, this interaction requires the cadherin and LNS domains of calsyntenin-3, as well as the LNS5-EGFc-LNS6 domains of α-neurexins. Calsyntenin-3 full-length form triggers pre-synapse differentiation, but calsyntenin-3-shed ectodomain suppresses the ability of α-neurexin partners in mediating pre-synapse differentiation. Calsyntenin-3 is present in pyramidal neurons throughout cortex and hippocampus, and is most highly expressed in interneurons. Young adult calsyntenin-3 knockout mice present deficits in both density and transmission for both excitatory and inhibitory synapses.

Chapter 3 shows that calsyntenin-3 regulates synaptic transmission in different neuronal types. Conditional calsyntenin-3 knockout in forebrain interneurons does not affect basal inhibitory transmission in CA1 pyramidal neurons, while conditional knockout in excitatory neurons enhances both basal excitatory and inhibitory transmission. Partial calsyntenin-3 knockout in primary hippocampal neuron culture and in juvenile calsyntenin-3 mice exhibit enhanced inhibitory transmission. Juvenile calsyntenin-3 knockout mice, however, show no difference in inhibitory transmission compared to wild-type littermates. Thus, calsyntenin-3 contributes in a developmentally regulated and at least partially non-cell-autonomous manner to synaptic transmission.

Chapter 4 discusses our discovery of unexpected germline recombination in distinct mouse Cre driver lines and its profound implications. The Cre-loxP system (and resulting Cre mouse lines) has been widely used for cell-type specific gene manipulations and helps decipher gene functions, especially in neuroscience research. We demonstrated that unexpected germline recombination occurs in many Cre lines based on the studies of two Cre lines within our lab and collected data for fifty-seven Cre lines worldwide. Consequently, this may sway the interpretation of past experimental results as well as moving forward. This work not only provides guidelines for breeding strategies and precautions aimed at future studies, but most importantly for the first time, comprehensively raises awareness of this phenomenon among the neuroscience community.

Lay Summary

As one of the most important organs in the body, the brain analyzes information, creates perceptions, and drives human behavior. To accomplish these complex functions, nerve cells form networks made up of specialized junctions known as synapses. Synapse development is a process mediated by binding of cell surface molecules, ‘synaptic organizing molecules’, which act as an anchor that ultimately bridges these two cells together. My research in Chapter 2 and 3 focuses on the molecular interaction and function of one such molecule, calsyntenin-3. Unveiling these mechanisms will not only help provide a deeper understanding of brain development, but may also lead to novel treatments for neuropsychiatric disorders. In Chapter 4, I present and discuss an underappreciated pitfall of a commonly used genetic tool in the neuroscience community, which may affect the interpretation of thousands of studies in the past as well as moving forward.

Preface

Parts of Chapter 2 (Figures 2.1-2.6, 2.13-2.17) were published in Katherine L. Pettem*, Daisaku Yokomaku*, **Lin Luo*,** Michael W. Linhoff*, Tuhina Prasad*, Steven A. Connor*, Tabrez J. Siddiqui, Hiroshi Kawabe, Fang Chen, Ling Zhang, Gabby Rudenko, Yu Tian Wang, Nils Brose and Ann Marie Craig (2013). The Specific α-Neurexin Interactor Calsyntenin-3 Promotes Excitatory and Inhibitory Synapse Development. Neuron *80*, 113–128. (*Co-first authors) I designed and performed about one third of all experiments, and contributed in editing the manuscript. In this dissertation, I did the bulk of experiments, while part of Figure 2.6 was done by Dr. Katherine Pettem and Figure 2.17 was done by Dr. Steve Connor. All other coauthors' work in the manuscript is not included in the dissertation.

Some other parts of Chapter 2 (Figures 2.7 & 2.8) were published in Zhuoyang Lu, Yun Wang, Fang Chen, Huimin Tong, M. V. V. V. Sekhar Reddy, **Lin Luo**, Suchithra Seshadrinathan, Lei Zhang, Luis Marcelo F. Holthauzen, Ann Marie Craig, Gang Ren and Gabby Rudenko (2014). Calsyntenin-3 Molecular Architecture and Interaction with Neurexin 1α. J. Biol. Chem. *289*, 34530–34542. I performed the cell based binding assays and co-immunoprecipitation assays and contributed in editing the manuscript. Thesis Figure 2.8 B, C and D were performed by Dr. Gabby Rudenko's lab. All other coauthors' work in the manuscript is not included in the dissertation.

The remaining parts of Chapter 2 (Figures 2.9-2.12) are original, unpublished data from collaboration with Dr. Peng Zhang under the supervision of Dr. Ann Marie Craig. I did the bulk

of the experiments and analysis. Dr. Peng Zhang conducted the heparinase treatment experiment in Figure 2.9 and provided valuable suggestions in other experiments.

Chapter 3 is original, unpublished data, designed and conducted by me with the supervision of Dr. Ann Marie Craig.

A version of Chapter 4 is submitted for publication as "Optimizing nervous system specific knockout with Cre driver lines: parental gender effects" by **Lin Luo**, Mateusz C. Ambrozkiewizc, Fritz Benseler, Cui Chen, Emilie Dumontier, Susanne Falkner, Elisabetta Furlanis, Andrea Gomez, Wei-Hsiang Huang, Mary Anne Hutchison, Laura Lavery, Emily Ling-Lin Pai, Ariane Pereira, Lisa Traunmüller, Jiexin Wang, Wenjia You, Nashat Abumaria, Kevin T. Beier, Constance L. Cepko, Jean-François Cloutier, Sandra Goebbels, Pascal S. Kaeser, Jeremy N. Kay, Wei Lu, Liqun Luo, Chris McBain, Marco A.M. Prado, Vania F. Prado, John L. R. Rubenstein, Gesine Saher, Joshua R. Sanes, Peter Scheiffele, Hisashi Umemori, Matthijs Verhage, Michisuke Yuzaki, Huda Yahya Zoghbi, Hiroshi Kawabe, and Ann Marie Craig. I conceptualized the idea, conducted the experiments and wrote the first draft of the manuscript, with Dr. Ann Marie Craig's input throughout the process. All other authors contributed unpublished data listed in Table 4.3.

I also contributed in the publication of Tatiana V Lipina*, Tuhina Prasad*, Daisaku Yokomaku*, **Lin Luo***, Steven A Connor, Hiroshi Kawabe, Yu Tian Wang, Nils Brose, John C Roder, Ann Marie Craig (2015), Cognitive Deficits in Calsyntenin-2-deficient Mice Associated with Reduced GABAergic Transmission, Neuropsychopharmacology doi: 10.1038/npp.2015.206

(*Co-first authors). I contributed in managing the mouse colonies, generating tissue immunofluorescence data, interpreting behavior results and writing part of the manuscript. This work is not included as figures in this dissertation, but cited as reference.

I also assisted in the publication of Yunhee Kang, Yuan Ge, Robert M Cassidy, Vivian Lam, **Lin Luo**, Kyung-Mee Moon, Renate Lewis, Robert S Molday, Rachel OL Wong, Leonard J Foster, Ann Marie Craig (2014), A Combined Transgenic Proteomic Analysis and Regulated Trafficking of Neuroligin-2, Journal of Biological Chemistry 289 (42), 29350-29364. I contributed some tissue immunofluorescence staining and quantification, and edited the manuscript. This work is not included as figures in this dissertation, but cited as reference.

Table of Contents

Abstract ..... **iii**

Lay Summary ..... **v**

Preface ..... **vi**

Table of Contents ..... **ix**

List of Tables ..... **xv**

List of Figures ..... **xvi**

List of Abbreviations ..... **xix**

Acknowledgements ..... **xxiii**

Chapter 1: Introduction 1

1.1 Synapses and synaptic organizing complexes 1

1.1.1 Structure of synapses 2

1.1.2 Synaptic organizing proteins 2

1.1.3 Neurexins 7

1.1.4 Neurexin ligands 9

1.1.5 Neuroligins 10

1.1.6 Neurexins as HSPGs 14

1.2 Calsyntenin-3 15

1.2.1 Expression pattern of calsyntenins 16

1.2.2 Cleavage of calsyntenins 17

1.2.3 Calsyntenin ortholog *CASY-1* in *C. elegans* 18

1.2.4 Calsyntenins as cargo proteins 18
1.2.5 Calsyntenin-2 in learning and memory 19
1.2.6 Calsyntenins as biomarkers for diseases 20
1.3 Cre-loxP system 21
1.3.1 History 21
1.3.2 Applications of Cre-loxP system 23
1.3.3 Caveats of using Cre mouse lines 26
1.4 Research questions 29
Chapter 2: Calsyntenin-3 interacts with α-Neurexins and promotes synapse development 32
2.1 Introduction 32
2.2 Rationales and hypothesis 33
2.3 Methods 35
2.3.1 DNA constructs 35
2.3.2 Primary neuron culture and COS cell coculture assay 37
2.3.3 Animals 38
2.3.4 Protein purification and cell surface binding assay 38
2.3.5 Western blot 40
2.3.6 Co-immunoprecipitation 42
2.3.7 Tissue immunofluorescence staining 42
2.3.8 Electron microscope 43
2.4 Results 43
2.4.1 Calsyntenin-3 binds to α-Neurexins but not β-Neurexins 43
2.4.2 Calsyntenin-3 is largely cleaved *in vitro* and *in vivo* 48

2.4.3 Released calsyntenin-3 ectodomain inhibits the synaptogenic activity of multiple α-neurexin partners 51
2.4.4 Cadherin and LNS domains of calsyntenin-3 are necessary for α-neurexin binding and synaptogenic activity 53
2.4.5 Calsyntenin-3 binds to LNS5-EGFc-LNS6 region of α-Neurexins 56
2.4.6 Calsyntenin-3 forms multimers 58
2.4.7 HS modification is required for presynaptic differentiation by Calsyntenin-3. 60
2.4.8 HS modification of neurexin-2α regulates its binding to ectodomain of calsyntenin-3 62
2.4.9 Calsyntenin-3 RA mutants are deficient at inducing presynaptic differentiation compared to WT 64
2.4.10 Calsyntenin-3 shows differential expression patterns *in vivo* 66
2.4.11 *Clstn3−/−* mice are deficient in both inhibitory and excitatory synapse development 70
2.5 Discussion 75
2.5.1 Unique binding properties of calsyntenin-3 to neurexins 75
2.5.2 Model of calsyntenin-3-neureixn trans-synaptic complex 77
2.5.3 The mechanism and function of calsyntenin-3 cleavage 78
2.5.4 Other members of the calsyntenin family 79
2.5.5 The heparin sulfate binding property of calsyntenin-3 80
Chapter 3: Calsyntenin-3 modulates synaptic transmission *in vitro* and *in vivo* 82
3.1 Introduction 82
3.2 Rationale and hypothesis 83

3.3 Methods 84
3.3.1 Animals 84
3.3.2 Acute hippocampal slices recording 85
3.3.3 Primary hippocampal culture and recording 86
3.3.4 Immunofluorescence 88
3.3.5 AAV injection 89
3.4 Results 89
3.4.1 Conditional *Clstn3* knockout in forebrain interneurons does not affect basal inhibitory transmission 89
3.4.2 Conditional *Clstn3* knockout in hippocampal CA1 pyramidal neurons enhances basal transmission 93
3.4.3 ~50% knockout of Clstn3 in primary hippocampal culture via nucleofection tends to increase inhibitory synaptic transmission 96
3.4.4 ~50% knockout of *Clstn3* in primary hippocampal culture via nucleofection increases inhibitory synapse density 98
3.4.5 Viral-inducted sparse knockout of *Clstn3* in juvenile mice increases inhibitory synaptic transmission 102
3.4.6 Basal inhibitory transmission is not changed in juvenile global *Clstn3* knockout mice compared to wildtype 105
3.5 Discussion 108
3.5.1 Calsyntenin-3 functions in different stages of synapse development 108
3.5.2 The discrepancy in function of postsynaptic calsyntenin-3 109
3.5.3 Function of Calsyntenin-3 in interneurons 112

3.5.4 Calsyntenin-3 function in synaptic plasticity 113
Chapter 4: Germline recombination of multiple "brain-specific" Cre lines 115
4.1 Introduction 115
4.2 Methods 116
4.2.1 Animals 116
4.2.2 Genotyping 117
4.2.3 Immunofluorescence 117
4.3 Results 118
4.3.1 Dlx5/6-Cre shows unexpected maternal germline recombination when crossed with *Clstn3*$^{f/f}$ mice 118
4.3.2 Dlx5/6-Cre shows maternal germline recombination when crossed Ai32 reporter mice 119
4.3.3 Gpr26-Cre shows unexpected paternal germline recombination when crossed with *Clstn3*$^{f/f}$ mice 122
4.3.4 Gpr26-Cre shows paternal germline recombination in offspring when crossed Ai32 reporter mice 123
4.3.5 Literature review of germline recombination of nominally "nervous system-specific" Cre lines 126
4.3.6 Collection of unpublished data on Cre line germline recombination frequencies from labs worldwide 128
4.4 Discussion 148
4.4.1 Unexpected germline recombination commonly happens with Cre lines 148

4.4.2 Driver gene expression or Cre activity in reproductive systems poorly predicts germline recombination prevalence 149
4.4.3 Using tail/ear tissue for genotyping material 150
4.4.4 Choosing the proper breeding strategy to achieve desired outcome 151
Chapter 5: Conclusion 153
5.1 General conclusion and impact 153
5.2 Future directions 155
5.2.1 Calsyntenin-3's molecular and cellular function 155
5.2.2 Social-emotional and cognitive function of calsyntenin-3 156
5.2.3 Next steps on the Cre mouse lines 158
Bibliography 159
Appendices 186
Appendix A Detailed comparisons on the different Cre lines under the same driver 186
Appendix B Detailed driver gene expression and Cre tissue activity in reproductive systems on 58 Cre lines 197

List of Tables

Table 2.1 DNA constructs and sources used in Chapter 2 37

Table 3.1 Summary of electrophysiology recordings from *Clstn3* knockout and conditional knockout mice and culture 107

Table 4.1 Primers used for genotyping in Chapter 4 117

Table 4.2 Lines that showed germline recombination, from the literature 128

Table 4.3 Collective data of germline recombination frequency on 57 Cre driver lines 146

Table 4.4 Summary of comparison between germline recombination prevalence and driver gene expression and Cre tissue activity patterns in reproductive systems 150

List of Figures

Figure 1.1 Illustration of trans-synaptic cell adhesion molecules..... 7

Figure 1.2 Selected Ligand Interactions of Neurexins..... 10

Figure 1.3 Samples of Cre-loxP cassettes..... 25

Figure 2.1 Calsyntenin-3 ectodomain binds to HA-Neurexin 1α at COS cell surface. 44

Figure 2.2 Calsyntenin-3 ectodomain binding to HA-Neurexin 1α is calcium-dependent 45

Figure 2.3 Calsyntenin-3 ectodomain binds to all α-Neurexins tested but not β-Neurexins..... 47

Figure 2.4 Calsyntenin-3 is largely cleaved *in vitro* and *in vivo* 51

Figure 2.5 Released calsyntenin-3 ectodomain inhibits the synaptogenic activity of multiple α-neurexin partners..... 53

Figure 2.6 The Cadherin and LNS domains are required for calsyntenin-3 synaptogenic activity and α-neurexin binding 55

Figure 2.7 Interaction of Calsyntenin-3 with neurexin-1α variants..... 57

Figure 2.8 Calsyntenin-3 forms multimers 59

Figure 2.9 HS modification is required for presynaptic differentiation by calsyntenin-3..... 61

Figure 2.10 HS modification of Nrx regulates its binding to ectodomain of Calsyntenin-3..... 64

Figure 2.11 Proposed mutations in calsyntenin-3..... 65

Figure 2.12 Calsyntenin-3 RA mutants are deficient at inducing presynaptic differentiation 66

Figure 2.13 Calsyntenin-3 expression level and cleavage level is consistent throughout development..... 67

Figure 2.14 Calsyntenin-3 expression is high in interneurons and moderate in pyramidal neurons 70

Figure 2.15 Neurexin level is intact in *Clstn3* -/- mice..... 71

Figure 2.16 Symmetric and asymmetric synapse density is reduced in *Clstn3 -/-* mice 73

Figure 2.17 Inhibitory and excitatory neurotransmission is compromised in *Clstn3*$^{-/-}$ mice.... 74

Figure 3.1 Expression of *Clstn3* conditional knockout mice in hippocampal CA1 region 92

Figure 3.2 Conditional *Clstn3* knockout in forebrain interneurons does not affect basal inhibitory transmission in CA1 pyramidal neurons..... 93

Figure 3.3 Conditional *Clstn3* knockout in CA1 pyramidal neurons increases basal inhibitory transmission 94

Figure 3.4 Conditional Clstn3 knockout in CA1 pyramidal neurons increases basal excitatory transmission 95

Figure 3.5 Nucleofected ~50% knockout of *Clstn3* in primary hippocampal culture increases inhibitory synaptic transmission 97

Figure 3.6 Nucleofected ~50% knockout of Clstn3 in primary hippocampal culture increases inhibitory synapse density..... 100

Figure 3.7 Nucleofected ~50% knockout of *Clstn3* in primary hippocampal culture does not affect excitatory synapse number..... 101

Figure 3.8 Expression pattern of AAV P0 injections 102

Figure 3.9 Viral-inducted sparse knockout of *Clstn3* in juvenile mice increases inhibitory synaptic transmission..... 104

Figure 3.10 Basal inhibitory transmission is not changed in juvenile *Clstn3* global knockout mice 107

Figure 4.1 Dlx5/6-Cre shows maternal germline recombination when crossed with *Clstn3*$^{f/f}$ mice 119

Figure 4.2 Dlx5/6-Cre shows maternal germline recombination when crossed Ai32 reporter mice 121

Figure 4.3 Gpr26-Cre shows paternal germline recombination in offspring when crossed with *Clstn3*$^{f/f}$ mice 123

Figure 4.4 Gpr26-Cre shows paternal germline recombination when crossed Ai32 reporter mice 125

List of Abbreviations

AAV	Adeno-associated virus
AChR	Nicotinic acetylcholine receptor
AD	Alzheimer's disease
AMCA	7-amino-4methylcoumarin-3-acetic acid
AMPA	A-amino-3-hydroxy-5-methyl-4-isoxazolepropionic acid
ANOVA	Analysis of variance
AP	Alkaline phosphatase
APP	Amyloid precursor protein
APV	(2R)-amino-5-phosphonovaleric acid
ARU	Animal resource unit
ASD	Autism spectrum disorder
Bicc	Bicuculline methiodide
bp	Base pair
BSA	Bovine serum albumin
C1	Calsyntenin-1
C2	Calsyntenin-2
C3	Calsyntenin-3
CAD	Cadherin
CaMKIIα	Calcium-calmodulin-activated protein kinase iiα
CD4	Cluster of differentiation 4
CD8	Cluster of differentiation 8
CFP	Cyan fluorescent protein
CHO	Carbohydrate attachment sequence
ChR2	Channelrhodopsin-2
cKO	Conditional knockout
Clstn	Calsyntenin
CNQX	Cyanquixaline (6-cyano-7-nitroquinoxaline-2,3-dione)
CNS	Central nervous system
CNVs	Copy number variants
COS	CV-1 in Origin with SV-40 genes
CREATE	Coordination of resources for conditional expression of mutated mouse alleles
CSF	Cerebrospinal fluid
ctl	Control
DAPI	4′,6-diamidino-2-phenylindole
DIO	Double-floxed Inverse Orientation
DIV	Days in vitro

DMEM	Dulbecco’s modified Eagle’s medium
DNA	Deoxyribonucleic acid
DTT	Dithiothreitol
ECS	Extracellular solution
EDTA	Ethylenediaminetetraacetic acid
EGF	Epidermal growth factor-like
eGFP	Enhanced green fluorescent protein
EGTA	Ethylene glycol-bis(β-aminoethyl ether)-N,N,N′,N′-tetraacetic acid
EM	Electron microscope
EX	Extracellular
EYFP	Enhanced yellow fluorescent protein
FAD	Familial Alzheimer’s disease
GABA	Gamma-aminobutyric acid
GAD	Glutamic acid decarboxylase
GAIN	(GPCR) autoproteolysis-inducing
GENSAT	Gene expression nervous system atlas
GPI	Glycophosphatidylinositol
HA	Human influenza hemagglutinin
HCV	Hepatitis C virus
HEK	Human Embryonic Kidney cells
HEPES	4-(2-hydroxyethyl)-1-piperazineethanesulfonic acid
HMW	High molecular weight
hpf	Hours postfertilization
HSPG	Heparan sulfate proteoglycan
Ig	Immunoglobulin
KA	Lysine to Alanine mutation
Kd	The equilibrium dissociation constant
kDa	Kilodalton
LMW	Low molecular weight
LNS	Laminin/neurexin/sex hormone-binding globulin
LRRTM	Leucine-rich repeat transmembrane protein
LSL	Loxp-stop-loxp
LTD	Long term depression
LTP	Long term potentiation
MAM	Meprin, A-5 protein, and receptor protein-tyrosine phosphatase
MAP2	Microtubule associated protein 2
mEPSC	Miniature excitatory postsynaptic currents
mIPSC	Miniature inhibitory postsynaptic currents
mM	Millimolar

mRNA	Messenger RNA
ms	Millisecond
MuSK	Muscle specific kinase
N/C-terminus	Amino/carboxy-terminus
NGL	Netrin-G ligand
NIH	National Institutes of Health
Ni-NTA	Nickel-charged chelating ligand nitrilotriacetic acid
Nlg2	Neuroligin 2
NMDA	N-Methyl-D-aspartate
Nrx	Neurexin
pA	Picoampere
PBS	Phosphate-buffered saline
PCR	Polymerase chain reaction
PDL	Poly-D-lysine
PKA	Protein kinase A
PLL	Poly-L-lysine
PTHS	Pitt-Hopkins syndrome
PTP	Protein tyrosine phosphatase
RA	Arginine to Alanine mutation
RNA	Ribonucleic acid
RNAseq	RNA sequencing
RT-PCR	Reverse transcription polymerase chain reaction
s.l.	Stratum lucidum
s.l.m.	Stratum lacunosum moleculare
s.o.	Stratum oriens
s.p.	Stratum pyramidale
s.p.d	Stratum pyramidale deep
s.p.s	Stratum pyramidale superficial
s.r.	Stratum radiatum
SA	Serine to Alanine mutation
SAM	Synaptic adhesion molecule
SDS-PAGE	Sodium dodecyl sulfate polyacrylamide gel electrophoresis
SEM	Standard error of the mean
seqFISH	Sequential Fluorescence In Situ Hybridization
SFARI	Simons foundation autism research initiative
shRNA	Small hairpin RNA
Slitrk3	Slit and NTRK-like family member 3
SNP	Single-nucleotide polymorphism
SS	Splicing site
TM	Transmembrane
TrkC	Neurotrophin receptor tyrosine kinase type C

TTX	Tetrodotoxin
UBC	The University of British Columbia
YFP	Yellow fluorescent protein
μm	Micrometer
μM	Micromolar

Acknowledgements

I offer my enduring gratitude to my supervisor Dr. Ann Marie Craig for her generous support during my entire PhD training and detailed professional guidance throughout my research projects. She has shown me, by her example, what a good scientist should be like, which will benefit me for a lifetime.

I am grateful to all of my supervisory committee members, Drs. Tim O'Connor, Shernaz Bamji and Yu Tian Wang for their support during my training and especially during the graduation process.

I thank all my colleagues in the Craig lab for their help and assistance in the past years. I particularly am grateful for Drs. Peng Zhang and Yuan Ge for providing coherent answers to my endless questions regarding project design and experiment details, Drs. Katherine Pettem and Tuhina Prasad for trusting me enough to let me take over the calsyntenin-2 and calsyntenin-3 projects, Drs. Steve Connor and Lidong Liu for teaching me electrophysiology techniques and helping to troubleshoot throughout my research, Drs. Hideto Takahashi, Ted Dobie and Tabrez Siddiqui for assistance on the *in vitro* studies in the early years, Dr. Peng Zhang for guidance on the heparan sulfate project, and Mr. Hong Lu for editing the dissertation and working out schedules to share the ephys rig. Special thanks to Xiling Zhou for excellent neuron culture preparation and Nazarine Fernandes for managing the mouse colonies in the early years.

Finally, I would like to express my most sincere thanks to my dear husband Ling Zhang and lovely daughter Liviana. You two are the best things happened to me.

Chapter 1: Introduction

The mammalian central nervous system is composed of billions of neurons and glial cells. Neurons and glial cells communicate with each other and send signals to the whole body to guide sensation, movement and decision making, or in a word – everything. The development and maintenance of a fully functional brain is critical for every vertebrate organism.

Synapses are the basic communication units in the brain, delivering signals between nerve cells through chemical neurotransmitters. The development of synapses requires adhesion of appropriate nerve cell processes accompanied by local recruitment of neurotransmitter release machinery and opposing neurotransmitter receptor signal transduction machinery. Cell surface synapse organizing complexes coordinate these processes. Part of this study is focused on characterizing a newly identified cell-adhesion complex, neurexin-calsyntenin-3, dissecting the mechanism of their interactions, and unveiling how they regulate synapse and brain functions.

Valuable genetic tools allow researchers, especially in neuroscience, to manipulate and study specific gene function. The Cre-loxP system is a powerful and popular tool to specifically manipulate and label genes in various cell types. While useful, one particular caveat while using Cre lines, unexpected germline recombination, has historically been underrated by the neuroscience community in general. Therefore, a comprehensive study of this subject was conducted on two Cre lines used in our lab and a repository of information has been collected from multiple research groups across the world, forming part of this dissertation.

1.1 Synapses and synaptic organizing complexes

Chemical synapses are the most common connections in the central nervous system. There are two main types of chemical synapses in the brain: excitatory and inhibitory, depending on the neurotransmitters released and received.

1.1.1 Structure of synapses

Both excitatory and inhibitory synapses are composed of a presynaptic terminal, a postsynaptic terminal and a synaptic cleft. In the presynaptic terminal, voltage-gated ion channels trigger the release of neurotransmitters into the synaptic cleft when electrical action potentials arrive (Harris and Weinberg, 2012; Stevens, 2003; Südhof and Malenka, 2008). The neurotransmitter receptors from the postsynaptic terminal bind to the transmitters, open up ion channels and induce changes in postsynaptic membrane potential, increasing or decreasing the likelihood of triggering a new action potential (Purves et al., 2001).

In excitatory synapses, presynaptic-released glutamate binds to postsynaptic AMPA (α-amino-3-hydroxy-5-methyl-4-isoxazolepropionic acid) receptors and NMDA (N-Methyl-D-aspartate) receptors (Dingledine et al., 1999). In inhibitory synapses, presynaptic-released GABA (gamma-aminobutyric acid) and glycine bind to postsynaptic $GABA_A$ receptors (GABAAR) or glycine receptors, respectively, resulting in hyperpolarization of the postsynaptic compartment and a decreased chance of the generation of a new action potential (Luján et al., 2005).

1.1.2 Synaptic organizing proteins

Synaptic organizing proteins typically refer to the synaptic adhesion molecules spanning the cleft and secreted factors, which recruit presynaptic neurotransmitter release machinery and/or postsynaptic receptors. Several dozens of these proteins/families have been identified, and they function in distinct but overlapping neuronal types, brain regions and developmental stages. Deletion or mutation in these proteins results in a plethora of behavioral outcomes and neuropsychological symptoms (Missler et al., 2012; Shen and Scheiffele, 2010; Siddiqui and Craig, 2011).

The most well-known assay used for studying synaptic organizing proteins is the artificial synapse formation assay, also known as the fibroblast-neuron coculture assay, where the protein in interest is expressed in non-neuronal cells (usually COS7 or HEK293), and co-cultured with primary neurons. If the protein is "synaptogenic", hemi-synapses will form at the contact sites between fibroblasts and neurons, and pre- or post-synaptic components will then be recruited (Biederer et al., 2002; Graf et al., 2004; Nam and Chen, 2005; Shen and Scheiffele, 2010). This assay has been instrumental in identifying new synaptic adhesion molecules, including in our lab's unbiased screens which led to the discovery of LRRTMs and TrkC as postsynaptic proteins that trigger differentiation of neurotransmitter release sites in axons (Linhoff et al., 2009; Takahashi et al., 2011, 2012).

These newly identified molecules are all transmembrane proteins, located at the postsynaptic sites and binding to presynaptic ligands (Linhoff et al., 2009; Takahashi et al., 2011). These pre- and post-synaptic partners that bind *in trans* across the synapses often mediate bidirectional signaling via protein-protein interactions, in addition to physically aligning the pre- and post-synaptic sites and contributing to cell adhesion. Several groups of cell-adhesion molecules have been identified, among which presynaptic neurexins and the LAR-type receptor tyrosine phosphatases (PTPσ, LAR, and PTPδ) constitute "hubs" that each interact with distinct classes of postsynaptic cell-adhesion molecules (Figure 1.1): neurexins and their ligands (neuroligins, LRRTMs, cerebellins, neurexophilins, calsyntenin-3, Hevin, CA10, etc.), RPTPs and their ligands (SALMs, TrkC, Slitrks, NGL-3, etc.). Ephrin-EphR complexes, SynCAMs and cadherins also contribute to synaptic adhesion (Südhof, 2018). Among the aforementioned proteins, neurexins and their postsynaptic ligands are most relevant to this dissertation and will be reviewed thoroughly.

Disruption or dysfunction of these synaptic organizing proteins results in dysregulation of synapse formation, maturation, transmission, plasticity and related behavior. When knocking out either component of the Cbln1–GluRδ2 complex, the mice exhibit ataxia, deficient long-term depression, reduced numbers of parallel fiber–Purkinje synapses, increased numbers of free spines, and mismatches in the length of postsynaptic density relative to active zone at many remaining synapses (Hirai et al., 2005; Kashiwabuchi et al., 1995). Deletion of neuroligin-1 in knockout mice selectively decreases the NMDAR/AMPAR ratio, whereas deletion of neuroligin-2 selectively decreases inhibitory synaptic responses (Chubykin et al., 2007; Poulopoulos et al., 2009). Moreover, synaptic adhesion molecules have been implicated in numerous brain-based diseases such as Autism Spectrum Disorder (Guang et al., 2018), Alzheimer's Disease (Leshchyns'ka and Sytnyk, 2016), addiction (Muskiewicz et al., 2018), epilepsy (Gorlewicz and Kaczmarek, 2018), and much more. The underlying mechanism of how disruptions in synaptic proteins lead to dysfunction in brain activity and function has remained unclear, which is a gap that requires the whole community's combined effort to fill.

Glia derived proteins have been emergently shown to be involved in organizing synapses and regulating synapse function, either by comprising a physical 'tripartite synapse' consisting of presynaptic, postsynaptic and glia components (Araque et al., 1999), or by secreting synaptic organizing proteins (Allen and Lyons, 2018; Van Horn and Ruthazer, 2019). For example, Hevin, a synaptogenic protein secreted by astrocytes, was found to assemble glutamatergic synapses by bridging neurexin-1alpha and neuroligin-1B, two isoforms that otherwise do not interact with each other (Singh et al., 2016). Later, neuroligins themselves were reported to be expressed in the central nervous system by glial cells, such as astrocytes and oligodendrocytes,

and perform important roles in controlling synaptic connectivity in a non-cell autonomous manner (Sakers and Eroglu, 2019).

Although dozens of synaptic organizing proteins have been identified (Figure 1.1), they are only the tip of the iceberg. With the recent state of the art advances in proteomics and RNA sequencing techniques, more and more players in the synaptosomes are being recognized, as well as the direct and indirect interactions between the organizing proteins and receptors, channels and kinases. More studies will be required to understand the mechanisms underlying the interactions and functions, including but not limited to how different synaptic organizing proteins coordinate in the same synapse, how activity and activity-dependent proteolytic cleavage fine-tune synaptic protein composition and function, how the expression and function of synaptic organizing proteins are spatially and temporally regulated.

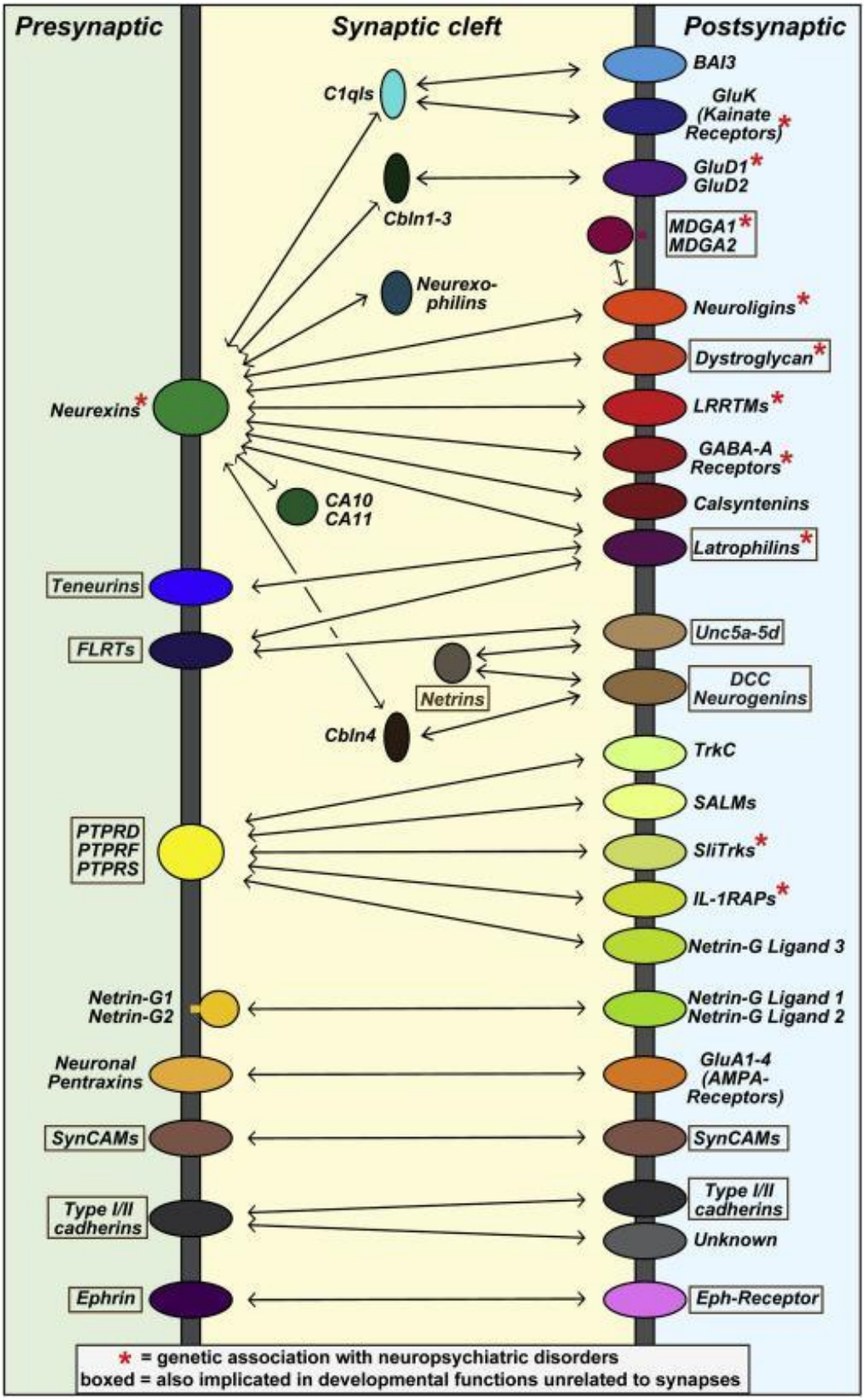
Presynaptic
Synaptic cleft
Postsynaptic
C1qls
BAI3
GluK (Kainate Receptors)*
GluD1* GluD2
Cbln1-3
MDGA1* MDGA2
Neurexo-philins
Neuroligins*
Dystroglycan*
Neurexins*
LRRTMs*
GABA-A Receptors*
CA10 CA11
Calsyntenins
Latrophilins*
Teneurins
Unc5a-5d
FLRTs
DCC Neurogenins
Netrins
Cbln4
TrkC
SALMs
PTPRD PTPRF PTPRS
SliTrks*
IL-1RAPs*
Netrin-G Ligand 3
Netrin-G1 Netrin-G2
Netrin-G Ligand 1 Netrin-G Ligand 2
Neuronal Pentraxins
GluA1-4 (AMPA-Receptors)
SynCAMs
SynCAMs
Type I/II cadherins
Type I/II cadherins
Unknown
Ephrin
Eph-Receptor
* = genetic association with neuropsychiatric disorders
boxed = also implicated in developmental functions unrelated to synapses

Figure 1.1 Illustration of trans-synaptic cell adhesion molecules

Summary of prominent cell adhesion molecule (CAM) interactions that were proposed to operate at the synapse. CAMs were placed on the pre- or postsynaptic side based on the overall published studies, but for many molecules firm assignments cannot yet be made. Image adapted and used by permission from (Südhof, 2018).

1.1.3 Neurexins

Neurexins were first discovered in 1992 as receptors for α-latrotoxin, a black widow spider neurotoxin that binds to presynaptic nerve terminals and causes massive neurotransmitter release (Ushkaryov et al., 1992). Mammalian neurexins are type-1 transmembrane proteins transcribed from 3 genes (neurexin-1, 2, 3), alternative promoters (α-, β-, γ-neurexins) and alternative splicing sites resulting in more than 3000 isoforms (Schreiner et al., 2014; Sterky et al., 2017; Ushkaryov and Südhof, 1993; Ushkaryov et al., 1992, 1994). α-neurexins contain six Laminin/Neurexin/Sex hormone-binding globulin (LNS) domains (LNS1-6) interspersed with three epidermal growth factor-like (EGF) repeats, followed by a highly glycosylated region, a transmembrane (TM) domain and a short cytoplasmic tail containing a PDZ binding domain. β-neurexins are transcribed from an internal promoter and are composed of an N-terminal β-neurexin-specific sequence that splices into the α-neurexin sequence N-terminal of its LNS6 domain; thus, β-neurexins are effectively N-terminally truncated α-neurexins with a short specific N-terminal motif. A recently discovered γ-neurexin is only transcribed from an internal promoter in the *Nrxn1* gene and splices into the Nrxn1α and Nrxn1β sequence C-terminal of the LNS6 domain, therefore only containing the cysteine-loop as an extracellular domain followed by the transmembrane domain and cytoplasmic sequence (Sterky et al., 2017). Nrxn1γ only binds to CA10 but no other ligands and thus is not the focus of this dissertation.

Different neurexin isoforms express differently in the brain. Neurexins are primarily expressed in neurons in the nervous system, while recent RNA-seq experiments also revealed Nrxn1 and Nrxn2 mRNAs in astrocytes and oligodendrocyte progenitor cells (Zhang et al., 2014). The three neurexin genes are transcribed in brain at similar levels, with α-neurexins being much more abundant than β-neurexins (Anderson et al., 2015; Aoto et al., 2013; Schreiner et al., 2014). Nrxn1α and Nrxn3α have 6 alternative splicing sites (SS1-SS6), and Nrxn2α has 5 (SS1-SS5), while SS4 and SS5 are present in the three β-neurexins (Ichtchenko et al., 1996; Schreiner et al., 2014; Ushkaryov and Südhof, 1993). The expression profile of different neurexin isoforms is pretty consistent within certain neuron subtypes and shows brain region specificity, suggesting that expression of synaptic cell-adhesion molecules overlaps with other key features of cellular identity and diversity (Fuccillo et al., 2015).

The three neurexin genes are all linked to various neuropsychiatric diseases in human. NRXN genomic alterations are frequently identified in autism spectrum disorders (ASD) and schizophrenia. Indeed, all of the NRXN family members are listed in public databases of risk genes for ASD and associated disorders, such as the SFARI (Simons Foundation Autism Research Initiative) gene database (https://sfari.org/), with moderate to high scores. NRXN mutations have been identified in multiple genetic studies for patients with ASD (Autism Genome Project Consortium et al., 2007; Feng et al., 2006; Guilmatre et al., 2009), Pitt-Hopkins syndrome (PTHS) (Duong et al., 2012; Harrison et al., 2011; Zweier et al., 2009), and schizophrenia (Gauthier et al., 2011; Kirov et al., 2008; Walsh et al., 2008).

α-Neurexins perform essential synaptic functions that are not shared with β-neurexins (Missler et al., 2003; Zhang et al., 2005), and the majority of disease-associated *NRXN* variations selectively affect α-neurexins and not β-neurexins (Ching et al., 2010; Gauthier et al., 2011;

Schaaf et al., 2012; Vaags et al., 2012). Mice that lack α-neurexins but express normal β-neurexin levels die at birth due to major deficits in synaptic function (Missler et al., 2003), and synaptic transmission can only be rescued by transgenic expression of neurexin-1α, but not of neurexin-1β (Zhang et al., 2005). Neurexophillins and dystroglycan interact with the α-specific LNS2 domain of neurexins (Missler et al., 1998; Sugita et al., 2001). IgSF21 selectively interacts with neurexin2α in LNS1, and positively regulates inhibitory presynaptic organization and GABA-mediated synaptic transmission in the hippocampal CA1 pyramidal neurons (Tanabe et al., 2017). Deletion of neurexin2α results in autism-related behaviors in mice (Dachtler et al., 2014).

1.1.4 Neurexin ligands

As a presynaptic organizing hub, neurexins interact with axonal intracellular proteins as well as postsynaptic transmembrane and soluble factors. At least seven protein families bind to neurexins and the interactions are largely regulated by alternative splicing (Figure 1.2). Most ligand binding depends on specific promoters or alternative splicing while acting consistently among three genes, but a recent study surprisingly found that IgSF21 only interacts with neurexin-2α but no other isoforms (Tanabe et al., 2017).

Neuroligin1 is a major glutamatergic synapse organizer, while neuroligin2 is found only in GABAergic synapses and neuroligin 3&4 function in both (Craig and Kang, 2007; Ichtchenko et al., 1996; Südhof, 2008). LRRTM1, and LRRTM2 selectively induce glutamatergic presynaptic differentiation (Linhoff et al., 2009; Siddiqui et al., 2010). Cbln1 and GluRδ2 function selectively in parallel fiber synaptogenesis between cerebellar granule cells and Purkinje cells (Matsuda et al., 2010; Uemura et al., 2010).

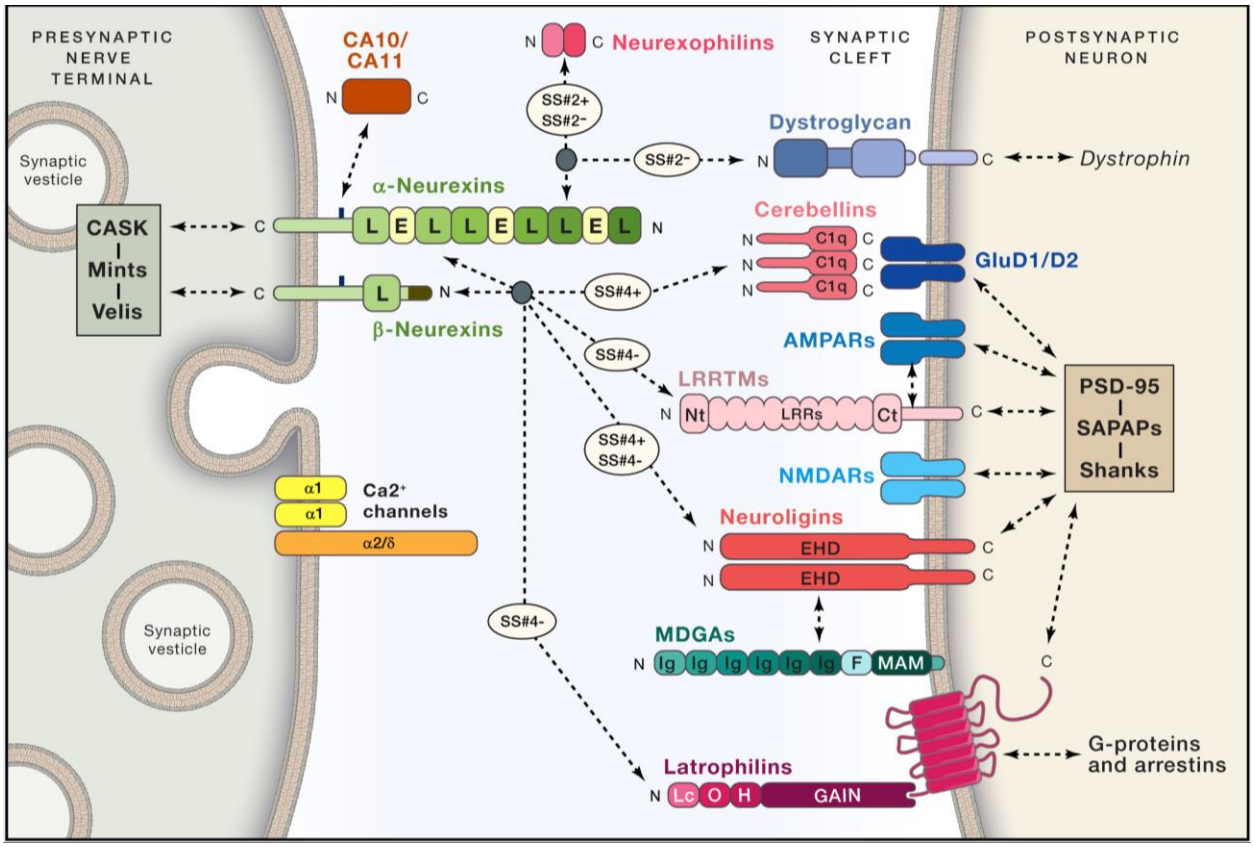

Figure 1.2 Selected Ligand Interactions of Neurexins

Schematic of the interactions of α- and β-neurexins with selected ligands in the context of the synapse. Requirements for neurexin splice variants are indicated; possible competition between ligands are indicated by junctions marked with a circle. Proteins are not drawn to scale (abbreviations: E, EGF-like domain; EHD, esterase homology domain; L, LNS-domain; LRRs, leucine-rich repeats; Nt and Ct, N- and C-terminal sequences surrounding LRRs; Ig, Ig-domain; F, fibronectin III domain; MAM, MAM-domain; Lc, lectin domain; O, olfactomedin-like domain; H, hormone-binding domain; GAIN, GAIN domain). Image adapted and used with permission from (Südhof, 2017).

1.1.5 Neuroligins

Aside from latrotoxins, neuroligins are the first known neurexin ligands and are the most studied postsynaptic organizing proteins, thus acting as an important positive control in various experiments in this study. At first, neuroligin1 was identified as a neuronal cell surface protein

that is enriched in synaptic plasma membranes and acts as a splice site-specific ligand for β-neurexins (Ichtchenko et al., 1995), followed by subsequent discoveries of the highly homologous neuroligin-2 and -3 (Ichtchenko et al., 1996). Later, several studies found that neurexin-neuroligin interaction is not only regulated by alternative splicing of neurexins, but also affected by a splicing insert B (SSB) in neuroligins: neuroligins with SSB bind to β-neurexins with or without SS4 at different affinities, while neuroligins without SSB can bind to both α- and β-neurexins (Boucard et al., 2005; Chih et al., 2006; Comoletti et al., 2006).

Neuroligins are type 1 transmembrane proteins that are composed of a single large extracellular domain consisting of a constitutively dimeric, enzymatically inactive esterase-homology domain, a single-pass transmembrane domain, and a short cytoplasmic tail containing PDZ binding sites. Four genes in vertebrates encode neuroligins (five in human), among which *Nlgn1*, *Nlgn2*, and *Nlgn3* are highly conserved evolutionarily (Ichtchenko et al., 1995, 1996). On the other hand, mouse *Nlgn4* variant has rapidly evolved from other mammalian *Nlgn4* genes and even exhibits sequence variations between different mouse strains (Bolliger et al., 2008). In the current study, neuroligin4 will be will not be extensively discussed. Human NLGN4Y, also known as NLGN5, only locates in the Y chromosome and will not be discussed (Skaletsky et al., 2003).

Neuroligin-1,2,3 are expressed throughout the central nervous system, with neuroligin1 specifically localized at glutamatergic synapses (Song et al., 1999), neuroligin-2 localized mainly at GABAergic and glycinergic (Graf et al., 2004; Varoqueaux et al., 2004), dopaminergic (Uchigashima et al., 2016) and cholinergic (Takács et al., 2013) synapses, and neuroligin-3 localized at both glutamatergic and GABAergic synapses (Budreck and Scheiffele, 2007).

Neuroligin-1 and 2 are the first molecules demonstrated in the fibroblast-neuron coculture assay described previously to induce presynaptic differentiation that triggered a new era for studying synaptic organizing proteins (Scheiffele et al., 2000). Following that, gain-of-function studies showed that overexpression of Neuroligin-1/2/3 increases the density of VGluT1 and VGaT clusters in cultured hippocampal neurons, whereas down-regulation of neuroligin isoform expression by RNA interference results in a loss of excitatory and inhibitory synapses which involves PSD-95 and neurexin1β (Chih et al., 2005; Levinson et al., 2005; Prange et al., 2004).

A series of *in vivo* studies revealed that neuroligins are essential in regulating excitatory and inhibitory synapse development and transmission. Knockout of neuroligin1 reduces NMDAR mediated excitatory but not inhibitory postsynaptic current amplitude in hippocampus and somatosensory cortex, accompanied with deficits in spatial learning and memory that correlate with impaired hippocampal long-term potentiation (Blundell et al., 2010; Chanda et al., 2017; Chubykin et al., 2007). On the other hand, neuroligin-2 knockout mainly reduces inhibitory puncta density and transmission, with a discrete behavioral phenotype that includes a marked increase in anxiety-like behavior, a decrease in pain sensitivity, and a slight decrease in motor coordination (Blundell et al., 2009; Chanda et al., 2017; Gibson et al., 2009). The preference of neuroligin-1 and 2 in regulating excitatory *vs.* inhibitory synaptic plasticity was also confirmed in dentate gyrus of hippocampus (Jedlicka et al., 2018). Conditional knockout of neuroligin-3 in Purkinje cells, as well as in parvalbumin positive interneurons, produces a small but significant reduction in NMDA-receptor-mediated postsynaptic currents (Baudouin et al., 2012; Polepalli et al., 2017), whereas mice carrying an ASD-linked R451C mutation show impaired social interactions but enhanced spatial learning abilities (Tabuchi et al., 2007).

The functions of neuroligins are overlapping as well as distinct. Although there is no apparent change of synapse number or size in single-, double-, or triple-knockouts, sparse knockdown of neuroligin-1 reduces synapse number and spine density in cortical layer 2/3 pyramidal neurons (Kwon et al., 2012), suggesting a competition mechanism. However, another comprehensive *in vitro* study, with careful comparison of global vs sparse knockouts as well as combinations of the three genes, demonstrated that neuroligins are required for the physiological organization of neurotransmitter receptors in postsynaptic specializations but they do not play a major role in synapse formation (Chanda et al., 2017).

Neuroligin-1 is subject to activity-dependent proteolytic cleavage, which could depress synaptic transmission by destabilizing its interaction with neurexins and abruptly reducing presynaptic release probability (Peixoto et al., 2012; Suzuki et al., 2012). The C-terminal domain generated by the cleavage was shown to be sufficient for increasing spine and synapse number as well as modulating synaptic plasticity (Liu et al., 2016). Further studies suggested proteolytic cleavage of neuroligin-3 in response to synaptic activity and protein kinase C signaling could also result in reduced synapse strength, and heterodimerization of neuroligin-3 with neuroligin-1 or 2 could drag the latter into the same cleavage pathway although they don't usually undergo this pathway (Bemben et al., 2019). The secreted N-terminal soluble neuroligin-3 was sufficient and necessary to promote robust high-grade glioma cell proliferation through PI3K-mTOR pathway, suggesting an unexpected mechanism in promoting neuronal activity-regulated cancer growth (Venkatesh et al., 2015). Neuroligin-2 cleavage in ER was believed to be essential for its own maturation and trafficking in Drosophila (Tu et al., 2017).

1.1.6 Neurexins as HSPGs

Heparan sulfate proteoglycans (HSPGs) are a class of proteins consisting of a core protein domain with one or several long linear HS glycosaminoglycan chains attached (Sarrazin et al., 2011). There are four commonly recognized types of HSPGs: cell-surface proteins with a transmembrane domain, such as syndecans; GPI-anchored membrane-associated proteins, such as glypicans; secreted extracellular proteins such as agrin, perlecan and collagen type XVIII; and the secretory vesicle proteoglycan, serglycin (Condomitti and de Wit, 2018; Sarrazin et al., 2011). Although low in the total number of identified members, HSPGs have been shown to be important in various biological contexts.

As ancient as HSPGs can be, their roles in synapse development have been acknowledged more and more in the last few decades. In cultured developing skeletal muscle fibers 35 years ago, agrin was arguably the first isolated synaptic organizing molecule, originally from the extracellular matrix of the Torpedo electric organ (consisting of stacks of electrocytes covered with modified neuromuscular junctions) as a high molecular weight protein factor that induces the aggregation of nicotinic acetylcholine receptors (AChRs). This was long before the role of neurexin in synapse development was identified (Godfrey et al., 1984). It was later confirmed that agrin acts via a receptor complex that includes muscle-specific kinase (MuSK), and agrin-null mice could not form functional neuromuscular junctions (Gautam et al., 1996; Glass et al., 1996).

In the central nervous system, researchers in our lab found that HSPGs are involved in excitatory synapse formation via HS-dependent interaction with postsynaptic LRRTM4 (Siddiqui et al., 2013). Another group independently identified glypican-4 as a presynaptic receptor of LRRTM4 using an unbiased proteomics-based approach (de Wit et al., 2013).

Glypican-4 could also bind PTPσ with nanomolar affinity and PTPσ was proposed to be a co-receptor of LRRTM4-glypican-4 complex on the presynaptic membrane to regulate excitatory synapse transmission (Ko et al., 2015). Another similar trans-synaptic complex GPR158-HSPG (glypican-4 especially) with LAR as the presynaptic co-receptor was identified later by the same group (Condomitti et al., 2018).

Recently, Dr. Peng Zhang and other colleagues in our lab expanded the breadth of how HSPGs are involved in synapse development to another level by confirming neurexins themselves as HSPGs (Zhang et al., 2018). Both α-neurexins and β-neurexins are modified by heparan sulfate (HS) glycosaminoglycan chains at the shared CHO region before transmembrane domain and the HS modification is essential for high affinity binding with neuroligins and LRRTMs. Mice lacking heparan sulfate on neurexin-1 showed reduced survival, as well as structural and functional deficits at central synapses. This study showed that neurexins not only bind proteins through their core protein domains, but can also interact with hundreds of HS binding proteins (Esko et al., 2015). With the interactome of neurexins redefined, a lot of other proteins and signaling pathways might be connected and another level of post-translational regulation of synaptic development and plasticity might be achieved.

1.2 Calsyntenin-3

Calsyntenin-3, as other calsyntenins (calsyntenin-1 and calsyntenin-2), is a type I transmembrane protein of the cadherin superfamily, distributed in synaptic membranes of the adult brain (Hintsch et al., 2002). The family was first identified as proteins released from synapse-forming spinal cord neurons and given the name “calsyntenin” because they are postsynaptic membrane proteins with a Ca^{2+}-binding cytoplasmic domain (Vogt et al., 2001).

Soon after, in a yeast two-hybrid screen to identify the molecular machinery which regulates APP trafficking, the family was identified again and given another name, Alcadein, Alzheimer-related cadherin-like protein (Araki et al., 2003). For consistency, the name "calsyntenin" is used throughout this dissertation.

Very recently, a completely distinct and unannotated form of *Clstn3b* (encoding calsyntenin-3β) was identified in brown adipose tissue (BAT), regulating adipose thermogenesis (Zeng et al., 2019). *Clstn3b* appears to contain three exons. The first exon, which is large and unique, lies within an intron of *Clstn3*, and the final two exons are shared with *Clstn3*. *Clstn3b* is evolutionarily divergent from *Clstn3* and lacks the entire N-terminal sequence that is important for interacting with neurexins. Thus, it is beyond the scope of this dissertation and will not be discussed.

1.2.1 Expression pattern of calsyntenins

Developmental expression patterns of calsyntenins are studied in mice, chickens and zebrafish. In zebrafish, calsyntenin-1 and calsyntenin-3 are expressed strongly in the forebrain, midbrain and hindbrain, while the expression of calsyntenin-2 is weak in the brain that only some expression is detectable in the telencephalon and diencephalon by 24 hours postfertilization (hpf). At 48hpf, all three genes are broadly expressed throughout the nervous system (Ortiz-Medina et al., 2015). In chicken, the expression patterns of the three calsyntenins are highly dynamic throughout neural development such that expression of calsyntenin-1 and calsyntenin-3 are more similar to each other than to calsyntenin-2, with calsyntenin-1 and -3 being more ubiquitous and calsyntenin-2 being more restricted and less variable (de Ramon Francàs et al., 2017). In mice, *in situ* hybridizations of different developmental stages (E14 - P48) revealed ubiquitous calsyntenin-1 mRNA expression throughout the body and in all brain regions while

calsyntenin-2 and -3 mRNAs are restricted to the CNS (Hintsch et al., 2002; Um et al.; Vogt et al., 2001).

1.2.2 Cleavage of calsyntenins

Calsyntenin proteins undergo extensive proteolytic cleavage. Calsyntenin-1 exists in three configurations: a full-length transmembrane protein, a membrane-bound C-terminal cleavage product, and a soluble N-terminal cleavage product. The resulting N-terminal segment is released into the extracellular fluids of the CNS, including the cerebrospinal fluid. The transmembrane stump is internalized and accumulates in the spine apparatus of spine synapses and in subsynaptic lamellar membranes of shaft synapses. This internalization after proteolytic cleavage of calsyntenin-1 removes its Ca^{2+}-binding domain from the cytoplasmic side of the postsynaptic membrane and translocates it to the cytoplasmic surface of the spine apparatus (Vogt et al., 2001). The full-length calsyntenin-1 is rarely detected on the cell surface, despite evidence showing that it is transported to the plasma membrane, suggesting that calsyntenin-1 is cleaved *en route* to and/or upon reaching the plasma membrane. An "uncleavable" mutant calsyntenin-1 readily accumulates on the cell surface and causes the aberrant peripheral retention of kinesin-1 (Maruta et al., 2012). Calsyntenin-1 enhances APP-X11L binding and forms a tripartite complex to enhance the X11L-mediated stabilization of APP metabolism and suppression of Aβ and sAPP secretion (Araki et al., 2003). All three calsyntenins were later confirmed to undergo α-cleavage by ADAM10 or 17, and then a secondary presenilin-dependent γ-cleavage that leads to the secretion of the amyloid-β-protein-like peptide and the liberation of an intracellular domain fragment (Araki et al., 2004; Hata et al., 2009a). A later study showed that Calsyntenin-1 is cleaved by ADAM10 in early endosomes while the calsyntenin-1/APP co-transport packages that are found along axons and in growth cones contain BACE1 but not

ADAM10. Down-regulation of calsyntenin-1 by RNAi results in axonal co-transport of APP and ADAM10, enhanced APP processing, and increased secretion of Aβ (Steuble et al., 2012).

1.2.3 Calsyntenin ortholog *CASY-1* in *C. elegans*

In *C. elegans*, calsyntenins only have one ortholog-CASY-1, which seems to be involved in all the three main functions of calsyntenins. CASY-1 was shown to regulate both GABAergic and glutamatergic synaptic transmission at neuromuscular junctions (Thapliyal et al., 2018a, 2018b) which is consistent with synaptic functions of calsyntenin-1 and 3 (Pettem et al., 2013; Ster et al., 2014). Also, CASY-1 is responsible for axon translocation of insulin receptor DAF-2c by interacting with kinesin-1, which is consistent with calsyntenin-1 in mice (Ohno et al., 2014). Moreover, CASY-1 was implicated in learning and memory in several studies (Hoerndli et al., 2009; Ikeda et al., 2008), which resembles calsyntenin-2 in mice (Lipina et al., 2016; Ranneva et al., 2017).

1.2.4 Calsyntenins as cargo proteins

In zebrafish, calsyntenin-1 regulates the transportation of Rab5-containing endosomes from the cell body to specific locations of developing axons (Ponomareva et al., 2014). Related to its function of mediating intracellular transportation of endosomes, in hepatitis C virus (HCV) infected cells it was shown that calsyntenin-1 contributes to the early stages of the viral replication cycle and the formation of the replication complex. Silencing calsyntenin-1 disrupts the viral replication cycle, confirming the reliance of HCV on this protein as a host factor (Awan et al., 2016).

In mammals, emerging evidence have shown that calsyntenins (especially calsyntenin-1) play an important role in amyloid precursor protein (APP) trafficking. Colocalization of calsyntenin-1 and APP have been shown in several studies in axons of hippocampal neuron

culture when co-transfected (Vagnoni et al., 2012) and in the trans-Golgi network in the soma (Vagnoni et al., 2011). Recently, calsyntenin-3 was also found to colocalize with APP in neuronal axons (Dinamarca et al., 2019). Calsyntenin-1 and APP colocalize and cotransport (Vagnoni et al., 2012), but there is not yet evidence suggesting a direct interaction. Rather, X11L was believed to be the bridge linking calsyntenin-1/3 with APP (Araki et al., 2003; Dinamarca et al., 2019).

Furthermore, as a kinesin adapter, calsyntenin-1 was also required for sensory axon branching and microtubule polarity in developing axon arbors (Lee et al., 2017). Another study using a knockout mouse model showed that calsyntenin-1 regulates targeting of dendritic NMDA receptors and dendritic spine maturation in CA1 hippocampal pyramidal cells during postnatal development (Ster et al., 2014), which in turn affects NMDA receptor-dependent LTP. Calsyntenin-3 was recently identified in a proteomic screen for the $GABA_B$ receptor complex and believed to play a role in its localization (Dinamarca et al., 2019; Schwenk et al., 2016). Together, these findings suggested that calsyntenins contribute to the development of the central nervous systems in multiple aspects.

1.2.5 Calsyntenin-2 in learning and memory

Calsyntenin-2 plays an important role in learning and memory. It is associated with verbal memory in young humans, semantic memory and global cognitive abilities in the elderly (Laukka et al., 2013), as well as old-age unipolar depression (Pantzar et al., 2014). An fMRI study showed effects of polymorphism in *CLSTN2* gene on functional neuronal connections between the parahippocampal gyrus of the right hemisphere, bilateral caudal nuclei, and frontal-cortical brain regions during word recognition (Jacobsen et al., 2009). Another genome-wide association study (GWAS) of brain images using MRI-derived temporal lobe volumetric

measurements also uncovered an association between *CLSTN2* and memory-related temporal lobe volume (Kohannim et al., 2012). Moreover, polymorphism of the calsyntenin-2 gene was associated with modulation of early and delayed recall of words in a large sample of Swiss origin (Papassotiropoulos et al., 2006). However, results pertaining to distinct *CLSTN2* alleles affecting hippocampal volume and memory performance in large populations remain controversial (Boraxbekk et al., 2015; Sédille-Mostafaie et al., 2012; Zhang et al., 2009) (Boraxbekk et al., 2015; Sédille-Mostafaie et al., 2012; Zhang et al., 2009).

To further characterize the function of calsyntenin-2 on learning and memory, in addition to genetic correlation studies, *CLSTN2* knockout (KO) mice were made in our lab and collaborative behavioral studies were conducted. In these studies, we showed that *Clstn2−/−* mice were hyperactive in the open field test and presented spatial learning and memory deficits in the Morris water maze and Barnes maze (Lipina et al., 2016). Furthermore, *Clstn2-/-* mice showed stereotypic behavior, and deficient social motivation and social recognition was only identified in males but not females (Ranneva et al., 2017).

1.2.6 Calsyntenins as biomarkers for diseases

Calsyntenins have been suggested as biomarkers for Alzheimer's disease (AD) because concomitantly altered C-termini for the calsyntenin-1 $p3_{35/38}$ fragments were observed in presenilin-1 familial Alzheimer's disease mutants that lead to an altered Aβ40/42 ratio of APP (Hata et al., 2009a). Furthermore, elevated levels of calsyntenin-1 $p3_{38}$ fragments were detected in the cerebrospinal fluid (CSF) of patients of various clinical populations including sporadic AD. Calsyntenin-3 was found significantly down-regulated in the CSF of familial Alzheimer disease mutant carriers comparing to negative controls (Ringman JM et al., 2012). *CLSTN2* was

also identified for linkage to late onset AD in a genetically isolated Dutch population (Liu et al., 2007).

Calsyntenin-1 isoform X2 was found in higher levels in the CSF of non-corticosteroid treated cervical spondylomyelopathy-affected great danes than in the CSF of clinically normal great danes (Martin-Vaquero et al., 2015). Calsyntenin-1 was also found in higher levels in the CSF of patients with Dementia with Lewy bodies (DLB) compared to healthy controls (Dieks et al., 2013). In a study on patients with lung adenocarcinoma that combined proteomics with bioinformatic prediction on signal peptides, calsyntenin-1 was found secreted in higher levels from both cell lines and serum, and may become a new serologic biomarker for the disease (Chu et al., 2017). In another study, a novel loss of copy number on chr3q23 was found in four ASD cases. This copy number variation (CNV) results in deletion of intron 2 of *CLSTN2* (AlAyadhi et al., 2016).

1.3 Cre-loxP system

1.3.1 History

Ever since the structure of DNA and the genome was discovered, scientists have been trying to manipulate genes in model organisms to study their functions. The advent of embryonic stem (ES) cell technology and gene targeting (homologous recombination between DNA sequences residing in the chromosome and newly introduced DNA sequences) strategies provided powerful tools to make that possible and changed mouse genetics ever since (Capecchi, 1989). However, genes, especially important ones, usually have multiple functions throughout the body as well as throughout the course of development, thus often making global and complete knockout of genes lethal. In other cases, the power of evolution mitigated such events

by creating multiple family members sharing similar functions, so the loss of one gene during an early point in development often does not show any phenotype since its functions are compensated by other family members. In 1980s, an effective way of manipulating gene function in a temporal-, spatial-, and tissue-specific manner was strongly desired.

Cre recombinase is a 38 kDa protein, first discovered and named in 1981 by Nat Sternberg in Bacteriophage P1 as a site-specific recombinase, recognizing a 34bp DNA sequence called loxP (also named by Nat Sternberg) (Sternberg and Hamilton, 1981). When two loxP sites are recognized by Cre, a DNA loop will form and the sequence in between is either deleted or flipped according to the orientation of the loxP sites. A potential use of this system as a gene manipulating tool was proposed in the original paper and finally came into reality in the late 1980s in yeast and transfected mammalian cells (Sauer, 1987; Sauer and Henderson, 1988).

In neuroscience, the first CamKII-Cre (T29-1) mouse was published in 1996, achieving hippocampal CA1 specific (forebrain specific in older mice) and pyramidal neuron specific deletion of NR1, demonstrating the essential role of CA1 NMDA receptors in synaptic plasticity and space representation *in vivo* (McHugh et al., 1996; Tsien et al., 1996a, 1996b). The story by Joe Tsien about the generation of this mouse line and how they published three Cell papers back to back from the project is a great and inspiring read (Tsien, 2018).

Since then, many individual labs have been developing Cre transgenic mouse lines under tissue specific drivers. National and international institutions also launched large-scale projects generating various mouse strains, aiming at better understanding gene functions in a cell-type specific manner. These projects include the Cre-driver project and GENSAT (Gene Expression Nervous System Atlas) project funded by the NIH Blueprint for Neuroscience Research, the CREATE (coordination of resources for conditional expression of mutated mouse alleles) project

funded by the European Union, the Pleiades Promoter Project, and the CanEuCre project developed here in British Columbia, Canada. To date, there are almost 800 mouse lines expressing Cre in the Jackson Laboratory Cre Repository. A PubMed search of "Cre" returns almost 20,000 articles, confirming the enormous usage of the system.

1.3.2 Applications of Cre-loxP system

The general application of Cre-loxP system requires two mouse lines: one with Cre expression under a certain driving promoter, the other line with two loxP sites flanking a sequence of interest. Crossing these two lines together will result in a double transgenic line, with the flanked sequence excised if the two loxP-sites are in the same orientation, or inverted if the two loxP-sites are oppositely oriented. Moreover, if the two loxP-sites are on different DNA molecules, translocation of sequences could also happen.

Since the system was first introduced, most of its applications were to knockout a certain gene in a spatial temporal or cell-type specific manner, by flanking a coding exon with loxP sites (Figure 1.3A). Later, researchers started to use the system in additional ways by designing various loxP cassettes, such as turning on a transgene by putting a stop cassette between loxP-sites before the transgene (Figure 1.3B). The stop cassette prevents gene expression without Cre, and when Cre is present, the stop cassette gets excised so the transgene expression proceeds. This has been extremely useful in introducing genetically modified sensors such as GCamPs and iGluSnFr, and stimulating tools in optogenetics such as channelrhodopsins in the desired cell types. A specific reporter can be introduced to make sure gene knockin or knockout has occurred. For example, a -loxP-exon-stop-loxP-EGFP- cassette only produces EGFP expression when the flanked exon is excised (Figure 1.3C).

In recent years, about a dozen loxP variants have been engineered (Duyne, 2015), providing more flexible and precise tools to control gene expression, as well as to overcome limitations in the system. The loxP-stop-loxP cassette is usually about 1.8kb, thus too big to be packaged in an AAV vector together with a transgene (Kuhlman and Huang, 2008). Also, two opposing wild-type loxP sites could undergo inversion for several rounds in the presence of Cre, making it difficult to determine the orientation of the resultant loxP-flanked sequence. Researchers developed a DIO (Double-floxed Inverse Orientation) cassette to achieve Cre-dependent gene expression by putting an inverted gene between two sets of loxP sequences (one set of wild-type loxPs and one set of mutant loxPs) which are not cross-compatible (Cardin et al., 2009). The inverted gene is not expressed without Cre, whereas with Cre the two loxP pairs will undergo an inversion followed by an excision, ending with an expressing gene between two incompatible loxP sites. A FLEX (Flip Excision) design with the same cassette was also published independently (Atasoy et al., 2008) (Figure 1.3D). Gene switch or conditional knockin could be achieved by flanking the target exon as well as an inverted mutation by a pair of mutated loxP sites, one mutated in the left end and the other in the right end. After inversion by Cre recombinase, the LE-RE loxP will be defective so the mutated gene is stably expressed (Zhang and Lutz, 2002) (Figure 1.3E).

Researchers also combine Cre-loxP system with other site-specific recombinase systems to gain more flexible and specific control. FLP-FRT system is very similar to Cre-loxP and the two were often used together for selection markers or reporter genes (Dymecki, 1996; Gronostajski and Sadowski, 1985). PhiC31 was identified from Streptomyces phage and can recombine two heterotypic sites (attB and attP) resulting in two new sites which are not the substrates for the integrase (Belteki et al., 2003; Thomason et al., 2001). The PhiC31/AttP

system was discovered before all the loxP variants mentioned above were engineered, but did not get as much use as the Cre-loxP system partially because there are already so many Cre driver lines available. There is also the Dre-rox system, very similar to and derived from Cre-loxP, which does not show any crossover recombination between Cre-rox or Dre-loxP, making it a great addition to the site-specific recombination toolbox (Anastassiadis et al., 2009).

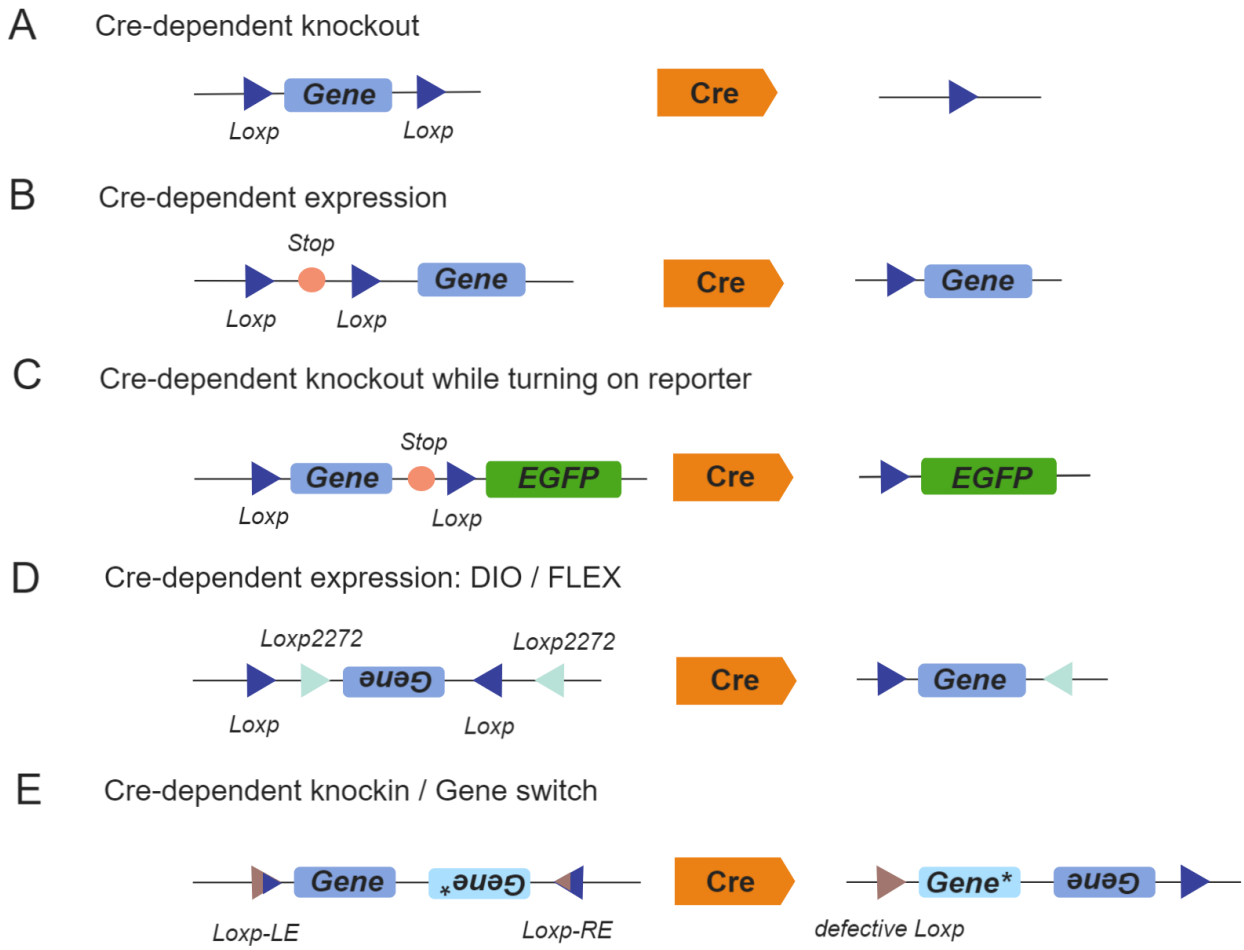

Figure 1.3 Samples of Cre-loxP cassettes

A. Targeted gene (usually one exon or several exons) is flanked by two loxP sites and excised with Cre expression.

B. Cre-dependent gene expression can be achieved by inserting a loxP-stop codon-loxP cassette before the transgene, so the gene expression is prevented by the stop cassette without Cre and can proceed when Cre is present.

C. When the transgene and a stop cassette are both flanked by loxP sites followed by an EGFP reporter sequence, Cre-dependent excision could knockout the gene and at the same time turn on expression of the reporter.

D. DIO/FLEX strategy for stable gene inversion. An inverted gene sequence is flanked by two sets of loxP sites that are not cross compatible. When Cre recombinase is present, either set of loxP get inverted and then the other set excised, ending with the gene in the right orientation and two incompatible loxP.

E. Cre-dependent knockin or gene switch strategy: the right oriented gene and inverted gene mutation are flanked by two mutant loxP sequences. When Cre is present, the flanked sequence is inverted so the wild-type gene gets scrambled and mutated gene can express in frame. LE-loxp: left end mutated loxP; RE-loxp: right end mutated loxP.

1.3.3 Caveats of using Cre mouse lines

During the past twenty years, as the Cre-loxP system was utilized more frequently by researchers, several different caveats have been observed, especially with regards to Cre-expressing mouse lines. In May 2019, a PubMed search of "Cre transgenic mouse" returns over 8000 articles. In view of this popularity, it appears particularly important to draw attention to the problems and pitfalls inherent in using the system, which if not careful considered can easily lead to faulty conclusions from experimental results.

Perhaps the most important problem in using Cre-dependent technology is that of Cre toxicity. *In vitro* studies using fibroblasts have shown that high level of Cre expression can inhibit cell growth and induce chromosomal DNA damage (Loonstra et al., 2001; Silver and Livingston, 2001). Cre recombinase was also shown as a PKA substrate in an *in vitro* kinase

assay, suggesting that the expression of Cre could result in global attenuation of the cAMP/PKA pathway (Gangoda et al., 2012). In addition, Cre activity could cause widespread apoptosis and lethal anemia during embryonic development, independent of introduced floxed sites (Naiche and Papaioannou, 2007). Cryptic loxP sites, sometimes called Pseudo-loxP sites, whose sequences are similar but different from consensus loxP sites, can also be recognized by the Cre recombinase and catalyzed as its substrate. Actually, a bioinformatics study revealed that in the mouse genome, cryptic loxP sites occur frequently and are homogeneously distributed in the genome, at a frequency of 1.2 per megabase (Semprini et al., 2007). These sites could undergo excision, inversion, or chromosomal translocation in the presence of Cre recombinase. However, one report argued that the level of apoptosis induced by Cre expression cannot always be attributed to activity at cryptic loxP sites, but rather correlates with the number of loxP sites introduced and that cell death is p53-dependent (Zhu et al., 2012).

Increasing evidence from widely used Cre lines suggests the importance of using Cre-positive non-floxed mice as experimental controls. Prm1-Cre (Tg(Prm1-cre)1Mrc) expression in post-mitotic spermatids led to immediate abortion of fertilized eggs with 100% penetrance, concomitant with massive DNA damages visualized as “scrambled DNA” in chromosome spreads of male pronuclei (Schmidt et al., 2000). Prolonged Cre expression driven by the α-myosin heavy chain promoter (αMyHC-Cre) can be cardio-toxically associated with fibrosis, inflammation, and DNA damage response, potentially resulting from off-target effects onto cryptic loxP sites (Pugach et al., 2015). One recent transcriptome analysis revealed that Le-Cre (Tg(Pax6-cre, GFP)1Pgr) hemizygous lenses deregulated the expression of fifteen murine genes, several of which are associated with apoptosis, independent of any floxed DNA deletion (Lam et al., 2019).

To avoid the developmental deficits potentially resulted from early Cre-mediated recombination in the genome, some researchers opted for either viral introduction of Cre or conditional Cre activation by tamoxifen. While the toxicity of tamoxifen onto CreER expressing cells has long been known (Higashi et al., 2009; Huh et al., 2010; Li et al., 2014; Takebayashi et al., 2008), one very recent study showed that viral vector-mediated Cre recombinase expression (AAV-eGFP-Cre) in substantia nigra induces lesions of the nigrostriatal pathway and drastic reproducible modifications of behavior, with increased basal locomotor activity as well as impaired locomotor response to cocaine compared with AAV-eGFP-injected controls (Rezai Amin et al., 2019).

There are also Cre lines showing mosaic or inconsistent expression patterns, including $GATA4^{Cre}$ in the early embryos (Pilon et al., 2008), and MMTV-Cre in postnatal mammary glands (Lu et al., 2008).

Other unexpected Cre expression or off-target effects in seemingly unrelated organs may not directly lead to cell death or growth arrest, but could also complicate result interpretation. Such evidence has been reported for: $Osr2^{tm2(cre)Jian}$ which is designed for palatal mesenchyme but also expresses in kidney glomeruli tissues (Lan et al., 2007); Tg(Pdx1-cre)89.1Dam which is designed to be β-cell or pancreas-specific but also expresses in the brain (Wicksteed et al., 2010); $Krt19^{tm1(cre)Mmt}$ which is designed for epithelia-specific recombination during organogenesis, but actually allows unexpected recombination in early embryonic development, resulting in recombination of a loxP-flanked allele throughout all tissues of the mouse, but with sparing of the extraembryonic endoderm, including the anterior visceral endoderm (Means et al., 2005).

Genetic background is another important but underrated factor in the pitfalls of using Cre mouse lines. Mice from different genetic background carrying the same mutation could show

different behavior and metabolism, which could also affect the expression pattern for Cre transgene and interpretation for experimental results. Many Cre lines are developed and maintained in individual labs and used on mixed backgrounds. A collaborative report from three labs reviewed at least 17 studies using the RIP-Cre mouse, and suggested that these RIP2-Cre mice, in the absence of genes targeted by loxP sites, are glucose intolerant (Lee et al., 2006). Another study argued that such phenotypic changes in RIP2-Cre mice are not obligatory upon Cre expression in β-cells, but may rather be controlled by a rigorous backcrossing strategy. When they bred the Cre line onto a nearly pure C57BL/6J background, no glucose intolerant was detected (Fex et al., 2007).

In conclusion, the Cre-loxp system is a very powerful tool to study gene function in various fields especially in neuroscience where the cell types are so complicated. Yet the use of Cre driver lines could come together with unexpected pitfalls, which if not taken seriously could really complicate the research and lead to erroneous conclusions.

1.4 Research questions

General research questions and organization of this dissertation are described here. Detailed rationale and hypothesis will be explained in each chapter.

Calsyntenin-3 was identified as a synaptogenic molecule, promoting synapse development in primary neuron cultures (Pettem et al., 2013). But the nature of its interaction with presynaptic partner α-neurexins and mechanism of how it regulates synapse development *in vivo* remained unclear. In **Chapter 2**, I try to answer these following questions:

- Does calsyntenin-3 bind to all neurexins? Is it regulated by promoter specificity or alternative splicing?
- Which protein domains are involved?
- Does endogenous calsyntenin-3 undergo similar cleavage as calsyntenin-1?

- How does the cleavage, if any, affect the function of calsyntenin-3?
- Does the heparan sulfate modification of neurexins affect its interaction with calsyntenin-3?
- When and where is calsyntenin-3 expressed in the brain?
- How does calsyntenin-3 regulate synapse development *in vivo*?

Based on my work in Chapter 2 and colleagues' research (Pettem et al., 2013), calsyntenin-3 expresses differentially in excitatory and inhibitory neurons. As an overall effect, both excitatory and inhibitory synapse development are compromised in young adult *Clstn3-/-* mice, with a slight shift of E/I balance towards the inhibitory side. In **Chapter 3**, I ask the questions below to further understand the role of calsyntenin-3 in regulating synapse development and transmission:

- What is calsyntenin-3's function in interneurons, where it is highly expressed?
- What is calsyntenin-3's function in excitatory pyramidal neurons?
- Does calsyntenin-3 mainly function on the presynaptic side or the postsynaptic side?
- Does calsyntenin-3 regulate synaptic transmission in an age-dependent manner similar to calsyntenin-1 and neuroligin-1?
- Is calsyntenin-3's function cell autonomous or does it depend on the environment?

To answer these questions, Cre-expressing transgenic mouse lines were used to generate Clstn3 conditional knockout mice targeting excitatory and inhibitory neurons specifically. During this process, we encountered unexpected germline recombination with both lines. This particular pitfall of using Cre mouse lines has not been well recognized by the neuroscience community and has been an enormous resource and time sink. In **Chapter 4**, we try to address the following questions to raise awareness of this phenomenon:

- Is unexpected germline recombination a common drawback for Cre lines? Or is it rare and we were just unlucky?

- For a given Cre line, is the germline recombination locus specific?
- Do Cre lines under the same promoter with different enhancers behave differently?
- Ultimately, what are steps we can take to avoid unexpected germline recombination events from happening?

Chapter 2: Calsyntenin-3 interacts with α-Neurexins and promotes synapse development

2.1 Introduction

Synapse-organizing complexes mediate local differentiation of presynaptic and postsynaptic specializations by recruiting molecular components and organelles involved in neurotransmitter release and reception. Emerging evidence indicates that multiple synapse-organizing complexes act in concert to regulate the density, composition, and function of synapses on each neuron (Missler et al., 2012; Siddiqui and Craig, 2011; Südhof, 2018).

The presynaptic neurexins constitute one of the best-characterized families of synapse-organizing proteins (Südhof, 2017). Each of the three neurexin genes in humans and rodents produces long α isoforms from an upstream promoter and shorter β isoforms from a downstream promoter. Alternative splicing creates additional diversity resulting in >3,000 potential neurexin isoforms (Tabuchi and Südhof, 2002). Neurexins have acquired particular notoriety because alterations in NRXN genes were found to contribute to nonsyndromic autism spectrum disorders and schizophrenia (Betancur et al., 2009; Südhof, 2008). Importantly, α-neurexins perform essential functions that are not shared with β-neurexins (Missler et al., 2003; Zhang et al., 2005), and the majority of disease-associated NRXN variations selectively affect α-neurexins, and not β-neurexins (Ching et al., 2010; Gauthier et al., 2011; Schaaf et al., 2012; Vaags et al., 2012). Despite the obvious functional importance of α-neurexins and the identification of multiple extracellular partners for neurexin isoforms, the only identified α-neurexin-specific interacting proteins are the small secreted neuropeptide-like neurexophilins (Missler and Südhof, 1998) and neurexin-2α specific interactor IgSF21 (Tanabe et al., 2017).

Neurexins control excitatory and inhibitory synapse development through isoform-selective interactions with different sets of postsynaptic partners, among which neuroligins were the first to be identified. As with neurexins, mutations in NLGN genes are linked to neurodevelopmental disorders (Jamain et al., 2003; Südhof, 2008) and their causative role is supported by animal models (Jamain et al., 2008). The main neuroligin at glutamatergic synapses, neuroligin-1 (with the B insert), binds only β-neurexins, whereas the other neuroligins, including neuroligin-2 which is the main neuroligin at GABAergic synapses, bind all neurexins (Boucard et al., 2005). Acting cooperatively with neuroligins at subsets of glutamatergic synapses, postsynaptic LRRTM1 and LRRTM2 bind α- and β-neurexins lacking an insert at splice site 4, whereas cerebellin-1 bridges postsynaptic GluRδ2 to neurexins containing an insert at splice site 4 (Ko et al., 2009; Linhoff et al., 2009; Siddiqui et al., 2010). Neurexins and these diverse postsynaptic binding partners control multiple aspects of synapse development, including stabilization and morphological and functional maturation (Ito-Ishida et al., 2012; Kwon et al., 2012; Südhof, 2017).

2.2 Rationales and hypothesis

In an unbiased mammalian expression screen developed in our lab to identify novel proteins involved in synaptic development based on co-cultures of non-neuronal cells with neurons, we identified calsyntenin-3 as a "synaptogenic" protein (Pettem et al., 2013). When expressed in COS cells, calsyntenin-3 can induce both excitatory and inhibitory presynaptic differentiation in contacting axons. An initial search for presynaptic binding partners revealed that calsyntenin-3 interacts with α-neurexins, critical organizers of synaptic structure and important players in synaptic transmission and plasticity (reviewed above). This dissertation aims to reveal the mechanism of calsyntenin-3's activity and function. Based on the properties of

calsyntenins and neurexins, as well as studies of other synaptic organizers, I formed the following hypotheses and aimed to characterize calsyntenin-3's interaction and function as detailed below:

I. In the initial test done by another lab member, calsyntenin-3 binds to neurexin-1α lacking the insert at splice site 4. The interaction between neurexins and postsynaptic ligands largely depends on specific promoters or alternative splicing, a phenomenon which is consistent among all of the three neurexins. We hypothesize that all three α-neurexins are able to interact with calsyntenin-3 at similar affinities and the insert at splice site 4 may or may not regulate this interaction.

II. The domains responsible for binding in both calsyntenin-3 and α-neurexins will be determined. Given α-neurexin-specific binding properties, we hypothesize that sequences within LNS1 to LNS5 of α-neurexins are involved, with or without contribution from LNS6. Regarding calsyntenin-3, we hypothesize that the two cadherin domains and the LNS domain are involved. A point mutation in the LNS domain Q441→K mimicking a mutation E→K in the C. elegans single calsyntenin ortholog CASY-1 which results in learning deficits (Ikeda et al., 2008) will also be tested.

III. Calsyntenin proteins undergo extensive proteolytic cleavage (Araki et al., 2004; Hata et al., 2009b), which affects their surface expression and co-transportation with APP (Maruta et al., 2012; Steuble et al., 2012). We hypothesize that the cleavage of calsyntenin-3 impacts its function in the context of synaptic organization.

IV. Neurexins have been recently found to be modified by heparan sulfate, extending their interactome beyond those based on protein-protein domain interactions (Zhang et al., 2018). The heparan sulfate modification affects the interaction of neurexins with postsynaptic ligands such as neuroligins and LRRTMS. We hypothesize that calsyntenin-3 also interacts with α-neurexins through these heparan sulfate chains.

V. Overexpressed calsyntenin-3 variant enhances excitatory and inhibitory presynaptic inputs in cultured neurons (Pettem et al., 2013). We hypothesize that loss of function *in vivo* studies in calsyntenin-3 knockout mice will provide more information of calsyntenin-3's function in synapse development in a context that is more physiologically relevant.

2.3 Methods

2.3.1 DNA constructs

The DNA constructs used in this Chapter are listed in the following table.

DNA vector	Source
HA-Neurexin1α(-S4)	(Siddiqui et al., 2010)
Neurexin1α(-S4) -CFP	(Kang et al., 2008)
Neurexin1α(+S4) -CFP	(Kang et al., 2008)
Neurexin1β(-S4) -CFP	(Kang et al., 2008)
Neurexin1β(+S4) -CFP	(Kang et al., 2008)
Neurexin2α(-S4) -CFP	(Kang et al., 2008)
Neurexin2α(+S4) -CFP	(Kang et al., 2008)
Neurexin2β'(-S4) -CFP	(Kang et al., 2008)
Neurexin2β'(+S4) -CFP	(Kang et al., 2008)

DNA vector	Source
Neurexin3α(-S4) -CFP	(Kang et al., 2008)
Neurexin3α(+S4) -CFP	(Kang et al., 2008)
Neurexin3β'(-S4) -CFP	(Kang et al., 2008)
Neurexin3β'(+S4) -CFP	(Kang et al., 2008)
Clstn3-FC	(Pettem et al., 2013)
LRRTM2-CFP	(Linhoff et al., 2009)
Slitrk3-CFP	(Takahashi et al., 2012)
Plain AP	(Linhoff et al., 2009)
Myc-His-C3secreted	(Pettem et al., 2013)
Nlg2-CFP	(Siddiqui et al., 2010)
Myc-C1-CFP	(Pettem et al., 2013)
Myc-C2-CFP	(Pettem et al., 2013)
Myc-C1EX-CD8-CFP	(Pettem et al., 2013)
Myc-C2EX-CD8-CFP	(Pettem et al., 2013)
Myc-C3EX-CD8-CFP	(Pettem et al., 2013)
Myc-C3ΔPCS-CFP	(Pettem et al., 2013)
Myc-C3CADonly -CFP	(Pettem et al., 2013)
Myc-C3ΔCAD-CFP	(Pettem et al., 2013)
Myc-C3ΔLNSQ/K-CFP	(Pettem et al., 2013)
Myc-C3ΔLNS-CFP	(Pettem et al., 2013)
N-Cadherin-CFP	(Kang et al., 2008)
N1α_L1L6-CFP	(Kang et al., 2008)
N1α_L3L6-CFP	(Kang et al., 2008)
N1α_L5L6-CFP	(Kang et al., 2008)
N1α-D1176A-CFP	(Kang et al., 2008)
Clstn2-CFP	(Pettem et al., 2013)
Clstn1-CFP	(Pettem et al., 2013)

DNA vector	Source
Myc-NGL3	(Zhang et al., 2018)
Myc-C3	(Pettem et al., 2013)
Myc-C3-4KA	This study
Myc-C3-5RA	This study
Myc-C3-6RA	This study
Myc-CD4	(Ge et al., 2018)

Table 2.1 DNA constructs and sources used in Chapter 2

2.3.2 Primary neuron culture and COS cell coculture assay

Dissociated primary hippocampal neuronal cultures were prepared from embryonic day 18 (E18) rats as previously described (Kaech and Banker, 2006). Hippocampi were dissociated by trypsinization. Dissociated neurons were plated onto poly-L-lysine-coated glass coverslips in 60-mm culture dishes at a density of 300,000 cells/dish and cocultured over a monolayer of glia. After 2 days, cytosine arabinoside (5 μM) was added to neuron cultures to prevent the overgrowth of glia. Cultures were maintained in serum-free minimal essential medium with N2 supplements, 0.1% ovalbumin, and 1 mM pyruvate, with replacement of ⅓ of the media per dish once per week. For coculture assays, neurons were treated with 100 μM 2-amino-5-phosphonopentanoic acid (APV, Research Biochemicals) beginning on day 7.

COS-7 and HEK293 cells were maintained in Dulbecco's modified Eagle's medium supplemented with 10% fetal bovine serum and transfected with TransIT-LT1 Transfection Reagent (Mirus). The flat shape of COS cells was preferred for coculture compared with the rounder shape of HEK cells preferred for confocal analyses of surface association. Transfected COS cells were trypsinized 24 h after transfection, washed, and plated at 200,000 cells/dish onto

neurons pre-grown for 13 days *in vitro* (DIV). After 24 h of coculture, cells were fixed for 15 min in warm phosphate-buffered saline with 4% paraformaldehyde and 4% sucrose. After surface staining by anti-Myc primary antibody (1:1000, IgG1; Invitrogen), COS-neuron cocultures are permeabilized with 0.25% Triton X-100 and incubated with anti-synaptophysin (1:1000; IgG1; BD Biosciences; 611880), anti-MAP2 (1:4000, chicken polyclonal IgY; Abcam; ab5392) and anti-tau-1 (1:2000; mIgG2a; clone PC1C6; Millipore; MAB3420; recognizes dephosphorylated tau) overnight at 4℃. Secondary antibodies used were raised in goat against the appropriate species and monoclonal isotype, highly cross-absorbed and conjugated to Alexa-488, Alexa-568 and Alexa-647 dyes (1:500, Invitrogen). AMCA (7-amino-4methylcoumarin-3-acetic acid)-conjugated anti-chicken IgY (donkey IgG; 1:200; Jackson ImmunoResearch; 703-155-155) was used for visualizing dendrites.

2.3.3 Animals

Clstn3-/- mice were described previously (Pettem et al., 2013). All mice were housed in ARU at the University of British Columbia. All procedures were approved by the Animal Care Committee at the University of British Columbia. Protocols include mice breeding A16-0090 and A16-0086, biosafety certificate B17-0067.

2.3.4 Protein purification and cell surface binding assay

Expression of Clstn3-Fc protein was performed by transfecting HEK293T cells with the encoding plasmid, and culturing in DMEM with 10% FBS and 0.5 mg/ml Zeocin (Invitrogen). After a 21-day selection period with Zeocin, the medium was replaced with serum-free AIM V synthetic medium (Invitrogen). The conditioned medium was collected every 2-3 days for three weeks and frozen at -80°C, for a total of 300-400 mL. Fc fusion protein was purified using protein-G sepharose 4 fastflow columns (GE Healthcare) and concentrated in PBS with

Centricon filters (Millipore). Purified Fc fusion proteins were immunoblotted, visualized by chemiluminescence using a Bio-Rad gel documentation system, and quantified by densitometry relative to a human IgG standard curve. Nlg2-Fc fusion protein was prepared as described previously (Gauthier et al., 2011).

HEK293T cells stably expressing neurexin1α-AP were generated by antibiotic selection as above. Supernatant collected from expressing cells was concentrated using Centricon Plus-70 ultrafiltration units (100 kDa cutoff; Millipore). The neurexin1α-AP fusion protein also contained Myc and His tags and was purified using Ni-NTA agarose eluting with 250 mM imidazole. Imidazole was replaced by PBS via buffer exchange using Centricon filters. Purified neurexin1α-AP fusion proteins were quantitated by SDS-PAGE relative to a BSA standard curve using Sypro Ruby gel stain (Invitrogen), UV illumination, and a Bio-Rad gel documentation system. The production of Myc-His-C3-ecto protein is similar to AP-tagged proteins and was purified by Ni-NTA agarose as described above.

To assess binding of fusion proteins, COS7 cells on coverslips were transfected with the indicated expression vectors and grown for 24 h. Live cells were incubated with fusion proteins (at 50 nM unless otherwise indicated) for 45 min at 4°C. Binding was assayed in the following "binding buffer": 168 mM NaCl, 2.6 mM KCl, 10 mM HEPES, pH 7.2, 2 mM $CaCl_2$, 2 mM $MgCl_2$, 10 mM D-glucose, and 100 µg/ml BSA. Cells were fixed in parafix solution (4% paraformaldehyde and 4% sucrose in PBS pH 7.4) for 15 min at 20°C, then incubated with blocking solution (PBS + 3% BSA and 5% normal goat serum) for 30 min at 37°C. This was followed by incubation with anti-HA antibodies (1:500; IgG2b; clone 12CA5; Roche) overnight at 4°C and secondary antibodies FITC-conjugated donkey anti-human IgG (H+L) (1:100,

Jackson ImmunoResearch) and Alexa-568 anti-IgG2b (1:1000, Invitrogen) for 1 h at 37°C to visualize bound Fc-fusion protein and surface HA, respectively. Binding of AP-fusion protein was visualized by incubation with either anti-alkaline phosphatase primary antibody (1:500, Sigma) and Alexa-568 anti-IgG2a (1:1000, Invitrogen), or anti-Myc primary antibody (1:1000, IgG1; Invitrogen) and Alexa-568 anti-IgG1 (1:1000, Invitrogen). Coverslips were mounted in elvanol (Tris-HCl, glycerol, and polyvinyl alcohol with 2% 1, 4-diazabi-cyclo[2,2,2]octane).

For protein binding on primary neurons, pLL3.7-syn-YFP-2A-V5-N2α or ΔHS constructs were transfected into primary rat hippocampal neurons by nucleofection. At DIV 3, neuron coverslips were incubated with conditioned medium containing the purified Myc-His-C3 protein for 1 hour in the cell culture incubator on an ice pack to inhibit endocytosis. After binding, the coverslips were washed with conditioned medium and neurobasal medium, followed by fixation with 4% paraformaldehyde. Then coverslips were stained with anti-Myc primary antibody (1:1000, IgG1; Invitrogen) and anti-V5 (1:5000; Thermo Fisher Scientific, R960 - CUS) followed by the appropriate secondary antibodies.

2.3.5 Western blot

For running western blots at various developmental stages, brain tissues were collected from P6, P21, P30, P60 wild-type mice in cold homogenization buffer (320 mM sucrose, 5 mM Hepes pH 7.4). The tissue samples were homogenized using a Dounce homogenizer in five volumes of homogenization buffer supplemented with cOmplete™ protease inhibitor tablets (Roche). Homogenized tissues were centrifuged at 1000 x g for 10 min at 4°C, the supernatant collected, and protein concentration determined with the Bio-Rad Protein Assay kit, using BSA as a standard (Sigma). Protein concentrations were normalized between samples and run on 8%

polyacrylamide gels. Gel transfer was performed onto Immobilon P membranes (Millipore) which were blocked in 5% skim milk in Tris-buffered saline/0.05% Tween-20 (Sigma) and incubated with primary calsyntenin-3 and β-actin antibodies (Pettem et al., 2013) and appropriate secondary antibodies. Immunoblots were detected using the SuperSignal Chemiluminescent kit (Thermo Scientific) and visualized by chemiluminescence using a Bio-Rad gel documentation system.

To detect the expression level of neurexins in *Clstn3 -/-* and *Clstn3+/+* mice, brain tissues were collected from P42 mice and P2' fractions were prepared as described before (Linhoff et al., 2009). Western blotting was conducted as described above and membranes were probed with anti-pan neurexin (1:2000, Millipore) and anti-α-tubulin (1:10000, Thermo) antibodies.

To test the effect of GM6001 on calsyntenin-3 cleavage, rat cortical neurons were plated on 12-well plates coated with poly-L-lysine (PLL) at a density of 1 million per well and cultured in the same medium as hippocampal neurons without addition of cytosine arabinoside. On DIV14, 10μM GM6001 was added to conditioned media 2 hours before harvesting lysate and media. Then, the media was collected, treated with protease inhibitor cocktail tablets (Roche) and placed on ice, and the cells were washed with phosphate buffered saline then scraped into lysis buffer (1% Triton X-100, 150mM NaCl, 20mM Tris pH 7.4, 1mM DTT, 1mM EDTA, plus protease inhibitor tablet). Lysates were centrifuged at 16000 x g for 15min at 4°C and the supernatant was collected. The protein concentrations of both media and lysate fractions were determined and western blot conducted as described above.

2.3.6 Co-immunoprecipitation

HEK cells were transfected with the indicated expression vectors using TransIT-LT1 transfection reagent (Mirus) and grown for 48 hours. Cell lysates were extracted with 1% Triton X-100 in TBS with cOmplete^{TM} protease inhibitor (Roche Applied Science), incubated with 1 µg of anti-HA antibody (Roche Applied Science) overnight at 4 °C and then with Protein G beads for 1 hour at 4°C. The beads were washed with 0.1% Triton X-100 three times and then eluted with SDS-sample buffer. Samples were analyzed by Western blot with an anti-GFP antibody (Invitrogen).

2.3.7 Tissue immunofluorescence staining

For immunofluorescence studies, brain tissue samples were collected from P30 *Clstn3 -/-* and littermate wild-type male mice. The mice were anaesthetized with 20% urethane and perfused transcardially with cold 0.1 M phosphate buffered saline (PBS) followed by 4 % paraformaldehyde + 4% sucrose in PBS (pH 7.4). Following perfusion, the brains were extracted and post-fixed in cold 4% paraformaldehyde overnight. The brains were then cryoprotected in 30% sucrose in PBS at 4˚C and frozen in OCT compound (Tissue-Tek; Sakura-Finetek) using dry ice. Coronal cryostat sections 20 µm thick were cut at hippocampal level and mounted on Superfrost Plus slides. For double staining with calsyntenin-3 and CaMKIIα/ Parvalbumin antibodies, the sections were then incubated in 100% methanol for 10 minutes at -20°C followed by PBS wash and then incubated in blocking solution (5% BSA + 5% Normal goat serum + 0.25 % Triton X100 in PBS) at 37°C for 1 hour. For all immunostaining, sections were incubated with primary antibodies diluted in the same blocking solution (overnight, 4°C) then with the appropriate secondary antibodies conjugated to Alexa 488, 568 or 647 (Molecular Probes/Invitrogen) (1 hour, 20°C). Sections were washed in PBS containing the nuclear

counterstain DAPI (4',6 diamidino-2- phenylindole), and mounted in elvanol (Tris-HCl, glycerol, and polyvinyl alcohol with 2% 1,4-diazabicyclo[2,2,2]octane).

For studying the expression pattern of calsyntenin-3, tiled images were captured on a Zeiss LSM 700 confocal microscope using a 20x lens with 0.5x magnification followed by the use of a stitch macro for further processing. For synaptic density quantification images, sets of sections were fixed and stained simultaneously and imaged with identical settings blind to the experimental condition on the Zeiss confocal microscope using a 40x 1.4 numerical aperture lens with 2.5x magnification and sequential scanning with individual lasers and optimized filters.

2.3.8 Electron microscope

Clstn3−/− and wild-type littermate mice were perfused transcardially with 4% paraformaldehyde and then PBS. Brain tissue was collected and postfixed with 4% paraformaldehyde for 24 hours. Hippocampal CA1 region was blocked and fixed with osmium oxide, dehydrated, embedded in a JEMBED/Spurr's mixture, and 70 nm sections were generated and stained with 2% uranyl acetate and Reynold's lead. Images of stratum pyramidale (>100) and stratum radiatum (>50) were obtained on a Hitachi H7600 transmission electron microscope. Symmetric and asymmetric synapses were visually identified and counted.

2.4 Results

2.4.1 Calsyntenin-3 binds to α-Neurexins but not β-Neurexins

Presumably, calsyntenin-3 induces presynaptic differentiation in co-culture assays by binding to presynaptic proteins. There are two major groups of presynaptic organizing proteins: neurexins and RPTPs (Siddiqui and Craig, 2011; Takahashi and Craig, 2013). Therefore we tested the interaction between calsyntenin-3 and representative members of these two families. I found that, like neuroligin-2-Fc, calsyntenin-3-Fc (C3-FC), purified soluble fusion proteins of

the calsyntenin-3 ectodomain with human immunoglobulin constant region, bound to COS cells expressing neurexin-1α, but not to cells expressing PTPσ or PTPδ on the surface (Figure 2.1A). Saturable binding was observed, and Scatchard analysis revealed an apparent dissociation constant of 43.7 nM for the interaction of C3-FC with cell-expressed neurexin-1α (Figure 2.1B). The binding affinity was lower than that between neuroligins and neurexins, or that between LRRTMs and neurexins (Siddiqui et al., 2010), but still suggested physiological interaction.

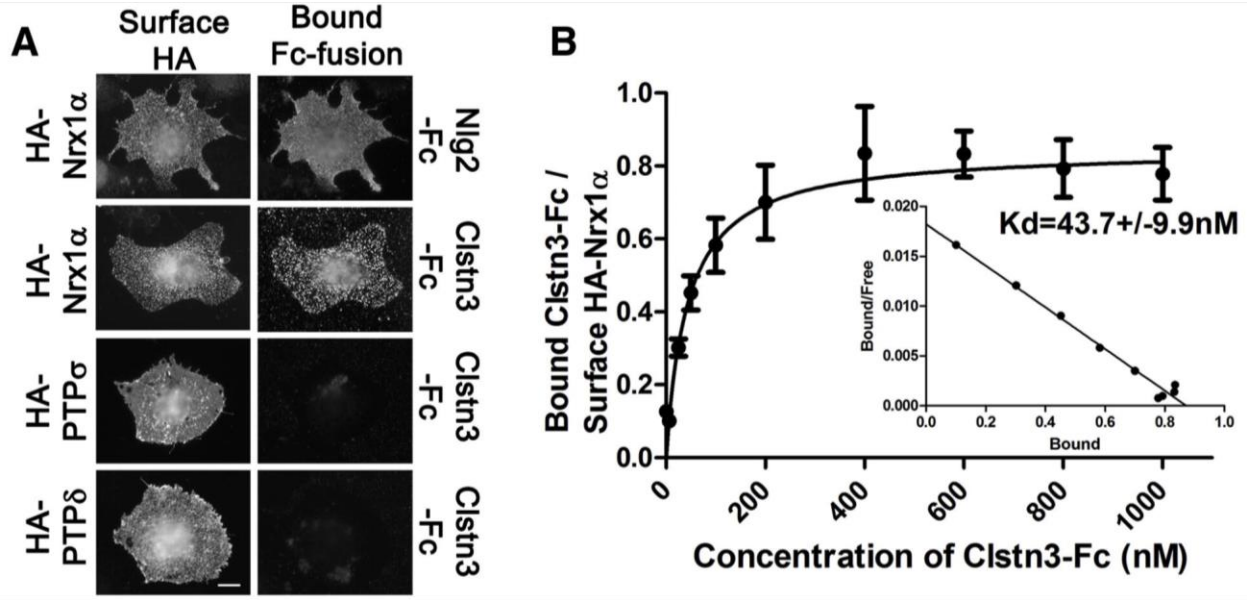

Figure 2.1 Calsyntenin-3 ectodomain binds to HA-Neurexin 1α at COS cell surface.

A. Like neuroligin-2-Fc (Nlg2-Fc), calsyntenin-3 fusion protein Clstn3-Fc bound to COS cells expressing HA-neurexin-1α (HA-Nrx1α) but did not bind to COS cells expressing HA-PTPσ or HA-PTPδ. The neurexin-1α variant lacking the insert at splice site 4 was used. Surface HA stain shown in the left column and Fc stain in the right. Scale bar = 20μm.

B. By Scatchard analysis, affinity of binding of Clstn3-Fc to HA-Neurexin1α was estimated at 43.7 ± 10.0 nM (n ≥ 15 cells each in two independent experiments).

Both neuroligin-1 and LRRTM2 bind to neurexins in a calcium-dependent manner (Siddiqui et al., 2010; Südhof, 2008). So I tested the calsyntenin-3-neurexin interaction in calcium-free binding buffer containing the calcium chelator EGTA. Indeed, the intensity of bound calsyntenin3-Fc on COS cell surface is less than one tenth of that in normal calcium containing binding buffer (Figure 2.2), indicating this interaction is calcium-dependent, just like LRRTMs and neuroligins.

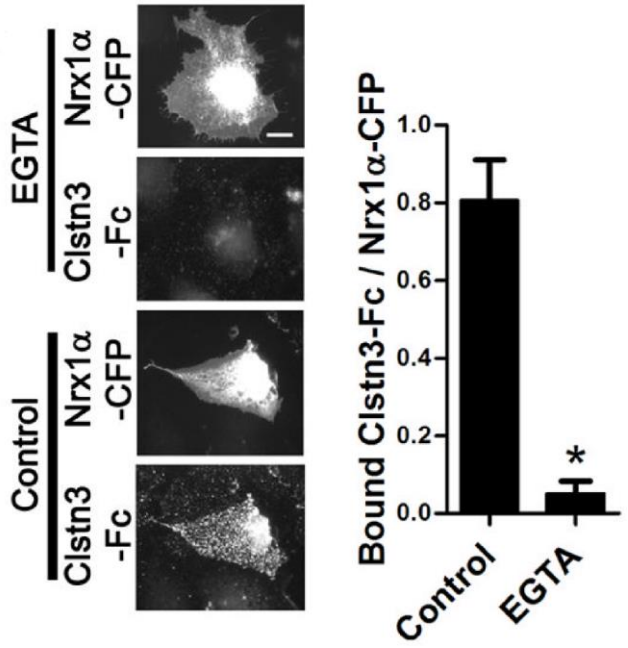

Figure 2.2 Calsyntenin-3 ectodomain binding to HA-Neurexin 1α is calcium-dependent

Binding of Clstn3-Fc to Nrx1α-CFP was abolished in calcium-free media containing 50 mM EGTA. Transfected Nrx1α-CFP and Fc staining are shown. Scale bar=20μm. $*p < 0.0001$, Student's t test (n = 24 cells each).

Next, we wondered whether calsyntenin-3 could interact with all major neurexin isoforms. As discussed above, neurexin promoter usage and alternative splicing at site 4 control its extracellular interactions. In our test, when expressed in COS cells, all α-neurexins (1, 2, and 3 with or without an insert at splice site 4) bound calsyntenin-3-Fc, whereas none of the six β-

neurexin variants tested bound calsyntenin-3-Fc (Figure 2.3A). Here the pseudo neurexin-2β' and 3β' contain the LNS domain from neurexin 2 and 3, respectively, fused to neurexin-1β-flanking sequences. Quantification of neurexin-1 binding showed that only neurexin-1α, but not neurexin-1β, mediated significant calsyntenin-3 binding compared with non-transfected cells; the presence or absence of an insert at splice site 4 in neurexin-1α had no effect on its apparent affinity with calsyntenin-3-Fc (Figure 2.3B). I also conducted the reciprocal experiment to validate the extent of binding. Calsyntenin-3 expressed on COS cells mediated binding of neurexin-1α ectodomain fused to AP (neurexin-1α-AP), but not of neurexin-1β-AP, further confirming the interaction (Figure 2.3C), while expressed neuroligin-2 could bind to both, as expected.

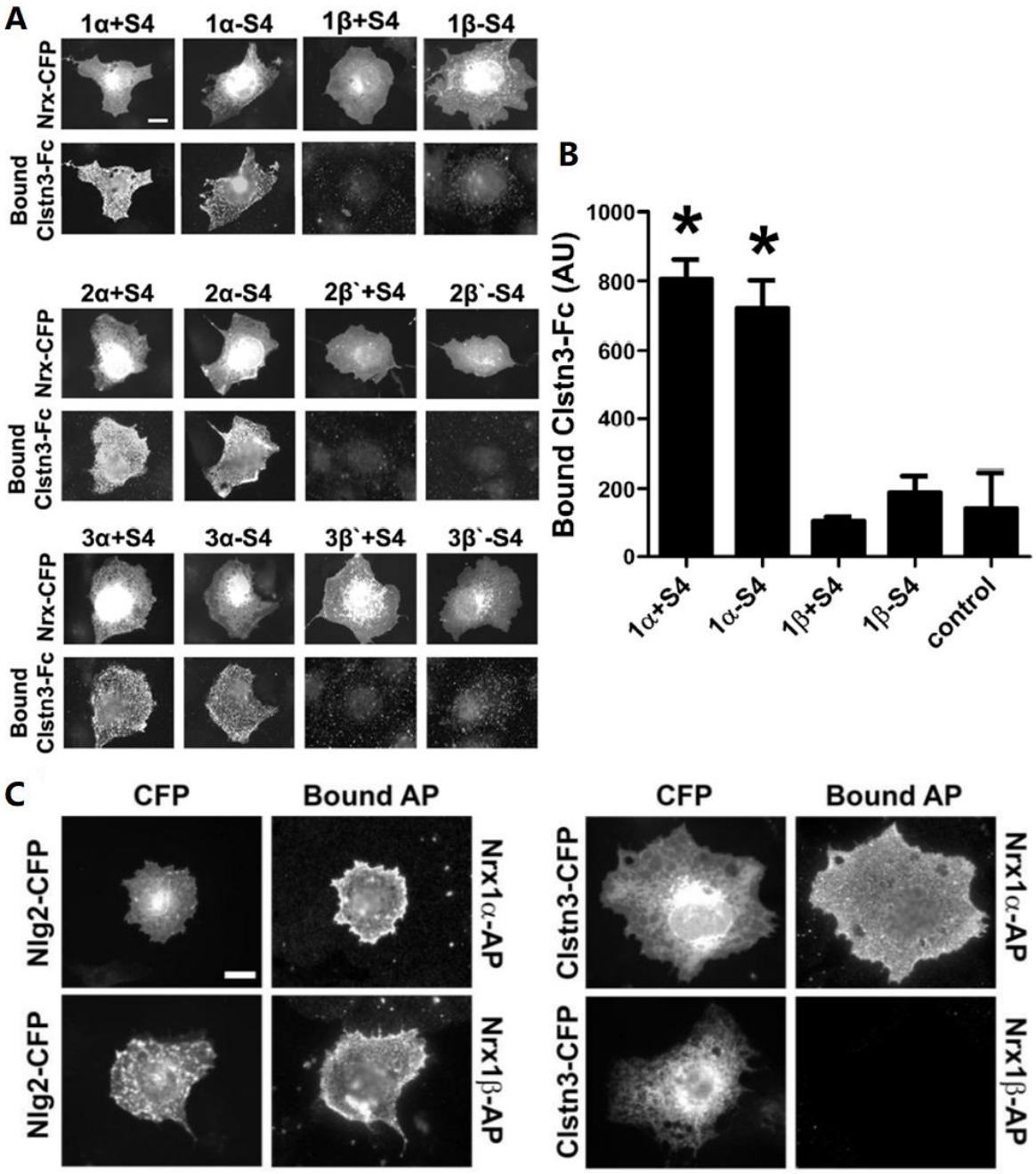

Figure 2.3 Calsyntenin-3 ectodomain binds to all α-Neurexins tested but not β-Neurexins

A. Clstn3-Fc bound to COS cells expressing all α-neurexin isoforms tested, α-neurexins 1, 2, and 3 containing (+S4) or lacking (−S4) the insert at splice site 4. Clstn3-Fc did not bind to COS cells expressing any β-neurexin isoform tested; 2β' and 3β' contained the LNS domain from neurexin 2 and 3, respectively, fused to neurexin-1β-flanking sequences. Scale bar = 20μm.

B. Quantification of Clstn3-Fc bound to COS cells expressing neurexin-1α or neurexin-1β containing (+S4) or lacking (−S4) the insert at splice site 4. ANOVA $p < 0.0001$ ($n \geqslant 20$ cells each); $*p < 0.001$ compared with negative control N-cadherin-CFP by post hoc Bonferroni multiple comparison test.

C. Both α- and β-neurexin fusion proteins Nrx1α-AP and Nrx1β-AP bound to COS cells expressing neuroligin-2 (Nlg2-CFP). But only Nrx1α-AP bound to cells expressing calsyntenin-3 (Clstn3-CFP).

2.4.2 Calsyntenin-3 is largely cleaved *in vitro* and *in vivo*

As discussed in the introduction, in a manner similar to amyloid β-precursor protein, calsyntenin-3 is subject to primary membrane-proximal proteolytic cleavage resulting in ectodomain shedding followed by secondary intramembranous cleavage by a presenilin-dependent γ-secretase (Araki et al., 2004; Hata et al., 2009a).

To determine whether the full-length and/or cleaved ectodomain forms of calsyntenin-3 are present in brain, we generated an antibody that detects an extracellular epitope present in calsyntenin-3, but not in calsyntenin-1 or -2 (Figure 2.4A). In mouse brain homogenate, this antibody detected both the full-length (~130kDa) and the large cleaved extracellular fragment (~115kDa) of calsyntenin-3 in roughly equal amounts (Figure 2.4A), indicating that about 50% of the calsyntenin-3 in the brain is in cleaved form. The percentage of calsyntenin-3 in cleaved form may actually be even higher because some of the cleavage products may end up in the cerebrospinal fluid (Hata et al.; Vogt et al., 2001). Since the studies on synaptic organizing proteins have been largely conducted in primary neuron cultures, I also evaluated the cleavage level of endogenous calsyntenin-3 in primary cortical neurons. Unlike in the mouse brain, the cleaved form accounted for more than 90% of all calsyntenin-3 in culture (Figure 2.4B).

After testing over 20 protease inhibitors and combinations, I finally found 10μM GM6001 was able to reduce the cleaved calsyntenin-3 in media by 70% (Figure 2.4C). GM6001

is a broad spectrum MMP inhibitor which could increase the survival of mice in a melanoma metastasis model, presumably by inhibiting cell invasion or tumor growth (Galardy et al., 1994). But unfortunately, this inhibitor also affects the cleavage of neuroligin-1 and some other synaptic proteins (Cirillo et al., 2016; Iwakura et al., 2017; Lemmens et al., 2016), and thus is not a useful tool to study specific effects of calsyntenin-3 cleavage.

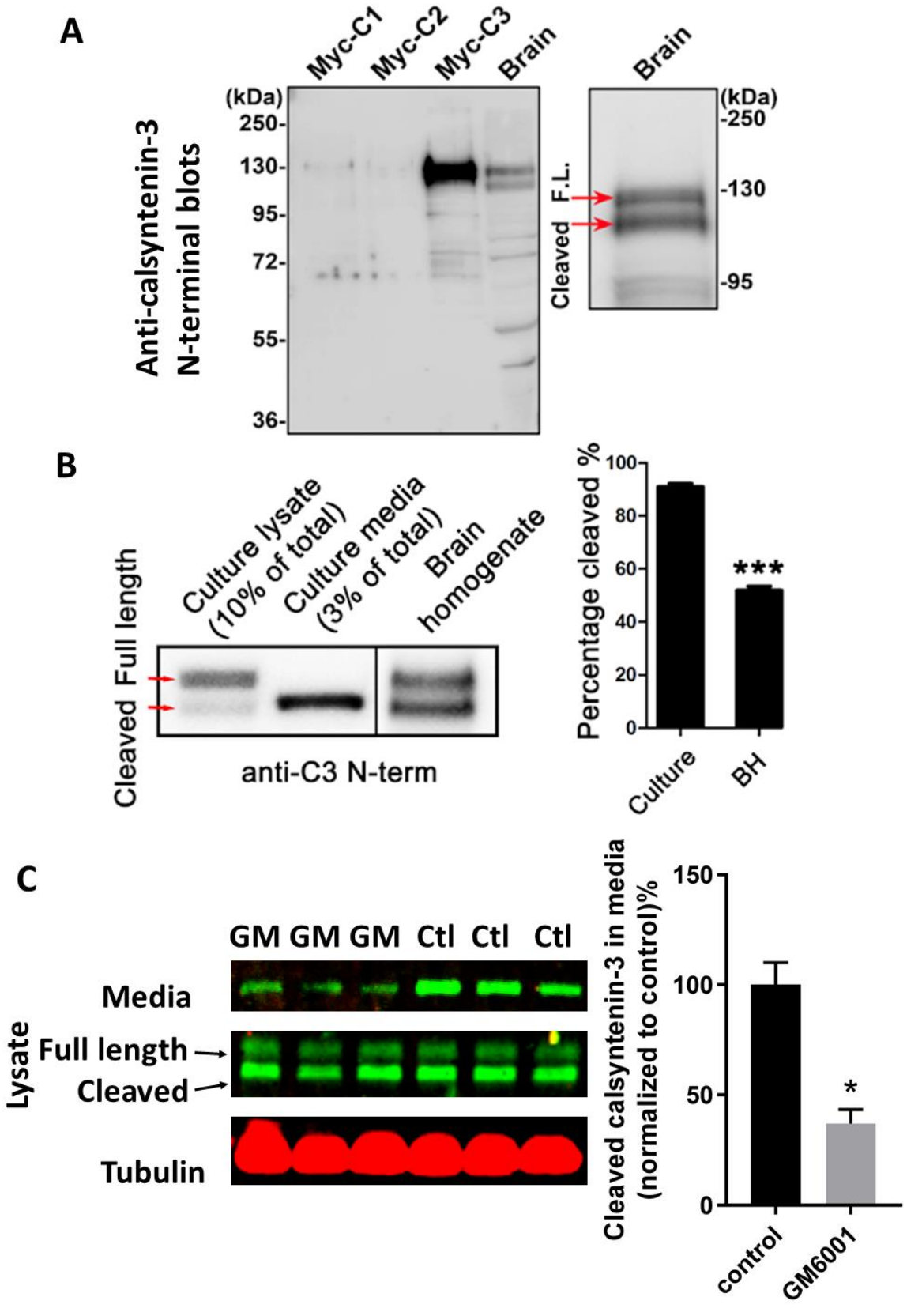
A
Myc-C1
Myc-C2
Myc-C3
Brain
Brain
(kDa)
250-
130-
95-
72-
55-
36-
Anti-calsyntenin-3
N-terminal blots
Cleaved F.L.
(kDa)
-250
-130
-95
B
Culture lysate
(10% of total)
Culture media
(3% of total)
Brain
homogenate
Cleaved Full length
anti-C3 N-term
Percentage cleaved %
100
80
60
40
20
0
***
Culture
BH
C
GM GM GM Ctl Ctl Ctl
Media
Lysate
Full length
Cleaved
Tubulin
Cleaved calsyntenin-3 in media
(normalized to control)%
150
100
50
0
*
control
GM6001

Figure 2.4 Calsyntenin-3 is largely cleaved *in vitro* and *in vivo*

A. An antibody raised against an N-terminal region of calsyntenin-3 recognizes Myc-calsyntenin-3 (Myc-C3) and shows little or no signal for Myc-calsyntenin-1 or Myc-calsyntenin-2 (Myc-C1, Myc-C2) expressed in COS cells. In mouse brain homogenate, the two major bands corresponded to full-length calsyntenin-3 and the cleaved extracellular fragment. The COS cell lysate analyzed here mainly contained full-length calsyntenin-3; the cleaved extracellular fragment was found mainly in COS cell media.
B. Western blot and quantification of percentage of endogenous calsyntenin-3 present in cleaved form in cortical culture at 14 DIV and in adult brain homogenate. Percentage cleaved was calculated as described. Student t test, *** $p < 0.001$, $n = 3$ experiments.
C. Western blots showing endogenous calsyntenin-3 in cortical culture media and lysate with or without GM6001 treatment. GM6001 reduced cleaved calsyntenin-3 protein in cortical culture media. GM, GM6001; Ctl, control. Student's t test, *$p=0.014$, $n=3$.

2.4.3 Released calsyntenin-3 ectodomain inhibits the synaptogenic activity of multiple α-neurexin partners

Considering the unusually large abundance of cleaved calsyntenin-3, I hypothesized that this form has a dominant-negative function by competing with the full-length form of calsyntenin-3. The cleaved form could bind to α-neurexins and occupy the interaction sites, so α-neurexins could not bind full-length calsyntenin-3 or other ligands. Conversely, it could induce the endocytosis of α-neurexins and reduce their surface availability, which in turn limits the presynaptic induction activity of other α-neurexin partners.

To test this hypothesis, I co-expressed the secreted form of calsyntenin-3 (Myc-C3secreted), or the presumably inert secreted protein alkaline phosphatase (AP) as a control, in the COS cells on co-culture assays with different synaptogenic molecules. Here I used a calsyntenin-3ΔPCS form rather than wild-type to achieve a lower cleavage level and higher

surface expression level, as described in (Pettem et al., 2013). In this form, 20 amino acids were deleted around the primary cleavage site of wild-type calsyntenin-3. Indeed, presynaptic induction by calsyntenin-3ΔPCS, neuroligin-2, or LRRTM2 which all act through binding neurexins (α-neurexins in part) (Boucard et al., 2005; Siddiqui et al., 2010), but not by Slitrk2 which acts through PTPσ (Yim et al., 2013), was significantly attenuated by presenting Myc-C3secreted compared with AP in the control (Figure 2.5). This demonstrated that the released calsyntenin-3 ectodomain inhibits the presynaptic-inducing activity of full-length calsyntenin-3 and other α-neurexin partners such as neuroligins and LRRTMs.

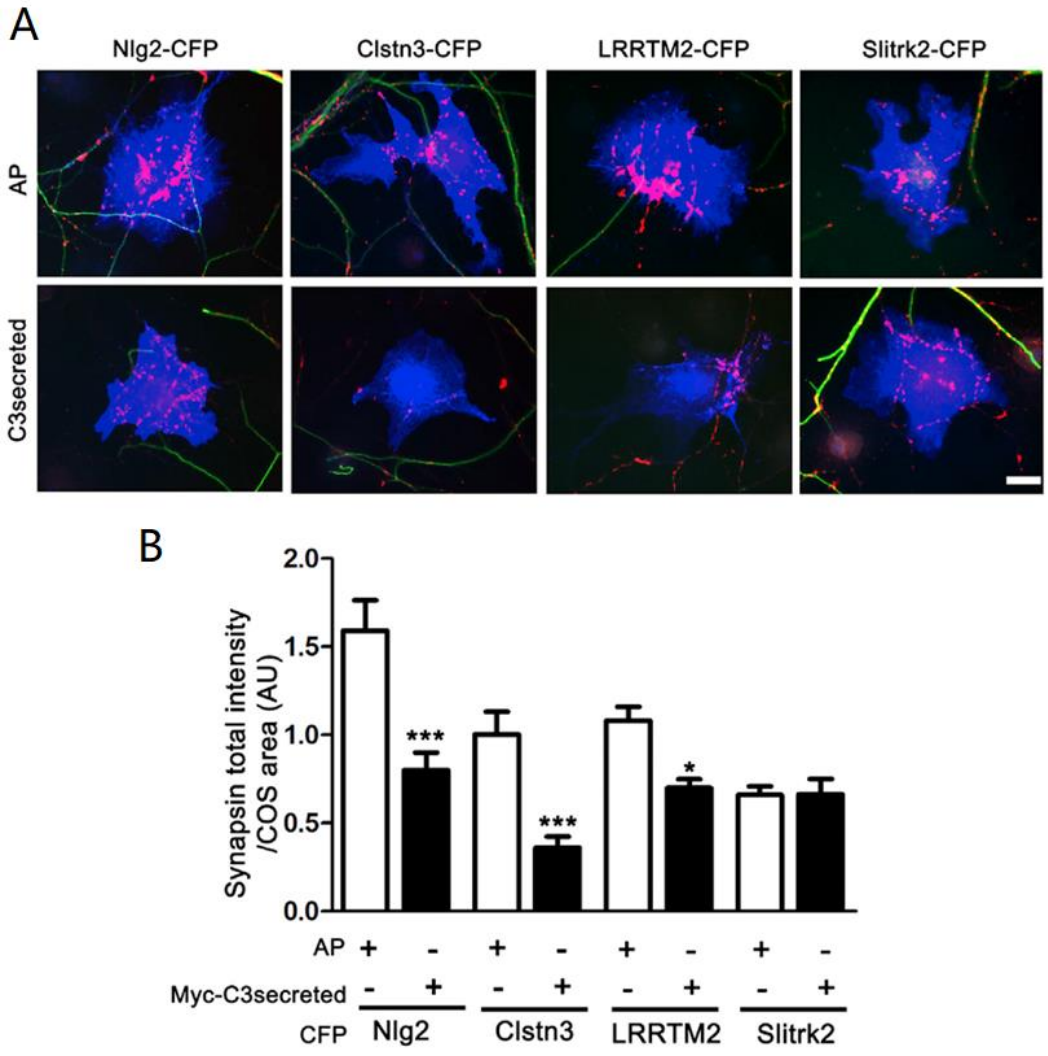

Figure 2.5 Released calsyntenin-3 ectodomain inhibits the synaptogenic activity of multiple α-neurexin partners

A. Representative co-culture images showing suppression of synaptogenic activity of CFP-tagged α-neurexin partners neuroligin-2 (Nlg2), calsyntenin-3 (Clstn3), and LRRTM2 by co-expression of Myc-C3secreted mimicking the shed calsyntenin-3 ectodomain compared with co-expression of AP in the control. Myc-C3secreted had no effect on the activity of Slitrk2 which acts via a non-neurexin presynaptic partner. Co-cultures were immunolabeled for synapsin (red) and MAP2 (green). Scale bar = 20μm.

B. Quantification of synaptogenic activity suppression of α-neurexin partners by Myc-C3secreted. Clusters of synapsin associated with CFP-positive COS cells and lacking MAP2 were measured. ANOVA, $p < 0.0001$ ($n = > 30$ cells each); $***p < 0.001$ and $*p < 0.05$ compared with AP control by post hoc Bonferroni multiple comparison test.

2.4.4 Cadherin and LNS domains of calsyntenin-3 are necessary for α-neurexin binding and synaptogenic activity

I next tested tagged calsyntenin-1 and calsyntenin-2 for α-neurexin binding. Consistent with the lack of co-culture activity, these calsyntenin family members could not mediate binding of neurexin-1α-AP (Figure 2.6). However, Myc-calsyntenin-1-CFP and Myc-calsyntenin-2-CFP showed poor surface trafficking compared with Myc-calsyntenin-3-CFP (Figure 2.6C). Therefore, variants with better surface expression were generated. Myc-C1EX-CD8-CFP and Myc-C2EX-CD8-CFP containing the extracellular domains up to the primary cleavage sites trafficked well to the COS cell surface, yet they could not mediate binding of neurexin-1α-AP or presynaptic induction in co-culture, unlike the homologous Myc-C3EX-CD8-CFP (Figure 2.6). Thus, among the three calsyntenins, calsyntenin-3 may be unique in its ability to bind α-neurexin and induce presynaptic differentiation.

To further unveil the mechanism of calsyntenin-3-neurexin interactions, we generated another series of deletion/mutation constructs to map the domains of calsyntenin-3 important for neurexin binding and presynaptic inducing activity (Figure 2.6A). Myc-calsyntenin-3-CFP and mutants were evaluated for their binding of neurexin-1α-AP and their synaptogenic activity in the co-culture assay (Figure 2.6B). Deleting the cadherin domains (Myc-C3ΔCAD-CFP) abolished both neurexin binding and synaptogenic activity, indicating that the cadherin domains are essential. However, the cadherin domains alone (Myc-C3CADonly-CFP) expressed on the COS cell surface were unable to bind neurexin-1α-AP or induce presynaptic differentiation in co-culture. On the other hand, deleting the LNS domain abolished both neurexin binding and synaptogenic activity. All mutants tested reached the COS cell surface with efficiencies similar to or better than Myc-calsyntenin-3-CFP (Figure 2.6C); thus, deficits of these mutants in neurexin binding and synaptogenic activity were not due to trafficking alterations. I further evaluated a point mutation in the LNS domain Q441→K mimicking the mutation E→K in the *C. elegans* single calsyntenin ortholog *CASY-1*, which results in defects in learning (Ikeda et al., 2008). This LNS point mutation significantly reduced but did not abolish both α-neurexin binding and synaptogenic activity.

The above results indicate that the cadherin and LNS domains of calsyntenin-3 are essential for α-neurexin binding and its synaptogenic activity. Altogether, the correlation of multiple constructs between α-neurexin binding and co-culture activity (Figure 2.6) supports the idea that α-neurexin mediates the presynaptic inducing activity of calsyntenin-3.

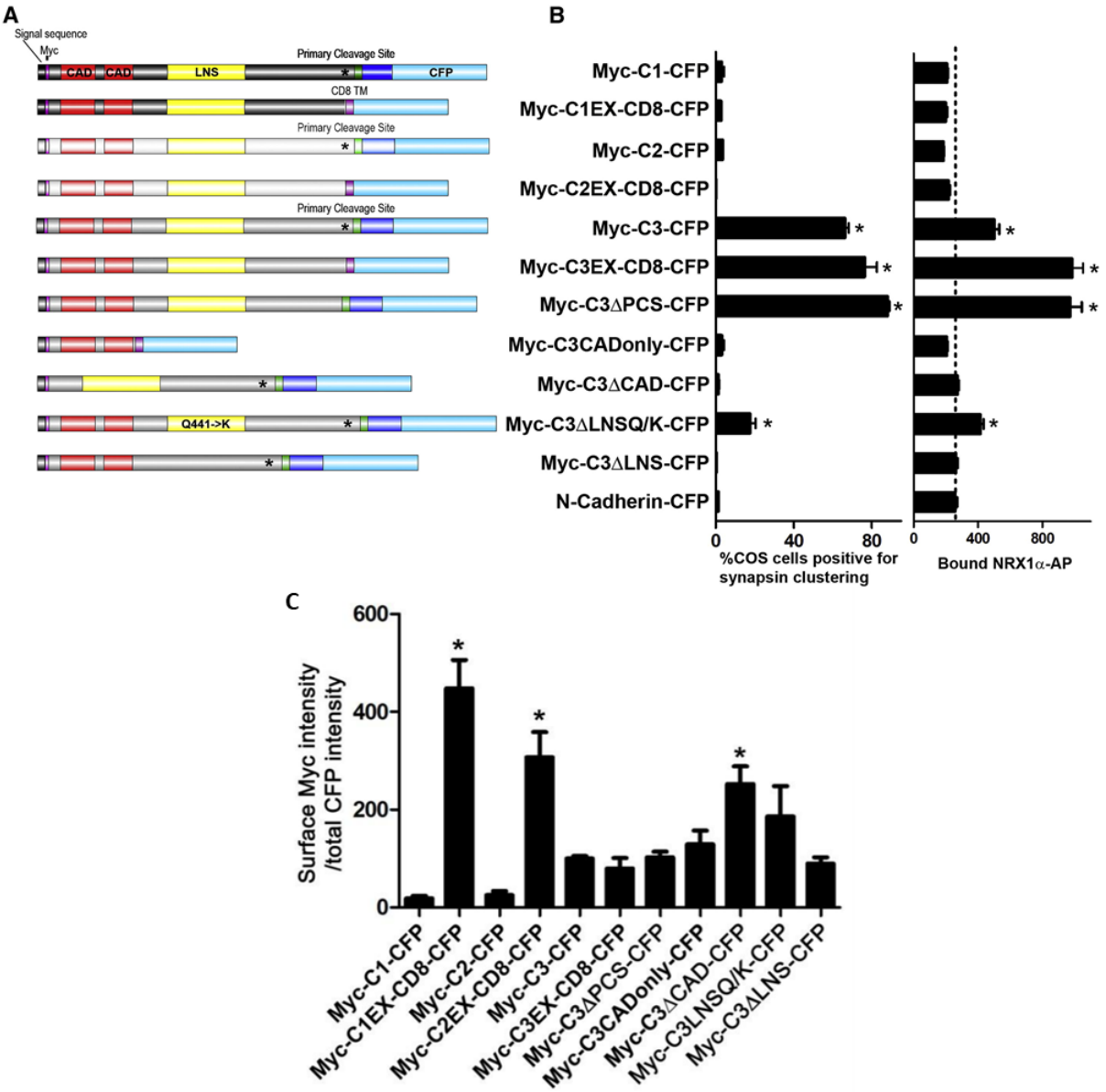

Figure 2.6 The Cadherin and LNS domains are required for calsyntenin-3 synaptogenic activity and α-neurexin binding

A. Domain structure of calsyntenin variants. The darker and lighter shading for calsyntenin-1 (C1) and calsyntenin-2 (C2) represents different but similar amino acid sequences as compared with calsyntenin-3 (C3).

B. Quantification of the percentages of COS cells expressing the indicated constructs that induced clustering of synapsin lacking MAP2 in the co-culture assay (left) and binding of neurexin-1α-AP to the indicated constructs expressed in COS cells (right). ANOVA, $p < 0.0001$ ($n = > 30$ cells each). $*p < 0.01$ compared with negative control N-cadherin-CFP by post hoc Bonferroni multiple comparison test. Data are presented as mean ± SEM.

C. Surface expression of calsyntenin constructs in COS cells. Only Myc-C1-CFP and Myc-C2-CFP showed poorer surface expression than Myc-C3-CFP, all other constructs trafficked to the cell surface at least as well as Myc-C3-CFP. ANOVA, $p < 0.0001$, $n \geqslant 10$ cells each; $*p < 0.001$ compared with Myc-C3-CFP by post-hoc Bonferroni test. Scale bar, 10 μm. Data are presented as mean ± SEM.

2.4.5 Calsyntenin-3 binds to LNS5-EGFc-LNS6 region of α-Neurexins

The domains of neurexin-1α mediating its interaction with calsyntenin-3 were identified in cell-based binding assays (Figure 2.7). The capabilities of a panel of neurexin-1α (n1α) mutants lacking various domains to bind soluble calsyntenin-3-Fc were evaluated in a cell based binding assay. Calsyntenin-3-Fc bound cells expressing n1α_L1L6, n1α_L3L6, and n1α_L5L6 in similar levels, indicating that LNS5, LNS6, and the intervening EGFc domains together are sufficient for the interaction. However, LNS6 alone was not sufficient as indicated by the lack of detectable calsyntenin-3 binding to neurexin-1β. Furthermore, the neurexin-1α mutation D1176A, which abolishes the Ca^{2+}-binding site in the LNS6 domain and prevents cell surface-expressed neurexin-1α from recruiting neuroligin-2 on the surface of dendrites in neuronal co-culture assays (Kang et al., 2008), had no effect on the interaction between calsyntenin-3-Fc and neurexin-1α, substantiating that calsyntenin-3 utilizes a different mechanism to bind neurexin-1α than neuroligin-2.

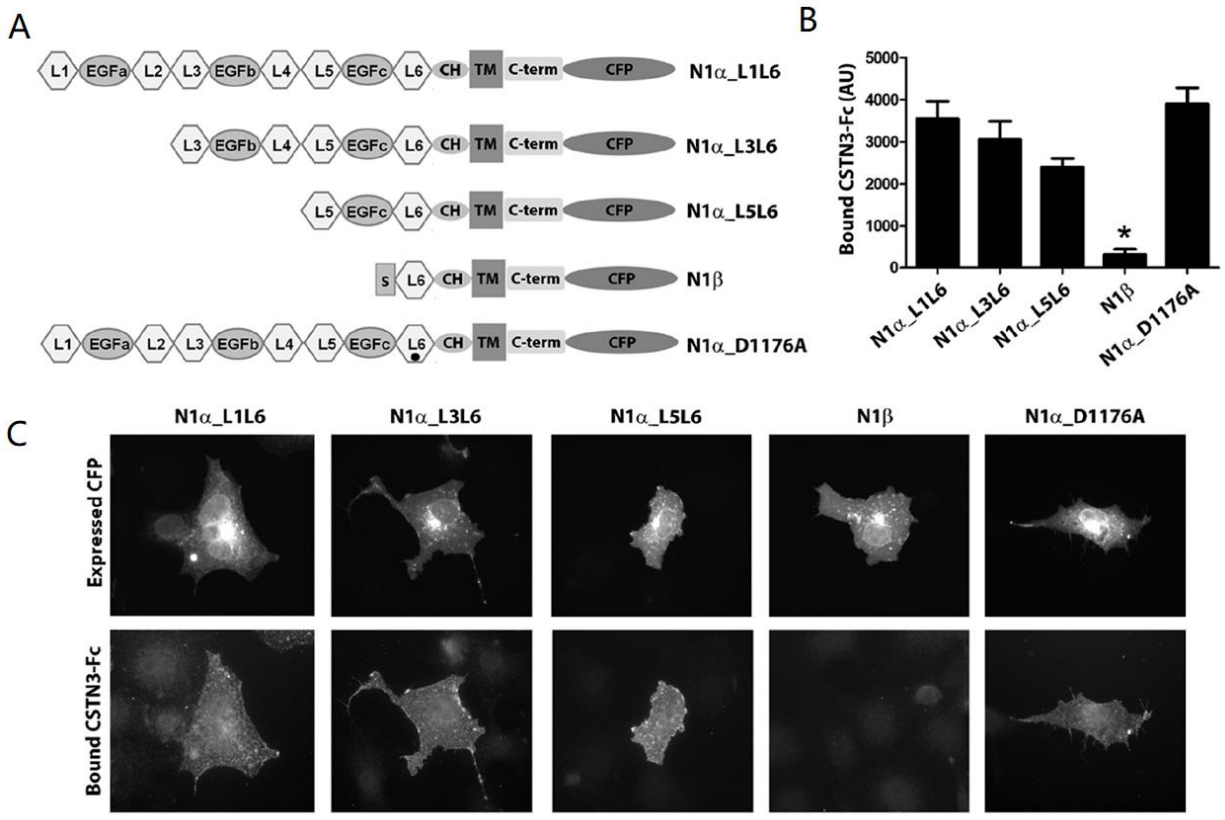

Figure 2.7 Interaction of Calsyntenin-3 with neurexin-1α variants

A. Domain structures of the n1α_L1L6 vector and mutants used in this study (N1α_L1L6, neurexin-1α LNS1-LNS6, the full-length of wild-type neurexin-1α; CH, glycosylated region; TM, transmembrane domain; C-term, intracellular domain; CFP, C-terminal CFP tag).

B. Quantification of soluble Cstn3-Fc bound to COS cells expressing the indicated neurexin constructs on the cell surface (ANOVA, $p < 0.0001$ ($n > 20$ cells each); *, $p < 0.001$ compared with n1α L1L6 by post hoc Bonferroni multiple comparison test).

C. Representative images of Cstn3-Fc bound to COS cells expressing n1α_L1L6, n1α_L3L6, n1α_L5L6, and n1α_D1176A but not n1β in cell-based binding assays.

2.4.6 Calsyntenin-3 forms multimers

Neuroligins form dimers. This dimerization is essential for neuroligin-neurexin interaction and synapse induction (Araç et al., 2007; Levinson and El-Husseini, 2007; Shipman and Nicoll, 2012). In zebrafish, calsyntenins were shown to mediate homophilic adhesion in beads aggregations assays through their amino-terminal cadherin repeats (Ortiz-Medina et al., 2015). Here I investigated whether calsyntenin-3 multimerizes with itself or other calsyntenin family members in a cellular environment. HA-tagged calsyntenin-3 was co-expressed in HEK cells with CFP-tagged calsyntenin-1, 2, 3, or the unrelated N-cadherin. HA-calsyntenin-3 was then pulled down and probed if a CFP-tagged partner co-immunoprecipitated. Results showed that HA-calsyntenin-3 co-immunoprecipitated calsyntenin-3-CFP, suggesting that calsyntenin-3 forms multimers with itself, a specific association, as indicated by lack of co-precipitation of calsyntenin-1-CFP or N-cadherin-CFP (Figure 2.8A).

To visualize the multimers, we collaborated with Dr. Gabby Rudenko's lab and generated negative-stain EM images. Indeed, we found both low molecular weight monomers (Cstn-LMW) and high molecular weight multimers (Cstn-HMW) (Figure 2.8B and C, respectively). The multimers contained an internal 4-fold axis, suggestive of a tetramer, based on self-rotation and cross-correlation analysis of electron tomographic density maps from two independent particles. The four monomers in the calsyntenin-3 tetramer are related by a 90° rotation around a common 4-fold axis as opposed to a dimer of dimers (Lu et al., 2014). Both monomers and tetramers could bind neurexin-1α at physiological affinities (Figure 2.8D).

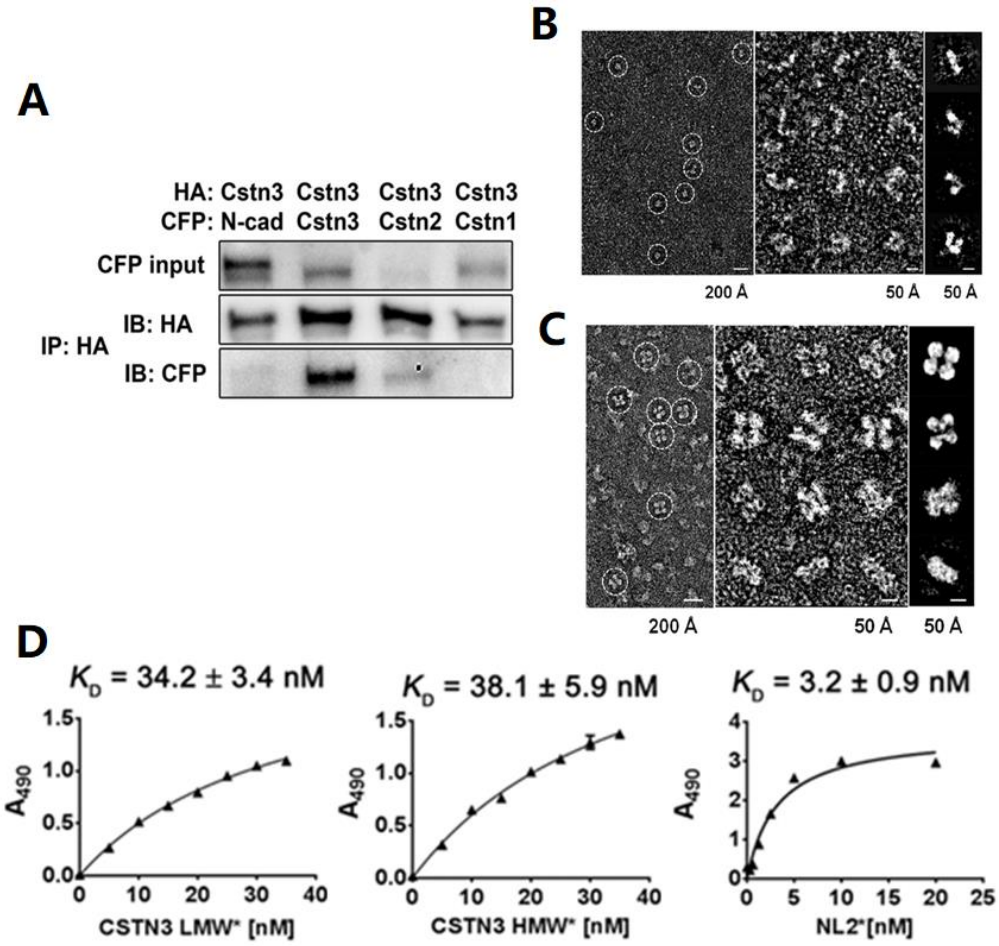

Figure 2.8 Calsyntenin-3 forms multimers

A. Cstn3 forms multimers in cell-based assays. HEK cells were co-transfected with HA-Cstn3 as well as N-cadherin-CFP, Cstn3-CFP, Cstn2-CFP, or Cstn1-CFP. Cell lysates were immunoprecipitated with anti-HA antibody and analyzed by Western blot (IB) compared with input (10% of immunoprecipitate (IP)). The relative signal intensity of co-immunoprecipitated proteins, normalized to precipitated HA-Cstn3 and input CFP signals, was 0.036 ± 0.016 for N-cadherin-CFP and 0.090 ± 0.044 for Cstn1-CFP relative to 1 for Cstn3-CFP (analysis of variance, $p < 0.0001$, and $p < 0.001$ comparing Cstn3 with Cstn1 or with N-cadherin in Bonferroni post hoc test, $n = 4$). The expression and co-immunoprecipitation data for Cstn2-CFP were highly variable.

B. Cstn3-LMW negative-stain EM images and three-dimensional reconstructions. Left, survey view of Cstn3 monomers (dashed circles). Middle, 12 representative raw images of Cstn3 monomers. Right, four representative reference-free class averages.

C. Cstn3-HMW negative stain EM images and three-dimensional reconstruction. Left, survey view of Cstn3 tetramers (dashed circles). Middle, 12 representative raw images of Cstn3 tetramers. Right, four representative reference-free class averages.

D. Increasing concentrations of biotinylated Cstn3-LMW (monomer), Cstn3-HMW (tetramer), and NL2 were incubated with immobilized neurexin1α and specific binding was shown.

2.4.7 HS modification is required for presynaptic differentiation by Calsyntenin-3

Recently, colleagues in our lab identified neurexins as HSPGs, and the HS modification is not just essential for the high affinity interaction of neurexins with neuroligins and LRRTMs, but also required for the presynaptic differentiation by these postsynaptic ligands (Zhang et al., 2018). Thus it was natural for us to wonder whether calsyntenin-3, as a postsynaptic neurexin ligand similar to neuroligins and LRRTMs, interacts with α-neurexins in a similar manner. Thus, we first investigated whether HS is required for calsyntenin-3 to induce presynaptic differentiation. Expression of calsyntenin-3 on COS7 cells followed by co-culture with neurons triggers local bassoon aggregation on the axon surface at points of COS7 cell contact, whereas acute removal of HS chains by adding a cocktail of heparinase 1, 2, and 3 during co-culture abolished the ability of calsyntenin-3 to induce presynaptic differentiation (Figure 2.9). On the other hand, the presynaptic induction activity of a non-neurexin binding partner NGL-3 was not affected by heparinase treatment.

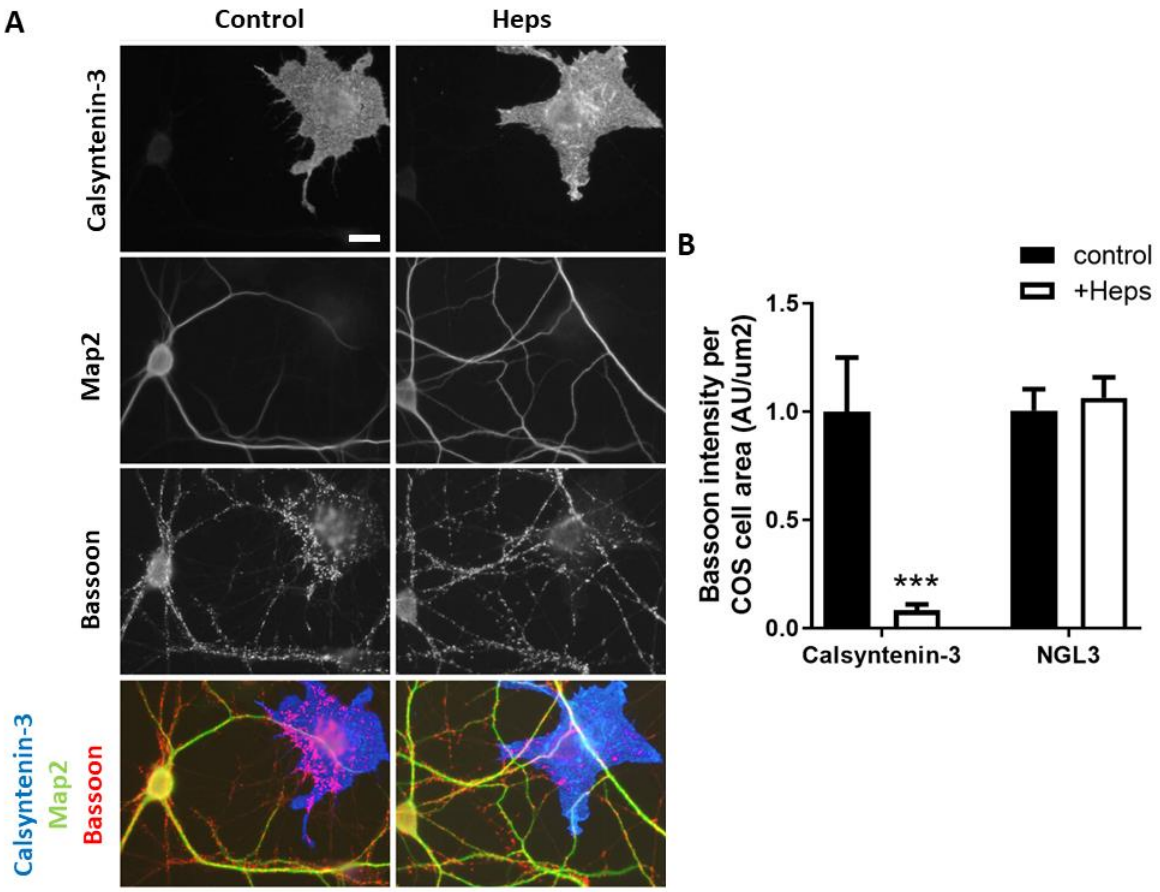

Figure 2.9 HS modification is required for presynaptic differentiation by calsyntenin-3

A. Heparinase (Heps) reduced clustering of presynaptic marker bassoon in contacting axons induced by calsyntenin-3 on COS7 cells. Heparinase was added after axon outgrowth only during the co-culture period. Scale bar = 10µm.

B. Quantification of co-culture experiment with or without heparinase treatment. Measures are integrated intensity of bassoon puncta, lacking microtubule associated protein 2 (MAP2) dendrite contact to exclude native synapses, per transfected COS7 cell contact area. Two way ANOVA, $p < 0.01$ for all protein identity, treatment and interaction effect. ***$P < 0.001$ by Bonferroni's post hoc multiple comparisons test comparing calsyntenin-3 heparinase treatment with control and $p>0.05$ comparing NGL3 heparinase treatment with control (n = 28-33).

2.4.8 HS modification of neurexin-2α regulates its binding to ectodomain of calsyntenin-3

To investigate whether this reduction by heparianse of the ability of calsyntenin-3 to induce presynaptic differentiation in contacting axons is due to its interaction with HS chains on α-neurexins, I did a cell surface binding assay with recombinant calsyntenin-3 ectodomain, similar to the experiment in Figure 2.1. But this time I chose to use DIV5 primary neuron culture instead of COS7 cells because the post-translational modifications on neurexin, expecially HS modification, might be different between neurons and non-neuronal fibroblast cells. Moreover, I generated a monomeric form of Myc-His-Clstn3ecto recombinant protein to avoid the possible dimerization of FC fusion proteins, given that we don't know yet whether multimerization of calsyntenin-3 have any effect on its interaction with neurexins.

Neurexin-2α instead of -1α was used in this assay to achieve a higher surface expression level (data not shown). To test the function of HS modification, we introduced a serine to alanine (SA) mutation on the CHO region of neurexin-2α, homologous with the reported SA mutation on neurexin-1β (Zhang et al., 2018). This mutation was shown to be free of HS modification in cultured neurons using western blot with 3G10 anti-HS stub antibody (Zhang et al., 2018). YFP-2A-V5-neurexin-2α and its SA mutant nucleofected into DIV0 neurons showed similar surface V5 levels on DIV5 (data not shown). Myc-His-Clstn3ecto bound strongly to YFP-2A-V5-neurexin-2α and relatively weakly to its SA mutant, while there is no above background binding to negative control V5-CD4 (Figure 2.10). I tried to fit the binding curves with a specific binding model but the binding between calsyntenin-3 with wild-type neurexin-2α never reached satuation with the concentrations tested.

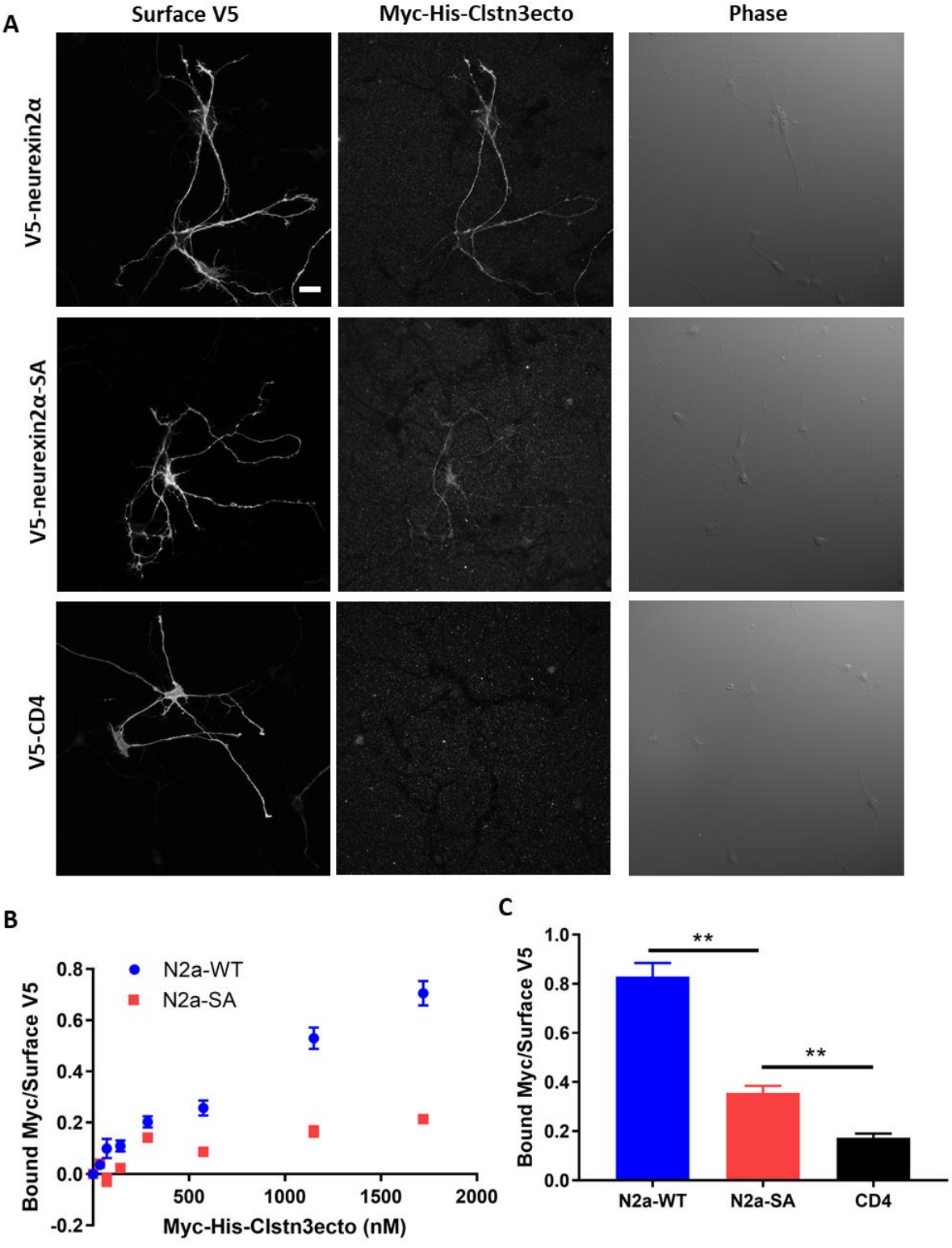
A
Surface V5
Myc-His-Clstn3ecto
Phase
V5-neurexin2α
V5-neurexin2α-SA
V5-CD4
B
N2a-WT
N2a-SA
Bound Myc/Surface V5
Myc-His-Clstn3ecto (nM)
0.8
0.6
0.4
0.2
0.0
-0.2
500
1000
1500
2000
C
Bound Myc/Surface V5
1.0
0.8
0.6
0.4
0.2
0.0
**
**
N2a-WT
N2a-SA
CD4

Figure 2.10 HS modification of Nrx regulates its binding to ectodomain of Calsyntenin-3

A. Recombinant calsyntenin-3 ectodomain bound more strongly to V5-neurexin-2α compared with V5-neurexin-2α-SA mutation expressed on the surface of neurons at 5 DIV. Surface V5 staining showed in the left column, bound Myc-His-Clstn3ecto in the middle and phase images of the field in the right. Scale bar =10μm.
B. Recombinant calsyntenin-3 ectodomain bound more strongly to V5-neurexin-2α compared with V5-neurexin-2α-SA mutation expressed on the surface of neurons at 5 DIV. Two way ANOVA, $p < 0.0001$ for all concentration, mutation and interaction effect. $P < 0.0001$ comparing N2α-WT with N2α-SA by Bonferroni's post hoc multiple comparisons test for the three highest concentrations.
C. Recombinant calsyntenin-3 ectodomain (1150nM) bound to V5-neurexin-2α-SA mutant compared with non-related V5-CD4 control and bound to V5-neurexin-2α stronger than SA mutant. $P < 0.0001$ by Kruskal-Wallis test and $^{**}p < 0.01$, by Dunn's post hoc multiple comparisons test.

2.4.9 Calsyntenin-3 RA mutants are deficient at inducing presynaptic differentiation compared to WT

Based on the above results and the fact that other neurexin ligands, neuroligins and LRRTMs, could bind HS chains on neurexin (Zhang et al., 2018), we wondered whether calsyntenin-3 could also interact with HS directly.

I searched the amino acid sequence of calsyntenin-3 and looked for regions with basic residues (Arginines and Lysines) close together that might mediate HS binding. I identified three such regions (Figure 2.11) and mutated the Arginines and Lysines to Alanines, resulting with so-called 4KA, 5RA, and 6RA mutations. I expressed these mutations in COS7 cells and co-cultured them with rat hippocampal neurons. The surface expression levels of the mutants were the same as wild-type Myc-Clstn3. While Myc-Clstn3-4KA could induce presynaptic differentiation to the same level as wild-type, the 5RA and 6RA mutants could only induce at

minimum levels compared with negative control Myc-CD4 (Figure 2.12). We propose the 5R and 6R regions as HS binding sites, and speculate that these two sites work cooperatively since mutating either one could diminish the ability of calsyntenin-3 to induce presynaptic differentiation. However, this hypothesis will require further validation, specifically assays of whether calsyntenin-3 directly binds HS and whether the 5RA and 6RA mutations disrupt such binding. Additionally, whether these mutations disrupt the interaction between calsyntenin-3 and the protein core of neurexins is still unknown and also requires further investigation.

Figure 2.11 Proposed mutations in calsyntenin-3

The proposed HS binding regions in calsyntenin-3 are shown, with residues in red blocks mutated to Alanines. (hs, homo sapiens; mm, Mus musculus.)

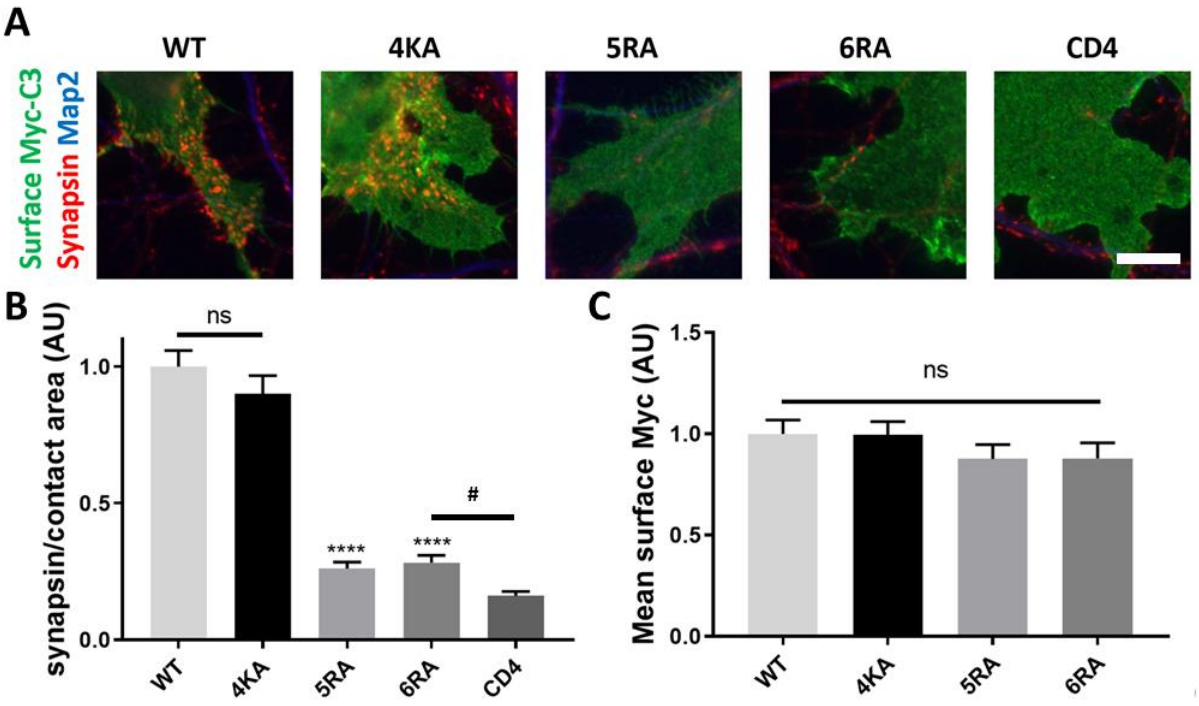

Figure 2.12 Calsyntenin-3 RA mutants are deficient at inducing presynaptic differentiation

A. Calsyntenin-3-5RA and -6RA are deficient at inducing presynaptic differentiation. Clustering of synapsin in contacting axons induced by calsyntenin-3 on COS7 cells was impaired by the 5RA and 6RA mutations.

B. Quantifications of synaptogenic activity of calsyntenin-3 mutants. Measures are integrated intensity of synapsin puncta per transfected COS7 cell-axon contact area lacking dendrite contact. $P < 0.0001$ by Kruskal-Wallis, and ****$p < 0.0001$ by Dunn's post hoc tests comparing calsyntenin-3-5RA and -6RA mutants with WT (n=55-57) from 2 independent experiments, #$p < 0.05$ comparing calsyntenin-3-6RA with negative control CD4.

C. Surface levels of calsyntenin-3 and mutants did not vary in these co-culture assays. $P>0.05$ by Kruskal-Wallis.

2.4.10 Calsyntenin-3 shows differential expression patterns *in vivo*

The markedly different ratios of full-length to cleaved calsyntenin-3 in neuron culture as compared with *in vivo* (Figure 2.4) and the opposing biological effects of the two forms of the

protein (Figure 2.5) highlighted the limitations of culture studies on calsyntenin-3, and prompted us to focus on studying the distribution and function of calsyntenin-3 *in vivo*.

The developmental expression and cleavage profiles of calsyntenin-3 were determined between postnatal days P6 and P60 by western blot analysis with the N-terminal antibody. Only modest nonsignificant changes in levels of calsyntenin-3 or in the ratio of cleaved to full-length forms were observed over this timeframe (Figure 2.13). The percentage of calsyntenin-3 in cleaved form was always in the range of 52% - 60%.

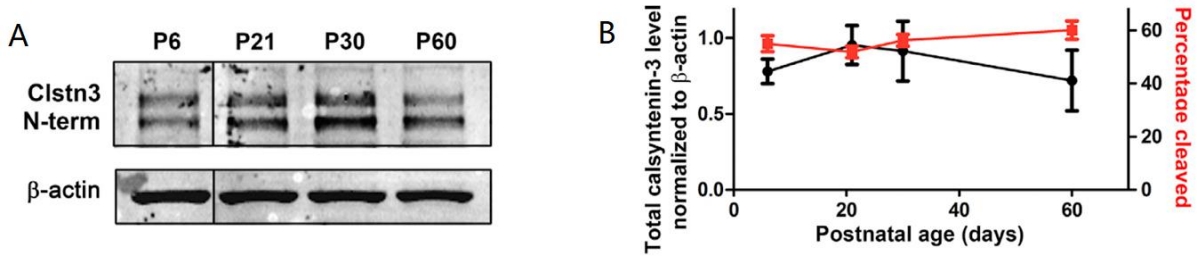

Figure 2.13 Calsyntenin-3 expression level and cleavage level is consistent throughout development

Sample western blot images (A) and quantification (B) of the expression level and fraction of total calsyntenin-3 present as the cleaved form during development. P6, postnatal day 6; P21, postnatal day 21; etc.

By immunofluorescence, calsyntenin-3 was detected widely in the brain including hippocampus and cortex (Figure 2.14) using an antibody raised against a C-terminal peptide that was validated using tissue lacking calsyntenin-3. Consistent with a previous report by Hintsch et al. (Hintsch et al., 2002), calsyntenin-3 was detected most strongly in interneurons identified by their location outside the main cell body layers of the hippocampus, by the absence of calcium-calmodulin-activated protein kinase IIα (CaMKIIα), and by the presence of parvalbumin in a subset of interneurons. Calsyntenin-3 was also detected at lower levels in CA1 and CA3 pyramidal neurons. In the dentate gyrus, scattered hilar neurons and interneurons exhibited high

levels of calsyntenin-3, whereas granule cells showed little or no calsysntenin-3. In neocortex, calsyntenin-3 was again most strongly expressed by interneurons including parvalbumin-positive neurons but also expressed by many pyramidal cells, particularly in layer V (Figure 2.14). Calsyntenin-3 was detected in soma, proximal dendrites, and additional processes. We did not detect clear synaptic puncta of calsyntenin-3, which may be due to limitations of antigen accessibility or antibody sensitivity because electron microscopic analyses detected calsyntenin-3 most prominently in postsynaptic specializations of asymmetric synapses in hippocampus, cortex, and cerebellum (Hintsch et al., 2002).

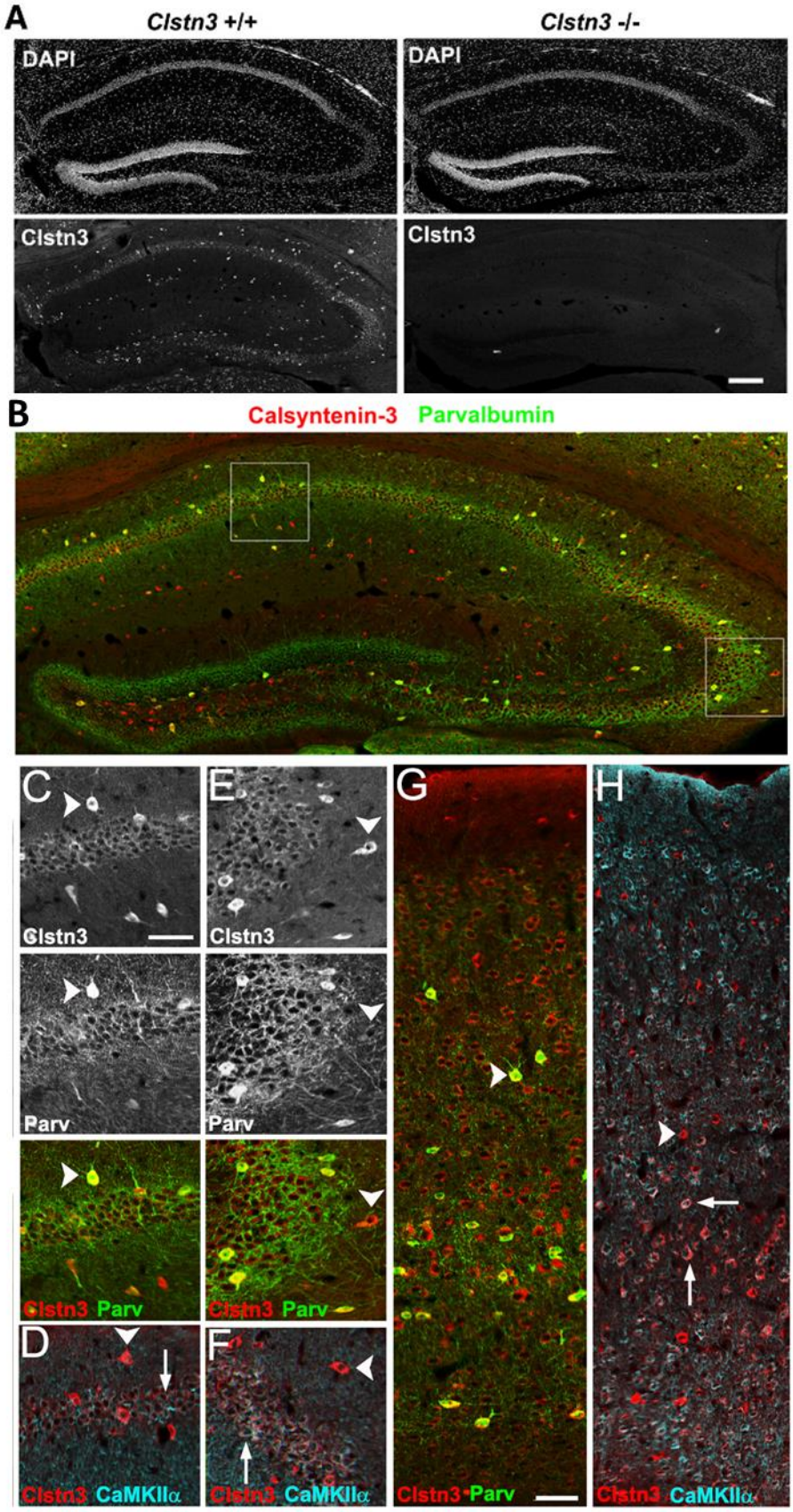
A
Clstn3 +/+
Clstn3 -/-
DAPI
DAPI
Clstn3
Clstn3
B
Calsyntenin-3
Parvalbumin
C
E
G
H
Clstn3
Clstn3
Parv
Parv
Clstn3 Parv
Clstn3 Parv
D
F
Clstn3 CaMKIIα
Clstn3 CaMKIIα
Clstn3 Parv
Clstn3 CaMKIIα

Figure 2.14 Calsyntenin-3 expression is high in interneurons and moderate in pyramidal neurons

A-F. In hippocampus, calsyntenin-3 immunoreactivity was detected most strongly in interneurons, both parvalbumin positive and parvalbumin negative (arrowheads in C and E, respectively). Parvalbumin-negative interneurons were identified by their position outside the pyramidal cell layer and by the absence of immunoreactivity for CaMKIIα (arrowheads in D and F). By comparison with Clstn3−/− tissue (A), wild-type pyramidal neurons (arrows) in CA1 (C and D) and in CA3 (E and F) were also immunopositive for calsyntenin-3, whereas no immunoreactivity was detectable in dentate granule cells.

G-H. In neocortex, calsyntenin-3 was widely expressed, at highest levels by interneurons (arrowheads) including parvalbumin-positive interneurons (G) but also by some pyramidal neurons particularly in layer V (arrows in H). Scale bars, 200 μm (A and B) and 50 μm (C–H).

2.4.11 *Clstn3−/−* mice are deficient in both inhibitory and excitatory synapse development

To determine the function of calsyntenin-3 *in vivo*, we generated *Clstn3−/−* mice (Pettem et al., 2013). Loss of calsyntenin-3 protein was confirmed by loss of calsyntenin-3 immunofluorescence in brain sections and by western blot of brain homogenates. *Clstn3−/−* mice showed no obvious deficit in survival or fertility. The overall brain morphology of *Clstn3−/−* mice was normal, as was the overall organization of the excitatory synapse marker VGlut1 and the inhibitory synapse marker glutamic acid decarboxylase GAD65 (Pettem et al., 2013). The level of α-neurexin was normal in *Clstn3−/−* mouse brain crude synaptosome fractions (Figure 2.15). However, quantitative high-resolution confocal analysis of hippocampal CA1 and dentate gyrus regions revealed significant regional reduction in VGlut1 and global reduction in GAD65 punctate immunofluorescence in mice lacking calsyntenin-3 compared with wild-type littermate controls (Pettem et al., 2013).

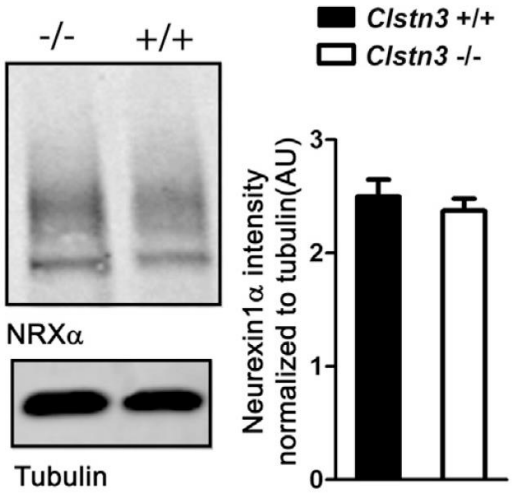

Figure 2.15 Neurexin level is intact in *Clstn3* -/- mice

Western blot and quantification showed that the level of α-neurexin was indistinguishable in crude synaptosome fractions of *Clstn3*−/− and *Clstn3*+/+ littermate mice. Student's t test, $p > 0.05$ ($n = 3$).

To determine whether the reduction in punctate VGlut1 and GAD65 immunofluorescence in CA1 of *Clstn3*−/− mice represents reduction in excitatory and inhibitory synapse density, I assessed asymmetric and symmetric synapse density by transmission electron microscopy (Figure 2.16). Indeed, in mice lacking calsyntenin-3, asymmetric synapse density was significantly reduced in CA1 stratum radiatum and symmetric synapse density was significantly reduced in CA1 stratum pyramidale, compared with wild-type littermate controls (Figure 2.16). Non-significant reductions of >30% were also seen for asymmetric synapses in stratum pyramidale and symmetric synapses in stratum radiatum, regions of low synapse density. Therefore it can be concluded that loss of calsyntenin-3 results in reduction in both excitatory and inhibitory synapse density.

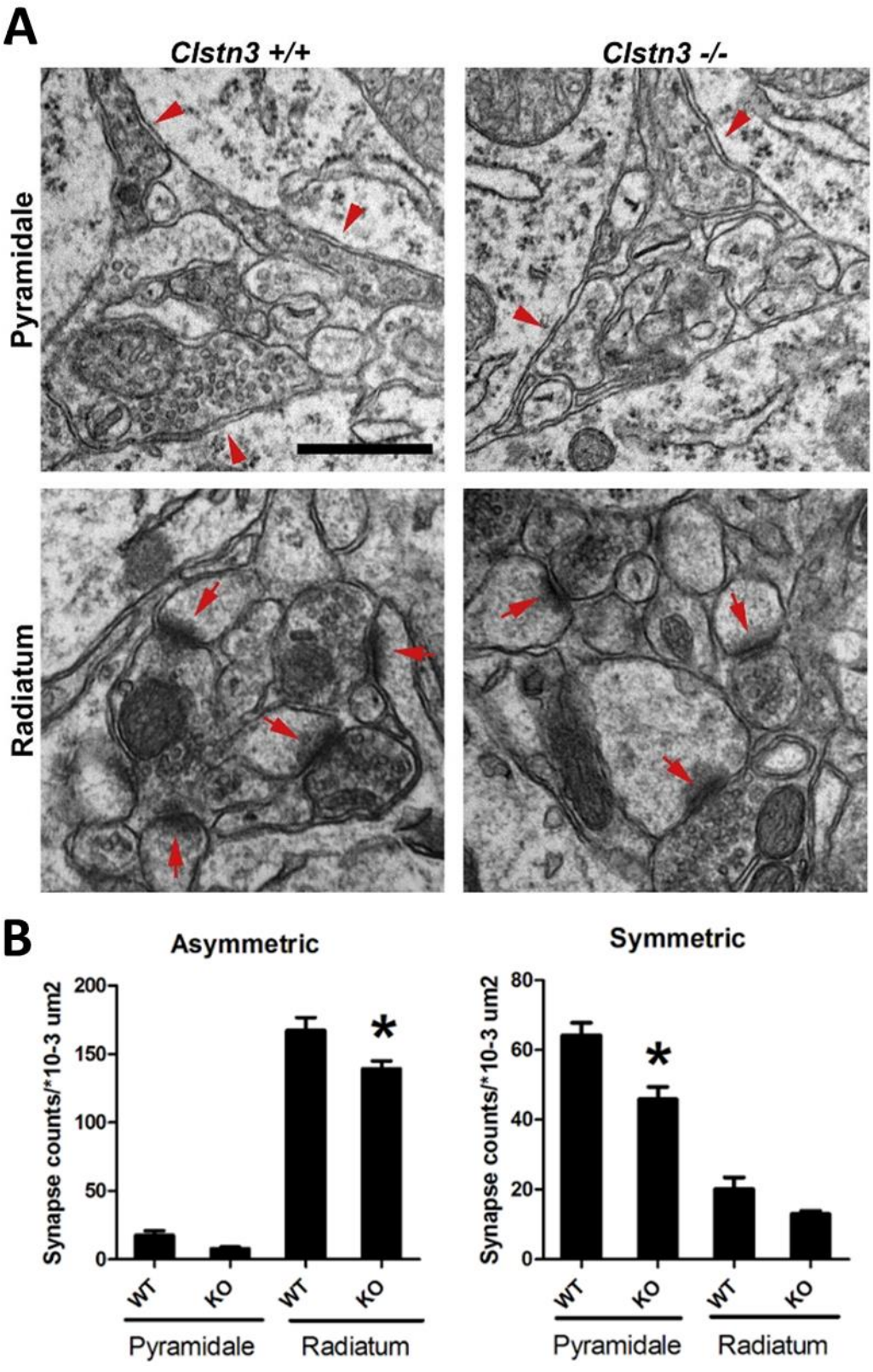
A
Clstn3 +/+
Clstn3 -/-
Pyramidale
Radiatum
B
Asymmetric
Symmetric
Synapse counts/*10-3 um2
200
150
100
50
0
80
60
40
20
0
*
*
WT
KO
WT
KO
Pyramidale
Radiatum
WT
KO
WT
KO
Pyramidale
Radiatum

Figure 2.16 Symmetric and asymmetric synapse density is reduced in *Clstn3 -/-* mice

Sample images (A) and quantification (B) of ultrastructure analysis showed asymmetric (arrows) and symmetric (arrowheads) synapse loss in hippocampal CA1 region of *Clstn3*−/− mice. ANOVA, $p < 0.0001$ ($n = 4$ mice each after averaging data from more than 50 images per mouse per region), age P50–P60; $*p < 0.01$ by post hoc Bonferroni multiple comparison test comparing *Clstn3*+/+ (WT) and *Clstn3*−/− (KO) for each region. Scale bar = 500nm.

We next sought to determine if synaptic transmission is altered in the absence of calsyntenin-3. Whole-cell recording was performed on CA1 pyramidal cells in *Clstn3*−/− and wild-type littermate hippocampal slices to quantify spontaneous miniature inhibitory postsynaptic currents (mIPSCs) and miniature excitatory postsynaptic currents (mEPSCs). Relative to wild-type littermates, mIPSC recordings from *Clstn3*−/− slices revealed a reduction in mIPSC frequency but not amplitude (corresponding to an increased interevent interval, Figure 2.17). Similarly, comparison of mEPSCs between *Clstn3*−/− and wild-type mice revealed reduction in frequency but not amplitude (Figure 2.17). Together, these results indicate that calsyntenin-3 is required for normal development of functional inhibitory and excitatory synapses.

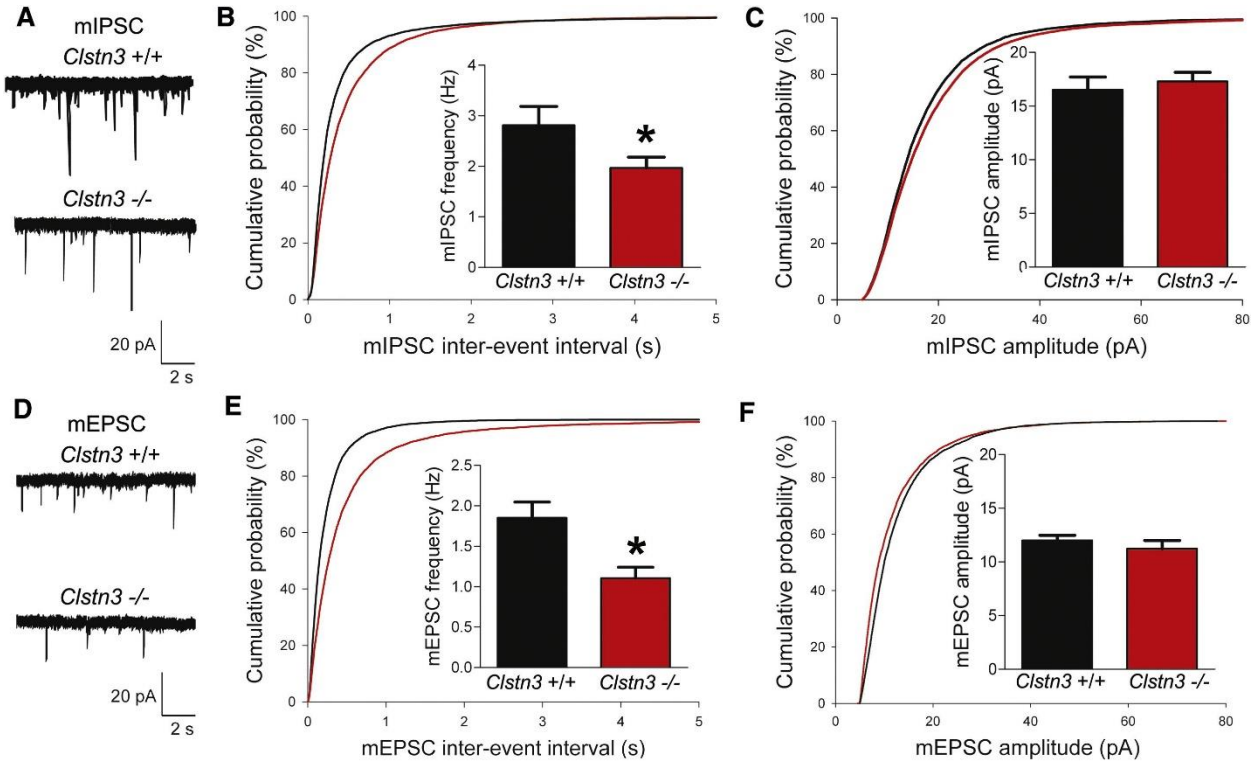

Figure 2.17 Inhibitory and excitatory neurotransmission is compromised in *Clstn3−/−* mice

A. Representative mIPSC recordings from hippocampal CA1 pyramidal neurons in acute slices from *Clstn3*+/+ and *Clstn3*−/− young adult mice.

B-C. Cumulative distributions of mIPSC interevent intervals (B) and amplitudes (C) in *Clstn3*+/+ and *Clstn3*−/− neurons (Kolmogorov-Smirnov test, $p < 0.001$ for interevent intervals). Insets display mean ± SEM for mIPSC frequency (B) and amplitude (C). mIPSC frequency but not amplitude was significantly reduced in *Clstn3*−/− neurons (Student's t test, $*p < 0.05$; n = 11 cells, *Clstn3*+/+; n = 21 cells, *Clstn3*−/−).

D. Representative mEPSC recordings from *Clstn3*+/+ and *Clstn3*−/− hippocampal CA1 pyramidal neurons.

E-F. Cumulative distributions of mEPSC interevent intervals (E) and amplitudes (F) in *Clstn3*+/+ and *Clstn3*−/− neurons (Kolmogorov-Smirnov test, $p < 0.001$ for interevent intervals). Insets display mean ± SEM for mEPSC frequency (E) and amplitude (F). mEPSC frequency but not amplitude was significantly reduced in *Clstn3*−/− neurons (Student's t test, $*p < 0.01$; n = 20 cells, *Clstn3*+/+; n = 22 cells, *Clstn3*−/−).

2.5 Discussion

Previously from an unbiased expression screen, calsyntenin-3 was identified as a synaptogenic protein in our lab (Pettem et al., 2013). Calsyntenin-3, but not the related calsyntenin-1 or calsyntenin-2, can trigger excitatory and inhibitory presynapse differentiation in contacting axons (Pettem et al., 2013). I took over the project from there and further explored the mechanism behind the synaptogenic activity. With cell-based binding assays I showed that calsyntenin-3 specifically binds to α-neurexins and not β-neurexins. Calsyntenin-3 undergoes prominent ectodomain shedding with at least half of calsyntenin-3 in mouse brain present in the cleaved form. Full-length calsytenin-3 is synaptogenic in co-culture. However, the released ectodomain of calsyntenin-3 not only lacks synaptogenic activity but also inhibits the presynaptic-inducing activity of multiple α-neurexin partners. Calsyntenin-3 is highly expressed in interneurons throughout hippocampus and cortex, and is expressed at lower levels in many pyramidal neurons. *Clstn3*$^{-/-}$ mice show reduced density of symmetric and asymmetric synapses, and lower mIPSC and mEPSC frequency in hippocampal CA1 neurons. Together, these data suggest that a α-neurexin-calsyntenin-3 complex is essential for normal inhibitory and excitatory synapse development and function.

2.5.1 Unique binding properties of calsyntenin-3 to neurexins

Unlike the binding specificity of calsyntenin-3 for α-neurexins, other neurexin partners such as neuroligins, LRRTMs, cerebellin-GluRδ, dystroglycan, and latrophilin bind to α- and β-neurexins or just β-neurexins (Boucard et al., 2005, 2012; Matsuda and Yuzaki, 2011; Siddiqui et al., 2010; Sugita et al., 2001; Uemura et al., 2010). Neurexin splice site 4, a key molecular switch that affects neurexin's interaction with many of these partners, did not appear to affect its interaction with calsyntenin-3 (Figure 2.3). In the domain mapping experiment, calsyntenin-3

binds to the LNS5-EGFc-LNS6 region of neurexin-1α, while neuroligins and LRRTMs preferably bind to LNS6 (Südhof, 2017). Although neurexin LNS6 alone is not sufficient for calsyntenin-3 binding, as indicated by the undetectable binding to β-neurexins, I deduce that the calsyntenin-3 binding site on neurexin-1α might be spatially close to LNS6 because calsyntenin-3 ectodomain can suppress the synapse-promoting activity of NL2 and LRRTM2, possibly by competing for neurexin interaction. In collaboration with Dr. Gabby Rudenko, we proposed that one calsyntenin-3 tetramer may recruit four α-neurexin molecules (Lu et al., 2014) in a way similar to how the tetramer of the postsynaptic GluRδ2 receptors assembles four neurexins, although this binding is indirect and requires a tripartite complex with cerebellins (Lee et al., 2012).

Mice lacking all three α-neurexins but with normal expression of β-neurexins die at birth due to impaired synaptic transmission linked to deficits in presynaptic calcium channel currents (Missler et al., 2003). *Clstn3*−/− mice exhibit relatively normal survival and lack the profound reductions in evoked synaptic transmission that were detected in mice lacking α-neurexins. Thus, it seems likely that neurexin partners other than calsyntenin-3 mediate its presynaptic calcium channel recruitment function. However, we found in mice lacking calsyntenin-3 a reduction of inhibitory synapse density that also happened to mice lacking α-neurexins. The small but significant increase in input-output curve in *Clstn3*−/− CA1 region compared with wild-type controls supports the idea that the contribution of calsyntenin-3 to inhibitory synapse development is important for circuit function (Pettem et al., 2013). Overall, calsyntenin-3 plays a stronger role in inhibitory synapses than in excitatory synapses.

2.5.2 Model of calsyntenin-3-neureixn trans-synaptic complex

In the simplest model, full-length calsyntenin-3 may act as a postsynaptic cell adhesion and synapse-organizing protein, similar to neuroligins, LRRTMs, and other presynaptic-inducing proteins. This model is consistent with the ability of calsyntenin-3 to induce presynaptic specializations when presented to axons *in trans* on COS cells or upon dendritic overexpression of calsyntenin-3ΔPCS (Pettem et al., 2013). Although we were unable to detect its specific synaptic localization, electron microscopy showed prominent enrichment of calsyntenin-3 in the postsynaptic specializations of asymmetric synapses in hippocampus, cortex, and cerebellum (Hintsch et al., 2002), consistent with this model. However, extensive calsyntenin-3 cleavage differentiates it from other synaptogenic proteins, and our data suggest that the cleaved form is important in buffering the synaptogenic activity of α-neurexin partners and balancing overall synapse development.

Consider calsyntenin-3's multiple unique characteristics, its prominent intracellular pools detected with our antibody (Figure 2.14), its functional importance for both inhibitory and excitatory synapses (Figure 2.16 and Figure 2.17), and its high degree of cleavage (Figure 2.4). It is reasonable to suspect that calsyntenin-3 may actually act, at least additionally, by a distinct mechanism that is unlike any of the other known neurexin ligands. Although the level of α-neurexin in crude synaptosomes was not affected by loss of calsyntenin-3 (Figure 2.15), it remained possible that calsyntenin-3 interacted *in cis* with α-neurexins to regulate neurexin trafficking and/or function. In my unpublished preliminary experiment results, calsyntenin-3 expressed in COS cells did not induce postsynaptic differentiation in contacting dendrites, while neurexin-1β as positive control did, ruling out the possibility of calsyntenin-3 acting directly as a presynaptic organizing protein. YFP-C3ΔPCS is co-localized with HA-neurexin1α in co-

transfected neurons on both dendrites and axons, indicating their co-transportation. In the mouse brain, loss of calsyntenin-3 results in widespread deficits in inhibitory synapses, evidenced by loss of GAD65 even in dentate granule cells that normally express little or no calsyntenin-3 (Pettem et al., 2013) (VGluT1 input onto this region was not changed), possibly due to loss of calsyntenin-3 in interneurons. Further work is needed to 1) assess subcellular distribution and circuit contribution of full-length and cleaved calsyntenin-3 in interneurons and pyramidal cells, and 2) determine the mechanisms by which calsyntenin-3 regulates synapse development, whether as an inducer or modulator.

2.5.3 The mechanism and function of calsyntenin-3 cleavage

Calsyntenin-3 undergoes proteolytic processing in a manner similar to amyloid precursor protein, involving primary cleavage that releases a large extracellular fragment, followed by secondary intramembranous cleavage by γ-secretase (Hata et al., 2009a). Neuroligin-1 was also found to undergo regulated ectodomain cleavage (Peixoto et al., 2012; Suzuki et al., 2012). The vast majority of neuroligin-1 in the brain is present in the full-length form (Peixoto et al., 2012), whereas less than half of calsyntenin-3 in the brain is present in the full-length form and over half as the shed ectodomains (Figure 2.4). Recombinant calsyntenin-3 can be partially cleaved by ADAM-10 and ADAM-17 (Hata et al., 2009a), although the identity of the primary proteases in the brain has not been determined yet. In cultured neurons, nearly all calsyntenin-3 were cleaved, and we were able to inhibit the cleavage by protease inhibitor GM6001. Nonetheless, GM6001 as a broad-spectrum inhibitor of MMPs can also inhibit the cleavage of neuroligin-1 and some other synaptic proteins (Cirillo et al., 2016; Iwakura et al., 2017; Lemmens et al., 2016). Therefore, it cannot be used to study the specific function of calsyntenin-3 cleavage.

Perhaps similar to the related calsyntenin-1 (Maruta et al., 2012), calsyntenin-3 may be largely cleaved *en route* to the cell surface. We deduce that calsyntenin-3 cleavage is linked to its trafficking in neurons because partially cleavable Myc-C3ΔPCS-CFP and Myc-C3EX-CD8-C3IN accumulated on the dendrite surface, but noncleaved Myc-C3EX-CD8-CFP did not (Pettem et al., 2013). Adding GM6001 in the culture resulted in no accumulation of wild-type Myc-C3 on the dendrite surface.

Cleavage of synaptic adhesion molecules could induce intracellular signaling and alter synaptic strength. Function of extracellular proteases (such as ADAMs and MMPs) is largely dependent on cell activity (Conant et al., 2015; Lemmens et al., 2016; Shinoe and Goda, 2015). I studied calsyntenin-3 cleavage in the context of cell activity manipulation by adding TTX, bicuculline, APV, NBQX, or potassium chloride in the rat primary cortical culture and using western blot to analyze endogenous calsyntenin-3 in culture media and lysate. Blocking action potentials by TTX reduced calsyntenin-3 cleavage, while blocking GABA receptor mediated inhibitory transmission by bicuculline increased calsyntenin-3 cleavage (in three different experiments, data not shown). However, the amounts of several other synaptic proteins also changed in similar trends under such manipulations, making it difficult to interpret the changes. A better understanding of the regulation of calsyntenin-3 proteolytic processing is desired considering our finding that full-length calsyntenin-3 and the released ectodomains can have opposing functions (Figure 2.5).

2.5.4 Other members of the calsyntenin family

Calsyntenin-1 and calsyntenin-2 have similar domain structures as calsyntenin-3, undergo similar cleavage (Araki et al., 2004; Hata et al., 2009a), and are enriched at postsynaptic sites (Hintsch et al., 2002; Vogt et al., 2001). However, calsyntenin-1 and calsyntenin-2 lack

synaptogenic activity, and have no interaction with neurexins (Figure 2.6). Calsyntenin-1 is an organelle adaptor that links kinesin-1 light chain to transport vesicles (Araki et al., 2007; Konecna et al., 2006; Vagnoni et al., 2012). No role of calsyntenin-3 has been demonstrated in organelle transportation. Indeed, such a function is unlikely because calsyntenin-3 lacks one of the two kinesin light-chain binding sites and has a variant residue in the other that reduces the affinity of kinesin interactions (Konecna et al., 2006). The difference in their proposed functions, calsyntenin-3 for synapse development and calsyntenin-1 for vesicle transport, is consistent with the difference in their COS7 cell surface expression where we observed that tagged calsyntenin-3 is higher than calsyntenin-1 (data not shown). Synapse-organizing function is not always shared among family members; for example, only TrkC but not TrkA or TrkB interacts with PTPσ to organize excitatory synapses (Takahashi et al., 2011).

2.5.5 The heparin sulfate binding property of calsyntenin-3

As for the heparan sulfate binding property of calsyntenin-3, our knowledge is still very limited. Future studies are required to confirm the direct interaction between calsyntenin-3 and heparan sulfate. I have tried the heparin column binding assay similar to what we did for neuroligins and LRRTMs (Zhang et al., 2018), in which purified calsyntenin-3 ectodomains were incubated with heparin conjugated beads and eluted with different concentrations of salt and heparin solutions. Surprisingly, except that a small fraction of calsyntenin-3 was dissociated with low concentration of sodium chloride, a large fraction stuck with the heparin beads even after elution with 2M sodium chloride plus 8M Urea (data not shown). Purified 5RA and 6RA mutated calsyntenin-3 exhibited similar behavior to the wild-type in this assay. Additional assays such as plate binding assays with purified proteins and heparin or cell based binding assays of

calsyntenin-3 with other HSPGs could be further utilized to confirm the direct interaction between calsyntenin-3 and heparan sulfate.

Chapter 3: Calsyntenin-3 modulates synaptic transmission *in vitro* and *in vivo*

3.1 Introduction

Synaptic transmission is the basic unit of communication in the central nervous system. This process involves neurotransmitter release machinery at the presynaptic terminal and neurotransmitter receptors at the postsynaptic terminal. Synaptic adhesion molecules spanning the synaptic cleft regulate synaptic transmission by their direct and indirect interactions with scaffolding proteins, vesicle release machines, calcium channels and postsynaptic receptors (Craig and Kang, 2007; Jang et al., 2017; Südhof, 2017). Dysfunction of synaptic adhesion molecules usually results in altered synaptic transmission and imbalance of the excitatory-inhibitory scale could potentially lead to neuropsychiatric disorders such as autism and schizophrenia (Haas et al., 2018; Howell and Smith, 2019; Liang et al., 2015).

Such regulation of synaptic adhesion molecules to synaptic transmission could be temporal, spatial and cell type specific. For example, conditional deletion of all neuroligins in cerebellar Purkinje cells caused loss of distal climbing-fiber synapses and weakened climbing-fiber but not parallel-fiber synapses (Zhang et al., 2015), conditional knockout of neuroligin2 in adult medial prefrontal cortex induced major reductions in synaptic inhibition only after 6–7 weeks, not 2-3 weeks, and caused parallel impairments in anxiety, fear memory and social interaction behaviors (Liang et al., 2015). Calsyntenin-1 regulates targeting of dendritic NMDA receptors and dendritic spine maturation. In the absence of calsyntenin-1, synaptic transmission was depressed in juvenile mice but not in adult mice (Ster et al., 2014).

3.2 Rationale and hypothesis

In Chapter 2 and (Pettem et al., 2013), we demonstrated that calsyntenin-3 regulates synaptic development and transmission as an overall effect of global knockout. However, the underlying mechanism has remained unclear. Calsyntenin-3 expresses highly in inhibitory interneurons and moderately in pyramidal neurons (Pettem et al., 2013). Although CLSTN3 null mice show reduced excitatory and inhibitory synapse density, the EPSP response is enhanced relative to wild-type littermates at higher stimulation intensities, suggesting that calsyntenin-3 may not contribute to the development of excitatory synapses at the same level as inhibitory synapses. In addition, calsyntenin-3 has been reported to be localized in the excitatory postsynaptic density by an immuno-EM study (Hintsch et al., 2002). Unfortunately, we were unable to confirm this localization by immunocytochemistry due to antibody accessibility and sensitivity. Therefore it's important to study calsyntenin-3's function in different neuron types to determine how it contributes to excitatory and inhibitory synaptic development, and whether it does so through pre- or post-synaptic mechanisms. Furthermore, we proposed that the full-length calsyntenin-3 promotes synapse development while its secreted form plays an opposite role to inhibit it (Figure 2.5), which we have yet to confirm *in vivo*. In the global knockout study mentioned above, both the full-length and secreted calsyntenin-3 are diminished in all cell types, thus only an overall effect can be observed. Based on these concerns, the following hypotheses are formed to further study calsyntenin-3's function in a temporal, spatial and cell type specific manner:

- Given the differential expression pattern of calsyntenin-3 in excitatory and inhibitory neurons, I hypothesize that calsyntenin-3 differentially regulates

synaptic transmission in these cell types. This investigation could be approached by using Cre lines that can specifically delete calsyntenin-3 in each cell type followed by electrophysiological recordings from the knockout cells or efferent cells receiving inputs.

- Given the transient effect of calsyntenin-1 knockout mice on synaptic transmission (Ster et al., 2014) and the time course of general synapse development, I hypothesize that calsyntenin-3 knockout phenotype is age-sensitive. This can be tested through recordings on the knockout mice during different time window throughout development.
- Considering the complexity of calsyntenin-3 cleavage and possible compensation from other family members or synaptic adhesion molecules, I hypothesize that the effect of calsyntenin-3 deletion is not cell autonomous. This can be evaluated by comparing sparse vs global knockout of calsyntenin-3.

3.3 Methods

3.3.1 Animals

Clstn3-/- mice and *Clstn3*$^{Flox/Flox}$ were described previously (Pettem et al., 2013). To get conditional knockout lines, *Clstn3*$^{Flox/+}$ line was crossed with Dlx5/6-cre [Tg(dlx6a-cre)1Mekk/J] line that express Cre recombinase in forebrain interneurons, or Gpr26-cre [Tg(Gpr26-cre)KO250Gsat/Mmucd] line that express Cre recombinase in deep layer of hippocampal CA1 pyramidal neurons.

All mice were housed in ARU at the University of British Columbia. All procedures were approved by the Animal Care Committee at the University of British Columbia. Protocols

include AAV P0 injection A17-0225, mice breeding A16-0090 and A16-0086, biosafety certificate B17-0067.

3.3.2 Acute hippocampal slices recording

For slice preparation from 6-8 week mice, following cervical dislocation, mouse brains were rapidly removed and placed in ice-cold slicing solution consisting of (in mM): 120 NMDG, 2.5 KCl, 1.2 NaH2PO4, 25 NaHCO3, 1.0 CaCl2, 7.0 MgCl2, 2.4 Na-pyruvate, 1.3 Na-ascorbate, 20 D-glucose with pH adjusted to 7.35 using HCl acid (unless stated, all chemicals and drugs were purchased from Sigma or BioShop, Canada). The hippocampus was dissected out and coronal brain slices (400 μm thickness) were cut using Vibratome (VT1000s, Leica) and transferred to oxygenated, ice-cold slicing solution. For slices from 2-week mice, the slicing buffer is artificial cerebrospinal fluid (ACSF) containing (in mM): 125 NaCl, 2.5 KCl, 2 CaCl2, 2 MgCl2, 1.25 NaH2PO4, 26 NaCO3, 25 glucose, pH 7.35 (oxygenated with 95% O2 and 5% CO2, 310-320 mOsm). Freshly cut slices were placed in a recovery chamber with carbogenated ACSF at 31°C for at least 30 min and then were kept at room temperature for 60 min before recording.

Recordings were performed at room temperature in a submerged recording chamber perfused continuously with carbogenated ACSF (2-3 ml/min). The patch pipettes were pulled from borosilicate glass capillary tubes (World Precision Instruments) using a pipette puller (P - 97, Sutter Instruments). The resistance of pipettes varied between 3-6 MΩ. For mEPSC recordings, CA1 neurons were voltage clamped at -70 mV. Recording pipettes were filled with solution containing (in mM) Cs gluconate 122.5, CsCl 17.5, $MgCl_2$ 2, HEPES 10, BAPTA 10, ATP 4, and QX314 5 (pH 7.2). Prior to recording mEPSCs, tetrodotoxin (TTX; 500 nM; Ascent

Scientific) and bicuculline methiodide (10 μM; Abcam) were added to block action potentials and $GABA_A$ receptor-mediated inhibitory synaptic currents, respectively. To verify that remaining responses were mEPSCs, CNQX (10 μM; Abcam) and DL-AP5 (50 μM; Abcam) were added towards the conclusion of some experiments to block remaining excitatory currents.

For mIPSC recordings, CA1 neurons were voltage clamped at –70 mV and the recording pipette was filled with solution containing (in mM): 140 CsCl, 0.1 $CaCl_2$, 2 $MgCl_2$, 10 HEPES, 10 EGTA, 4 ATP(K), with pH adjusted to 7.2 using CsOH. Slices were treated with CNQX (10 μM), DL-AP5 (50 μM) and TTX (500 nM) to block excitatory synaptic transmission. Bicuculline methiodide (10 μM) was added towards the end of some experiments to confirm that the remaining responses were mIPSCs. mEPSCs and mIPSCs were recorded using pClamp 11. Recordings were low-pass filtered at 2 kHz, and series resistance was left uncompensated. Cells with changes >20% in series resistance during recording were discarded.

Analyses for frequency and amplitude were conducted using MiniAnalysis software. Statistical analyses were completed using GraphPad Prism 7. Student's t-tests were conducted to test for differences between groups with n = number of cells. Data are presented as mean ± SEM.

3.3.3 Primary hippocampal culture and recording

Dissociated primary hippocampal neuronal cultures were prepared from embryonic day 18 (E18) mice as previously described (Kaech and Banker, 2006). Hippocampi were dissociated by papain solution and nutation. Dissociated neurons were transfected using nucleofection (AMAXA Biosystems, Lonza) and plated onto poly-L-lysine-coated glass coverslips in 60-mm culture dishes at a density of 300,000 cells/dish and cocultured over a monolayer of glia. After 2 days, cytosine arabinoside (5 μM) was added to neuron cultures to prevent the overgrowth of

glia. Cultures were maintained in serum-free minimal essential medium with N2 supplements, 0.1% ovalbumin, and 1 mM pyruvate, with replacing ⅓ of the media per dish once per week. For coculture assays, neurons were treated with 100 μM 2-amino-5-phosphonopentanoic acid (APV, Research Biochemicals) beginning on day 7.

For recording in cultured hippocampal neurons, whole-cell recordings were made from the cultures at room temperature (20-22°C) at 15-17 DIV. Neurons were continuously perfused (1 mL/min) with the extracellular solution (ECS) containing (in mM): NaCl 140, CaCl2 1.3, KCl 5.4, MgCl2 1, HEPES 25, glucose 33 (pH 7.35; osmolality 300-310 mosmol/Kg). mEPSCs were recorded in the presence of 0.5 μM tetrodotoxin and 10 μM bicuculline methiodide; mIPSCs were recorded in the presence of 0.5 μM tetrodotoxin, 10 μM 6-cyano-7-nitroquinoxaline-2,3-dione (CNQX) and 100 μM APV. The patch pipettes were pulled from borosilicate glass capillary tubes (World Precision Instruments) using a PP-830 pipette puller (Narishige). The resistance of pipettes was 4-6 MΩ. For mEPSC recording, the patch pipette solution contained (in mM): Cs gluconate 122.5, CsCl 17.5, $MgCl_2$ 2, HEPES 10, BAPTA 10, ATP 4, and QX314 5 (pH 7.2; osmolality 280-290 mosmol/Kg). For mIPSC recording, the patch pipette solution contained (in mM): CsCl 140, $CaCl_2$ 0.1, $MgCl_2$ 2, HEPES 10, BAPTA 10, ATP 4, and QX314 5 (pH 7.2; osmolality 280-290 mosmol/Kg). The series resistance in these recordings varied from 8 to 13 MΩ, and recordings where series resistance varied by more than 10% were rejected. No electronic compensation for series resistance was employed. Cells that demonstrated a change in "leak" current of more than 10% were rejected from the analysis.

Analyses for frequency and amplitude were conducted using MiniAnalysis software. Statistical analyses were completed using GraphPad Prism 7. Kolmogorov-Smirnov tests were

used for determination of cumulative probability normality. Student's t-tests were conducted to test for differences between groups with n=number of cells. Data are presented as mean ± SEM.

3.3.4 Immunofluorescence

For calsyntenin-3 staining in the brain slices, P30 mice were deeply anesthetized with CO_2. Brains were transferred to pre-cooled to -38°C 2-methylbutane immediately after decapitation. After freezing for approximately 30 seconds in 2-methylbutane, brains were transferred to a cryostat set to -18°C and sliced into 20µm sections. Slices were mounted onto coated slides and transferred to pre-cooled to -20°C methanol and kept there for 5 minutes as fixation followed by PBS wash and then incubated in blocking solution (5% BSA + 5% Normal goat serum + 0.25 % Triton X100 in PBS) at 37°C for 1 hour. Sections were incubated with a Calsyntenin-3 C-terminal antibody (1:500, antibody generated in our lab and described in (Pettem et al., 2013)) diluted in the same blocking solution (overnight, 4°C) then with the goat anti-rabbit secondary antibodies conjugated to Alexa 568 (Molecular Probes/Invitrogen) (1 hour, 20°C). Sections were washed in PBS containing the nuclear counterstain DAPI (4',6 diamidino-2- phenylindole), and mounted in elvanol (Tris-HCl, glycerol, and polyvinyl alcohol with 2% 1,4-diazabicyclo[2,2,2]octane).

For synaptic staining in primary culture, neurons were fixed in parafix solution (4% paraformaldehyde and 4% sucrose in PBS pH 7.4) for 15 min followed by permeabilization with PBST (PBS + 0.25 % Triton X-100) or in -20°C methanol for 10 min (for neuroligin2 antibody staining, a gift from Dr. Nils Brose). They were then incubated with blocking solution (PBS + 3% BSA and 5% normal goat serum) for 30 min at 37°C, followed by incubation with primary antibodies in blocking solution (overnight, 20°C) and secondary antibodies conjugated to Alexa 488, 568 or AMCA (Molecular Probes/Invitrogen) (45 min, 37°C). Coverslips were mounted in

elvanol (Tris-HCl, glycerol, and polyvinyl alcohol with 2% 1,4- diazabi-cyclo[2,2,2]octane). Primary antibodies used are anti-PSD-95 family (1:500; IgG2a; clone 6G6-1C9; Thermo Scientific; recognizes PSD-95, PSD-93, SAP102 and SAP97), anti-gephyrin (1:500; IgG1; mAb7a; Synaptic Systems), rabbit anti-VGlut1 (1:2000; Synaptic Systems; 135 302), rabbit anti-VGAT (1:1000; Synaptic Systems; 131 003), and anti-MAP2 (1:4000, chicken polyclonal IgY; Abcam; ab5392).

3.3.5 AAV injection

The packaging of AAV was performed by the University of Pennsylvania Vector Core. On the day of birth (P0), C57BL/6 neonates were anesthetized using isoflurane and bilaterally injected with 1µl of viral vector into each cerebral lateral ventricle through a finely drawn glass micropipette as described previously (Kim et al., 2013, 2014). Pups were recovered in 2% oxygen for 15 min before returning them to the dam and monitored daily for 3 days for body weight, milk in stomach and signs of movement.

3.4 Results

3.4.1 Conditional *Clstn3* knockout in forebrain interneurons does not affect basal inhibitory transmission

To explore the function of calsyntenin-3 in interneurons and excitatory neurons separately, I utilized two Cre transgenic mouse lines, the Dlx5a-Cre (B6-Tg(dlx5a-cre)1Mekk/J) and Gpr26-Cre (B6-Tg(Gpr26-cre)KO250Gsat/Mmucd). The Dlx5a-Cre line was generated in 2000 (Zerucha et al., 2000) and has been used in over 70 peer-reviewed publications to specifically target forebrain interneurons according to Jackson Laboratory's Mouse Genome Informatics Database (Boon et al., 2018; Sasamoto et al., 2017; Winkler et al., 2018). The MGI

database tissue activity image shows Cre expression in forebrain interneurons (Figure 3.1A). My calsyntenin-3 C-terminal antibody staining results confirmed that, in my Clstn3$^{f/f}$; Dlx5a-Cre mice, calsyntenin-3 was not expressed in interneurons while its expression in pyramidal neurons was intact (Figure 3.1B).

Gpr26-Cre_KO250 (Gpr26-Cre in the following text) was generated by the GENSAT project (http://gensat.org/) and displayed specific expression in hippocampal CA1 and sparse expression in other brain regions, including layer V cortex and thalamus (Gerfen et al., 2013; Harris et al., 2014). Allen Brain Atlas Mouse Connectivity shows Cre expression in pyramidal neurons in hippocampal CA1, but not CA2 or CA3 (Figure 3.1A). My calsyntenin-3 C-terminal antibody staining results confirmed that, in my Clstn3$^{f/f}$; Gpr26-Cre mice, calsyntenin-3 was not expressed in the deep layer of CA1 pyramidal neuron layer next to stratum oriens while its expression in the superficial layer and in interneurons remained intact (Figure 3.1B).

To be consistent with the previous study in Figure 2.17, I recorded mIPSCs in these conditional knockout mice during week 6-8. Surprisingly, despite the high expression level of calsyntenin-3 in interneurons, neither mIPSC frequency or amplitude in *Clstn3*$^{f/f}$; Dlx5a-Cre CA1 pyramidal neurons was changed compared with that of *Clstn3*$^{f/f}$ mice (Figure 3.2), suggesting that calsyntenin-3 does not regulate inhibitory synapse development in the presynaptic side at the basal level.

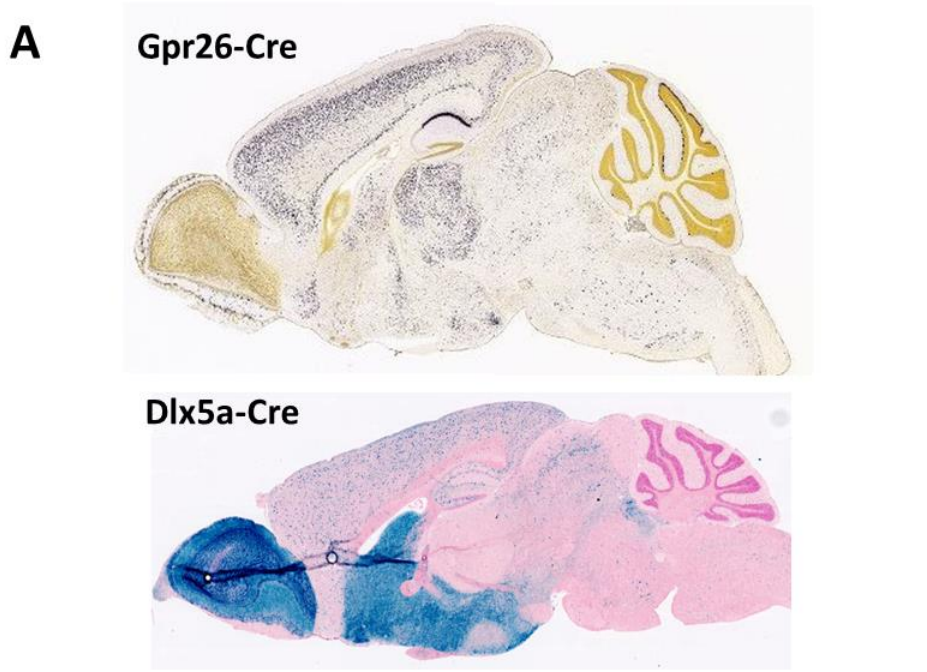
A
Gpr26-Cre
Dlx5a-Cre
B
Wildtype
Clstn3 -/-
DAPI Calsyntenin-3
Clstn3flox/flox::Gpr26-Cre
Clstn3flox/flox::Dlx5a-Cre
DAPI Calsyntenin-3

Figure 3.1 Expression of *Clstn3* conditional knockout mice in hippocampal CA1 region

A. Expression patterns of Cre recombinase in Gpr26-Cre and Dlx5a-Cre mouse lines. ISH image adapted from Allen Brain Atlas Mouse Connectivity Gpr26-Cre_KO250; Ai14(RCL-tdT) from P28 mouse brain and Tg(dlx5a-cre)1Mekk with Cre reporter lacZ staining from P56 mouse brain.

B. Expression patterns of *Clstn3* global knockout and conditional knockout mice in hippocampal CA1. Red, calsyntenin-3 C-terminal antibody staining; Blue, DAPI. Scale bar=50μm.

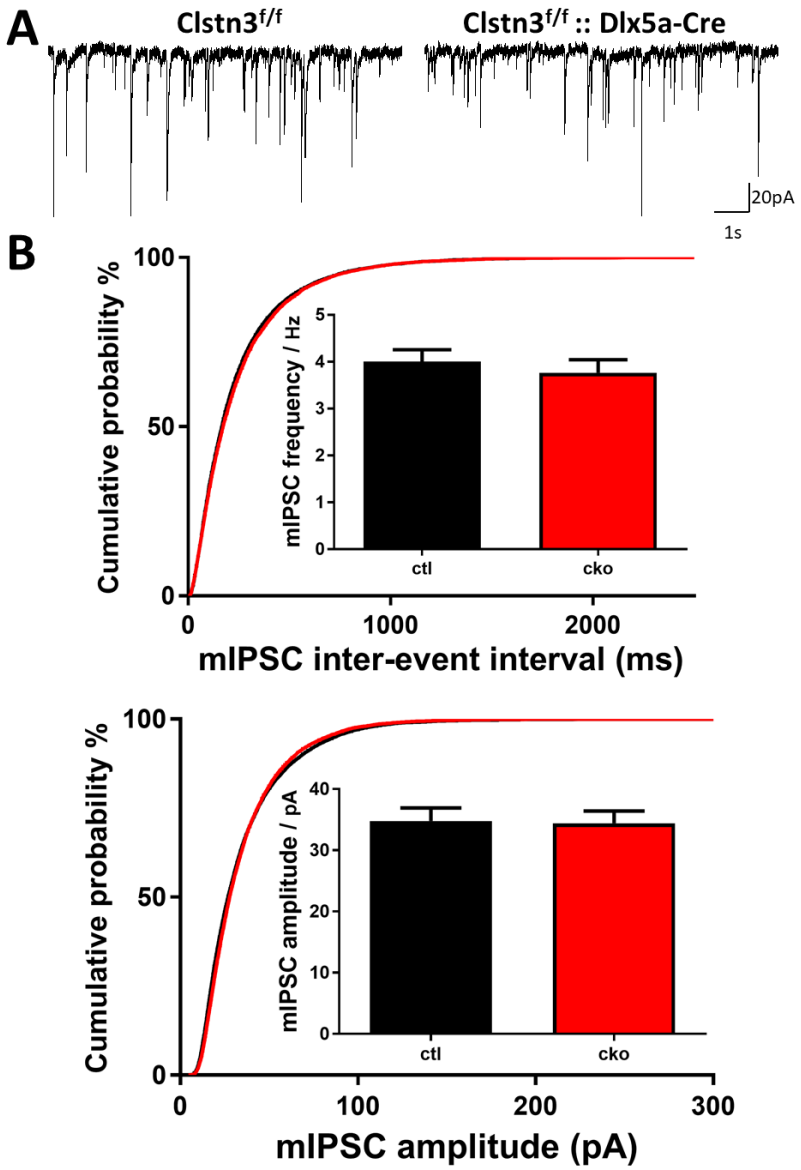

Figure 3.2 Conditional *Clstn3* knockout in forebrain interneurons does not affect basal inhibitory transmission in CA1 pyramidal neurons

(A) Representative mIPSC recordings from hippocampal CA1 pyramidal neurons in acute slices from *Clstn3*$^{f/f}$ and *Clstn3*$^{f/f}$; Dlx5a-Cre young adult mice.

(B) Cumulative distributions of mIPSC interevent intervals and amplitudes in *Clstn3*$^{f/f}$ and *Clstn3*$^{f/f}$; Dlx5a-Cre neurons. Insets display mean ± SEM for mIPSC frequency and amplitude. (Student's t test, $p > 0.05$. n=27 cells for *Clstn3*$^{f/f}$ and n=23 cells for *Clstn3*$^{f/f}$; Dlx5a-Cre).

3.4.2 Conditional *Clstn3* knockout in hippocampal CA1 pyramidal neurons enhances basal transmission

To explore the function of calsyntenin-3 in excitatory neurons, I recorded mEPSCs and mIPSCs on the deep layer of CA1 pyramidal neurons, where Cre recombinase was expressed, in 6-8 weeks old *Clstn3*$^{f/f}$; Gpr26-Cre mice (Figure 3.1). Unlike the global *Clstn3* knockout mice, the pyramidal neuron specific conditional *Clstn3* knockout mice showed enhanced basal transmission with increased mIPSC amplitude and mEPSC frequency, compared with *Clstn3*$^{f/f}$ control mice (Figure 3.3Figure 3.4).

The discrepancy between conditional *Clstn3* knockout mice and global *Clstn3* knockout mice could result from: 1) laminar organization of CA1 pyramidal neurons; 2) existing secreted form of calsyntenin-3 from neighboring cells; 3) developmental stage of the deletion; 4) global vs partial deletion causing competition between neighboring cells.

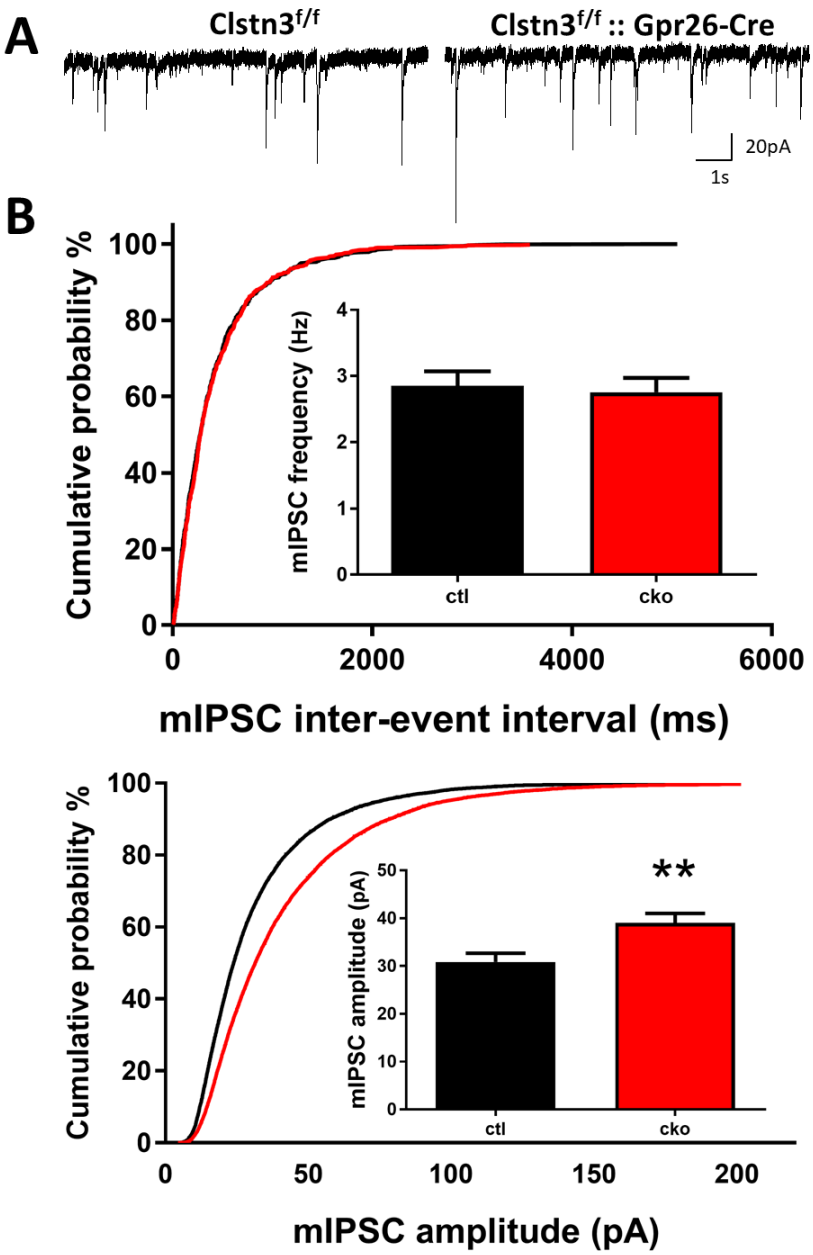

Figure 3.3 Conditional *Clstn3* knockout in CA1 pyramidal neurons increases basal inhibitory transmission

A. Representative mIPSC recordings from hippocampal CA1 pyramidal neurons in acute slices from *Clstn3*$^{f/f}$ and *Clstn3*$^{f/f}$; Gpr26-Cre young adult mice.

B. Cumulative distributions of mIPSC interevent intervals and amplitudes in *Clstn3*$^{f/f}$ and *Clstn3*$^{f/f}$; Gpr26-Cre neurons. Insets display mean ± SEM for mIPSC frequency and amplitude. (Student's t test, **p < 0.01. n=32 cells for *Clstn3*$^{f/f}$ and n=30 cells for *Clstn3*$^{f/f}$; Gpr26-Cre).

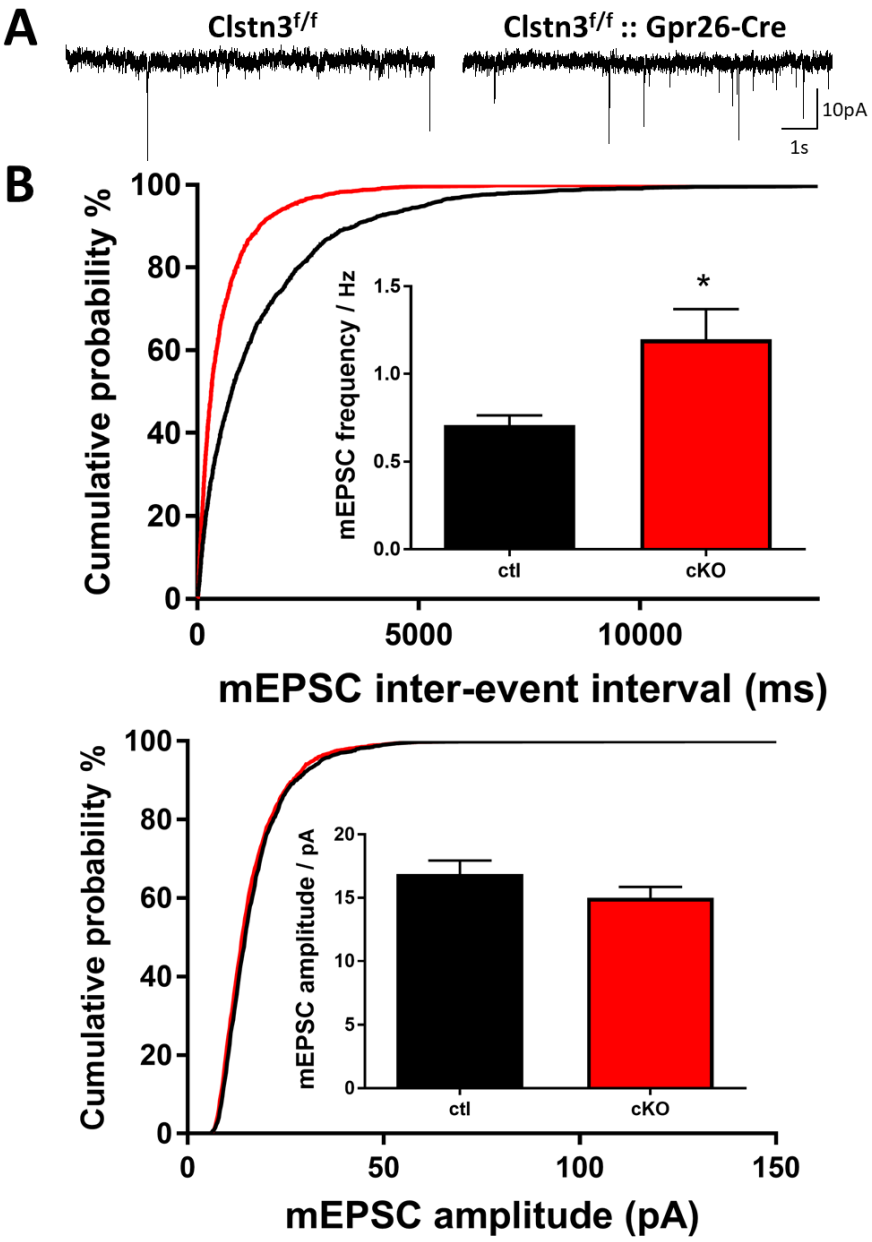

Figure 3.4 Conditional Clstn3 knockout in CA1 pyramidal neurons increases basal excitatory transmission

A. Representative mEPSC recordings from hippocampal CA1 pyramidal neurons in acute slices from *Clstn3*$^{f/f}$ and *Clstn3*$^{f/f}$; Gpr26-Cre young adult mice.

B. Cumulative distributions of mEPSC interevent intervals and amplitudes in *Clstn3*$^{f/f}$ and *Clstn3*$^{f/f}$; Gpr26-Cre neurons. Insets display mean ± SEM for mEPSC frequency and amplitude. (Student's t test, $*p < 0.05$. n=14 cells for *Clstn3*$^{f/f}$ and n=18 cells for *Clstn3*$^{f/f}$; Gpr26-Cre).

3.4.3 ~50% knockout of Clstn3 in primary hippocampal culture via nucleofection tends to increase inhibitory synaptic transmission

To test the possibility of global vs partial deletion effects in the Gpr26-Cre dependent *Clstn3* conditional knockout mice, I did mIPSC recordings in the cultured neurons mimicking the partial conditional knockout effect. Primary hippocampal cultures were obtained from *Clstn3*$^{flox/flox}$ mice and nucleofected with either pSyn-mCherry or pSyn-mCherry-2A-Cre on DIV0 to achieve about 100% knockout in 50% neurons, similar to in the CA1 region of Gpr26-Cre mice. Recordings on the mCherry-positive neurons in the "knockout" group revealed a trend of increased mIPSC frequency ($p = 0.09$) but no change of mIPSC amplitude compared with the control group (Figure 3.5).

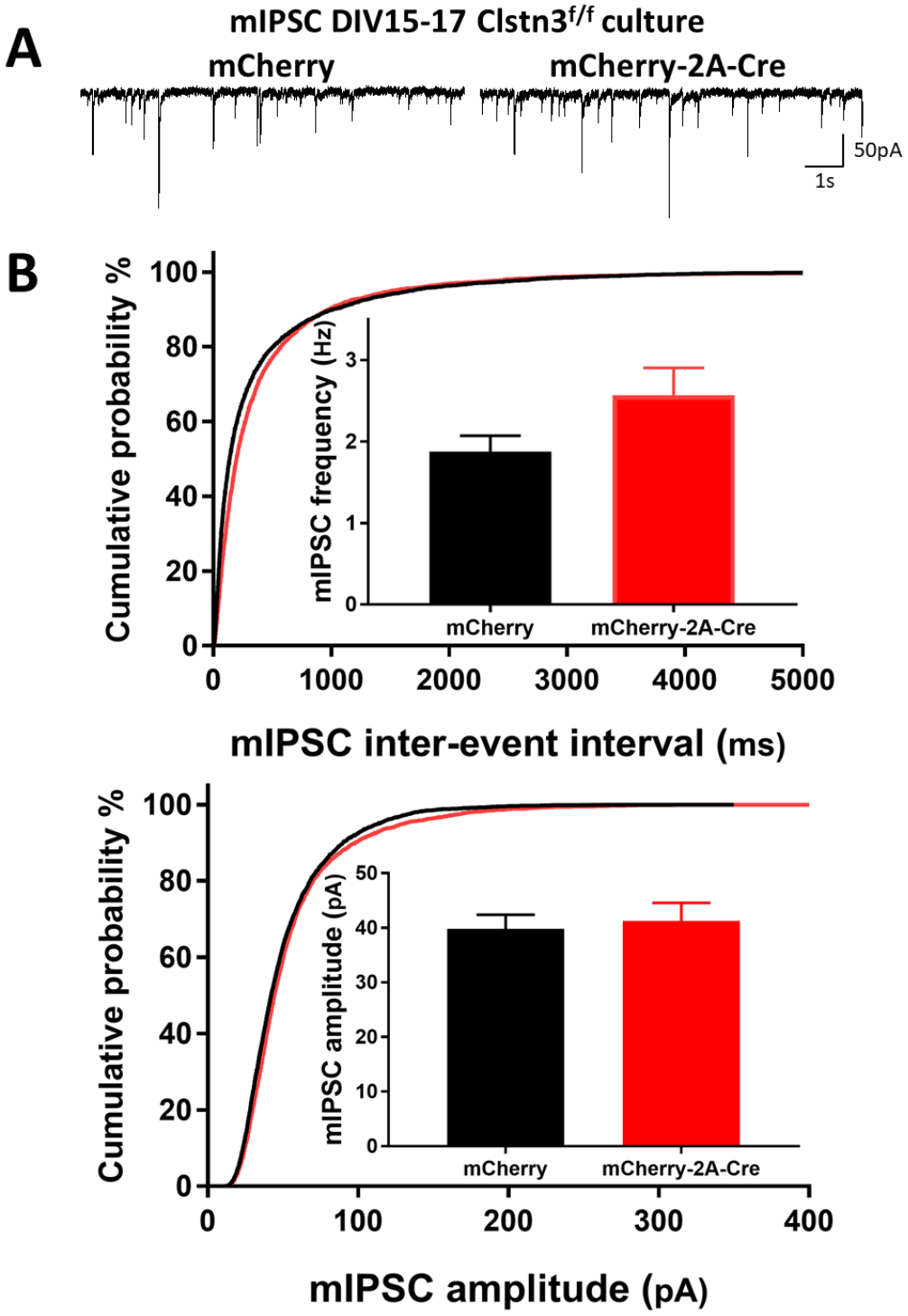

Figure 3.5 Nucleofected ~50% knockout of *Clstn3* in primary hippocampal culture increases inhibitory synaptic transmission

A. Representative mIPSC recordings from DIV15-17 cultured hippocampal neurons from *Clstn3*$^{f/f}$ mice, nucleofected with pSyn-mCherry or pSyn-mCherry-2A-Cre.

B. Cumulative distributions of mIPSC interevent intervals and amplitudes in DIV15-17 cultured hippocampal neurons from *Clstn3*$^{f/f}$ mice, nucleofected with pSyn-mCherry or pSyn-mCherry-2A-Cre. Insets display mean ± SEM for mIPSC frequency and amplitude. (Student's t test, p = 0.09 for frequency. n = 25 cells for pSyn-mCherry and n = 29 cells for pSyn-mCherry-2A-Cre).

3.4.4 ~50% knockout of *Clstn3* in primary hippocampal culture via nucleofection increases inhibitory synapse density

I also stained the same cultures on DIV17 for excitatory and inhibitory synaptic markers, VGAT/Gephyrin, VGAT/neuroligin2, and VGluT1/PSD95. The puncta number of VGAT, puncta number of Gephyrin, and neuroligin-2 colocalized with VGAT per dendritic area were all increased in the mCherry-2A-Cre transfected cells (Figure 3.6), consistent with the trend of mIPSC recording results. The puncta densities of PSD95 and VGluT1 remained unchanged (Figure 3.7).

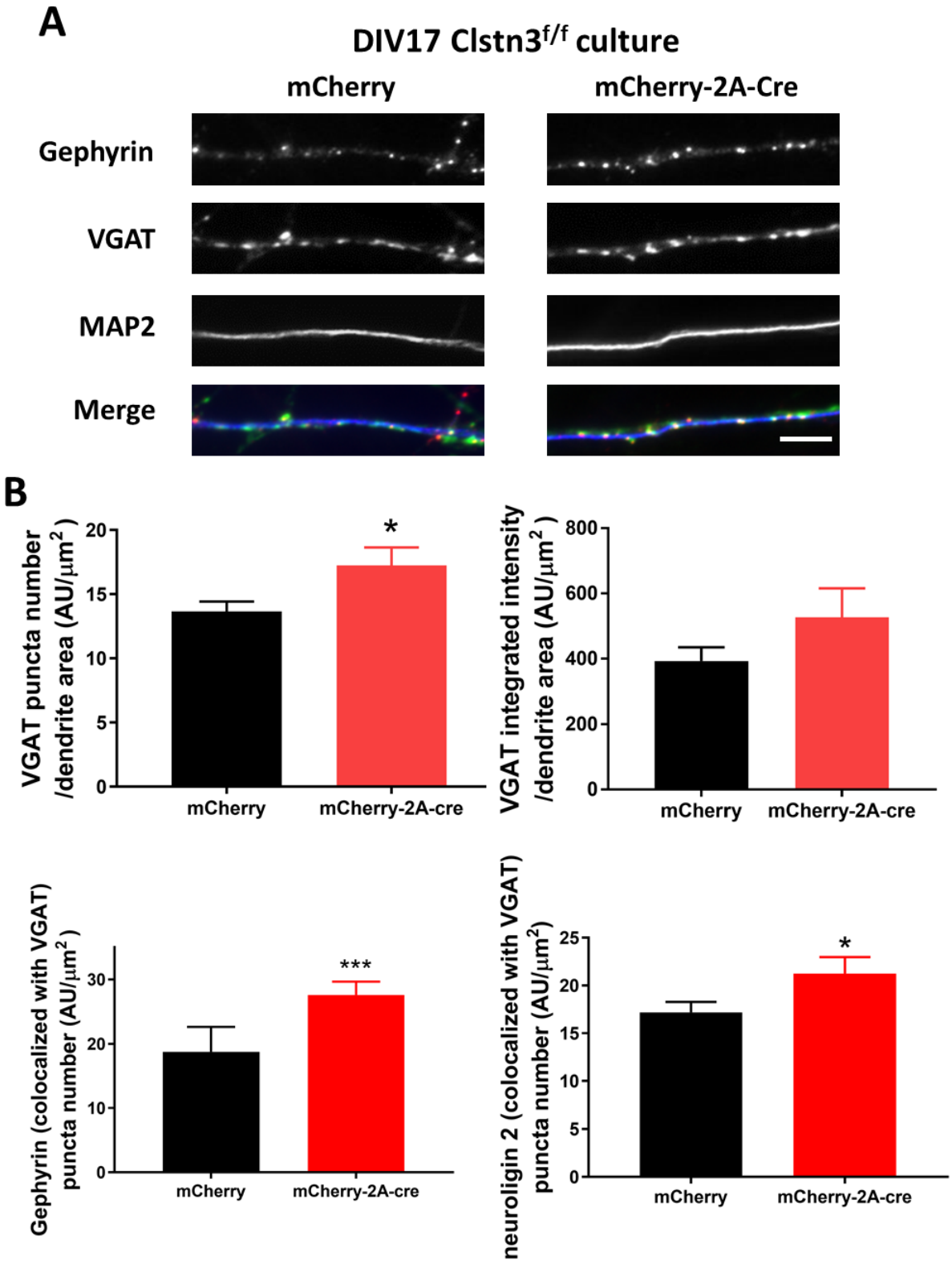
A
DIV17 Clstn3f/f culture
mCherry
mCherry-2A-Cre
Gephyrin
VGAT
MAP2
Merge
B
VGAT puncta number /dendrite area (AU/μm2)
VGAT integrated intensity /dendrite area (AU/μm2)
Gephyrin (colocalized with VGAT) puncta number (AU/μm2)
neuroligin 2 (colocalized with VGAT) puncta number (AU/μm2)
mCherry
mCherry-2A-cre
*
***

Figure 3.6 Nucleofected ~50% knockout of Clstn3 in primary hippocampal culture increases inhibitory synapse density

A. Sample images of inhibitory marker staining from DIV17 cultured hippocampal neurons from Clstn3$^{f/f}$ mice, nucleofected with pSyn-mCherry or pSyn-mCherry-2A-Cre. Scale bar = 10μm.

B. Quantification of VGAT puncta number, VGAT integrated intensity, gephyrin puncta number (colocalized with VGAT) and neuroligin 2 puncta number (colocalized with VGAT) per dendritic area from DIV17 cultured hippocampal neurons from *Clstn3$^{f/f}$* mice, nucleofected with pSyn-mCherry or pSyn-mCherry-2A-Cre. (Student's t test, *$p < 0.05$, ***$P < 0.001$)

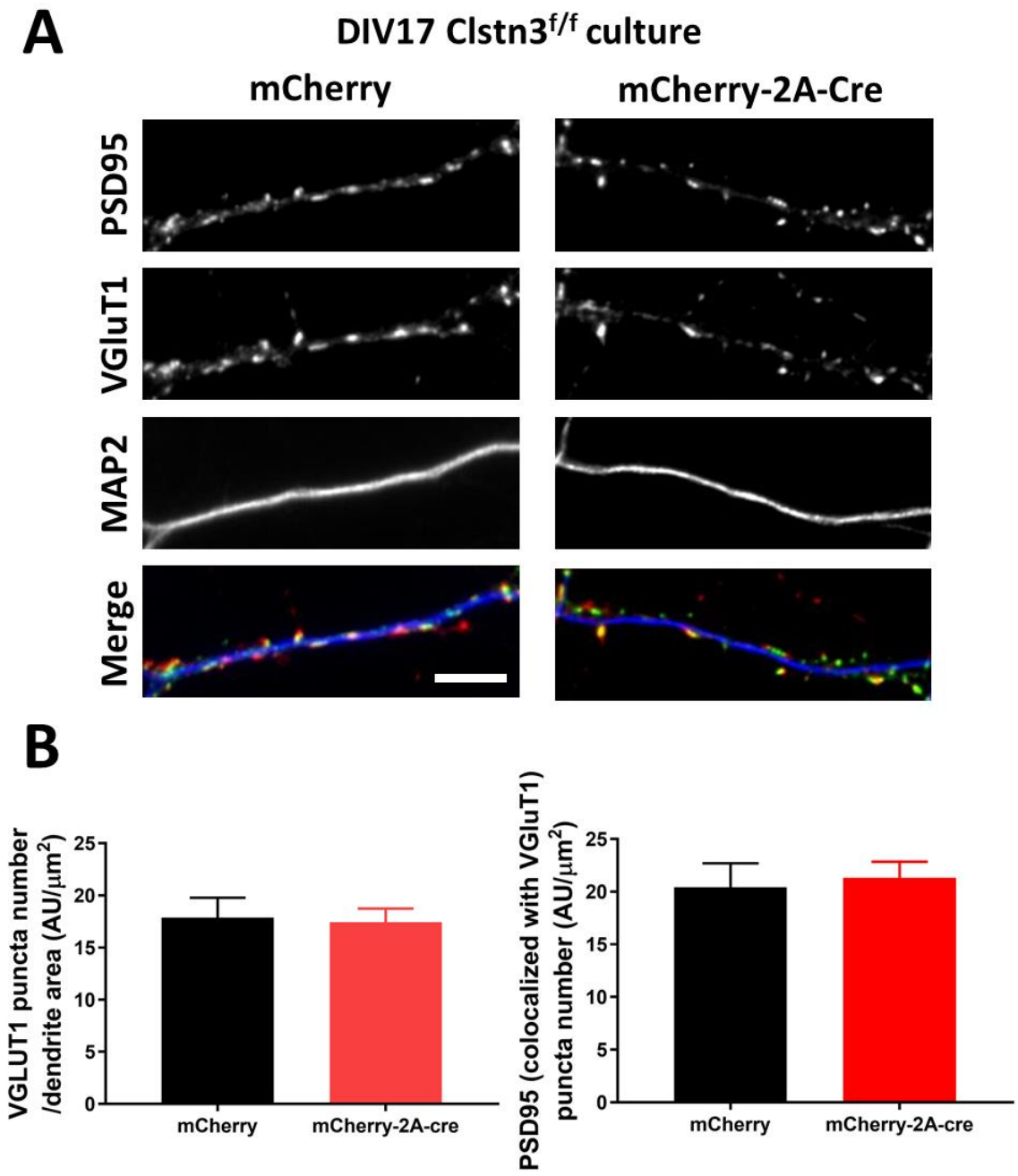

Figure 3.7 Nucleofected ~50% knockout of *Clstn3* in primary hippocampal culture does not affect excitatory synapse number

A. Sample images of excitatory marker staining from DIV17 cultured hippocampal neurons from Clstn3$^{f/f}$ mice, nucleofected with pSyn-mCherry or pSyn-mCherry-2A-Cre. Scale bar=10μm.

B. Quantification of VGluT1 and PSD95 puncta number per dendritic area from DIV17 cultured hippocampal neurons from Clstn3$^{f/f}$ mice, nucleofected with pSyn-mCherry or pSyn-mCherry-2A-Cre. (Student's t test, $p>0.05$)

3.4.5 Viral-inducted sparse knockout of *Clstn3* in juvenile mice increases inhibitory synaptic transmission

To confirm the results from cultured neurons *in vivo*, I recorded mIPSCs in sparse *Clstn3* knockout cells in AAV-Cre injected *Clstn3*$^{f/f}$ mice. Two strategies for viral induction were tested and compared: the AAV5-Cre and AAV9-DIO-GFP combination, or AAV9-Cre-GFP. The *Clstn3*$^{f/f}$ mice were injected at P0 or P1 with a glass pipette and monitored for 3 days. At P14, the brains were extracted and sectioned for imaging. The AAV5-Cre and AAV9-DIO-GFP combination showed sparse GFP pattern in the CA1 region with several GFP positive cells per field while AAV9-Cre-GFP showed a near global pattern with about 80% of pyramidal neurons infected (Figure 3.8). So in later experiments, the AAV5-Cre and AAV9-DIO-GFP combination was used to achieve sparse knockout with AAV9-GFP in separate animals as control.

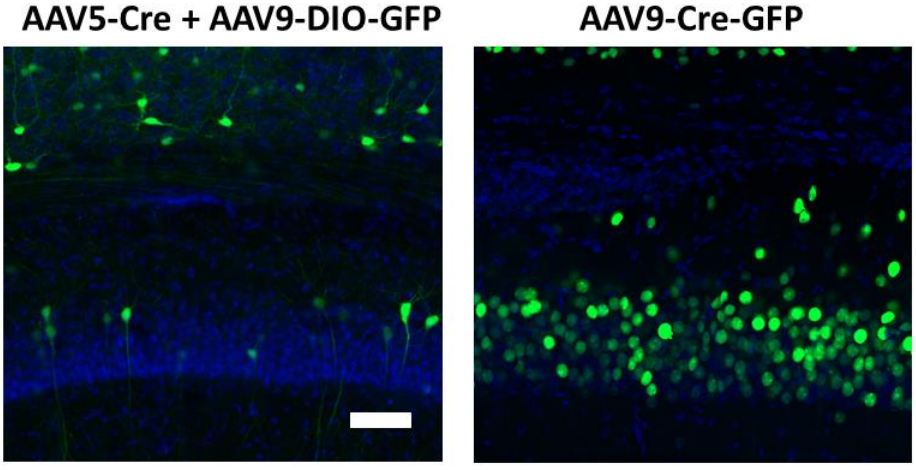

Figure 3.8 Expression pattern of AAV P0 injections

Sample images for hippocampal CA1 region of AAV-injected *Clstn3*$^{f/f}$ mice at P14. Blue, DAPI; Green, GFP. Scale bar = 50μm.

mIPSCs were recorded in GFP-positive CA1 pyramidal neurons at P14-16. Consistent with the culture results, significantly higher frequency of mIPSC was observed in the knockout cells (Figure 3.9), while the amplitude of mIPSC appeared similar.

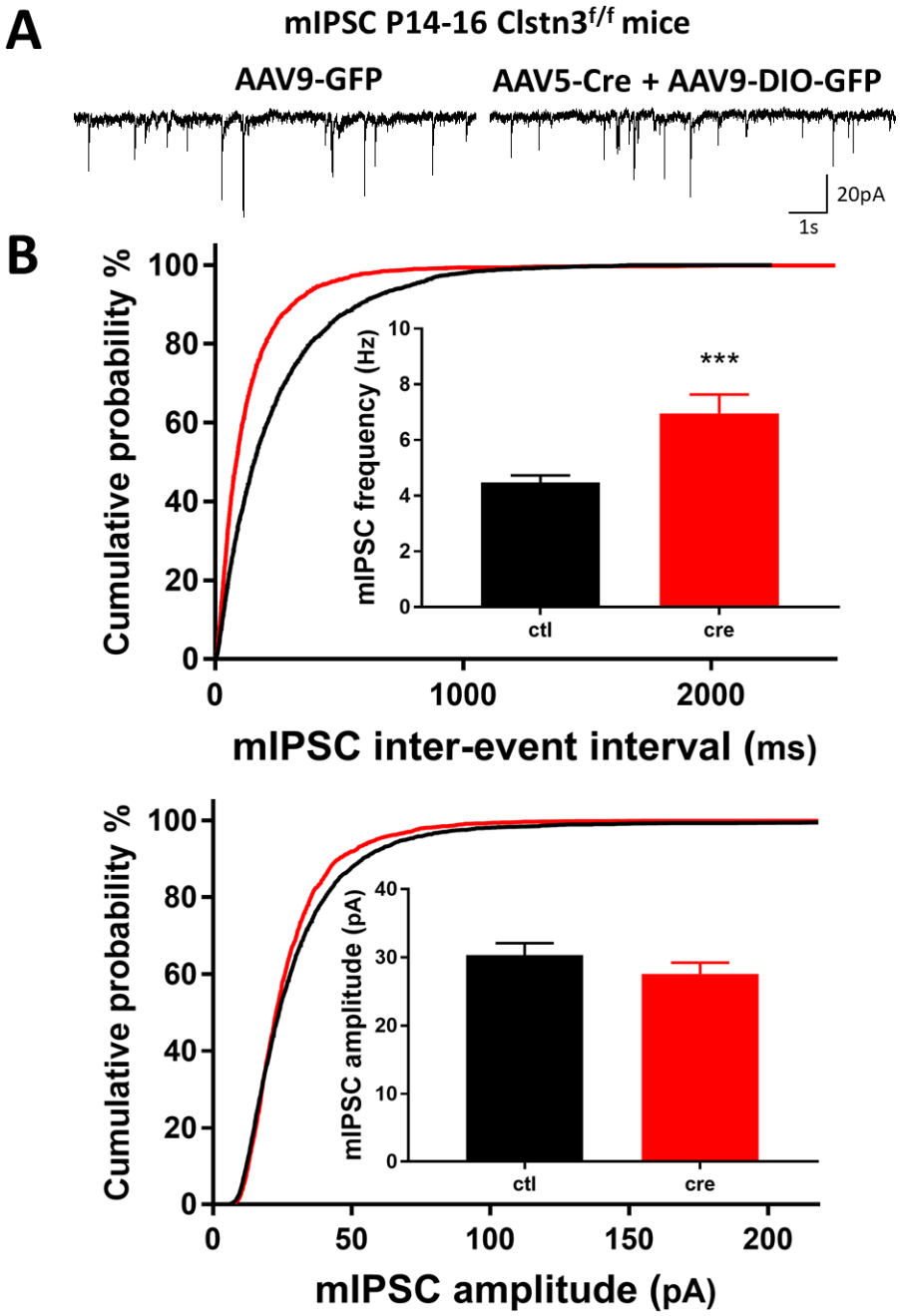

Figure 3.9 Viral-inducted sparse knockout of *Clstn3* in juvenile mice increases inhibitory synaptic transmission

A. Representative mIPSC recordings from hippocampal CA1 pyramidal neurons from P14-16 *Clstn3*$^{f/f}$ mice, AAV-injected AAV9-GFP or AAV5-Cre + AAV9-DIO-GFP.

B. Cumulative distributions of mIPSC inter-event intervals and amplitudes in hippocampal neurons from *Clstn3*$^{f/f}$ mice, AAV-injected AAV9-GFP or AAV5-Cre + AAV9-DIO-GFP. Insets display mean ± SEM for mIPSC frequency and amplitude. (Student's t test, ***p < 0.001. n = 19 cells for AAV9-GFP and n = 14 cells for AAV5-Cre + AAV9-DIO-GFP).

3.4.6 Basal inhibitory transmission is not changed in juvenile global *Clstn3* knockout mice compared to wildtype

Considering all the recording results together, with AAV-injected juvenile mice consistent with the 2-week culture data, and the conditional knockout by Gpr26-Cre contradicting global knockout results, we deduced that the major contributing factors here could be age differences and/or competition from neighboring normal neurons. To solve this puzzle, I recorded global *Clstn3* knockout mice at 2 weeks (P14-16). Surprisingly, no change was observed on mIPSC frequency or amplitude in these mice compared to the wild-type littermates.

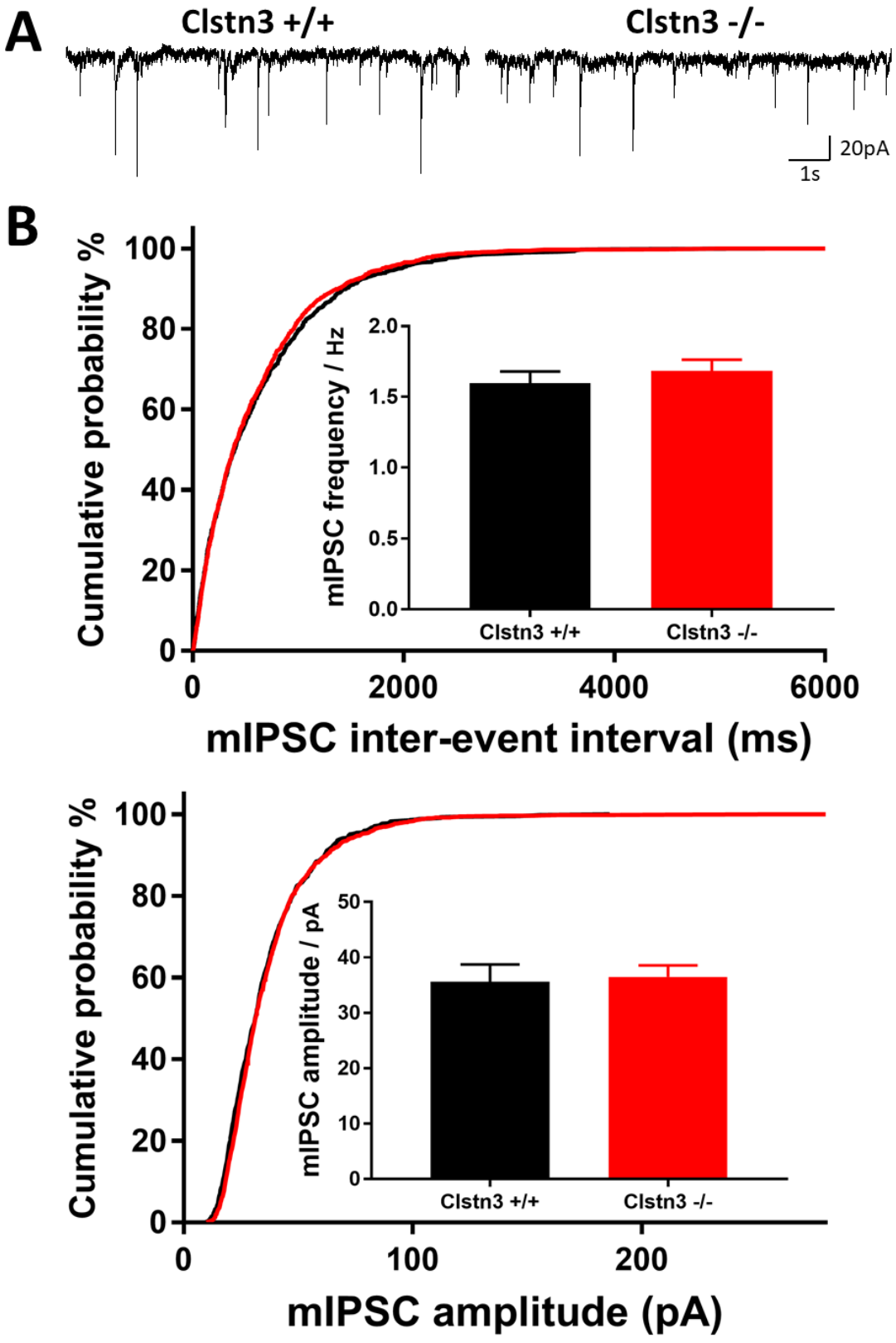
A
Clstn3 +/+
Clstn3 -/-
20pA
1s
B
Cumulative probability %
100
80
60
40
20
0
0
2000
4000
6000
mIPSC inter-event interval (ms)
mIPSC frequency / Hz
2.0
1.5
1.0
0.5
0.0
Clstn3 +/+
Clstn3 -/-
Cumulative probability %
100
80
60
40
20
0
0
100
200
mIPSC amplitude (pA)
mIPSC amplitude / pA
50
40
30
20
10
0
Clstn3 +/+
Clstn3 -/-

Figure 3.10 Basal inhibitory transmission is not changed in juvenile *Clstn3* global knockout mice

A. Representative mIPSC recordings from hippocampal CA1 pyramidal neurons from P15-16 *Clstn3+/+ and Clstn3-/-* mice.

B. Cumulative distributions of mIPSC inter-event intervals and amplitudes in hippocampal neurons from P15-16 *Clstn3+/+ and Clstn3-/-* mice. Insets display mean ± SEM for mIPSC frequency and amplitude. (Student's t test, $p > 0.05$. n = 9 cells for Clstn3+/+ and n = 13 cells for Clstn3-/-).

As summarized in table 3.1, we conclude that calsyntenin-3 regulates basal synaptic transmission from the postsynaptic side, but the effect differs from system to system, depending on the age, manipulated neuron types and whether the deletion is sparse or global. Future studies will be required to fully decipher the function of calsyntenin-3 and will be suggested in the discussion.

All CA1 cells	***Clstn3-/-* Global**	***Clstn3-/-* global**	***Clstn3*$^{f/f}$ Dlx5/6-Cre**	***Clstn3*$^{f/f}$ Gpr26-Cre**	***Clstn3*$^{f/f}$ Mouse AAV-Cre (Sparse)**	***Clstn3*$^{f/f}$ Culture AAV-Cre (~50%)**
age	2wk	6-10 wk	6-8 wk	6-8 wk	2 wk	14 DIV
mIPSC amplitude	No diff	No diff	No diff	Increased	No diff	No diff
mIPSC frequency	No diff	reduced	No diff	No diff	Increased	Tend to be increased
Inhibitory synapse number		Reduced (EM)				Increased
mEPSC amplitude		No diff		No diff		
mEPSC frequency		reduced		Increased		
Excitatory synapse number		Reduced (EM)				No diff

Table 3.1 Summary of electrophysiology recordings from *Clstn3* knockout and conditional knockout mice and culture

3.5 Discussion

In this Chapter, I examined calsyntenin-3's function in regulating basal synaptic transmission using cell type-specific deletion. We concluded that calsyntenin-3 does not play an essential role in the presynaptic side of inhibitory synapses, based on the recordings from *Clstn3*$^{f/f}$; Dlx5/6-Cre mice. Rather, calsyntenin-3 does affect basal transmission of both inhibitory and excitatory synapses from the postsynaptic side, based on the recordings on Gpr26-Cre dependent conditional *Clstn3* knockout mice and AAV-inducted sparse *Clstn3* knockout mice. Whether calsyntenin-3 has any specific effect on the presynaptic side of excitatory synapses was not studied yet and may be evaluated by recording mEPSCs from subiculum neurons from *Clstn3*$^{f/f}$; Gpr26-Cre mice. Besides the conditional knockout mice, the global knockout and culture studies show a mixture of presynaptic and postsynaptic effects. Additionally in each condition, there are differences related to the time of recording (age of mice or primary culture), and knockout pattern (global or sparse).

3.5.1 Calsyntenin-3 functions in different stages of synapse development

In the central nervous system, synapses are formed mostly during embryonic and postnatal periods (in mice, before birth until about P14 to 21), while synaptic specification, maturation, and elimination mostly happen during puberty or post pubescent periods and continue throughout life (Südhof, 2018). Synaptic adhesion molecules play important roles throughout the entirety of these processes, but their effect could also be transient. For example, NP1/2 knockouts exhibited reduced clustering of GluR4 in hippocampus (Sia et al., 2007) as well as reduced AMPA-mediated but normal NMDA-mediated retinogeniculate transmission

during early postnatal days. But in adulthood, the affected retinogeniculate transmission not only recovered in NP1/2 knockouts but eventually became excessive (Koch and Ullian, 2010).

I did not observe any difference in mIPSC frequency or amplitude when recording the global calsyntenin-3 knockout mice at 2 weeks, but another colleague did notice a reduction in mIPSC frequency at 6-10 weeks, suggesting that as an overall effect, caslyntenin-3 does not affect synapse formation but rather regulates synapse maintenance. Similarly, a previous study on global neuroligin-1/2/3 triple knockout culture observed that inhibitory puncta density was not changed in DIV14-16 neurons but was significantly reduced in DIV28 neurons (Chanda et al., 2017).

We also have unpublished results showing identical fEPSP input-output curves for *Clstn3-/-* and *Clstn3+/+* mice at 2-3 weeks (data not shown). In young adult mice, however, fEPSP responses were significantly stronger in *Clstn3−/−* than in *Clstn3+/+* littermate controls (Pettem et al., 2013). This difference in input-output curves is consistent with our observations pertaining to mIPSC frequencies. To further investigate calsyntenin-3's function in synapse maturation and maintenance, one can use a global Cre mouse line with a later point of activation or an inducible Cre line.

3.5.2 The discrepancy in function of postsynaptic calsyntenin-3

It has been known for a while now that hippocampal principal cells differ from dorsal to ventral and from proximal to distal (Cenquizca and Swanson, 2007; Kaifosh and Losonczy, 2016; Slomianka et al., 2011). In recent years, thanks to advances in single-cell RNA-seq and seqFISH technology, another axis of laminar organization within the CA1 region has been recognized: the stratum pyramidale (s.p.) deep and superficial (Cembrowski et al., 2016; Shah et

al., 2016). There are developmental, genetic, morphological, and intrinsic electrophysiological differences between the deep and superficial pyramidal neurons which exhibit biased micro-circuits and afferent–efferent connectivity within and outside the hippocampus (reviewed in Soltesz and Losonczy, 2018). The miniature recordings shown in Figure 2.17 for *Clstn3* global knockout mice were performed through blind random patching in the whole CA1 region, while the recordings I did for the Gpr26-Cre dependent *Clstn3* conditional knockout were performed by visualized patching only in the deep layer of dorsal CA1. The heterogeneity of the recordings on the global *Clstn3* knockout mice may have just concealed the real differences from a certain subtype of cells.

Besides the technical difference, in the global *Clstn3* knockout mice, all the cells lack calsyntenin-3 from embryonic day 1, while in the Gpr-26 dependent conditional knockout, all cells outside of the CA1 s.p. deep layer still express calsyntenin-3, including all the interneurons. Based on Chapter 2, calsyntenin-3 plays an overall promoting role in terms of synaptic development, when the effect of both the full-length and secreted forms, from both interneurons and excitatory neurons are all combined. Conversely, in the conditional knockout mice, things are more complicated.

First, while the full-length calsyntenin-3 is eliminated in the Cre-expressing cells, secreted form of calsyntenin-3 from neighboring cells could be accumulating at/near the synaptic clefts, as the excitatory synapses onto pyramidal neurons are mixed together in the stratum radiatum and oriens. I hypothesized that the full-length calsyntenin-3 is promoting while its secreted form is inhibiting synapse development in Chapter 2, but have not yet been able to conclude anything *in vivo*.

Second, expression of calsyntenin-3 in the s.p. deep layer cells is only diminished later in development. According to Allen Brain Atlas Mouse Connectivity, there is almost no Cre expression in CA1 in the Gpr26-Cre line at P4. Although the expression is high at P14, we do not know for sure whether calsyntenin-3 is expressed or not between P4 and P14 which is exactly the critical time window for synapse formation. It is possible that calsyntenin-3 mediates both synapse formation and elimination; thus in the conditional knockout mice, calsyntenin-3 is present during the formation period but eliminated during the elimination period, resulting in overall up-regulated development.

Lastly, competition may exist between the postsynaptic sites with calsyntenin-3 and those without in the conditional *Clstn3* knockout mice. Previous study has shown that only sparse knockdown but not global knockout of neuroligin-1 leads to lower density of excitatory synapses and spines (Kwon et al., 2012). In the case of conditional *Clstn3* knockout cells, absence of calsyntenin-3 frees up presynaptic neurexins which may then have more availability for other postsynaptic partners (such as neuroligins and LRRTMs) compared with neighboring postsynaptic sites presented with calsyntenin-3. This leads to higher synapse density and/or stronger basal synaptic transmission in the conditional knockout cells. This is a reasonable speculation based on the assumptions that calsyntenin-3 possibly competes with neuroligins and LRRTMs for binding to neurexins (Figure 2.5); the binding affinity of calsyntenin-3 is lower than that of neuroligins and LRRTMs (Figure 2.1, Siddiqui et al., 2010); and calsyntenin-3 is less capable than neuroligins and LRRTMs in recruiting postsynaptic receptors.

3.5.3 Function of Calsyntenin-3 in interneurons

The expression level of calsyntenin-3 in interneurons is much higher than in excitatory neurons (Figure 2.14). But the mIPSC recordings in the pyramidal neurons of *Clstn3*$^{f/f}$; Dlx5/6-Cre conditional knockout mice suggested that calsyntenin-3 does not play an essential role in the presynaptic side of inhibitory synapses, at least not in spontaneous basal transmission. Future experiments such as interneuron recordings are required to determine the function of calsyntenin-3 in these cells from the postsynaptic side.

We have attempted to cross the interneuron conditional knockout mice with a reporter line G42-GFP (CB6-Tg(Gad1-EGFP)G42Zjh/J), which expresses GFP in a subset of parvalbumin-positive interneurons (Chattopadhyaya et al., 2004). However, during the initial characterization, we found there are only up to five GFP-positive cells per acute hippocampal slice in the CA1 region in these triple transgenic mice, which are not always the most healthy ones to patch onto (data not shown), consistent with a previous study (Cabezas et al., 2013). We gave up this approach since it would produce an enormous surplus of animals for the quantitative analyses.

Another possible strategy is to inject AAV9-DIO-GFP in these Clstn3$^{f/f}$; Dlx5a-Cre conditional knockout mice and record the GFP-positive neurons, but due to the expression pattern of Dlx5a-Cre, all interneuron subtypes in the forebrain were labeled and the heterogeneity of electrophysiological properties prevents an accurate explanation of the results. To avoid this heterogeneity, I have also double stained GAD67 (labeling all interneurons) and Parvalbumin in CA1 stratum oriens to estimate the fraction of parvalbumin-positive interneurons in this region. Parvalbumin-positive interneurons counted for more than 70% of all the interneurons there, and if I exclude GAD67+/Parv- interneurons close to the upper edge of oriens

(near the cortex), parv+ ones counted for about 90% (from 18 images, 6 slices, 2 adult animals). Thus, recording from the GFP-positive cells within this region might be good enough to hit most parvalbumin-positive fast spiking interneurons. Alternatively, the recording pipette could be filled with biocytin and the slice could be fixed and double stained with parvalbumin after recording.

3.5.4 Calsyntenin-3 function in synaptic plasticity

In Chapters 2 and 3, we showed that calsyntenin-3 regulates synapse number and basal synaptic transmission, but more and more literature have been suggesting that synaptic adhesion molecules are involved in more processes beyond synapse formation. For example, genetic deletion of neuroligins preferentially caused a decrease in NMDAR-mediated responses in cultured hippocampal neurons (Chubykin et al., 2007) and that conditional deletion of neuroligins from hippocampal CA1 pyramidal neurons *in vivo* blocked NMDAR-dependent LTP and simultaneously reduced the ratio of NMDAR- to AMPAR-mediated EPSCs (Jiang et al., 2017; Wu et al., 2019). In contrast, genetic deletion of LRRTM1 and 2 *in vivo* in CA1 neurons dramatically impaired LTP and caused a decrease in AMPAR-mediated, but not NMDAR-mediated, synaptic transmission (Bhouri et al., 2018).

For the calsyntenins family, basal excitatory synaptic transmission is decreased in juvenile *Clstn1-/-* mice, while levels of GluN2B subunit-containing NMDA receptors and NMDA receptor-dependent LTP are increased compared with wild type controls, changes which are not observed after adulthood (Ster et al., 2014). Unpublished data from Dr. Bo Gong shows that hippocampal CA1 LTP is impaired in juvenile *Clstn3-/-* mice but not in young adult mice. GABA antagonist picrotoxin was unable to rescue the LTP in knockout mice, indicating the

effect is not due to acute changes in inhibitory synapses, consistent with Figure 3.10. Evoked NMDAR responses and LTD were both intact in these mice. It is possible that the changes in synaptic plasticity in juvenile Clstn3-/- mice are related to a lack of activity dependent cleavage of calsyntenin-3. In the wildtype mice, cleavage of calsyntenin-3 may lead to endocytosis and turnover of coupling proteins in the postsynaptic density thus creating insertion sites for receptors.

Chapter 4: Germline recombination of multiple "brain-specific" Cre lines

4.1 Introduction

Advances in modern neuroscience research rely on transgenic animal models incorporating site-specific recombinase technology to achieve gene manipulations in a spatially and temporally controlled manner. Among all genetic tools, the Cre-loxP system has arguably been the most frequently used approach since it was first discovered in bacteriophage P1 (Sternberg and Hamilton, 1981) and harnessed for genetic manipulations in mammalian cells (Sauer and Henderson, 1988) and in transgenic mice (Gu et al., 1994; Tsien et al., 1996a). Cre recombinase recognizes a 34 bp loxP site, mediating deletion of DNA between inverted loxP sites, and mediating inversion of DNA between loxP sites of the same orientation. Manipulation of genetic material flanked by loxP sites, in floxed genes, has been facilitated by the large-scale generation of mouse Cre driver lines with diverse expression patterns in the nervous system (Daigle et al., 2018; Gerfen et al., 2013; Taniguchi et al., 2011). Thus, the Cre-loxP system has become a mainstay for conditional gene knockout and knock-in in mice, and recently in rats (Bäck et al., 2019; Witten et al., 2011). However, several caveats have been noted, including Cre-mediated toxicity and metabolic phenotypes due to illegitimate recombination, mosaic and/or inconsistent recombination activity, and unexpected expression of Cre in unwanted cell types (Harno et al., 2013; Murray et al., 2012; Schmidt et al., 2000; Tachibana et al., 2018; Wojcinski et al., 2019).

A particularly under-appreciated and limiting caveat in terms of major unwanted consequences is non-intentional germline recombination from Cre driver lines. When Cre expression and associated recombinase activity occur in germ cells, the excised floxed allele will be present in all cells instead of in the region- and cell-type- specific patterns that we normally anticipate. A recent review describes how unexpected germline recombination could happen and

how to detect such events (Song and Palmiter, 2018), but information about affected Cre driver lines has been overwhelmingly scarce, with only a few sporadic reports (Choi et al., 2014a; Kobayashi and Hensch, 2013a; Liput, 2018; Zhang et al., 2013a). Awareness of the occurrence of germline recombination in "nervous system-specific" Cre driver lines is essential to avoid mistakes in genotyping and data interpretation. Furthermore, beyond simple awareness, information about parental gender effects on germline recombination in specific Cre driver lines could guide optimal breeding schemes to save researchers valuable time and resources. Yet such a meta-analysis has been lacking.

Therefore, we used two Cre lines, Dlx5/6-Cre and Gpr26-Cre expressing in different neuron populations, as examples to demonstrate unexpected germline recombination occurring selectively in either the female or male Cre-carrying parents, respectively. To generate a more comprehensive resource, we compiled information on germline recombination frequencies from a total of 57 different Cre driver lines commonly used for nervous system-specific genetic manipulations. We hope that our short report will serve as a collective resource to guide optimal usage of Cre driver lines.

4.2 Methods

4.2.1 Animals

All animal experiments were performed in compliance with provincial and institutional guidelines. Clstn3$^{f/f}$ mice were generated in our lab and described before (Pettem et al., 2013). Ai32 mice (Jax # 012569) were a kind gift from Dr. Timothy Murphy (Madisen et al., 2012). All Cre lines used are described in Tables 4.3 and 4.4.

4.2.2 Genotyping

Genotyping was done via PCR using P8-10 tail tissue, with primers used in Table 4.1.

Primer name	5’ to 3’ sequence	Length of product
Clstn3F	GTACCGGTTATGATTGTATTCTCTTGGGTGTGGGGATG	Flox: 413bp
Clstn3R	CAAGAGTAGAGCCCAGTTTCCTGAAATCTCAGTCGTTTAC	WT: 315bp
Clstn3KO-F	GTACCGGTTATGATTGTATTCTCTTGGGTGTGGGGATG	332bp
Clstn3KO-R	GAGGAGGTACTTGGAATGGGTCT	
Cre-F	GCGGTCTGGCAGTAAAAACTATC	~100bp
Cre-R	GTGAAACAGCATTGCTGTCACTT	
Ai32-tg-F	ACATGGTCCTGCTGGAGTTC	253bp
Ai32-tg-R	GGCATTAAAGCAGCGTATCC	
Ai32-WT-F	AAGGGAGCTGCAGTGGAGTA	297bp
Ai32-WT-R	CCGAAAATCTGTGGGAAGTC	
Ai32-LSL-F	TCTGGATCCCCATCAAGCTG	88bp
Ai32-LSL-R	TGCAGGTCGAGGGACCTAAT	

Table 4.1 Primers used for genotyping in Chapter 4

4.2.3 Immunofluorescence

Offspring from Ai32 crosses were euthanized at P14-16, and brains extracted and sectioned in ice cold artificial cerebrospinal fluid (ACSF) containing (in mM): 124 NaCl, 3 KCl, 1.25 NaH2PO4, 1 MgSO47H2O, 2 CaCl2, 26 NaHCO3 and 15 D-glucose which was bubbled continuously with carbogen (95% O2/ 5% CO2) to adjust the pH to 7.3. 300µm slices were then recovered in 31℃ ACSF for 20 min and fixed in 4 % paraformaldehyde + 4% sucrose in PBS (pH 7.4) for 12 min. They were then washed in PBS containing the nuclear counterstain DAPI (4’, 6 diamidino-2- phenylindole), and mounted in elvanol (Tris-HCl, glycerol, and polyvinyl

alcohol with 2% 1, 4-diazabicyclo[2, 2, 2]octane). Tiled and individual images were captured on a Zeiss LSM 700 confocal microscope.

4.3 Results

4.3.1 Dlx5/6-Cre shows unexpected maternal germline recombination when crossed with *Clstn3$^{f/f}$* mice

The Dlx5/6-Cre line (Tg(dlx5a-cre)1Mekk) was generated in 2000 (Zerucha et al., 2000) and has been used in over 70 papers to specifically target forebrain interneurons according to Jackson Laboratory's Mouse Genome Informatics database. We combined this transgene with the *Clstn3$^{f/f}$* (B6-Clstn3^{tm1Amcr}/J) allele (Pettem et al., 2013) then crossed *Clstn3$^{f/f}$*; Dlx5/6-Cre with *Clstn3$^{f/f}$* mice, a typical approach to generate experimental conditional knockout animals. We genotyped the offspring with one set of primers for *Clstn3* floxed and wild type alleles, a second set for *Clstn3* knockout, and a third set for Cre using tail tissue. We expected to observe only the *Clstn3* floxed band (no wild type or knockout) regardless of Cre. Yet 88% (73/83) of the offspring expressed a *Clstn3* knockout allele when the female parent carried Cre, while not one of the 52 offspring we tested had the knockout allele when the Cre recombinase was from the male parent (Figure 4.1). Thus, a high fraction of female mice carrying the Dlx5/6-Cre and floxed genes apparently expressed Cre in the female germ cells resulting in maternal germline recombination. This unexpected germline deletion could be circumvented by transmitting Cre strictly paternally. Note that during the crosses to combine the Cre and floxed genes, the first cross of *Clstn3$^{f/f}$* with Dlx5/6-Cre mice would not be problematic as the Cre transgene and floxed allele would not be together in germ cells, but the second cross using *Clstn3$^{f/+}$*; Dlx5/6-Cre mice would also be susceptible to maternal germline recombination.

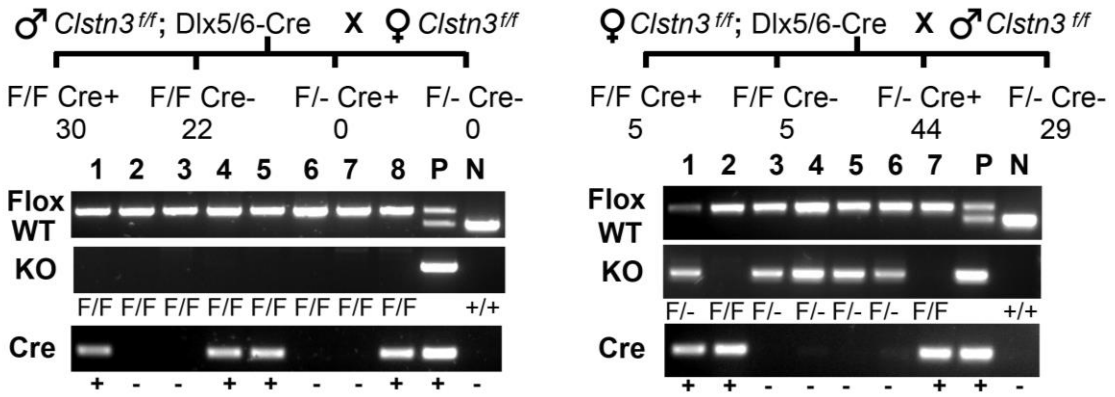

Figure 4.1 Dlx5/6-Cre shows maternal germline recombination when crossed with *Clstn3$^{f/f}$* mice

Pedigree and sample genotyping results of offspring when *Clstn3$^{f/f}$*; Dlx5/6-Cre mice were crossed with Clstn3$^{f/f}$. The Cre recombinase came from either the male or female parent. F/F Cre+ indicates Clstn3$^{f/f}$; Dlx5/6-Cre; F/F Cre- indicates *Clstn3$^{f/f}$* without Cre; F/- Cre+ indicates *Clstn3$^{f/-}$*; Dlx5/6-Cre in which germline recombination has occurred resulting in a global knockout allele; F/- Cre- indicates *Clstn3$^{f/-}$* without Cre in which germline recombination has occurred resulting in a global knockout allele, P and N indicate controls. Numbers below genotypes indicate the total number of offspring obtained with that genotype.

4.3.2 Dlx5/6-Cre shows maternal germline recombination when crossed Ai32 reporter mice

To test whether this maternal germline recombination is locus-specific, we crossed the Dlx5/6-Cre mice with an Ai32 reporter line (B6;129S-Gt(ROSA)26Sor $^{tm32(CAG-COP4*H134R/EYFP)Hze}$/J) (Madisen et al., 2012). The Ai32 mouse line contains a LoxP – stop codons – three SV40 poly(A) sequences – LoxP – EYFP-ChR2 – WPRE – bGH poly(A) – AttB – PGK promoter – FRT – Neo – PGK poly(A) – AttP cassette at the Rosa 26 locus. The genotyping method provided by Jackson lab targets the EYFP and WPRE sequences, so it cannot distinguish the transgene before and after recombination. Therefore, we designed a new primer set targeting the loxP-stop-loxP-EYFP region, with the forward primer targeting the stop cassette that would

be deleted by Cre recombinase. Thus, PCR product with these primers is present in the tail tissue of transgenic mice without Cre-dependent recombination ("LSL-tg" in Fig 4.2A) and absent in mice with germline recombination ("tg" in Fig 4.2A). When female $Rosa^{LSL\text{-}tg/+}$; Dlx5/6-Cre mice were crossed with male wild type mice, 46.2% (18/39) of offspring with the transgene had a recombined tg allele instead of the original LSL-tg (Figure 4.2A). In contrast, no germline recombination was observed when male $Rosa^{LSL\text{-}tg/+}$; Dlx5/6-Cre mice were crossed with female wild type mice (0/33 offspring with the transgene). This germline recombination activity in female but not male germ cells is consistent with the finding from the $Clstn3^{f/f}$ crosses. However, the recombination frequencies differed per target allele (46.2% for $Rosa^{LSL\text{-}tg}$ and 88.0% for $Clstn3^{f}$ even after accounting for differences in the breeding schemes), perhaps related to differences in chromosomal location or the length of loxP-flanked sequences (Liu et al., 2013; Zheng et al., 2000).

To support the PCR results with Dlx5/6-Cre and the Ai32 reporter, we confirmed germline versus local Cre recombination by fluorescence imaging for expression of the Cre-dependent transgene EYFP-channelrhodopsin2 (EYFP-ChR2; Figure 4.2B-D). $Rosa^{LSL\text{-}tg/+}$ mice showed no EYFP signal above background levels. $Rosa^{LSL\text{-}tg/+}$; Dlx5/6-Cre mice showed a pattern of EYFP-ChR2 consistent with expression in axons and dendrites of interneurons, as expected. For example, expression was high in inhibitory axon inputs to stratum pyramidale in hippocampal CA1 and CA3 regions, low in the CA3 stratum lucidum region rich in excitatory synapses, and not detectable in non-neuronal cells. When germline recombination happened, the $Rosa^{tg/+}$; Dlx5/6-Cre offspring showed a ubiquitous EYFP-ChR2 expression pattern spanning all brain regions in all cell types, including neurons, glia cells, and blood vessels (Figure 4.2B-D). Note that the laser power for the EYFP channel used to image the recombined mouse

hippocampus was only 15% of that for the other two genotypes. Cre-negative *Rosa*$^{tg/+}$ mice showed the same phenotype as *Rosa*$^{tg/+}$; Dlx5/6-Cre (data not shown).

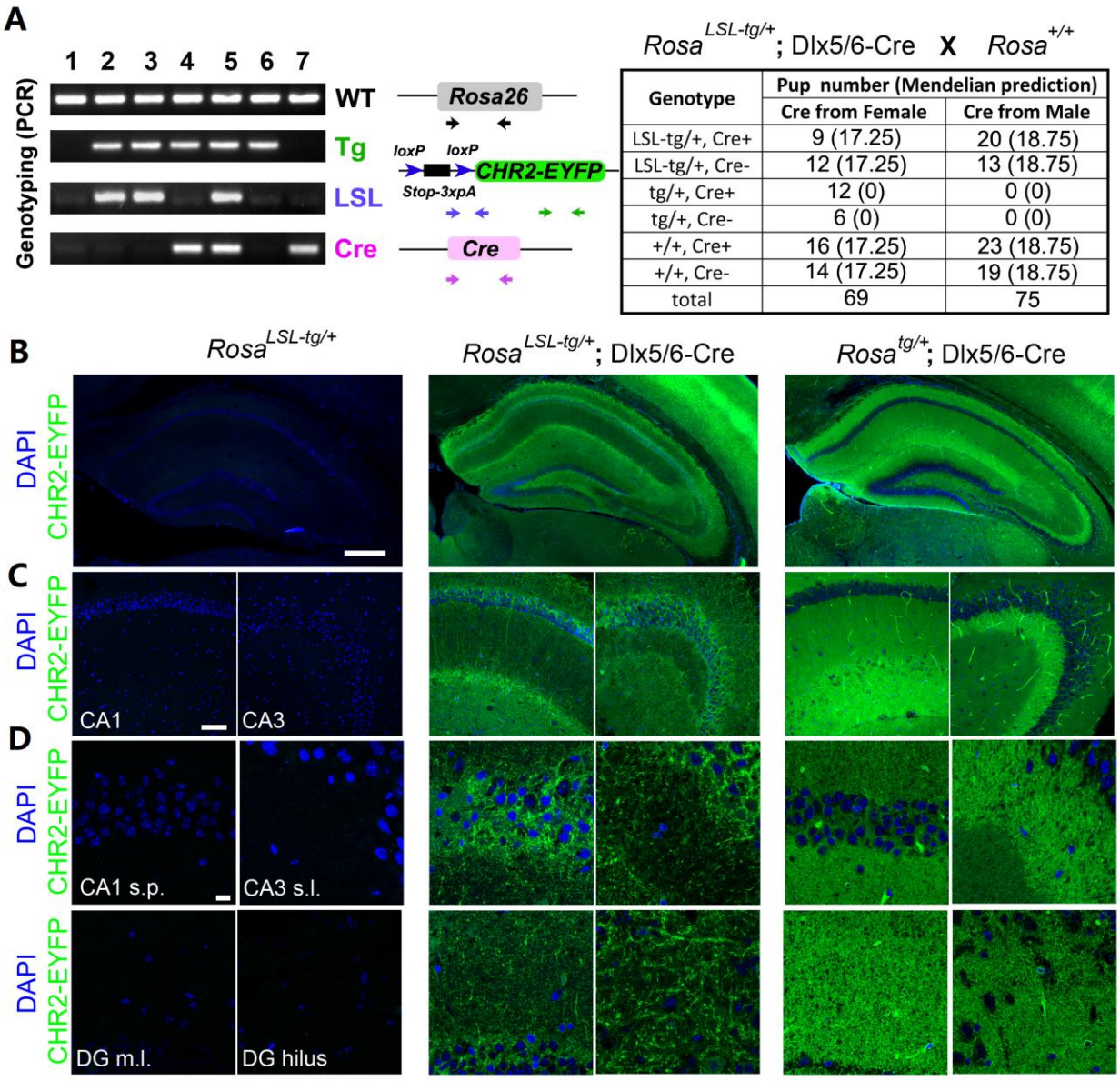

Genotype	Pup number (Mendelian prediction)	
	Cre from Female	Cre from Male
LSL-tg/+, Cre+	9 (17.25)	20 (18.75)
LSL-tg/+, Cre-	12 (17.25)	13 (18.75)
tg/+, Cre+	12 (0)	0 (0)
tg/+, Cre-	6 (0)	0 (0)
+/+, Cre+	16 (17.25)	23 (18.75)
+/+, Cre-	14 (17.25)	19 (18.75)
total	69	75

Figure 4.2 Dlx5/6-Cre shows maternal germline recombination when crossed Ai32 reporter mice

A. Sample genotyping results and offspring numbers when Gt(ROSA)26Sor$^{tm32(CAG-COP4*H134R/EYFP)Hze}$/J reporter line mice were crossed with Dlx5/6-Cre. LSL-tg indicates lox-stop-lox sequences before the transgene channelrhodopsin-2(H134R)-EYFP (CHR2-EYFP) on the Rosa locus; tg indicates Rosa

transgene after germline recombination by Cre resulting in global transgene expression. Genotypes of the animals are: 1, +/+, Cre-; 2&3, LSL-tg/+, Cre-; 4, tg/+, Cre+; 5, LSL-tg/+, Cre+; 6, tg/+, Cre-; 7, +/+, Cre+.

B-D. Tiled images of the hippocampus (B) and sample CA1 and CA3 regions (C) showing CHR2-EYFP transgene expression and DAPI nuclear stain for selected offspring from panel A. Further zoomed in images are shown for hippocampal CA1 stratum pyramidale (s.p.), CA3 stratum lucidum (s.l.), dentate gyrus molecular layer (DG m.l.), and dentate gyrus hilus regions (D). Note that the laser power used for the EYFP channel in the far right panel for images from *Rosa26*$^{tg/+}$; Dlx5/6-Cre mice was only 15% of that for the rest. Scale bars = 500 μm (B); 100 μm (C); 20 μm (D).

4.3.3 Gpr26-Cre shows unexpected paternal germline recombination when crossed with *Clstn3*$^{f/f}$ mice

Given the experience with Dlx5/6-Cre and the recommendations on the Jackson Labs website: "For many *cre* strains, but not all, using *cre*-positive **males** for breeding avoids potential germline deletion of your *loxP*-flanked allele."(https://www.jax.org/news-and-insights/jax-blog/2016/may/are-your-cre-lox-mice-deleting-what-you-think-they-are), we stuck to the breeding strategy of keeping Cre recombinase transmitted paternally. However, we found that Gpr26-Cre showed selective paternal germline recombination, indicating that there is no single optimal breeding strategy to fit all Cre lines.

Gpr26-Cre (Tg(Gpr26-cre)KO250Gsat/Mmucd) was generated by the GENSAT project (http://gensat.org/) and displays specific CA1 expression in hippocampus and sparse expression in other brain regions, including layer V cortex and thalamus (Gerfen et al., 2013; Harris et al., 2014). We chose this line for its specific expression in CA1 pyramidal neurons, which actually turned out to be only in the deep sublayer (near stratum oriens) but not the superficial sublayer of CA1 stratum pyramidale in our characterization (data not shown and Figure 4.4). We observed

germline deletion when crossing *Clstn3*$^{f/f}$; Gpr26-Cre with *Clstn3*$^{f/f}$ mice, only this time germline recombination was dependent on the expression of paternal Cre as opposed to maternal Cre (Figure 4.3).

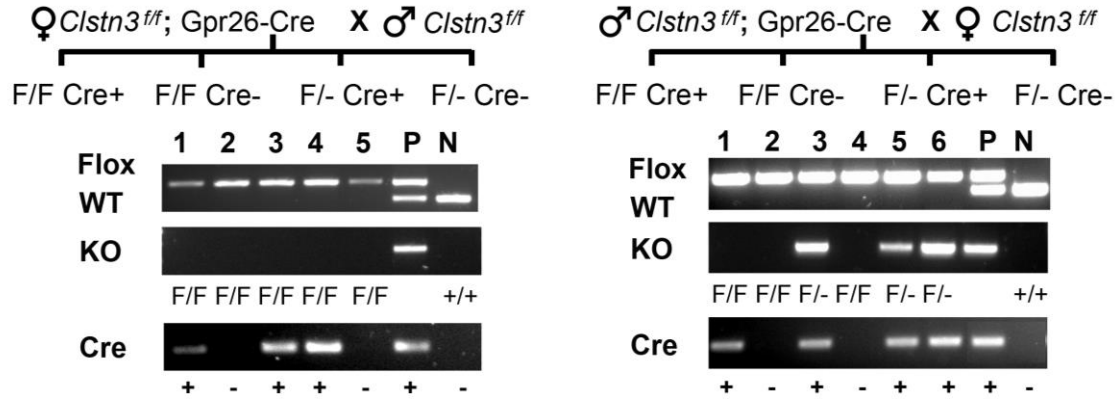

Figure 4.3 Gpr26-Cre shows paternal germline recombination in offspring when crossed with *Clstn3*$^{f/f}$ mice

Pedigree and sample genotyping results of offspring when *Clstn3*$^{f/f}$; Gpr26-Cre mice were crossed with *Clstn3*$^{f/f}$. The Cre recombinase came from either the male or female parent. F/F Cre+ indicates *Clstn3*$^{f/f}$; Gpr26-Cre; F/F Cre- indicates *Clstn3*$^{f/f}$ without Cre; F/- Cre+ indicates *Clstn3*$^{f/-}$; Gpr26-Cre in which germline recombination has occurred resulting in a global knockout allele; F/- Cre- indicates *Clstn3*$^{f/-}$ without Cre in which germline recombination has occurred resulting in a global knockout allele, P and N indicate controls.

4.3.4 Gpr26-Cre shows paternal germline recombination in offspring when crossed Ai32 reporter mice

To test whether selective paternal germline recombination also occurs with another target locus, we crossed Gpr26-Cre mice with the Ai32 reporter line and assessed F2 progeny with PCR genotyping of tail tissue and EYFP-ChR2 imaging of brain sections. When male *Rosa*$^{LSL\text{-}tg/+}$; Gpr26-Cre mice were crossed with wild type females, 27.6% (8/29) of the offspring with the transgene had a recombined allele, whereas when Cre was transmitted through the female parent, all the loxP-stop-loxP sequences remained intact (Figure 4.4A). As expected, *Rosa*$^{LSL\text{-}tg/+}$mice

showed no EYFP signal above background levels, and *Rosa*$^{LSL\text{-}tg/+}$; Gpr26-Cre mice expressed EYFP-ChR2 specifically in the hippocampal CA1 region with weak expression in the cortex (Figure 4.4B-D). In contrast, for animals with germline recombination, i.e. *Rosa*$^{tg/+}$ mice, EYFP-ChR2 was expressed globally. In the hippocampus, *Rosa*$^{LSL\text{-}tg/+}$; Gpr26-Cre mice had strong EYFP-ChR2 expression in the CA1 stratum radiatum and oriens layers but not in CA3, while *Rosa*$^{tg/+}$ mice had EYFP expression in both regions and in all cell types, including non-neuronal cells such as blood vessels (Figure 4.4).

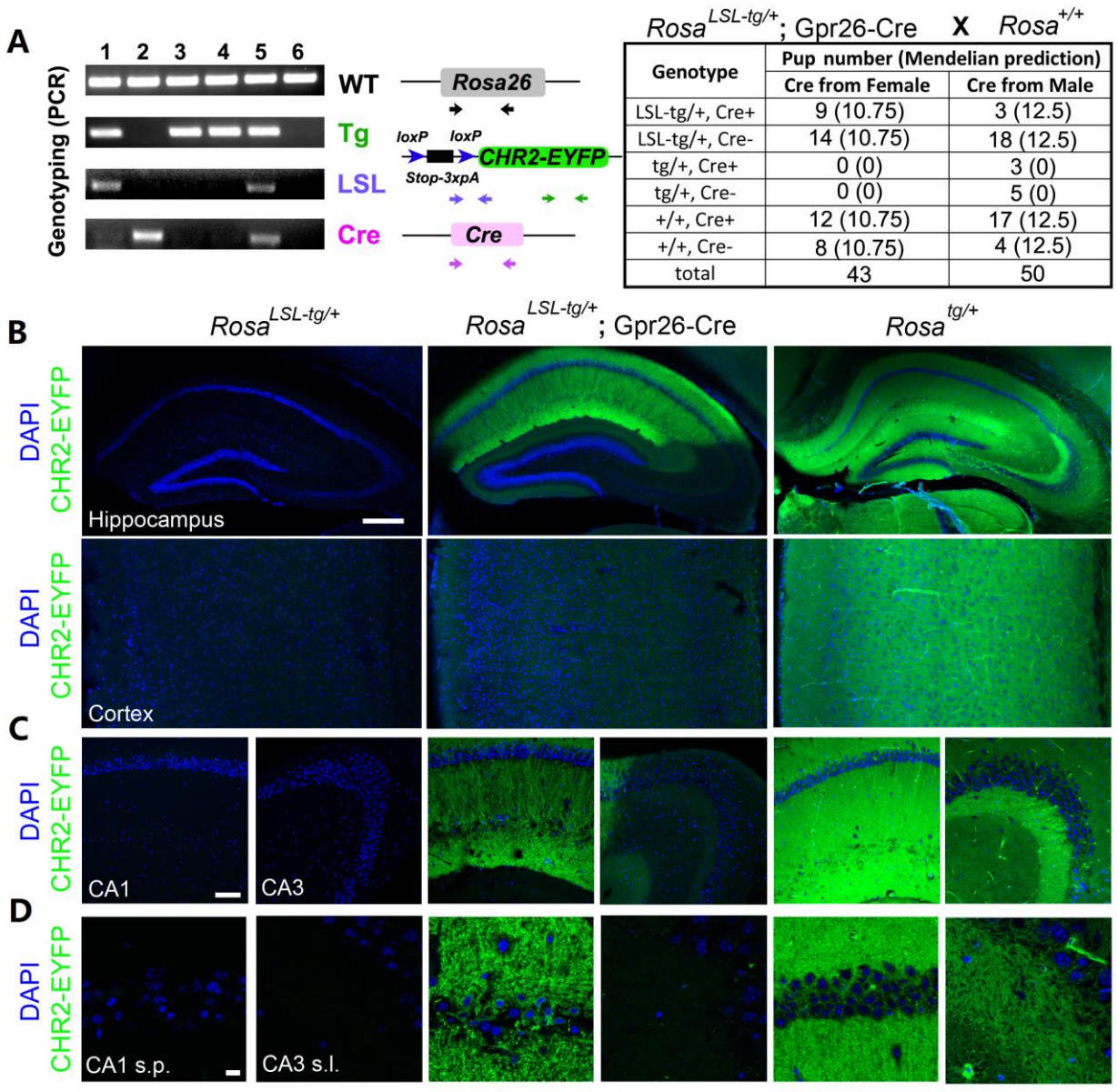

$Rosa^{LSL\text{-}tg/+}$; Gpr26-Cre X $Rosa^{+/+}$

Genotype	Pup number (Mendelian prediction)	
	Cre from Female	Cre from Male
LSL-tg/+, Cre+	9 (10.75)	3 (12.5)
LSL-tg/+, Cre-	14 (10.75)	18 (12.5)
tg/+, Cre+	0 (0)	3 (0)
tg/+, Cre-	0 (0)	5 (0)
+/+, Cre+	12 (10.75)	17 (12.5)
+/+, Cre-	8 (10.75)	4 (12.5)
total	43	50

Figure 4.4 Gpr26-Cre shows paternal germline recombination when crossed Ai32 reporter mice

A. Sample genotyping results and offspring numbers when Gt(ROSA)26Sor$^{tm32(CAG\text{-}COP4*H134R/EYFP)Hze}$/J reporter line mice were crossed with Gpr26-Cre. LSL-tg indicates lox-stop-lox sequences before the transgene channelrhodopsin-2(H134R)-EYFP (CHR2-EYFP) on the Rosa locus; tg indicates Rosa transgene after germline recombination by Cre resulting in global transgene expression. Genotypes of the animals are: 1, LSL-tg/+, Cre-; 2, +/+, Cre+; 3&4, tg/+, Cre-; 5, LSL-tg/+, Cre+; 6, +/+, Cre-.

B-D. Tiled images of the hippocampus and cortex (B) and sample CA1 and CA3 regions (C) showing CHR2-EYFP transgene expression and DAPI nuclear stain for selected offspring from panel B. Further zoomed in images are shown for hippocampal CA1 stratum pyramidale (s.p.) and CA3 stratum lucidum (s.l.) (D). Note that the laser power used for the EYFP channel in the far right panel for images from *Rosa*$^{tg/+}$ mice was only 15% of that for the rest. Scale bars = 500 μm (B); 100 μm (C); 20 μm (D).

4.3.5 Literature review of germline recombination of nominally "nervous system-specific" Cre lines

As significant germline recombination happened in both of these Cre lines designed for gene knockout in specific neuron types, we wondered about the prevalence of this phenomenon in other Cre lines and thus turned to the current literature. To the best of our knowledge, there are only a handful of papers focused on germline recombination in Cre driver lines intended for nervous system-specific recombination (Kobayashi and Hensch, 2013a; Liput, 2018; Weng et al., 2008; Zhang et al., 2013a), and several other papers that mention this issue, typically in the methods, listed in Table 4.2. Lines reported to undergo significant germline recombination include the widely used Nestin-Cre, GFAP-Cre, CaMKIIα-Cre, and Synapsin1-Cre lines (Zhang et al., 2013; Choi et al., 2014; Rempe et al., 2006), which collectively were used in over 1500 papers according to Jackson Laboratory's Mouse Genome Informatics database. Furthermore, in this data collected from the literature, most (6/7) of the Cre driver lines tested showed a parental gender effect. We suspect that this data represents the tip of an iceberg, as for the majority of Cre driver lines information has not been readily available on either the extent of germline recombination or parental gender bias.

Cre line common name	Full Cre line name/source	Target gene /Reporter	Breeding strategy[1]	Germline recombination efficiency, Cre from father[2]	Germline recombination efficiency, Cre from mother[2]	Reference
CaMKIIα-Cre	B6.Cg-Tg(Camk2a-cre)2Szi/J	Lepr$^{tm1.1Chua}$	A	High	0	(McMinn et al., 2005)
		Chat/Slc18a3$^{tm1.2Vpra}$	A or C	High	ND	(Castro et al., 2009)
CaMKIIα-Cre	Tg(Camk2a-cre)93Kln	Gnao1	B	72.09% (31/43)	ND	(Choi et al., 2014a)
		B6;129S4-Gt(ROSA)26Sor^{tm1Sor}/J	B	98.5% (64/65)	ND	
Emx1-Cre	Emx1$^{tm1(cre)Ito}$	B6.129(FVB)-Gabra1^{tm1Geh}/J	A	36%	36%	(Zeller et al., 2008a)
GFAP-cre	Tg(GFAP-cre)25Mes	Gja1^{tm1Kwi}	C	16.67% (7/42) of Cre negative offspring	50% (8/16) of Cre negative offspring	(Zhang et al., 2013a)
Nestin-Cre	Tg(Nes-cre)1Kln/J	Gja1^{tm8Kwi}	Not specified	28.57% (4/14) of Cre negative offspring		
Nes-Cre1	Tg(Nes-cre)1Atp	Runx1	D	Observed in Cre negative offspring, frequency not reported		(Buchholz et al., 2000a)
Pcp2/L7-Cre	B6.129-Tg(Pcp2-cre)2Mpin/J	Tsc1$^{tm1.1Djk}$	A or E	~5%		(Tsai et al., 2012a)
Pou4f2-Cre	Pou4f2$^{tm1(cre)Bnt}$/J	Ai9[5]	B	100%	0	(Simmons et al., 2016a)
Pvalb-2A-Cre	B6.Cg-Pvalb$^{tm1.1(cre)Aibs}$/J	B6.129S4-*Clock*^{tm1Rep}/J	F	50% (24/48)	<5%	(Kobayashi and Hensch, 2013a)
Rgs9-cre	Rgs9$^{tm1(cre)Yql}$	B6.Cg-Rem2$^{tm3551(T2A-mkate2)Arte}$	A	7.6%	55.1%	(Liput, 2018)
Synapsin1-Cre	B6.Cg-Tg(Syn1-cre)671Jxm/J	Hif1a^{tm1Rsjo}	C	67%	0	(Rempe et al., 2006a)

Table 4.2 Lines that showed germline recombination, from the literature

[1]Breeding strategy:

A: Target$^{f/+}$; Promoter-Cre X Target$^{f/f}$

B: Target$^{f/+}$; Promoter-Cre X Target$^{+/+}$

C: Target$^{f/f}$; Promoter-Cre X Target$^{f/f}$

D: Target$^{f/f}$; Promoter-Cre X Target$^{+/+}$

E: Target$^{f/+}$; Promoter-Cre ⊗

F: Target$^{f/+}$; Promoter-Cre X Target$^{f/+}$

[2] The numbers (x/y) indicate that x offspring with germline recombination were found from y total offspring with the target locus in cumulative data from multiple litters. ND indicates not determined, crossings were not done in this configuration.

4.3.6 Collection of unpublished data on Cre line germline recombination frequencies from labs worldwide

A comprehensive resource of relevant information on Cre driver lines could be invaluable to mitigate undesired germline recombination by serving as a guide for choosing among similar Cre lines and for designing optimal breeding schemes. We thus gathered information from many laboratories to present new combined data on germline recombination rates and parental gender effects for Cre driver lines for neuroscience research. The collective data from all unpublished sources is reported in Table 4.3. The previously published lines listed in Table 4.2 are also integrated in Table 4.3 for easy comparisons of data from multiple sources for the same lines or related lines under drivers with common promoter elements.

Of the 58 Cre driver lines analyzed, just over half (56.9 %) exhibited germline recombination. Furthermore, of the 23 Cre driver lines for which information is available on parental gender effects, the majority (82.6%) showed a gender bias, with 52.2% demonstrating germline recombination solely or selectively through the male parent and 30.4% solely or

selectively through the female parent. These findings highlight the importance of assessing potential germline recombination for every mouse and the value of tracking parental gender bias towards optimizing breeding schemes to minimize unwanted germline recombination.

Different Cre driver lines with common promoter and enhancer elements may behave differently regarding germline recombination. Perhaps the most interesting comparison is for the pairs of Cre driver lines targeting common transcriptional regulatory elements by both random transgenic insertion and knockin approaches. For one such pair, Grik4-Cre, germline recombination was observed with both approaches. However, for two of these pairs, Pcp2/L7-Cre and VGAT/VIAAT-Cre, germline recombination was observed for the transgenic line but not the knockin line. While we cannot rule out differences related to target locus specificity, intrinsic differences between these related Cre driver lines seems likely. Factors contributing to germline recombination in the transgenic lines may include ectopic expression due to a limited regulatory region and/or transgene insertion site, and high expression due to mutli-copy integration (although the latter would not apply to the Pcp2/L7-Cre transgenic line which was generated through ES cells to avoid multi-copy integration (Barski et al., 2000)). Both Nestin-Cre transgenic lines showed germline recombination although information on frequencies is lacking. The four CaMKII-Cre transgenic lines were generated with similar targeting strategies (Tsien et al., 1996; Minichiello et al., 1999; Dragatsis and Zeitlin, 2000). While three showed only paternal germline recombination (one was not tested through the female parent), the fourth line also showed a lower rate of maternal germline recombination. Differences were also observed between the two Emx1-Cre knockin lines, with one showing equal paternal and maternal germline recombination and the other only maternal germline recombination. In comparing the two Pvalb-Cre knockin lines, Pvalb-IRES-Cre did not exhibit germline

recombination in multiple crosses from different labs, while Pvalb-2A-Cre showed germline recombination through both parents. These findings are consistent with the much stronger neuronal Cre activity in Pvalb-2A-Cre mice than in Pvalb-IRES-Cre mice (Madisen et al., 2010) and detection of Cre activity in spermatids of Pvalb-2A-Cre but not Pvalb-IRES-Cre mice (Kobayashi and Hensch, 2013a). Using tools such as an IRES to attenuate Cre expression may be beneficial for knockin driver lines where Cre expression in germ cells is lower than that in the nervous system. Song and Palmiter (2018) reported that they were able to reduce unwanted germline recombination in 2 of 3 attempts by generating a new Cre driver line with attenuated Cre expression by altering the codons, removing a nuclear localization signal, or adding destabilizing signals. For detailed descriptions and comparisons of the transgene/insertion constructs of these lines, see Appendix A.

The germline recombination prevalence could also depend on the specific target locus. Among the Cre driver lines crossed with multiple target loci, 65.5% (19/29) showed consistent results for all targets in terms of occurrence of germline recombination and parental gender bias where known. Quantitative data for multiple targets was available for only three of these lines, and all showed target-specific differences to some extent. As mentioned above, Dlx5/6-Cre showed nearly double the maternal germline recombination frequency for the *Clstn3*^{f} locus as for the Ai32 *Rosa*$^{LSL\text{-}tg}$ locus. CaMKIIα-Cre (T29-1) showed paternal germline recombination frequencies ranging from 21.4% to 31.3% for multiple target loci, while CaMKIIα-Cre (Tg(Camk2a-cre)93Kln) showed paternal germline recombination frequencies ranging from 72.1% to 98.5%. Furthermore, 20.7% (6/29) of the Cre driver lines showed germline recombination at some target loci but not others. These lines showing target locus-dependent recombination were Gad2-IRES-Cre (B6.Cg-Gad2$^{tm2(cre)Zjh}$/J), Grik4-Cre (B6-Tg(Grik4-cre)G32-

4Stl/J), Sst-IRES-Cre (B6-Sst$^{tm2.1(cre)Zjh}$), VGluT1-IRES2-Cre-D (Slc17a7tm1.1(cre)Hze/J), VGluT3-Cre (Tg(Slc17a8-icre)1Edw/SealJ), and VIP-Cre (B6-Vip$^{tm1(cre)Zjh}$/J) . Such target locus specificity could be due to differences in chromosomal location, the length of loxP-flanked sequences or epigenetic modification on the DNA sequence (Liu et al., 2013; Long and Rossi, 2009; Zheng et al., 2000).

Based on these results, we conclude that unexpected germline recombination is a common occurrence in widely used Cre lines, and often shows parental preference, with higher rates in one strategy and lower in the other, or actually only happens in one kind of germ cells, sperms or eggs. Different Cre lines driven by the same promoter could exhibit different levels of germline recombination activity, and such rates of the same Cre line in different crosses could vary due to locus sensitivity. Future researchers should be well aware of this phenomenon and take the necessary precautions when using Cre lines (recommendations in Discussion).

Cre line common name	Full Cre line name/source	Target gene /Reporter	Breeding strategy[1]	Germline recombination efficiency, Cre from father[2]	Germline recombination efficiency, Cre from mother[2]	Reference/associated publication[3]	Contributors[4]
799-CreER-IRES-GFP	Tg(hs799-cre/ERT2,-GFP)405Jlr	Mafb$^{tm1.1Good}$ Maf$^{tm2.1Cbm}$ Ai14[5]	H	0	Observed	(Pai et al., 2019; Silberberg et al., 2016)	Emily Ling-Lin Pai, John L. R. Rubenstein John.rubenstein@ucsf.edu
A2a-Cre	B6-Tg(Adora2a-Cre)KG139GSat	Ai14[5]	E or G	0	0	NA	Kevin T. Beier kbeier@uci.edu
	B6.FVB(Cg)-Tg(Adora2a-cre)KG139Gsat/Mmucd/GENSAT	Gt(ROSA)26Sor^{tm2} (CAG-tdTomato)Fawa	F	0	0	NA	Hisashi Umemori hisashi.umemori@childrens.harvard.edu
Bhlhb5-Cre	Bhlhe22$^{tm3.1(cre)Meg}$	Ai9[5]	B	0	0	NA	Wenjia You, Constance L. Cepko cepko@genetics.med.harvard.edu
Calb2-IRES-Cre	B6(Cg)-Calb2$^{tm1(cre)Zjh}$/J	Ai9[5]	B	0	0	NA	Wenjia You, Constance L. Cepko cepko@genetics.med.harvard.edu
CaMKIIα-Cre	Tg(Camk2a-cre)159Kln	Fdft1^{tm1Kan}	C	16.2% (12/74)	6.3% (3/48)	NA	Gesine Saher, Klaus A Nave saher@em.mpg.de

Cre line common name	Full Cre line name/source	Target gene /Reporter	Breeding strategy[1]	Germline recombination efficiency, Cre from father[2]	Germline recombination efficiency, Cre from mother[2]	Reference/associated publication[3]	Contributors[4]
CaMKII α-Cre	Tg(Camk2a-cre)93Kln	Gnao1	B	72.1% (31/43)	ND	(Choi et al., 2014b)	NA
		B6;129S4-Gt(ROSA)26Sor^{tm1Sor}/J	B	98.5% (64/65)	ND		
CaMKII α-Cre	B6.Cg-Tg(Camk2a-cre)2Szi/J	Lepr$^{tm1.1Chua}$	A	Observed	0	(McMinn et al., 2005)	NA
		Chat/Slc18a3$^{tm1.2Vpra}$	A or C	Observed	ND	(Castro et al., 2009)	NA
CaMKII α-Cre (T29-1)	Tg(Camk2a-cre)T29-1Stl	Khdrbs3$^{tm1.1Schei}$/J	C	31.3% (5/16)	0% (0/7)	NA	Elisabetta Furlanis, Lisa Traunmüller, Peter Scheiffele peter.scheiffele@unibas.ch
		Rpl22$^{tm1.1Psam}$/J	C	21.4% (6/28)	0% (0/21)		
Chat-Cre	B6;129S6-Chat$^{tm2(cre)Lowl}$/J	Megf10$^{tm1c(KOMP)Jrs}$	A or C	0	0	NA	Ariane Pereira, Jeremy N. Kay jeremy.kay@duke.edu
		Tgfb3^{tm1Moaz}					
		Flrt2$^{tm1c(EUCOMM)Wtsi}$					
		ROSA$^{mT/mG5}$					
		Ai14[5]					
		Rpl22$^{tm1.1Psam}$/J	B	ND	0 (0/15)	NA	

Cre line common name	Full Cre line name/source	Target gene /Reporter	Breeding strategy[1]	Germline recombination efficiency, Cre from father[2]	Germline recombination efficiency, Cre from mother[2]	Reference/associated publication[3]	Contributors[4]
Cux2-CreERT2	B6.Cg-Cux2$^{tm3.1(cre/ERT2)Mull}$/Mmmh		E	0 (0/23)	0 (0/23)		Susanne Falkner, Peter Scheiffele peter.scheiffele@unibas.ch
D2-cre	Tg(Drd2-cre)ER44Gsat/Mmucd	Chat/Slc18a3$^{tm1.2Vpra}$	A or C	0	0	NA	Marco A.M. Prado mprado@robarts.ca Vania F. Prado vprado@robarts.ca
DAT-Cre	Slc6a3$^{tm1.1(cre)Bkmn}$/J	Gria1^{tm2Rsp}	A or C	0	ND	(Hutchison et al., 2018)	Mary Anne Hutchison, Wei Lu luw4@mail.nih.gov
		Gria2^{tm3Rsp}					
		Gria3^{tm1Rsp}					
		Grin1^{tm1Rsp}					
		Ai14[5]					
	B6.SJL-SLc6a3$^{tm1.1(cre)Bkmn}$/J	Ai14[5]	E or G	0	0	NA	Kevin T. Beier kbeier@uci.edu
		Gt(ROSA)26Sor$^{tm2(CAG-tdTomato)Fawa}$	E, F	0	0	NA	Hisashi Umemori hisashi.umemori@childrens.harvard.edu
		Rims1^{tm3Sud}/J	A or C	0	0	(Liu et al., 2018)	Jiexin Wang, Pascal S. Kaeser kaeser@hms.harvard.edu
		Rims2$^{tm1.1Sud}$/J					
		Ai34[5]					
		Clstn3^{tm1Amcr}/J	C	0 (0/52)	88.0% (73/83)	NA	Lin Luo, Ann Marie Craig

Cre line common name	**Full Cre line name/source**	**Target gene /Reporter**	**Breeding strategy**[1]	**Germline recombination efficiency, Cre from father**[2]	**Germline recombination efficiency, Cre from mother**[2]	**Reference/associated publication**[3]	**Contributors**[4]
Dlx5/6-Cre	B6-Tg(dlx5a-cre)1Mekk/J	Ai32[5]	B	0 (0/33)	46.2% (18/39)	NA	acraig@mail.ubc.ca
DlxI12B-Cre	*Tg(I12b–cre)1Jlr*	Mafb$^{tm1.1Good}$	H	Observed	ND	NA	Emily Ling-Lin Pai, John L. R. Rubenstein John.rubenstein@ucsf.edu
		Maf$^{tm2.1Cbm}$					
		Ai14[5]					
Drd1-Cre	B6-Tg(Drd1-Cre)EY262GSat	Ai14[5]	E or G	0	0	NA	Kevin T. Beier kbeier@uci.edu
	B6.FVB(Cg)-Tg(Drd1-cre)EY262Gsat/Mmucd/GENSAT	Gt(ROSA)26Sor^{tm2} (CAG-tdTomato)Fawa	F	0	0	NA	Hisashi Umemori hisashi.umemori@childrens.harvard.edu
Emx1-Cre	Emx1$^{tm1(cre)Ito}$	B6.129(FVB)-Gabra1^{tm1Geh}/J	A	36%	36%	(Zeller et al., 2008b)	NA
Emx1-Cre	B6.129S2-Emx1$^{tm1(cre)Krj}$/J	Wwp2$^{tm1.1Hkb}$	C	Observed	0	(Ambrozkiewicz et al., 2018)	Mateusz C. Ambrozkiewizc, Fritz Benseler, Hiroshi Kawabe kawabe@em.mpg.de
		Rai1$^{tm2.1Luo}$/	A	40%	ND	NA	Wei-Hsiang Huang, Liqun Luo lluo@stanford.edu

Cre line common name	**Full Cre line name/source**	**Target gene /Reporter**	**Breeding strategy**[1]	**Germline recombination efficiency, Cre from father**[2]	**Germline recombination efficiency, Cre from mother**[2]	**Reference/associated publication**[3]	**Contributors**[4]
En1-Cre	En1tm2(cre)Wrst/J	Chat/Slc18a3$^{tm1.2Vpra}$	A	33.3% (10/30)	29.2% (7/24)	NA	Marco A.M. Prado mprado@robarts.ca Vania F. Prado vprado@robarts.ca
Foxd1-Cre	B6;129S4-Foxd1$^{tm1(GFP/cre)Amc}$/J	Ai9[5]	B	0	0	NA	Wenjia You, Constance L. Cepko cepko@genetics.med.harvard.edu
Foxg1-cre	129(Cg)-Foxg1tm1(cre)Skm/J	Chat/Slc18a3$^{tm1.2Vpra}$	A or C	Observed	ND	NA	Marco A.M. Prado mprado@robarts.ca Vania F. Prado vprado@robarts.ca
Gad2-IRES-Cre	B6.Cg-Gad2$^{tm2(cre)Zjh}$/J	stxbp1^{tm1Mver}	E or G	~50%		(Kovacevic et al., 2018)	Matthijs Verhage matthijs@cncr.vu.nl
	B6N.Cg-Gad2$^{tm2(cre)Zjh}$/J	Rai1$^{tm2.1Luo}$/J	A	0	ND	NA	Wei-Hsiang Huang, Liqun Luo lluo@stanford.edu
	B6-GAD2$^{tm2(cre)Zjh}$/J	Ai14[5]	E or G	0	0	NA	Kevin T. Beier kbeier@uci.edu

Cre line common name	Full Cre line name/source	Target gene /Reporter	Breeding strategy[1]	Germline recombination efficiency, Cre from father[2]	Germline recombination efficiency, Cre from mother[2]	Reference/associated publication[3]	Contributors[4]
GFAP-cre	Tg(GFAP-cre)25Mes	Gja1^{tm1Kwi}	C	16.7% (7/42) of Cre negative offspring	50% (8/16) of Cre negative offspring	(Zhang et al., 2013b)	NA
Gpr26-Cre	B6-Tg(Gpr26-cre)KO250Gsat/Mmucd	Clstn3^{tm1Amcr}/J	C	Observed	0	NA	Lin Luo, Ann Marie Craig acraig@mail.ubc.ca
		Ai32[5]	B	27.6% (8/29)	0 (0/23)	NA	
Grik4-Cre	B6-Tg(Grik4-cre)G32-4Stl/J	Khdrbs3$^{tm1.1Schei}$/J	E	37.5% (12/32)		NA	Lisa Traunmüller, Andrea Gomez, Peter Scheiffele peter.scheiffele@unibas.ch
			C	0% (0/42)	ND		
		Rpl22$^{tm1.1Psam}$/J	C	0% (0/10)	ND		
		Fgf22$^{tm1a(EUCOMM)Hmgu}$	A, B, C, F, G	0%		(Terauchi et al., 2017)	Hisashi Umemori hisashi.umemori@childrens.harvard.edu
Grik4-Cre	Grik4$^{tm1(cre)Ksak}$	Ai9[5]	C	Observed		NA	Yu Itoh, Tomohiko Maruo, Kenji Sakimura, Kenji Mandai, and Yoshimi Takai mandai@med.kitasato-u.ac.jp
Htr3a-Cre	Tg(Htr3a-cre)NO152Gsat/Mmucd	Ai14[5]	multiple	~20-50%		NA	Kenneth Pelkey, Chris J. McBain mcbainc@mail.nih.gov

Cre line common name	Full Cre line name/source	Target gene /Reporter	Breeding strategy[1]	Germline recombination efficiency, Cre from father[2]	Germline recombination efficiency, Cre from mother[2]	Reference/associated publication[3]	Contributors[4]
Isl1-Cre	Isl1$^{tm1(cre)Sev}$/J	Ptf1a^{tm3Cvw}	A	0	0	NA	Ariane Pereira, Jeremy N. Kay jeremy.kay@duke.edu
Klf3-CreERT2	B6;129P-Klf3$^{tm1(cre/ERT2)Pzg}$/J	Ai9[5]	B	0	0	NA	Wenjia You, Constance L. Cepko cepko@genetics.med.harvard.edu
Nestin-Cre	Tg(Nes-cre)1Kln/J	Gja1^{tm8Kwi}	Not specified	28.6% (4/14) of Cre negative offspring		(Zhang et al., 2013b)	NA
		Ai34[5]	B	Observed	Observed	NA	Jiexin Wang, Pascal S. Kaeser kaeser@hms.harvard.edu
		Rai1$^{tm2.1Luo}$/J	A	80%	ND	(Huang et al., 2016)	Wei-Hsiang Huang, Liqun Luo lluo@stanford.edu
Nestin-Cre	Tg(Nes-cre)1Atp	Runx1	D	Observed in Cre negative offspring, frequency not reported		(Buchholz et al., 2000b)	NA
		Fgf8$^{tm1.3Mrt}$	A	100%	0	(Trumpp et al., 1999)	
		Wwp1$^{tm1.1Hkb}$	C	0	0	NA	

Cre line common name	Full Cre line name/source	Target gene /Reporter	Breeding strategy[1]	Germline recombination efficiency, Cre from father[2]	Germline recombination efficiency, Cre from mother[2]	Reference/associated publication[3]	Contributors[4]
NEX-Cre	Neurod6$^{tm1(cre)Kan}$	Wwp2$^{tm1.1Hkb}$		0	0		Sandra Goebbels, Klaus A Nave sgoebbels@em.mpg.de
Ngn2-CreER^{TM}	Neurog2$^{tm1(cre/Esr1*)}$ And	Ai9[5]	B	0	0	NA	Wenjia You, Constance L. Cepko cepko@genetics.med.harvard.edu
Nkx2.1-Cre	C57BL/6J-Tg(Nkx2-1-cre)2Sand/J	RCE:loxp[5]	multiple	~10-30%		NA	Kenneth Pelkey, Chris J. McBain mcbainc@mail.nih.gov
		Ai14[5]					
		Chat/Slc18a3$^{tm1.2Vpra}$	C	6.1% (16/262)	13.1% (28/214)	NA	Marco A.M. Prado mprado@robarts.ca Vania F. Prado vprado@robarts.ca
	B6.CD1-Tg(Nkx2-1-cre)2Sand	Mafb$^{tm1.1Good}$	H	Observed	Observed	(Pai et al., 2019)	Emily Ling-Lin Pai, John L. R. Rubenstein John.rubenstein@ucsf.edu
		Maf$^{tm2.1Cbm}$					
		Ai14[5]					
Ntsr1-Cre	B6.Cg-Tg(Ntsr1-cre)GN220Gsat/Mmucd	Rpl22$^{tm1.1Psam}$/J	C	ND	0 (0/21)	NA	Susanne Falkner, Peter Scheiffele peter.scheiffele@unibas.ch
			E	8.1% (3/37)			

Cre line common name	Full Cre line name/source	Target gene /Reporter	Breeding strategy[1]	Germline recombination efficiency, Cre from father[2]	Germline recombination efficiency, Cre from mother[2]	Reference/associated publication[3]	Contributors[4]
Pcp2/L7-Cre	B6.129-Tg(Pcp2-cre)2Mpin/J	Tsc1$^{tm1.1Djk}$	A or E	~5%		(Tsai et al., 2012b)	NA
		Adgrb3^{tm1Yazu}	C	Observed	0	(Kakegawa et al., 2015)	Michisuke Yuzaki myuzaki@keio.jp
		Atg5^{tm1Nmz}	C	Observed	0	(Nishiyama et al., 2007)	
		PhotonSABER$^{f/f}$	C	Observed	0	(Kakegawa et al., 2018)	
Pcp2/L7-Cre	B6.129-Pcp2$^{tm1(cre)Nobs}$	Rpl22$^{tm1.1Psam}$/J	C	0 (0/11)	ND	NA	Elisabetta Furlanis, Peter Scheiffele peter.scheiffele@unibas.ch
			G	0 (0/4)	0 (0/4)		
Pou4f2-Cre	Pou4f2$^{tm1(cre)Bnt}$/J	Ai9[5]	B	100%	0	(Simmons et al., 2016b)	NA
Pvalb-2A-Cre	B6.Cg-Pvalb$^{tm1.1(cre)Aibs}$/J	B6.129S4-*Clock*^{tm1Rep}/J	F	50% (24/48)	<5%	(Kobayashi and Hensch, 2013b)	NA
Pvalb-IRES-Cre	B6.129P2-Pvalb$^{tm1(cre)Arbr}$/J	Khdrbs3$^{tm1.1Schei}$/J	D	ND	0 (0/23)	NA	Elisabetta Furlanis, Lisa Traunmüller, Peter Scheiffele peter.scheiffele@unibas.ch
		Rpl22$^{tm1.1Psam}$/J	A	ND	0 (0/19)		
			B	0 (0/24)	ND		

Cre line common name	Full Cre line name/source	Target gene /Reporter	Breeding strategy[1]	Germline recombination efficiency, Cre from father[2]	Germline recombination efficiency, Cre from mother[2]	Reference/associated publication[3]	Contributors[4]
			F	0 (0/11)	ND		
			E	0 (0/16)	0 (0/16)		
			G	0 (0/3)	0 (0/3)		
		Trpm7^{tm1Clph}	C	0	0	NA	Cui Chen, Nashat Abumaria abumaria@fudan.edu.cn
Rbp4-Cre	B6.Cg-Tg(Rbp4-cre)KL100Gsat/Mmucd	Rpl22$^{tm1.1Psam}$/J	E	0 (0/14)	0 (0/14)	NA	Susanne Falkner, Peter Scheiffele peter.scheiffele@unibas.ch
			B	ND	0 (0/16)		
	B6.FVB(Cg)-Tg(Rbp4-cre)KL100Gsat/Mmucd/GENSAT	Gt(ROSA)26Sor^{tm2} (CAG-tdTomato)Fawa	A, C, F	0	0	NA	Hisashi Umemori hisashi.umemori@childrens.harvard.edu
Rgs9-cre	Rgs9$^{tm1(cre)Yql}$	B6.Cg-Rem2$^{tm3551(T2A-mkate2)Arte}$	A	7.6%	55.1%	(Liput, 2018)	NA
		Rpl22$^{tm1.1Psam}$/J	E	0 (0/17)	0 (0/17)	NA	

Cre line common name	Full Cre line name/source	Target gene /Reporter	Breeding strategy[1]	Germline recombination efficiency, Cre from father[2]	Germline recombination efficiency, Cre from mother[2]	Reference/associated publication[3]	Contributors[4]
Rorb-Cre	B6.129S-Rorb$^{tm1.1(cre)Hze}$/J		G	0 (0/22)	0 (0/22)		Susanne Falkner, Peter Scheiffele peter.scheiffele@unibas.ch
			C	ND	0 (0/20)		
Scnn1a-Cre	B6;C3-Tg(Scnn1a-cre)2Aibs/J	Rpl22$^{tm1.1Psam}$/J	A	0 (0/17)	ND	NA	Elisabetta Furlanis, Peter Scheiffele peter.scheiffele@unibas.ch
			C	0 (0/17)	ND		
Scx-Cre	Tg(Scx-GFP/cre)1Stzr	Ai9[5]	B	0	0	NA	Wenjia You, Constance L. Cepko cepko@genetics.med.harvard.edu
SERT-Cre	B6.129(Cg)-*Slc6a4$^{tm1(cre)Xz}$*/J	Stxbp1^{tm1Mver}	A	high	high	(Dudok et al., 2011)	Matthijs Verhage matthijs@cncr.vu.nl
Sim1-Cre	Tg(Sim1-cre)1Lowl/J	Rai1$^{tm2.1Luo}$/J	A	0	ND	NA	Wei-Hsiang Huang, Liqun Luo lluo@stanford.edu
Six3-Cre	Tg(Six3-cre)69Frty/GcoJ	Isl1$^{tm1.1Whk}$	A	Observed across all strains	Observed across all strains	NA	Ariane Pereira, Jeremy N. Kay jeremy.kay@duke.edu
		Syk$^{tm1.2Tara}$					
		Tgfb3^{tm1Moaz}					
		Flrt2$^{tm1c(EUCOMM)Wtsi}$					

Cre line common name	Full Cre line name/source	Target gene /Reporter	Breeding strategy[1]	Germline recombination efficiency, Cre from father[2]	Germline recombination efficiency, Cre from mother[2]	Reference/associated publication[3]	Contributors[4]
		Ptf1a^{tm3Cvw}					
		Pcdhg^{tm2Xzw} *Pcdha^{em1Jrs}*	multiple	Observed	Observed	(Ing-Esteves et al., 2018)	Joshua R. Sanes sanesj@mcb.harvard.edu
		Chat/Slc18a3$^{tm1.2Vpra}$	A or C	Observed	Observed	NA	Marco A.M. Prado mprado@robarts.ca Vania F. Prado vprado@robarts.ca
Sst-IRES-Cre	B6-Sst$^{tm2.1(cre)Zjh}$	Ai9[5]		<5%		NA	Elisabetta Furlanis, Lisa Traunmüller, Peter Scheiffele peter.scheiffele@unibas.ch
		Khdrbs3$^{tm1.1Schei}$/J	E	0 (0/5)	0 (0/5)		
			C	0 (0/16)	0 (0/10)		
		Rpl22$^{tm1.1Psam}$/J	E	0 (0/26)	0 (0/26)		
			C	0 (0/12)	0 (0/2)		
	B6;129S4;CD1-Sst$^{tm2.1(cre)Zjh}$	Mafb$^{tm1.1Good}$ Maf$^{tm2.1Cbm}$ Ai14[5]	H	0	0	(Pai et al., 2019)	Emily Ling-Lin Pai, John L. R. Rubenstein John.rubenstein@ucsf.edu
Synapsin1-Cre	B6.Cg-Tg(Syn1-cre)671Jxm/J	Hif1a^{tm1Rsjo}	C	67%	0	(Rempe et al., 2006b)	NA
		Erc2$^{tm1.1Sud}$/J	A	ND	0	NA	Jiexin Wang, Pascal S. Kaeser

Cre line common name	Full Cre line name/source	Target gene /Reporter	Breeding strategy[1]	Germline recombination efficiency, Cre from father[2]	Germline recombination efficiency, Cre from mother[2]	Reference/associated publication[3]	Contributors[4]
							kaeser@hms.harvard.edu
Thy1-CreER	Tg(Thy1-cre/ERT2,-EYFP)HGfng/PyngJ	Fgf22$^{tm1a(EUCOMM)Hmgu}$	A, B, C, D, E, F	0	0	NA	Hisashi Umemori hisashi.umemori@childrens.harvard.edu
VAChT.Cre.Fast	B6;129-Tg(SLC18A3-cre)KMisa/0	Chat/Slc18a3$^{tm1.2Vpra}$	A or C	0	0	NA	Marco A.M. Prado mprado@robarts.ca Vania F. Prado vprado@robarts.ca
VGAT/VIAAT-Cre	Slc32a1$^{tm2(cre)Lowl}$/J	Rai1$^{tm2.1Luo}$/J	A	0	ND	NA	Wei-Hsiang Huang, Liqun Luo lluo@stanford.edu
VGAT/VIAAT-Cre	B6.FVB-Tg(Slc32a1-cre)2.1Hzo/FrkJ/	Dnmt3a$^{tm3.1Enl}$	A or F	Observed	NA in young mothers, Observed in older	NA	Laura Lavery, Huda Y. Zoghbi hzoghbi@bcm.edu
VGluT1-IRES2-Cre-D	Slc17a7$^{tm1.1(cre)Hze}$/J	Ai34[5]	A or B	50% (13/26)	66.6% (6/9)	NA	Jiexin Wang, Pascal S. Kaeser kaeser@hms.harvard.edu

Cre line common name	Full Cre line name/source	Target gene /Reporter	Breeding strategy[1]	Germline recombination efficiency, Cre from father[2]	Germline recombination efficiency, Cre from mother[2]	Reference/associated publication[3]	Contributors[4]
	B6;129S-Slc17a7$^{tm1.1(cre)Hze}$/J	Rai1$^{tm2.1Luo}$/J	A	0	ND	NA	Wei-Hsiang Huang, Liqun Luo lluo@stanford.edu
VGluT2-IRES-cre	Slc17a6$^{tm2(cre)Lowl}$/J	Rai1$^{tm2.1Luo}$/J	A	0	ND	NA	Wei-Hsiang Huang, Liqun Luo lluo@stanford.edu
		Ai14[5]	E or G	0	0	NA	Kevin T. Beier kbeier@uci.edu
VGluT3-Cre	Tg(Slc17a8-icre)1Edw/SealJ	Chat/Slc18a3$^{tm1.2Vpra}$	A or C	0	0	NA	Marco A.M. Prado mprado@robarts.ca Vania F. Prado vprado@robarts.ca
		Ai14[5]	multiple	~30%		NA	Kenneth Pelkey, Chris J. McBain mcbainc@mail.nih.gov
VIP-Cre	B6-Vip$^{tm1(cre)Zjh}$/J	Khdrbs3$^{tm1.1Schei}$/J	C	0 (0/22)	ND	NA	Lisa Traunmüller, Peter Scheiffele peter.scheiffele@unibas.ch
			E	0 (0/7)	0 (0/7)		
		Rpl22$^{tm1.1Psam}$/J	E	0 (0/31)	0 (0/31)		
		Ai9[5]		<10%			

Cre line common name	Full Cre line name/source	Target gene /Reporter	Breeding strategy[1]	Germline recombination efficiency, Cre from father[2]	Germline recombination efficiency, Cre from mother[2]	Reference/associated publication[3]	Contributors[4]
Wnt1-Cre	B6.Cg-*H2afv*$^{Tg(Wnt1-cre)11Rth}$ Tg(Wnt1-GAL4)11Rth/J	Neo1$^{tm1.1Jfcl}$	F	0	ND	NA	Emilie Dumontier, Jean-François Cloutier jf.cloutier@mcgill.ca

Table 4.3 Collective data of germline recombination frequency on 57 Cre driver lines

[1]Breeding strategy:

A: Target$^{f/+}$; Promoter-Cre X Target$^{f/f}$

B: Target$^{f/+}$; Promoter-Cre X Target$^{+/+}$

C: Target$^{f/f}$; Promoter-Cre X Target$^{f/f}$

D: Target$^{f/f}$; Promoter-Cre X Target$^{+/+}$

E: Target$^{f/+}$; Promoter-Cre ⊗

F: Target$^{f/+}$; Promoter-Cre X Target$^{f/+}$

G: Target$^{f/f}$; Promoter-Cre ⊗

H: Target$^{f/f}$; Promoter-Cre X Target$^{f/+}$

[2] The numbers (x/y) indicate that x offspring with germline recombination were found from y offspring with the target locus in cumulative data from multiple litters. ND indicates not determined, crossings were not done in this configuration. A single number spanning both the 'Cre from father' and 'Cre from mother' columns indicates data from crosses in which the effect of parental gender was not determined; further crosses are needed to determine whether the germline recombination is of paternal or maternal origin or both.

[3] Where no contributors are listed, the information is from the reference. Where contributors are listed, the associated publication reported findings from the crosses but not information about germline recombination. NA indicates not applicable.

[4] Contributors providing information on germline recombination. Electronic address of principal investigators are listed.

[5] Ai9: B6.Cg-Gt(ROSA)26Sor$^{tm9(CAG-tdTomato)Hze}$/J; Ai14: B6.Cg-Gt(ROSA)26Sor$^{tm14(CAG-tdTomato)Hze}$/J; Ai32: B6;129S-Gt(ROSA)26Sor$^{tm32(CAG-COP4*H134R/EYFP)Hze}$/J; ROSA$^{mT/mG}$: Gt(ROSA)26Sor$^{tm4(ACTB-tdTomato,-EGFP)Luo}$/J; RCE:loxp : Gt(ROSA)26Sor$^{tm1.1(CAG-EGFP)Fsh}$/Mmjax; Ai34: 129S-Gt(ROSA)26Sor$^{tm34.1(CAG-Syp/tdTomato)Hze}$/J

4.4 Discussion

4.4.1 Unexpected germline recombination commonly happens with Cre lines

In this study, we demonstrated an underappreciated caveat of using the Cre-loxP system to manipulate gene expression in cell-type and region-specific manners. Various Cre transgenic lines are believed to express only in a certain cell type, yet can penetrate to germ cells to some degree. This in turn excises the loxP-flanked sequence and passes onto the progeny, resulting in unexpected germline recombination. The progeny will be a hemizygous ($gene^{fl/\Delta}$ or $gene^{+/\Delta}$ depending on the breeding strategy) rather than a homozygous or heterozygous ($gene^{fl/fl}$ or $gene^{+/fl}$, respectively), making results complicated to interpret. Such activity has been brought forth and described several times sporadically (Table 4.2) (Song and Palmiter, 2018). However, for the first time, we are reporting unpublished data as part of an international collaborative effort to show how widely used Cre lines are affected. Collectively, the Cre lines we reported that exhibit germline recombination activity have contributed to over 3300 research articles in total. Researchers are still testing for the best breeding schemes individually, resulting in a huge time and resource sink for the whole neuroscience community. We hope our report will draw more attention to this issue and serve as a reference for future research.

The general conclusions of this study does not only apply to the Cre-loxP system, but also all recombinase systems utilizing transgenic/knockin animals including the Flp-Frt system. Especially when the two systems are combined from different driver lines to achieve more specific manipulations, germline recombination could occur in either, enormously magnifying the effects in subsequent crossings.

4.4.2 Driver gene expression or Cre activity in reproductive systems poorly predicts germline recombination prevalence

As discussed in the introduction, many of these driver genes are expressed in the ovary or testes, which is very likely the reason why this germline recombination happens. For the Cre lines I tested, Gpr26 was expressed in the testes (Jones et al., 2007), and Dlx5/6 in both the ovary and testes (Bouhali et al., 2011; Nishida et al., 2008). However, studies using western blot or RT-PCR could not provide accurate information about the cell type that express certain genes. Therefore, one could not know whether it's in germ cells or only supporting peripheral neuronal cells, making it difficult to determine whether or not germline recombination could actually occur.

Furthermore, even when the genes are expressed in primordial or mature germ cells, the probability of recombination also depends on the expression level of the specific Cre line. As discussed above, the Pvalb-2A-Cre line showed EYFP in spermatids when crossed with Ai32 reporter mice, but the other widely used Pvalb-IRES-Cre line did not show the same phenomenon (Kobayashi and Hensch, 2013a).

Information about gene expression and Cre recombinase activity in different tissue and organs can also be found at Jackson lab's Mouse Genome Informatics database (http://www.informatics.jax.org/) (Bult et al., 2019; Smith et al., 2019). These data are either extracted from published literature or generated by Jackson Lab (MGI Direct Data Submission). The native gene expression results are from a mixture of mRNA *in situ* hybridization, immunohistochemistry, tissue specific RT-PCR, *in situ* knockin reporter expression etc., while the Cre tissue activity are mostly from recombinase reporter expression and some Cre antibody

staining. Still, despite its utility, the information is not yet complete. Moreover, driver gene expression and Cre activity in the reproductive system demonstrated by a certain reporter line, cannot precisely predict the possibility for germline recombination. According to my analysis with the data from MGI database, only a small fraction of the 58 cre lines show consistency between germline recombination prevalence and either the driver gene expression or Cre tissue activity (See summary in Table 4.4 and data for each single line in Appendix B). We eagerly encourage all researchers using Cre lines to deposit data in the Jackson Cre-portal and share experiences including, but not limited to germline recombination rates observed.

	Percentage of Cre lines where germline recombination rate and parental is consistent with **driver gene expression** in reproductive systems	Percentage of Cre lines where germline recombination rate and parental is consistent with **Cre tissue activity** in reproductive systems
Not enough information	43.1% (25/58)	62.1% (36/58)
Not consistent	37.9% (22/58)	19.0% (11/58)
Consistent	19.0% (11/58)	19.0% (11/58)

Table 4.4 Summary of comparison between germline recombination prevalence and driver gene expression and Cre tissue activity patterns in reproductive systems

4.4.3 Using tail/ear tissue for genotyping material

There are also concerns that PCR reactions using the tail or ear tissue could be contaminated by the peripheral nerve cells where the loxP sequence might be recombined by leaky Cre expression but not inherited from the germline. This assumption could be true and can make the genotyping results difficult to interpret when an unexpected knockout allele is observed like in Figures 4.1 and 4.3, but this can be resolved when more factors are taken into consideration. First, the knockout allele in Cre-negative offspring rules out the possibility of

leaky expression. In fact, numbers of Cre-positive and Cre-negative offspring with germline recombination were comparable in our analyses (Figures 4.1, 4.2, and 4.3). Second, if there is contamination from the nerve cells, it should happen regardless of the breeding scheme used, yet we only saw recombination through maternal or paternal transmission. One way to avoid the leaky expression of Cre is to use cells that developmentally differ from nerve cells, for example blood cells, for genotyping, but we would not consider that necessary given the reasons above.

4.4.4 Choosing the proper breeding strategy to achieve desired outcome

Unexpected germline recombination at a high rate could ultimately cost lots of time and research resources. We strongly recommend researchers to consider the following suggestions when using Cre lines:

1. Always genotype every animal for the wild-type, floxed and recombined alleles. This is the only way to make sure all the animals you used are their expected genotypes.
2. If the Cre line you are using is listed here, you should know which breeding strategy you should use to avoid germline recombination.
3. If your line is not listed here, test breeding strategies with Cre recombinase from either the male parent or the female parent. Given the strong parental gender effect, there is usually one better way to mitigate or even avoid undesired germline recombined alleles altogether.
4. Checking the Jackson Lab Cre portal for Cre activity in reproductive systems could potentially give an indication, though not a precise prediction, about the likelihood of germline recombination. Do note that these datasets were acquired using one certain reporter line and expression in different cell types are not always clearly distinguished.

5. In the Methods of all papers using Cre driver lines, authors should clearly indicate that all WT, floxed and recombined alleles are assessed by genotyping, report the frequencies of germline recombination and parental bias, and deposit their observations in Jackson Cre portal.

Chapter 5: Conclusion

5.1 General conclusion and impact

Synapses are the basic units of communication in the brain, where chemical neurotransmitters signal between connected nerve cells. Synapse development requires adhesion of appropriate nerve cell processes accompanied by local recruitment of neurotransmitter release machinery from the presynaptic side and neurotransmitter reception at the postsynaptic side. These processes are coordinated by synaptic organizing complexes spanning the synaptic cleft. The first part of this dissertation focused on calsyntenin-3, a synaptic adhesion molecule newly identified in our lab, and involved both *in vitro* and *in vivo* studies combining biochemistry, immunofluorescence, electron microscopy, and electrophysiological recording techniques.

In Chapter 2, I showed that calsyntenin-3 interacts with α-neurexins, but not β-neurexins at nanomolar affinity. The interaction is calcium dependent, and the cadherin and LNS domains of calsyntenin-3 and LNS5-EGFc-LNS6 of α-neurexins are required. The heparan sulfate modification of neurexins also regulates their interaction with calsyntenin-3. The transmembrane form of calsyntenin-3 triggers presynapse differentiation in contacting axons. However, calsyntenin-3-shed ectodomain, which represents about half the calsyntenin-3 pool in brain, suppresses the ability of multiple α-neurexin partners to induce presynapse differentiation. Calsyntenin-3 is present in many pyramidal neurons throughout cortex and hippocampus but is most highly expressed in interneurons. Young adult Clstn3−/− mice show reductions in excitatory and inhibitory synapse density by electron microscopy and corresponding deficits in synaptic transmission.

In Chapter 3, I further studied the function of calsyntenin-3 in regulating synaptic transmission in different neuronal types using conditional knockout mice and primary hippocampal neuron culture. Conditional calsyntenin-3 knockout in forebrain interneurons does not affect basal inhibitory transmission in CA1 pyramidal neurons, while conditional calsyntenin-3 knockout in excitatory neurons increases both basal inhibitory and excitatory transmission. In primary neuron culture and juvenile sparse knockout mice, the inhibitory transmission is also consistently enhanced. The inhibitory transmission in juvenile Clstn3−/− mice is not altered compared with wild type littermates.

These two chapters together with other work in our lab added a new member in the already complicated super family of synaptic adhesion molecules. In a simple model, calsyntenin-3 acts as a traditional postsynaptic adhesion molecule similar to neuroligins and LRRTMs. But several properties make calsyntenin-3 unique: its extensive cleavage, binding to LNS5-EGFc-LNS6 region of α-neurexins, differential expression pattern, and age- and context-dependent regulation of synaptic transmission. This study broadened our view of synapse organization and shed light on a new target for α-neurexin-related cognitive and psychiatric disorders.

The Cre-loxP system has been widely utilized for decades to achieve cell-type specific manipulations, providing a valuable tool for understanding gene function, especially in neuroscience research. However, we highlight varying probabilities of unexpected germline recombination in distinct Cre-lines that are not widely known, thus affecting the interpretation of experiments in the past as well as moving forward. In Chapter 4, we showcased the prevalence of unexpected germline recombination events using two example Cre lines and provided a

comprehensive reference list of commonly used lines with similar activity with supporting data collected for 57 Cre driver lines. This resource will not only inform future research by providing guidelines for breeding strategies and precautions while using Cre-lines, but more importantly, also draw more attention to non-trivial germline recombination in the entire neuroscience community.

5.2 Future directions

Despite the huge effort my colleagues and I dedicated to deciphering its interactions and function, little is known about calsyntenin-3 relative to the enormous studies on neurexins and neuroligins in the field. Further investigations that are similar to the current study have been discussed in each Chapter. Below I will propose several possible future directions that could potentially further our understanding of calsyntenin-3 and its implication in neuropsychiatric disorders. I will also talk about the next steps on the Cre mouse lines project.

5.2.1 Calsyntenin-3's molecular and cellular function

In Chapter 2 and Pettem et al., 2013, we showed that calsyntenin-3 binds to α-neurexins, but not β-neurexins directly regardless of the insert at splice site 4. Cleaved products of calsyntenin-3 accounts for 90% and at least 50% of the total amount, in the neuronal culture and *in vivo*, respectively. In turn, these fragments can suppress the presynaptic induction activity of multiple α-neurexin binding partners. It is still not clear whether this is because calsyntenin-3 binds to α-neurexins competitively with other partners or calsyntenin-3 can regulate the trafficking of α-neurexins thus reducing the amount available on the neuronal surface. The proper localization and function of α-neurexins is very important to the survival and normal function of neurons and mice (Grayton et al., 2013; Missler et al., 2003). Therefore, it is

important to determine whether calsyntenin-3 can regulate α-neurexin trafficking and the function of calsyntenin-3 cleavage. Calsyntenin-3 can form both monomers and tetramers *in vitro*, and both forms can bind to neurexin1α at physiological affinities (Figure 2.8), but the different functions of the two forms remains unknown. Multimerization of synaptic adhesion molecules can be important for their normal function (Shipman and Nicoll, 2012).

The role of calsyntenin-3 in regulating α-neurexin trafficking and synaptic localization could be assessed by co-transfecting calsyntenin-3 and potential mutants with α-neurexin (YFP-2A-neurexin-2α) in primary cultured neurons and staining for surface neurexin at DIV4 and synaptic neurexin at DIV14. The non-cleavable form of calsyntenin-3 (Myc-C3EX-CD8), the cleaved fragment (Myc-C3secreted) and the proposed HS-binding deficient forms (Myc-C35RA and Myc-C36RA) could be included in this test. If we could find and validate a non-multimerizing form of calsyntenin-3, it could also be included. Surface level of endogenous α-neurexins could be assessed by biotinylation-based assays in acute slices or high density cortical cultures obtained from Clstn3-/- mice and wild type littermates. Rescuing constructs such as the ones mentioned above could be introduced through AAV injection or *in utero* electroporation in mice, or nucleofection in cultures. In addition, the non-multimerizing mutant could be evaluated in the co-culture assay to determine whether the multimerization is required for presynaptic induction.

5.2.2 Social-emotional and cognitive function of calsyntenin-3

Synaptic organizing proteins, especially neurexins and their postsynaptic partners, are often implicated in regulating social-emotional and cognitive behaviors. Compared with littermate control mice, neurexin-1α deficient mice displayed autistic-like behaviors such as a

decrease in prepulse inhibition, an increase in grooming behaviors, an impairment in nest-building activity, and an improvement in motor learning (Etherton et al., 2009). Another independent study revealed altered social approach, reduced social investigation, and reduced locomotor activity in novel environments in homozygous Nrxn1α knockout mice (Grayton et al., 2013). Deletion of neurexin-2α resulted in a similar autism related anxiety-like phenotype with less exploratory activity (Dachtler et al., 2014). Consistent impaired social guidance behavior was observed in Nrxn1 knockout rats (Twining et al., 2017). Selective deletion of Nrxn3 in somatostatin-expressing (SST+) interneurons in the anterior cingulate cortex markedly increased observational fear and impaired inhibitory synaptic transmission from SST+ neurons (Keum et al., 2018).

For the calsyntenin family, besides multiple studies showing C. elegans ortholog CASY-1's association with learning and memory (Hoerndli et al., 2009; Ikeda et al., 2008; Ohno et al., 2014; Thapliyal et al., 2018b) and the genetic link between CLSTN2 variants and human episodic memory (Boraxbekk et al., 2015; Duning et al., 2013; Jacobsen et al., 2009; Pantzar et al., 2014; Preuschhof et al., 2010; Sédille-Mostafaie et al., 2012), behavioral studies have also been conducted in genetic mouse models. Our collaborators showed that Clstn2-/- mice were hyperactive in the open field and showed deficits in spatial learning and memory in the Morris water maze and Barnes maze, while deficient social motivation and social recognition were only observed in Clstn2-/- males (Lipina et al., 2016; Ranneva et al., 2017). Clstn1-/- mice were not tested for behavioral phenotypes but did show deficits in NMDA receptor dependent synaptic plasticity (Ster et al., 2014), which is highly correlated with cognitive functions (Lynch, 2004; Stuchlik, 2014).

Given the above evidence in α-neurexins deficient and calsyntenin-2 deficient mice and the perspective of calsyntenin-3 regulating neurexin trafficking, it is worth to investigate the behavioral changes in calsyntenin-3 deficient or overexpression mice. Autistic-like, anxiety-related, and learning and memory-associated behaviors are all within the scope and can be justified. This approach may lead to new neuropsychiatric disease models and potentially provide a new direction to rescue the autistic-like behaviors in α-neurexins deficient mice.

5.2.3 Next steps on the Cre mouse lines

In Chapter 4, we showed examples of two Cre lines and reported the germline recombination frequency on 57 popularly used Cre transgenic lines. But this seemingly large number is just a starting point to raise awareness comparing with the almost 3000 Cre-expressing alleles in the Jackson Laboratory Cre Repository or the nearly 700 with nervous system expression. There is a summary of tissue activity under each Cre line in JAX Cre Portal and a link that says "Your Observations Welcome" where they encourage researchers to contribute characterizations of the Cre lines. We will deposit our data into the portal. Additionally, we are planning to suggest that they list germline recombination as a specific data point or "warning", as the current simple description of "expression in reproductive system" is far from adequate considering the severe consequences unexpected germline recombination could lead to.

Bibliography

Akashi, K., Kakizaki, T., Kamiya, H., Fukaya, M., Yamasaki, M., Abe, M., Natsume, R., Watanabe, M., and Sakimura, K. (2009). NMDA Receptor GluN2B (GluRε2/NR2B) Subunit Is Crucial for Channel Function, Postsynaptic Macromolecular Organization, and Actin Cytoskeleton at Hippocampal CA3 Synapses. J. Neurosci. *29*, 10869–10882.

AlAyadhi, L.Y., Hashmi, J.A., Iqbal, M., Albalawi, A.M., Samman, M.I., Elamin, N.E., Bashir, S., and Basit, S. (2016). High-resolution SNP genotyping platform identified recurrent and novel CNVs in autism multiplex families. Neuroscience *339*, 561–570.

Allen, N.J., and Lyons, D.A. (2018). Glia as architects of central nervous system formation and function. Science *362*, 181–185.

Anastassiadis, K., Fu, J., Patsch, C., Hu, S., Weidlich, S., Duerschke, K., Buchholz, F., Edenhofer, F., and Stewart, A.F. (2009). Dre recombinase, like Cre, is a highly efficient site-specific recombinase in E. coli, mammalian cells and mice. Dis. Model. Mech. *2*, 508–515.

Anderson, G.R., Aoto, J., Tabuchi, K., Földy, C., Covy, J., Yee, A.X., Wu, D., Lee, S.-J., Chen, L., Malenka, R.C., et al. (2015). β-Neurexins Control Neural Circuits by Regulating Synaptic Endocannabinoid Signaling. Cell *162*, 593–606.

Aoto, J., Martinelli, D.C., Malenka, R.C., Tabuchi, K., and Südhof, T.C. (2013). Presynaptic Neurexin-3 Alternative Splicing trans-Synaptically Controls Postsynaptic AMPA Receptor Trafficking. Cell *154*, 75–88.

Araç, D., Boucard, A.A., Özkan, E., Strop, P., Newell, E., Südhof, T.C., and Brunger, A.T. (2007). Structures of Neuroligin-1 and the Neuroligin-1/Neurexin-1β Complex Reveal Specific Protein-Protein and Protein-Ca2+ Interactions. Neuron *56*, 992–1003.

Araki, Y., Tomita, S., Yamaguchi, H., Miyagi, N., Sumioka, A., Kirino, Y., and Suzuki, T. (2003). Novel cadherin-related membrane proteins, Alcadeins, enhance the X11-like protein-mediated stabilization of amyloid beta-protein precursor metabolism. J. Biol. Chem. *278*, 49448–49458.

Araki, Y., Miyagi, N., Kato, N., Yoshida, T., Wada, S., Nishimura, M., Komano, H., Yamamoto, T., De Strooper, B., Yamamoto, K., et al. (2004). Coordinated metabolism of Alcadein and amyloid beta-protein precursor regulates FE65-dependent gene transactivation. J. Biol. Chem. *279*, 24343–24354.

Araki, Y., Kawano, T., Taru, H., Saito, Y., Wada, S., Miyamoto, K., Kobayashi, H., Ishikawa, H.O., Ohsugi, Y., Yamamoto, T., et al. (2007). The novel cargo Alcadein induces vesicle association of kinesin-1 motor components and activates axonal transport. EMBO J. *26*, 1475–1486.

Araque, A., Parpura, V., Sanzgiri, R.P., and Haydon, P.G. (1999). Tripartite synapses: glia, the unacknowledged partner. Trends Neurosci. *22*, 208–215.

Atasoy, D., Aponte, Y., Su, H.H., and Sternson, S.M. (2008). A FLEX Switch Targets Channelrhodopsin-2 to Multiple Cell Types for Imaging and Long-Range Circuit Mapping. J. Neurosci. *28*, 7025–7030.

Autism Genome Project Consortium, Szatmari, P., Paterson, A.D., Zwaigenbaum, L., Roberts, W., Brian, J., Liu, X.-Q., Vincent, J.B., Skaug, J.L., Thompson, A.P., et al. (2007). Mapping autism risk loci using genetic linkage and chromosomal rearrangements. Nat. Genet. *39*, 319–328.

Awan, Z., Tay, E.S.E., Eyre, N.S., Wu, L.E., Beard, M.R., Boo, I., Drummer, H.E., George, J., and Douglas, M.W. (2016). Calsyntenin-1 mediates hepatitis C virus replication. J. Gen. Virol. *97*, 1877–1887.

Bäck, S., Necarsulmer, J., Whitaker, L.R., Coke, L.M., Koivula, P., Heathward, E.J., Fortuno, L.V., Zhang, Y., Yeh, C.G., Baldwin, H.A., et al. (2019). Neuron-Specific Genome Modification in the Adult Rat Brain Using CRISPR-Cas9 Transgenic Rats. Neuron *102*, 105-119.e8.

Barski, J.J., Dethleffsen, K., and Meyer, M. (2000). Cre recombinase expression in cerebellar Purkinje cells. Genes. N. Y. N 2000 *28*, 93–98.

Baudouin, S.J., Gaudias, J., Gerharz, S., Hatstatt, L., Zhou, K., Punnakkal, P., Tanaka, K.F., Spooren, W., Hen, R., Zeeuw, C.I.D., et al. (2012). Shared Synaptic Pathophysiology in Syndromic and Nonsyndromic Rodent Models of Autism. Science *338*, 128–132.

Belteki, G., Gertsenstein, M., Ow, D.W., and Nagy, A. (2003). Site-specific cassette exchange and germline transmission with mouse ES cells expressing phiC31 integrase. Nat. Biotechnol. *21*, 321–324.

Bemben, M.A., Nguyen, T.A., Li, Y., Wang, T., Nicoll, R.A., and Roche, K.W. (2019). Isoform-specific cleavage of neuroligin-3 reduces synapse strength. Mol. Psychiatry *24*, 145.

Betancur, C., Sakurai, T., and Buxbaum, J.D. (2009). The emerging role of synaptic cell-adhesion pathways in the pathogenesis of autism spectrum disorders. Trends Neurosci. *32*, 402–412.

Bhouri, M., Morishita, W., Temkin, P., Goswami, D., Kawabe, H., Brose, N., Südhof, T.C., Craig, A.M., Siddiqui, T.J., and Malenka, R. (2018). Deletion of LRRTM1 and LRRTM2 in adult mice impairs basal AMPA receptor transmission and LTP in hippocampal CA1 pyramidal neurons. Proc. Natl. Acad. Sci. U. S. A. *115*, E5382–E5389.

Biederer, T., Sara, Y., Mozhayeva, M., Atasoy, D., Liu, X., Kavalali, E.T., and Südhof, T.C. (2002). SynCAM, a Synaptic Adhesion Molecule That Drives Synapse Assembly. Science *297*, 1525–1531.

Blundell, J., Tabuchi, K., Bolliger, M.F., Blaiss, C.A., Brose, N., Liu, X., Südhof, T.C., and Powell, C.M. (2009). Increased anxiety-like behavior in mice lacking the inhibitory synapse cell adhesion molecule neuroligin 2. Genes Brain Behav. *8*, 114–126.

Blundell, J., Blaiss, C.A., Etherton, M.R., Espinosa, F., Tabuchi, K., Walz, C., Bolliger, M.F., Südhof, T.C., and Powell, C.M. (2010). Neuroligin-1 Deletion Results in Impaired Spatial Memory and Increased Repetitive Behavior. J. Neurosci. *30*, 2115–2129.

Bolliger, M.F., Pei, J., Maxeiner, S., Boucard, A.A., Grishin, N.V., and Südhof, T.C. (2008). Unusually rapid evolution of Neuroligin-4 in mice. Proc. Natl. Acad. Sci. *105*, 6421–6426.

Boon, J., Clarke, E., Kessaris, N., Goffinet, A., Molnár, Z., and Hoerder-Suabedissen, A. (2018). Long-range projections from sparse populations of GABAergic neurons in murine subplate. J. Comp. Neurol.

Boraxbekk, C.J., Ames, D., Kochan, N.A., Lee, T., Thalamuthu, A., Wen, W., Armstrong, N.J., Kwok, J.B.J., Schofield, P.R., Reppermund, S., et al. (2015). Investigating the influence of KIBRA and CLSTN2 genetic polymorphisms on cross-sectional and longitudinal measures of memory performance and hippocampal volume in older individuals. Neuropsychologia *78*, 10–17.

Boucard, A.A., Chubykin, A.A., Comoletti, D., Taylor, P., and Südhof, T.C. (2005). A Splice Code for trans-Synaptic Cell Adhesion Mediated by Binding of Neuroligin 1 to α- and β-Neurexins. Neuron *48*, 229–236.

Boucard, A.A., Ko, J., and Südhof, T.C. (2012). High affinity neurexin binding to cell adhesion G-protein-coupled receptor CIRL1/latrophilin-1 produces an intercellular adhesion complex. J. Biol. Chem. *287*, 9399–9413.

Bouhali, K., Dipietromaria, A., Fontaine, A., Caburet, S., Barbieri, O., Bellessort, B., Fellous, M., Veitia, R.A., and Levi, G. (2011). Allelic reduction of Dlx5 and Dlx6 results in early follicular depletion: a new mouse model of primary ovarian insufficiency. Hum. Mol. Genet. *20*, 2642–2650.

Buchholz, F., Refaeli, Y., Trumpp, A., and Bishop, J.M. (2000a). Inducible chromosomal translocation of AML1 and ETO genes through Cre/loxP-mediated recombination in the mouse. EMBO Rep. *1*, 133–139.

Buchholz, F., Refaeli, Y., Trumpp, A., and Bishop, J.M. (2000b). Inducible chromosomal translocation of AML1 and ETO genes through Cre/loxP-mediated recombination in the mouse. EMBO Rep. *1*, 133–139.

Budreck, E.C., and Scheiffele, P. (2007). Neuroligin-3 is a neuronal adhesion protein at GABAergic and glutamatergic synapses. Eur. J. Neurosci. *26*, 1738–1748.

Bult, C.J., Blake, J.A., Smith, C.L., Kadin, J.A., Richardson, J.E., and Mouse Genome Database Group (2019). Mouse Genome Database (MGD) 2019. Nucleic Acids Res. *47*, D801–D806.

Cabezas, C., Irinopoulou, T., Cauli, B., and Poncer, J.C. (2013). Molecular and functional characterization of GAD67-expressing, newborn granule cells in mouse dentate gyrus. Front. Neural Circuits *7*.

Capecchi, M.R. (1989). The new mouse genetics: Altering the genome by gene targeting. Trends Genet. *5*, 70–76.

Cardin, J.A., Carlén, M., Meletis, K., Knoblich, U., Zhang, F., Deisseroth, K., Tsai, L.-H., and Moore, C.I. (2009). Driving fast-spiking cells induces gamma rhythm and controls sensory responses. Nature *459*, 663–667.

Castro, B.M. de, Jaeger, X.D., Martins-Silva, C., Lima, R.D.F., Amaral, E., Menezes, C., Lima, P., Neves, C.M.L., Pires, R.G., Gould, T.W., et al. (2009). The Vesicular Acetylcholine Transporter Is Required for Neuromuscular Development and Function. Mol. Cell. Biol. *29*, 5238–5250.

Cembrowski, M.S., Bachman, J.L., Wang, L., Sugino, K., Shields, B.C., and Spruston, N. (2016). Spatial Gene-Expression Gradients Underlie Prominent Heterogeneity of CA1 Pyramidal Neurons. Neuron *89*, 351–368.

Cenquizca, L.A., and Swanson, L.W. (2007). Spatial organization of direct hippocampal field CA1 axonal projections to the rest of the cerebral cortex. Brain Res. Rev. *56*, 1–26.

Chanda, S., Hale, W.D., Zhang, B., Wernig, M., and Südhof, T.C. (2017). Unique versus Redundant Functions of Neuroligin Genes in Shaping Excitatory and Inhibitory Synapse Properties. J. Neurosci. *37*, 6816–6836.

Chao, H.-T., Chen, H., Samaco, R.C., Xue, M., Chahrour, M., Yoo, J., Neul, J.L., Gong, S., Lu, H.-C., Heintz, N., et al. (2010). Dysfunction in GABA signalling mediates autism-like stereotypies and Rett syndrome phenotypes. Nature *468*, 263–269.

Chattopadhyaya, B., Cristo, G.D., Higashiyama, H., Knott, G.W., Kuhlman, S.J., Welker, E., and Huang, Z.J. (2004). Experience and Activity-Dependent Maturation of Perisomatic GABAergic Innervation in Primary Visual Cortex during a Postnatal Critical Period. J. Neurosci. *24*, 9598–9611.

Chih, B., Engelman, H., and Scheiffele, P. (2005). Control of Excitatory and Inhibitory Synapse Formation by Neuroligins. Science *307*, 1324–1328.

Chih, B., Gollan, L., and Scheiffele, P. (2006). Alternative Splicing Controls Selective Trans-Synaptic Interactions of the Neuroligin-Neurexin Complex. Neuron *51*, 171–178.

Ching, M.S.L., Shen, Y., Tan, W.-H., Jeste, S.S., Morrow, E.M., Chen, X., Mukaddes, N.M., Yoo, S.-Y., Hanson, E., Hundley, R., et al. (2010). Deletions of NRXN1 (neurexin-1) predispose to a wide spectrum of developmental disorders. Am. J. Med. Genet. Part B Neuropsychiatr. Genet. Off. Publ. Int. Soc. Psychiatr. Genet. *153B*, 937–947.

Choi, C.-I., Yoon, S.-P., Choi, J.-M., Kim, S.-S., Lee, Y.-D., Birnbaumer, L., and Suh-Kim, H. (2014a). Simultaneous deletion of floxed genes mediated by CaMKIIα-Cre in the brain and in male germ cells: application to conditional and conventional disruption of Goα. Exp. Mol. Med. *46*, e93.

Choi, C.-I., Yoon, S.-P., Choi, J.-M., Kim, S.-S., Lee, Y.-D., Birnbaumer, L., and Suh-Kim, H. (2014b). Simultaneous deletion of floxed genes mediated by CaMKIIα-Cre in the brain and in male germ cells: application to conditional and conventional disruption of Goα. Exp. Mol. Med. *46*, e93.

Chubykin, A.A., Atasoy, D., Etherton, M.R., Brose, N., Kavalali, E.T., Gibson, J.R., and Südhof, T.C. (2007). Activity-Dependent Validation of Excitatory versus Inhibitory Synapses by Neuroligin-1 versus Neuroligin-2. Neuron *54*, 919–931.

Cirillo, G., Colangelo, A.M., De Luca, C., Savarese, L., Barillari, M.R., Alberghina, L., and Papa, M. (2016). Modulation of Matrix Metalloproteinases Activity in the Ventral Horn of the Spinal Cord Re-stores Neuroglial Synaptic Homeostasis and Neurotrophic Support following Peripheral Nerve Injury. PloS One *11*, e0152750.

Comoletti, D., Flynn, R.E., Boucard, A.A., Demeler, B., Schirf, V., Shi, J., Jennings, L.L., Newlin, H.R., Südhof, T.C., and Taylor, P. (2006). Gene Selection, Alternative Splicing, and Post-translational Processing Regulate Neuroligin Selectivity for β-Neurexins. Biochemistry *45*, 12816–12827.

Condomitti, G., and de Wit, J. (2018). Heparan Sulfate Proteoglycans as Emerging Players in Synaptic Specificity. Front. Mol. Neurosci. *11*.

Condomitti, G., Wierda, K.D., Schroeder, A., Rubio, S.E., Vennekens, K.M., Orlandi, C., Martemyanov, K.A., Gounko, N.V., Savas, J.N., and de Wit, J. (2018). An Input-Specific Orphan Receptor GPR158-HSPG Interaction Organizes Hippocampal Mossy Fiber-CA3 Synapses. Neuron *100*, 201-215.e9.

Craig, A.M., and Kang, Y. (2007). Neurexin-neuroligin signaling in synapse development. Curr. Opin. Neurobiol. *17*, 43–52.

Dachtler, J., Glasper, J., Cohen, R.N., Ivorra, J.L., Swiffen, D.J., Jackson, A.J., Harte, M.K., Rodgers, R.J., and Clapcote, S.J. (2014). Deletion of α-neurexin II results in autism-related behaviors in mice. Transl. Psychiatry *4*, e484.

Daigle, T.L., Madisen, L., Hage, T.A., Valley, M.T., Knoblich, U., Larsen, R.S., Takeno, M.M., Huang, L., Gu, H., Larsen, R., et al. (2018). A Suite of Transgenic Driver and Reporter Mouse Lines with Enhanced Brain-Cell-Type Targeting and Functionality. Cell *174*, 465-480.e22.

de Wit, J., O'Sullivan, M.L., Savas, J.N., Condomitti, G., Caccese, M.C., Vennekens, K.M., Yates, J.R., and Ghosh, A. (2013). Unbiased Discovery of Glypican as a Receptor for LRRTM4 in Regulating Excitatory Synapse Development. Neuron *79*, 696–711.

Dieks, J.-K., Gawinecka, J., Asif, A.R., Varges, D., Gmitterova, K., Streich, J.-H., Dihazi, H., Heinemann, U., and Zerr, I. (2013). Low-abundant cerebrospinal fluid proteome alterations in dementia with Lewy bodies. J. Alzheimers Dis. JAD *34*, 387–397.

Dinamarca, M.C., Raveh, A., Schneider, A., Fritzius, T., Früh, S., Rem, P.D., Stawarski, M., Lalanne, T., Turecek, R., Choo, M., et al. (2019). Complex formation of APP with GABA B receptors links axonal trafficking to amyloidogenic processing. Nat. Commun. *10*, 1331.

Dingledine, R., Borges, K., Bowie, D., and Traynelis, S.F. (1999). The Glutamate Receptor Ion Channels. Pharmacol. Rev. *51*, 7–62.

Dragatsis, I., and Zeitlin, S. (2000). CaMKIIα-cre transgene expression and recombination patterns in the mouse brain. Genesis *26*, 133–135.

Dubois, N.C., Hofmann, D., Kaloulis, K., Bishop, J.M., and Trumpp, A. (2006). Nestin-Cre transgenic mouse line Nes-Cre1 mediates highly efficient Cre/loxP mediated recombination in the nervous system, kidney, and somite-derived tissues. Genes. N. Y. N 2000 *44*, 355–360.

Dudok, J.J., Groffen, A.J.A., Toonen, R.F.T., and Verhage, M. (2011). Deletion of Munc18-1 in 5-HT neurons results in rapid degeneration of the 5-HT system and early postnatal lethality. PloS One *6*, e28137.

Duning, K., Wennmann, D.O., Bokemeyer, A., Reissner, C., Wersching, H., Thomas, C., Buschert, J., Guske, K., Franzke, V., Flöel, A., et al. (2013). Common exonic missense variants in the C2 domain of the human KIBRA protein modify lipid binding and cognitive performance. Transl. Psychiatry *3*, e272.

Duong, L., Klitten, L.L., Møller, R.S., Ingason, A., Jakobsen, K.D., Skjødt, C., Didriksen, M., Hjalgrim, H., Werge, T., and Tommerup, N. (2012). Mutations in NRXN1 in a family multiply

affected with brain disorders: NRXN1 mutations and brain disorders. Am. J. Med. Genet. Part B Neuropsychiatr. Genet. Off. Publ. Int. Soc. Psychiatr. Genet. *159B*, 354–358.

Duyne, G.D.V. (2015). Cre Recombinase. Microbiol. Spectr. *3*.

Dymecki, S.M. (1996). Flp recombinase promotes site-specific DNA recombination in embryonic stem cells and transgenic mice. Proc. Natl. Acad. Sci. U. S. A. *93*, 6191–6196.

Esko, J.D., H. Prestegard, J., and Linhardt, R.J. (2015). Proteins That Bind Sulfated Glycosaminoglycans. In Essentials of Glycobiology, A. Varki, R.D. Cummings, J.D. Esko, P. Stanley, G.W. Hart, M. Aebi, A.G. Darvill, T. Kinoshita, N.H. Packer, J.H. Prestegard, et al., eds. (Cold Spring Harbor (NY): Cold Spring Harbor Laboratory Press), p.

Etherton, M.R., Blaiss, C.A., Powell, C.M., and Südhof, T.C. (2009). Mouse neurexin-1alpha deletion causes correlated electrophysiological and behavioral changes consistent with cognitive impairments. Proc. Natl. Acad. Sci. U. S. A. *106*, 17998–18003.

Feng, J., Schroer, R., Yan, J., Song, W., Yang, C., Bockholt, A., Cook, E.H., Skinner, C., Schwartz, C.E., and Sommer, S.S. (2006). High frequency of neurexin 1β signal peptide structural variants in patients with autism. Neurosci. Lett. *409*, 10–13.

Fex, M., Wierup, N., Nitert, M.D., Ristow, M., and Mulder, H. (2007). Rat insulin promoter 2-Cre recombinase mice bred onto a pure C57BL/6J background exhibit unaltered glucose tolerance. J. Endocrinol. *194*, 551–555.

Fuccillo, M.V., Földy, C., Gökce, Ö., Rothwell, P.E., Sun, G.L., Malenka, R.C., and Südhof, T.C. (2015). Single-Cell mRNA Profiling Reveals Cell-Type-Specific Expression of Neurexin Isoforms. Neuron *87*, 326–340.

Galardy, R.E., Cassabonne, M.E., Giese, C., Gilbert, J.H., Lapierre, F., Lopez, H., Schaefer, M.E., Stack, R., Sullivan, M., Summers, B., et al. (1994). Low Molecular Weight Inhibitors in Corneal Ulcerationa. Ann. N. Y. Acad. Sci. *732*, 315–323.

Gangoda, L., Doerflinger, M., Lee, Y.Y., Rahimi, A., Etemadi, N., Chau, D., Milla, L., O'Connor, L., and Puthalakath, H. (2012). Cre transgene results in global attenuation of the cAMP/PKA pathway. Cell Death Dis. *3*, e365.

Gautam, M., Noakes, P.G., Moscoso, L., Rupp, F., Scheller, R.H., Merlie, J.P., and Sanes, J.R. (1996). Defective neuromuscular synaptogenesis in agrin-deficient mutant mice. Cell *85*, 525–535.

Gauthier, J., Siddiqui, T.J., Huashan, P., Yokomaku, D., Hamdan, F.F., Champagne, N., Lapointe, M., Spiegelman, D., Noreau, A., Lafrenière, R.G., et al. (2011). Truncating mutations in NRXN2 and NRXN1 in autism spectrum disorders and schizophrenia. Hum. Genet. *130*, 563–573.

Ge, Y., Kang, Y., Cassidy, R.M., Moon, K.-M., Lewis, R., Wong, R.O.L., Foster, L.J., and Craig, A.M. (2018). Clptm1 Limits Forward Trafficking of GABA A Receptors to Scale Inhibitory Synaptic Strength. Neuron *97*, 596-610.e8.

Gerfen, C.R., Paletzki, R., and Heintz, N. (2013). GENSAT BAC Cre-Recombinase Driver Lines to Study the Functional Organization of Cerebral Cortical and Basal Ganglia Circuits. Neuron *80*, 1368–1383.

Gibson, J.R., Huber, K.M., and Südhof, T.C. (2009). Neuroligin-2 deletion selectively decreases inhibitory synaptic transmission originating from fast-spiking, but not from somatostatin-positive interneurons. J. Neurosci. Off. J. Soc. Neurosci. *29*, 13883.

Glass, D.J., Bowen, D.C., Stitt, T.N., Radziejewski, C., Bruno, J., Ryan, T.E., Gies, D.R., Shah, S., Mattsson, K., Burden, S.J., et al. (1996). Agrin acts via a MuSK receptor complex. Cell *85*, 513–523.

Godfrey, E.W., Nitkin, R.M., Wallace, B.G., Rubin, L.L., and McMahan, U.J. (1984). Components of Torpedo electric organ and muscle that cause aggregation of acetylcholine receptors on cultured muscle cells. J. Cell Biol. *99*, 615–627.

Gorlewicz, A., and Kaczmarek, L. (2018). Pathophysiology of Trans-Synaptic Adhesion Molecules: Implications for Epilepsy. Front. Cell Dev. Biol. *6*, 119.

Gorski, J.A., Talley, T., Qiu, M., Puelles, L., Rubenstein, J.L.R., and Jones, K.R. (2002). Cortical Excitatory Neurons and Glia, But Not GABAergic Neurons, Are Produced in the Emx1-Expressing Lineage. J. Neurosci. *22*, 6309–6314.

Graf, E.R., Zhang, X., Jin, S.-X., Linhoff, M.W., and Craig, A.M. (2004). Neurexins Induce Differentiation of GABA and Glutamate Postsynaptic Specializations via Neuroligins. Cell *119*, 1013–1026.

Grayton, H.M., Missler, M., Collier, D.A., and Fernandes, C. (2013). Altered Social Behaviours in Neurexin 1α Knockout Mice Resemble Core Symptoms in Neurodevelopmental Disorders. PLoS ONE *8*, e67114.

Gronostajski, R.M., and Sadowski, P.D. (1985). The FLP recombinase of the Saccharomyces cerevisiae 2 microns plasmid attaches covalently to DNA via a phosphotyrosyl linkage. Mol. Cell. Biol. *5*, 3274–3279.

Gu, H., Marth, J.D., Orban, P.C., Mossmann, H., and Rajewsky, K. (1994). Deletion of a DNA polymerase beta gene segment in T cells using cell type-specific gene targeting. Science *265*, 103–106.

Guang, S., Pang, N., Deng, X., Yang, L., He, F., Wu, L., Chen, C., Yin, F., and Peng, J. (2018). Synaptopathology Involved in Autism Spectrum Disorder. Front. Cell. Neurosci. *12*, 470.

Guilmatre, A., Dubourg, C., Mosca, A.-L., Legallic, S., Goldenberg, A., Drouin-Garraud, V., Layet, V., Rosier, A., Briault, S., Bonnet-Brilhault, F., et al. (2009). Recurrent rearrangements in synaptic and neurodevelopmental genes and shared biologic pathways in schizophrenia, autism, and mental retardation. Arch. Gen. Psychiatry *66*, 947–956.

Haas, K.T., Compans, B., Letellier, M., Bartol, T.M., Grillo-Bosch, D., Sejnowski, T.J., Sainlos, M., Choquet, D., Thoumine, O., and Hosy, E. (2018). Pre-post synaptic alignment through neuroligin-1 tunes synaptic transmission efficiency. ELife *7*.

Harno, E., Cottrell, E.C., and White, A. (2013). Metabolic Pitfalls of CNS Cre-Based Technology. Cell Metab. *18*, 21–28.

Harris, K.M., and Weinberg, R.J. (2012). Ultrastructure of Synapses in the Mammalian Brain. Cold Spring Harb. Perspect. Biol. *4*, a005587.

Harris, J.A., Hirokawa, K.E., Sorensen, S.A., Gu, H., Mills, M., Ng, L.L., Bohn, P., Mortrud, M., Ouellette, B., Kidney, J., et al. (2014). Anatomical characterization of Cre driver mice for neural circuit mapping and manipulation. Front. Neural Circuits *8*.

Harrison, V., Connell, L., Hayesmoore, J., McParland, J., Pike, M.G., and Blair, E. (2011). Compound heterozygous deletion of NRXN1 causing severe developmental delay with early onset epilepsy in two sisters. Am. J. Med. Genet. A. *155A*, 2826–2831.

Hata, S., Fujishige, S., Araki, Y., Kato, N., Araseki, M., Nishimura, M., Hartmann, D., Saftig, P., Fahrenholz, F., Taniguchi, M., et al. (2009a). Alcadein cleavages by amyloid beta-precursor protein (APP) alpha- and gamma-secretases generate small peptides, p3-Alcs, indicating Alzheimer disease-related gamma-secretase dysfunction. J. Biol. Chem. *284*, 36024–36033.

Hata, S., Fujishige, S., Araki, Y., Kato, N., Araseki, M., Nishimura, M., Hartmann, D., Saftig, P., Fahrenholz, F., Taniguchi, M., et al. (2009b). Alcadein Cleavages by Amyloid β-Precursor Protein (APP) α- and γ-Secretases Generate Small Peptides, p3-Alcs, Indicating Alzheimer Disease-related γ-Secretase Dysfunction. J. Biol. Chem. *284*, 36024–36033.

Hata, S., Fujishige, S., Araki, Y., Taniguchi, M., Urakami, K., Peskind, E., Akatsu, H., Araseki, M., Yamamoto, K., Martins, R.N., et al. Alternative processing of γ-secretase substrates in common forms of mild cognitive impairment and alzheimer's disease: Evidence for γ-secretase dysfunction. Ann. Neurol. *69*, 1026–1031.

Higashi, A.Y., Ikawa, T., Muramatsu, M., Economides, A.N., Niwa, A., Okuda, T., Murphy, A.J., Rojas, J., Heike, T., Nakahata, T., et al. (2009). Direct hematological toxicity and illegitimate chromosomal recombination caused by the systemic activation of CreERT2. J. Immunol. Baltim. Md 1950 *182*, 5633–5640.

Hintsch, G., Zurlinden, A., Meskenaite, V., Steuble, M., Fink-Widmer, K., Kinter, J., and Sonderegger, P. (2002). The calsyntenins--a family of postsynaptic membrane proteins with distinct neuronal expression patterns. Mol. Cell. Neurosci. *21*, 393–409.

Hippenmeyer, S., Vrieseling, E., Sigrist, M., Portmann, T., Laengle, C., Ladle, D.R., and Arber, S. (2005). A developmental switch in the response of DRG neurons to ETS transcription factor signaling. PLoS Biol. *3*, e159.

Hirai, H., Pang, Z., Bao, D., Miyazaki, T., Li, L., Miura, E., Parris, J., Rong, Y., Watanabe, M., Yuzaki, M., et al. (2005). Cbln1 is essential for synaptic integrity and plasticity in the cerebellum. Nat. Neurosci. *8*, 1534–1541.

Hoerndli, F.J., Walser, M., Fröhli Hoier, E., de Quervain, D., Papassotiropoulos, A., and Hajnal, A. (2009). A Conserved Function of C. elegans CASY-1 Calsyntenin in Associative Learning. PLoS ONE *4*, e4880.

Howell, B.W., and Smith, K.M. (2019). Synaptic structural protein dysfunction leads to altered excitation inhibition ratios in models of autism spectrum disorder. Pharmacol. Res. *139*, 207–214.

Huang, W.-H., Guenthner, C.J., Xu, J., Nguyen, T., Schwarz, L.A., Wilkinson, A.W., Gozani, O., Chang, H.Y., Shamloo, M., and Luo, L. (2016). Molecular and Neural Functions of Rai1, the Causal Gene for Smith-Magenis Syndrome. Neuron *92*, 392–406.

Huh, W.J., Mysorekar, I.U., and Mills, J.C. (2010). Inducible activation of Cre recombinase in adult mice causes gastric epithelial atrophy, metaplasia, and regenerative changes in the absence of "floxed" alleles. Am. J. Physiol. Gastrointest. Liver Physiol. *299*, G368-380.

Hutchison, M.A., Gu, X., Adrover, M.F., Lee, M.R., Hnasko, T.S., Alvarez, V.A., and Lu, W. (2018). Genetic inhibition of neurotransmission reveals role of glutamatergic input to dopamine neurons in high-effort behavior. Mol. Psychiatry *23*, 1213–1225.

Ichtchenko, K., Hata, Y., Nguyen, T., Ullrich, B., Missler, M., Moomaw, C., and Südhof, T.C. (1995). Neuroligin 1: A splice site-specific ligand for β-neurexins. Cell *81*, 435–443.

Ichtchenko, K., Nguyen, T., and Südhof, T.C. (1996). Structures, alternative splicing, and neurexin binding of multiple neuroligins. J. Biol. Chem. *271*, 2676–2682.

Ikeda, D.D., Duan, Y., Matsuki, M., Kunitomo, H., Hutter, H., Hedgecock, E.M., and Iino, Y. (2008). CASY-1, an ortholog of calsyntenins/alcadeins, is essential for learning in Caenorhabditis elegans. Proc. Natl. Acad. Sci. *105*, 5260–5265.

Ing-Esteves, S., Kostadinov, D., Marocha, J., Sing, A.D., Joseph, K.S., Laboulaye, M.A., Sanes, J.R., and Lefebvre, J.L. (2018). Combinatorial Effects of Alpha- and Gamma-Protocadherins on Neuronal Survival and Dendritic Self-Avoidance. J. Neurosci. *38*, 2713–2729.

Ito-Ishida, A., Miyazaki, T., Miura, E., Matsuda, K., Watanabe, M., Yuzaki, M., and Okabe, S. (2012). Presynaptically released Cbln1 induces dynamic axonal structural changes by interacting with GluD2 during cerebellar synapse formation. Neuron *76*, 549–564.

Iwakura, Y., Wang, R., Inamura, N., Araki, K., Higashiyama, S., Takei, N., and Nawa, H. (2017). Glutamate-dependent ectodomain shedding of neuregulin-1 type II precursors in rat forebrain neurons. PloS One *12*, e0174780.

Iwasato, T., Datwani, A., Wolf, A.M., Nishiyama, H., Taguchi, Y., Tonegawa, S., Knöpfel, T., Erzurumlu, R.S., and Itohara, S. (2000). Cortex-restricted disruption of NMDAR1 impairs neuronal patterns in the barrel cortex. Nature *406*, 726.

Jacobsen, L.K., Picciotto, M.R., Heath, C.J., Mencl, W.E., and Gelernter, J. (2009). Allelic variation of calsyntenin 2 (CLSTN2) modulates the impact of developmental tobacco smoke exposure on mnemonic processing in adolescents. Biol. Psychiatry *65*, 671–679.

Jamain, S., Quach, H., Betancur, C., Råstam, M., Colineaux, C., Gillberg, I.C., Soderstrom, H., Giros, B., Leboyer, M., Gillberg, C., et al. (2003). Mutations of the X-linked genes encoding neuroligins NLGN3 and NLGN4 are associated with autism. Nat. Genet. *34*, 27–29.

Jamain, S., Radyushkin, K., Hammerschmidt, K., Granon, S., Boretius, S., Varoqueaux, F., Ramanantsoa, N., Gallego, J., Ronnenberg, A., Winter, D., et al. (2008). Reduced social interaction and ultrasonic communication in a mouse model of monogenic heritable autism. Proc. Natl. Acad. Sci. U. S. A. *105*, 1710–1715.

Jang, S., Lee, H., and Kim, E. (2017). Synaptic adhesion molecules and excitatory synaptic transmission. Curr. Opin. Neurobiol. *45*, 45–50.

Jedlicka, P., Muellerleile, J., and Schwarzacher, S.W. (2018). Synaptic Plasticity and Excitation-Inhibition Balance in the Dentate Gyrus: Insights from In Vivo Recordings in Neuroligin-1, Neuroligin-2, and Collybistin Knockouts. Neural Plast. *2018*, 6015753.

Jiang, M., Polepalli, J., Chen, L.Y., Zhang, B., Südhof, T.C., and Malenka, R.C. (2017). Conditional ablation of neuroligin-1 in CA1 pyramidal neurons blocks LTP by a cell-autonomous NMDA receptor-independent mechanism. Mol. Psychiatry *22*, 375–383.

Jones, P.G., Nawoschik, S.P., Sreekumar, K., Uveges, A.J., Tseng, E., Zhang, L., Johnson, J., He, L., Paulsen, J.E., Bates, B., et al. (2007). Tissue distribution and functional analyses of the constitutively active orphan G protein coupled receptors, GPR26 and GPR78. Biochim. Biophys. Acta BBA - Gen. Subj. *1770*, 890–901.

Kaech, S., and Banker, G. (2006). Culturing hippocampal neurons. Nat. Protoc. *1*, 2406–2415.

Kaifosh, P., and Losonczy, A. (2016). Mnemonic Functions for Nonlinear Dendritic Integration in Hippocampal Pyramidal Circuits. Neuron *90*, 622–634.

Kang, Y., Zhang, X., Dobie, F., Wu, H., and Craig, A.M. (2008). Induction of GABAergic postsynaptic differentiation by alpha-neurexins. J. Biol. Chem. *283*, 2323–2334.

Kashiwabuchi, N., Ikeda, K., Araki, K., Hirano, T., Shibuki, K., Takayama, C., Inoue, Y., Kutsuwada, T., Yagi, T., and Kang, Y. (1995). Impairment of motor coordination, Purkinje cell synapse formation, and cerebellar long-term depression in GluR delta 2 mutant mice. Cell *81*, 245–252.

Keum, S., Kim, A., Shin, J.J., Kim, J.-H., Park, J., and Shin, H.-S. (2018). A Missense Variant at the Nrxn3 Locus Enhances Empathy Fear in the Mouse. Neuron *98*, 588-601.e5.

Kim, J.-Y., Ash, R.T., Ceballos-Diaz, C., Levites, Y., Golde, T.E., Smirnakis, S.M., and Jankowsky, J.L. (2013). Viral transduction of the neonatal brain delivers controllable genetic mosaicism for visualising and manipulating neuronal circuits in vivo. Eur. J. Neurosci. *37*, 1203–1220.

Kim, J.-Y., Grunke, S.D., Levites, Y., Golde, T.E., and Jankowsky, J.L. (2014). Intracerebroventricular viral injection of the neonatal mouse brain for persistent and widespread neuronal transduction. J. Vis. Exp. JoVE 51863.

Kirov, G., Gumus, D., Chen, W., Norton, N., Georgieva, L., Sari, M., O'Donovan, M.C., Erdogan, F., Owen, M.J., Ropers, H.-H., et al. (2008). Comparative genome hybridization suggests a role for NRXN1 and APBA2 in schizophrenia. Hum. Mol. Genet. *17*, 458–465.

Ko, J., Fuccillo, M.V., Malenka, R.C., and Sudhof, T.C. (2009). LRRTM2 Functions as a Neurexin Ligand in Promoting Excitatory Synapse Formation. Neuron *64*, 791–798.

Ko, J.S., Pramanik, G., Um, J.W., Shim, J.S., Lee, D., Kim, K.H., Chung, G.-Y., Condomitti, G., Kim, H.M., Kim, H., et al. (2015). PTPσ functions as a presynaptic receptor for the glypican-4/LRRTM4 complex and is essential for excitatory synaptic transmission. Proc. Natl. Acad. Sci. *112*, 1874–1879.

Kobayashi, Y., and Hensch, T.K. (2013a). Germline recombination by conditional gene targeting with Parvalbumin-Cre lines. Front. Neural Circuits *7*, 168.

Kobayashi, Y., and Hensch, T.K. (2013b). Germline recombination by conditional gene targeting with Parvalbumin-Cre lines. Front. Neural Circuits *7*.

Koch, S.M., and Ullian, E.M. (2010). Neuronal Pentraxins Mediate Silent Synapse Conversion in the Developing Visual System. J. Neurosci. *30*, 5404–5414.

Kohannim, O., Hibar, D.P., Stein, J.L., Jahanshad, N., Hua, X., Rajagopalan, P., Toga, A.W., Jack, C.R., Weiner, M.W., de Zubicaray, G.I., et al. (2012). Discovery and Replication of Gene Influences on Brain Structure Using LASSO Regression. Front. Neurosci. *6*, 115.

Konecna, A., Frischknecht, R., Kinter, J., Ludwig, A., Steuble, M., Meskenaite, V., Indermühle, M., Engel, M., Cen, C., Mateos, J.-M., et al. (2006). Calsyntenin-1 docks vesicular cargo to kinesin-1. Mol. Biol. Cell *17*, 3651–3663.

Kovacevic, J., Maroteaux, G., Schut, D., Loos, M., Dubey, M., Pitsch, J., Remmelink, E., Koopmans, B., Crowley, J., Cornelisse, L.N., et al. (2018). Protein instability, haploinsufficiency, and cortical hyper-excitability underlie STXBP1 encephalopathy. Brain J. Neurol. *141*, 1350–1374.

Kuhlman, S.J., and Huang, Z.J. (2008). High-Resolution Labeling and Functional Manipulation of Specific Neuron Types in Mouse Brain by Cre-Activated Viral Gene Expression. PLOS ONE *3*, e2005.

Kwon, H.-B., Kozorovitskiy, Y., Oh, W.-J., Peixoto, R.T., Akhtar, N., Saulnier, J.L., Gu, C., and Sabatini, B.L. (2012). Neuroligin-1–dependent competition regulates cortical synaptogenesis and synapse number. Nat. Neurosci. *15*, 1667–1674.

Lam, P.T., Padula, S.L., Hoang, T.V., Poth, J.E., Liu, L., Liang, C., LeFever, A.S., Wallace, L.M., Ashery-Padan, R., Riggs, P.K., et al. (2019). Considerations for the use of Cre recombinase for conditional gene deletion in the mouse lens. Hum. Genomics *13*, 10.

Lan, Y., Wang, Q., Ovitt, C.E., and Jiang, R. (2007). A unique mouse strain expressing Cre recombinase for tissue-specific analysis of gene function in palate and kidney development. Genes. N. Y. N 2000 *45*, 618–624.

Laukka, E.J., Lövdén, M., Herlitz, A., Karlsson, S., Ferencz, B., Pantzar, A., Keller, L., Graff, C., Fratiglioni, L., and Bäckman, L. (2013). Genetic effects on old-age cognitive functioning: a population-based study. Psychol. Aging *28*, 262–274.

Lee, J.-Y., Ristow, M., Lin, X., White, M.F., Magnuson, M.A., and Hennighausen, L. (2006). RIP-Cre Revisited, Evidence for Impairments of Pancreatic β-Cell Function. J. Biol. Chem. *281*, 2649–2653.

Lee, S.-J., Uemura, T., Yoshida, T., and Mishina, M. (2012). GluRδ2 Assembles Four Neurexins into Trans-Synaptic Triad to Trigger Synapse Formation. J. Neurosci. *32*, 4688–4701.

Lee, T.J., Lee, J.W., Haynes, E.M., Eliceiri, K.W., and Halloran, M.C. (2017). The Kinesin Adaptor Calsyntenin-1 Organizes Microtubule Polarity and Regulates Dynamics during Sensory Axon Arbor Development. Front. Cell. Neurosci. *11*.

Lemmens, K., Bollaerts, I., Bhumika, S., de Groef, L., Van Houcke, J., Darras, V.M., Van Hove, I., and Moons, L. (2016). Matrix metalloproteinases as promising regulators of axonal regrowth in the injured adult zebrafish retinotectal system. J. Comp. Neurol. *524*, 1472–1493.

Leshchyns'ka, I., and Sytnyk, V. (2016). Synaptic Cell Adhesion Molecules in Alzheimer's Disease. Neural Plast. *2016*, 6427537.

Levinson, J.N., and El-Husseini, A. (2007). A Crystal-Clear Interaction: Relating Neuroligin/Neurexin Complex Structure to Function at the Synapse. Neuron *56*, 937–939.

Levinson, J.N., Chéry, N., Huang, K., Wong, T.P., Gerrow, K., Kang, R., Prange, O., Wang, Y.T., and El-Husseini, A. (2005). Neuroligins Mediate Excitatory and Inhibitory Synapse Formation INVOLVEMENT OF PSD-95 AND NEUREXIN-1β IN NEUROLIGIN-INDUCED SYNAPTIC SPECIFICITY. J. Biol. Chem. *280*, 17312–17319.

Li, Y., Choi, P.S., Casey, S.C., and Felsher, D.W. (2014). Activation of Cre recombinase alone can induce complete tumor regression. PloS One *9*, e107589.

Liang, J., Xu, W., Hsu, Y.-T., Yee, A.X., Chen, L., and Südhof, T.C. (2015). Conditional neuroligin-2 knockout in adult medial prefrontal cortex links chronic changes in synaptic inhibition to cognitive impairments. Mol. Psychiatry *20*, 850–859.

Linhoff, M.W., Laurén, J., Cassidy, R.M., Dobie, F.A., Takahashi, H., Nygaard, H.B., Airaksinen, M.S., Strittmatter, S.M., and Craig, A.M. (2009). An unbiased expression screen for synaptogenic proteins identifies the LRRTM protein family as synaptic organizers. Neuron *61*, 734–749.

Lipina, T.V., Prasad, T., Yokomaku, D., Luo, L., Connor, S.A., Kawabe, H., Wang, Y.T., Brose, N., Roder, J.C., and Craig, A.M. (2016). Cognitive Deficits in Calsyntenin-2-deficient Mice Associated with Reduced GABAergic Transmission. Neuropsychopharmacology *41*, 802–810.

Liput, D.J. (2018). Cre-Recombinase Dependent Germline Deletion of a Conditional Allele in the Rgs9cre Mouse Line. Front. Neural Circuits *12*.

Liu, A., Zhou, Z., Dang, R., Zhu, Y., Qi, J., He, G., Leung, C., Pak, D., Jia, Z., and Xie, W. (2016). Neuroligin 1 regulates spines and synaptic plasticity via LIMK1/cofilin-mediated actin reorganization. J Cell Biol *212*, 449–463.

Liu, C., Kershberg, L., Wang, J., Schneeberger, S., and Kaeser, P.S. (2018). Dopamine Secretion Is Mediated by Sparse Active Zone-like Release Sites. Cell *172*, 706-718.e15.

Liu, F., Arias-Vásquez, A., Sleegers, K., Aulchenko, Y.S., Kayser, M., Sanchez-Juan, P., Feng, B.-J., Bertoli-Avella, A.M., van Swieten, J., Axenovich, T.I., et al. (2007). A genomewide screen for late-onset Alzheimer disease in a genetically isolated Dutch population. Am. J. Hum. Genet. *81*, 17–31.

Liu, J., Willet, S.G., Bankaitis, E.D., Xu, Y., Wright, C.V.E., and Gu, G. (2013). Non-parallel recombination limits Cre-LoxP-based reporters as precise indicators of conditional genetic manipulation. Genes. N. Y. N 2000 *51*, 436–442.

Long, M.A., and Rossi, F.M.V. (2009). Silencing Inhibits Cre-Mediated Recombination of the Z/AP and Z/EG Reporters in Adult Cells. PLOS ONE *4*, e5435.

Loonstra, A., Vooijs, M., Beverloo, H.B., Allak, B.A., van Drunen, E., Kanaar, R., Berns, A., and Jonkers, J. (2001). Growth inhibition and DNA damage induced by Cre recombinase in mammalian cells. Proc. Natl. Acad. Sci. U. S. A. *98*, 9209–9214.

Lu, P., Ewald, A.J., Martin, G.R., and Werb, Z. (2008). Genetic mosaic analysis reveals FGF receptor 2 function in terminal end buds during mammary gland branching morphogenesis. Dev. Biol. *321*, 77–87.

Lu, Z., Wang, Y., Chen, F., Tong, H., Reddy, M.V.V.V.S., Luo, L., Seshadrinathan, S., Zhang, L., Holthauzen, L.M.F., Craig, A.M., et al. (2014). Calsyntenin-3 Molecular Architecture and Interaction with Neurexin 1α. J. Biol. Chem. *289*, 34530–34542.

Luján, R., Shigemoto, R., and López-Bendito, G. (2005). Glutamate and GABA receptor signalling in the developing brain. Neuroscience *130*, 567–580.

Lynch, M.A. (2004). Long-term potentiation and memory. Physiol. Rev. *84*, 87–136.

Madisen, L., Zwingman, T.A., Sunkin, S.M., Oh, S.W., Zariwala, H.A., Gu, H., Ng, L.L., Palmiter, R.D., Hawrylycz, M.J., Jones, A.R., et al. (2010). A robust and high-throughput Cre reporting and characterization system for the whole mouse brain. Nat. Neurosci. *13*, 133–140.

Madisen, L., Mao, T., Koch, H., Zhuo, J., Berenyi, A., Fujisawa, S., Hsu, Y.-W.A., Garcia Iii, A.J., Gu, X., Zanella, S., et al. (2012). A toolbox of Cre-dependent optogenetic transgenic mice for light-induced activation and silencing. Nat. Neurosci. *15*, 793–802.

Martin-Vaquero, P., da Costa, R.C., Allen, M.J., Moore, S.A., Keirsey, J.K., and Green, K.B. (2015). Proteomic analysis of cerebrospinal fluid in canine cervical spondylomyelopathy. Spine *40*, 601–612.

Maruta, C., Saito, Y., Hata, S., Gotoh, N., Suzuki, T., and Yamamoto, T. (2012). Constitutive Cleavage of the Single-Pass Transmembrane Protein Alcadeinα Prevents Aberrant Peripheral Retention of Kinesin-1. PLoS ONE *7*, e43058.

Matsuda, K., and Yuzaki, M. (2011). Cbln family proteins promote synapse formation by regulating distinct neurexin signaling pathways in various brain regions. Eur. J. Neurosci. *33*, 1447–1461.

Matsuda, K., Miura, E., Miyazaki, T., Kakegawa, W., Emi, K., Narumi, S., Fukazawa, Y., Ito-Ishida, A., Kondo, T., Shigemoto, R., et al. (2010). Cbln1 is a ligand for an orphan glutamate receptor delta2, a bidirectional synapse organizer. Science *328*, 363–368.

Mayford, M., Baranes, D., Podsypanina, K., and Kandel, E.R. (1996). The 3′-untranslated region of CaMKIIα is a cis-acting signal for the localization and translation of mRNA in dendrites. Proc. Natl. Acad. Sci. *93*, 13250–13255.

McHugh, T.J., Blum, K.I., Tsien, J.Z., Tonegawa, S., and Wilson, M.A. (1996). Impaired Hippocampal Representation of Space in CA1-Specific NMDAR1 Knockout Mice. Cell *87*, 1339–1349.

McMinn, J.E., Liu, S.-M., Liu, H., Dragatsis, I., Dietrich, P., Ludwig, T., Boozer, C.N., and Chua, S.C. (2005). Neuronal deletion of Lepr elicits diabesity in mice without affecting cold tolerance or fertility. Am. J. Physiol.-Endocrinol. Metab. *289*, E403–E411.

Means, A.L., Chytil, A., Moses, H.L., Coffey, R.J., Wright, C.V.E., Taketo, M.M., and Grady, W.M. (2005). Keratin 19 gene drives Cre recombinase expression throughout the early postimplantation mouse embryo. Genesis *42*, 23–27.

Minichiello, L., Korte, M., Wolfer, D., Kühn, R., Unsicker, K., Cestari, V., Rossi-Arnaud, C., Lipp, H.-P., Bonhoeffer, T., and Klein, R. (1999). Essential Role for TrkB Receptors in Hippocampus-Mediated Learning. Neuron *24*, 401–414.

Missler, M., Hammer, R.E., and Südhof, T.C. (1998). Neurexophilin binding to alpha-neurexins. A single LNS domain functions as an independently folding ligand-binding unit. J. Biol. Chem. *273*, 34716–34723.

Missler, M., Zhang, W., Rohlmann, A., Kattenstroth, G., Hammer, R.E., Gottmann, K., and Südhof, T.C. (2003). Alpha-neurexins couple Ca2+ channels to synaptic vesicle exocytosis. Nature *423*, 939–948.

Missler, M., Sudhof, T.C., and Biederer, T. (2012). Synaptic Cell Adhesion. Cold Spring Harb. Perspect. Biol. *4*, a005694–a005694.

Murray, S.A., Eppig, J.T., Smedley, D., Simpson, E.M., and Rosenthal, N. (2012). Beyond knockouts: cre resources for conditional mutagenesis. Mamm. Genome Off. J. Int. Mamm. Genome Soc. *23*, 587–599.

Muskiewicz, D.E., Uhl, G.R., and Hall, F.S. (2018). The Role of Cell Adhesion Molecule Genes Regulating Neuroplasticity in Addiction. Neural Plast. *2018*, 9803764.

Naiche, L.A., and Papaioannou, V.E. (2007). Cre activity causes widespread apoptosis and lethal anemia during embryonic development. Genesis *45*, 768–775.

Nakazawa, K., Quirk, M.C., Chitwood, R.A., Watanabe, M., Yeckel, M.F., Sun, L.D., Kato, A., Carr, C.A., Johnston, D., Wilson, M.A., et al. (2002). Requirement for Hippocampal CA3 NMDA Receptors in Associative Memory Recall. Science *297*, 211–218.

Nam, C.I., and Chen, L. (2005). Postsynaptic assembly induced by neurexin-neuroligin interaction and neurotransmitter. Proc. Natl. Acad. Sci. *102*, 6137–6142.

Nishida, H., Miyagawa, S., Vieux-Rochas, M., Morini, M., Ogino, Y., Suzuki, K., Nakagata, N., Choi, H.-S., Levi, G., and Yamada, G. (2008). Positive Regulation of Steroidogenic Acute Regulatory Protein Gene Expression through the Interaction between Dlx and GATA-4 for Testicular Steroidogenesis. Endocrinology *149*, 2090–2097.

Ohno, H., Kato, S., Naito, Y., Kunitomo, H., Tomioka, M., and Iino, Y. (2014). Role of synaptic phosphatidylinositol 3-kinase in a behavioral learning response in C. elegans. Science *345*, 313–317.

Ortiz-Medina, H., Emond, M.R., and Jontes, J.D. (2015). Zebrafish calsyntenins mediate homophilic adhesion through their amino-terminal cadherin repeats. Neuroscience *286*, 87–96.

Pai, E.L.-L., Vogt, D., Clemente-Perez, A., McKinsey, G.L., Cho, F.S., Hu, J.S., Wimer, M., Paul, A., Fazel Darbandi, S., Pla, R., et al. (2019). Mafb and c-Maf Have Prenatal Compensatory and Postnatal Antagonistic Roles in Cortical Interneuron Fate and Function. Cell Rep. *26*, 1157-1173.e5.

Pantzar, A., Laukka, E.J., Atti, A.R., Papenberg, G., Keller, L., Graff, C., Fratiglioni, L., and Bäckman, L. (2014). Interactive effects of KIBRA and CLSTN2 polymorphisms on episodic memory in old-age unipolar depression. Neuropsychologia *62*, 137–142.

Papassotiropoulos, A., Stephan, D.A., Huentelman, M.J., Hoerndli, F.J., Craig, D.W., Pearson, J.V., Huynh, K.-D., Brunner, F., Corneveaux, J., Osborne, D., et al. (2006). Common Kibra alleles are associated with human memory performance. Science *314*, 475–478.

Peixoto, R.T., Kunz, P.A., Kwon, H., Mabb, A.M., Sabatini, B.L., Philpot, B.D., and Ehlers, M.D. (2012). Transsynaptic signaling by activity-dependent cleavage of neuroligin-1. Neuron *76*, 396–409.

Pettem, K.L., Yokomaku, D., Luo, L., Linhoff, M.W., Prasad, T., Connor, S.A., Siddiqui, T.J., Kawabe, H., Chen, F., Zhang, L., et al. (2013). The Specific α-Neurexin Interactor Calsyntenin-3 Promotes Excitatory and Inhibitory Synapse Development. Neuron *80*, 113–128.

Pilon, N., Raiwet, D., Viger, R.S., and Silversides, D.W. (2008). Novel pre- and post-gastrulation expression of Gata4 within cells of the inner cell mass and migratory neural crest cells. Dev. Dyn. *237*, 1133–1143.

Polepalli, J.S., Wu, H., Goswami, D., Halpern, C.H., Südhof, T.C., and Malenka, R.C. (2017). Modulation of excitation on parvalbumin interneurons by neuroligin-3 regulates the hippocampal network. Nat. Neurosci. *20*, 219–229.

Ponomareva, O.Y., Holmen, I.C., Sperry, A.J., Eliceiri, K.W., and Halloran, M.C. (2014). Calsyntenin-1 Regulates Axon Branching and Endosomal Trafficking during Sensory Neuron Development In Vivo. J. Neurosci. *34*, 9235–9248.

Poulopoulos, A., Aramuni, G., Meyer, G., Soykan, T., Hoon, M., Papadopoulos, T., Zhang, M., Paarmann, I., Fuchs, C., Harvey, K., et al. (2009). Neuroligin 2 drives postsynaptic assembly at perisomatic inhibitory synapses through gephyrin and collybistin. Neuron *63*, 628–642.

Prange, O., Wong, T.P., Gerrow, K., Wang, Y.T., and El-Husseini, A. (2004). A balance between excitatory and inhibitory synapses is controlled by PSD-95 and neuroligin. Proc. Natl. Acad. Sci. *101*, 13915–13920.

Preuschhof, C., Heekeren, H.R., Li, S.-C., Sander, T., Lindenberger, U., and Bäckman, L. (2010). KIBRA and CLSTN2 polymorphisms exert interactive effects on human episodic memory. Neuropsychologia *48*, 402–408.

Pugach, E.K., Richmond, P.A., Azofeifa, J.G., Dowell, R.D., and Leinwand, L.A. (2015). Prolonged Cre expression driven by the α-myosin heavy chain promoter can be cardiotoxic. J. Mol. Cell. Cardiol. *86*, 54–61.

Purves, D., Augustine, G.J., Fitzpatrick, D., Katz, L.C., LaMantia, A.-S., McNamara, J.O., and Williams, S.M. (2001). Two Families of Postsynaptic Receptors. Neurosci. 2nd Ed.

de Ramon Francàs, G., Alther, T., and Stoeckli, E.T. (2017). Calsyntenins Are Expressed in a Dynamic and Partially Overlapping Manner during Neural Development. Front. Neuroanat. *11*.

Ranneva, S.V., Pavlov, K.S., Gromova, A.V., Amstislavskaya, T.G., and Lipina, T.V. (2017). Features of emotional and social behavioral phenotypes of calsyntenin2 knockout mice. Behav. Brain Res. *332*, 343–354.

Rempe, D., Vangeison, G., Hamilton, J., Li, Y., Jepson, M., and Federoff, H.J. (2006a). Synapsin I Cre transgene expression in male mice produces germline recombination in progeny. Genes. N. Y. N 2000 *44*, 44–49.

Rempe, D., Vangeison, G., Hamilton, J., Li, Y., Jepson, M., and Federoff, H. j. (2006b). Synapsin I Cre transgene expression in male mice produces germline recombination in progeny. Genesis *44*, 44–49.

Rezai Amin, S., Gruszczynski, C., Guiard, B.P., Callebert, J., Launay, J.-M., Louis, F., Betancur, C., Vialou, V., and Gautron, S. (2019). Viral vector-mediated Cre recombinase expression in substantia nigra induces lesions of the nigrostriatal pathway associated with perturbations of dopamine-related behaviors and hallmarks of programmed cell death. J. Neurochem.

Ringman JM, Schulman H, Becker C, and et al (2012). PRoteomic changes in cerebrospinal fluid of presymptomatic and affected persons carrying familial alzheimer disease mutations. Arch. Neurol. *69*, 96–04.

Saito, H., Tsumura, H., Otake, S., Nishida, A., Furukawa, T., and Suzuki, N. (2005). L7/Pcp-2-specific expression of Cre recombinase using knock-in approach. Biochem. Biophys. Res. Commun. *331*, 1216–1221.

Sakers, K., and Eroglu, C. (2019). Control of neural development and function by glial neuroligins. Curr. Opin. Neurobiol. *57*, 163–170.

Sarrazin, S., Lamanna, W.C., and Esko, J.D. (2011). Heparan sulfate proteoglycans. Cold Spring Harb. Perspect. Biol. *3*.

Sasamoto, K., Nagai, J., Nakabayashi, T., He, X., and Ohshima, T. (2017). Cdk5 is required for the positioning and survival of GABAergic neurons in developing mouse striatum. Dev. Neurobiol. *77*, 483–492.

Sauer, B. (1987). Functional expression of the cre-lox site-specific recombination system in the yeast Saccharomyces cerevisiae. Mol. Cell. Biol. *7*, 2087–2096.

Sauer, B., and Henderson, N. (1988). Site-specific DNA recombination in mammalian cells by the Cre recombinase of bacteriophage P1. Proc. Natl. Acad. Sci. U. S. A. *85*, 5166–5170.

Schaaf, C.P., Boone, P.M., Sampath, S., Williams, C., Bader, P.I., Mueller, J.M., Shchelochkov, O.A., Brown, C.W., Crawford, H.P., Phalen, J.A., et al. (2012). Phenotypic spectrum and genotype-phenotype correlations of NRXN1 exon deletions. Eur. J. Hum. Genet. EJHG *20*, 1240–1247.

Scheiffele, P., Fan, J., Choih, J., Fetter, R., and Serafini, T. (2000). Neuroligin Expressed in Nonneuronal Cells Triggers Presynaptic Development in Contacting Axons. Cell *101*, 657–669.

Schmidt, E.E., Taylor, D.S., Prigge, J.R., Barnett, S., and Capecchi, M.R. (2000). Illegitimate Cre-dependent chromosome rearrangements in transgenic mouse spermatids. Proc. Natl. Acad. Sci. *97*, 13702–13707.

Schreiner, D., Nguyen, T.-M., Russo, G., Heber, S., Patrignani, A., Ahrné, E., and Scheiffele, P. (2014). Targeted Combinatorial Alternative Splicing Generates Brain Region-Specific Repertoires of Neurexins. Neuron *84*, 386–398.

Schwenk, J., Pérez-Garci, E., Schneider, A., Kollewe, A., Gauthier-Kemper, A., Fritzius, T., Raveh, A., Dinamarca, M.C., Hanuschkin, A., Bildl, W., et al. (2016). Modular composition and dynamics of native $GABA_B$ receptors identified by high-resolution proteomics. Nat. Neurosci. *19*, 233–242.

Sédille-Mostafaie, N., Sebesta, C., Huber, K.R., Zehetmayer, S., Jungwirth, S., Tragl, K.H., Fischer, P., and Krugluger, W. (2012). The role of memory-related gene polymorphisms, KIBRA and CLSTN2, on replicate memory assessment in the elderly. J. Neural Transm. Vienna Austria 1996 *119*, 77–80.

Semprini, S., Troup, T.J., Kotelevtseva, N., King, K., Davis, J.R.E., Mullins, L.J., Chapman, K.E., Dunbar, D.R., and Mullins, J.J. (2007). Cryptic loxP sites in mammalian genomes: genome-wide distribution and relevance for the efficiency of BAC/PAC recombineering techniques. Nucleic Acids Res. *35*, 1402–1410.

Shah, S., Lubeck, E., Zhou, W., and Cai, L. (2016). In Situ Transcription Profiling of Single Cells Reveals Spatial Organization of Cells in the Mouse Hippocampus. Neuron *92*, 342–357.

Shen, K., and Scheiffele, P. (2010). Genetics and cell biology of building specific synaptic connectivity. Annu. Rev. Neurosci. *33*, 473–507.

Shipman, S.L., and Nicoll, R.A. (2012). Dimerization of postsynaptic neuroligin drives synaptic assembly via transsynaptic clustering of neurexin. Proc. Natl. Acad. Sci. U. S. A. *109*, 19432–19437.

Sia, G.-M., Béïque, J.-C., Rumbaugh, G., Cho, R., Worley, P.F., and Huganir, R.L. (2007). Interaction of the N-Terminal Domain of the AMPA Receptor GluR4 Subunit with the Neuronal Pentraxin NP1 Mediates GluR4 Synaptic Recruitment. Neuron *55*, 87–102.

Siddiqui, T.J., and Craig, A.M. (2011). Synaptic organizing complexes. Curr. Opin. Neurobiol. *21*, 132–143.

Siddiqui, T.J., Pancaroglu, R., Kang, Y., Rooyakkers, A., and Craig, A.M. (2010). LRRTMs and Neuroligins Bind Neurexins with a Differential Code to Cooperate in Glutamate Synapse Development. J. Neurosci. Off. J. Soc. Neurosci. *30*, 7495–7506.

Siddiqui, T.J., Tari, P.K., Connor, S.A., Zhang, P., Dobie, F.A., She, K., Kawabe, H., Wang, Y.T., Brose, N., and Craig, A.M. (2013). An LRRTM4-HSPG Complex Mediates Excitatory Synapse Development on Dentate Gyrus Granule Cells. Neuron *79*, 680–695.

Silberberg, S.N., Taher, L., Lindtner, S., Sandberg, M., Nord, A.S., Vogt, D., Mckinsey, G.L., Hoch, R., Pattabiraman, K., Zhang, D., et al. (2016). Subpallial Enhancer Transgenic Lines: a Data and Tool Resource to Study Transcriptional Regulation of GABAergic Cell Fate. Neuron *92*, 59–74.

Silver, D.P., and Livingston, D.M. (2001). Self-excising retroviral vectors encoding the Cre recombinase overcome Cre-mediated cellular toxicity. Mol. Cell *8*, 233–243.

Simmons, A.B., Bloomsburg, S.J., Billingslea, S.A., Merrill, M.M., Li, S., Thomas, M.W., and Fuerst, P.G. (2016a). Pou4f2 knock-in Cre mouse: A multifaceted genetic tool for vision researchers. Mol. Vis. *22*, 705–717.

Simmons, A.B., Bloomsburg, S.J., Billingslea, S.A., Merrill, M.M., Li, S., Thomas, M.W., and Fuerst, P.G. (2016b). Pou4f2 knock-in Cre mouse: A multifaceted genetic tool for vision researchers. Mol. Vis. *22*, 705–717.

Singh, S.K., Stogsdill, J.A., Pulimood, N.S., Dingsdale, H., Kim, Y.H., Pilaz, L.-J., Kim, I.H., Manhaes, A.C., Rodrigues, W.S., Pamukcu, A., et al. (2016). Astrocytes Assemble Thalamocortical Synapses by Bridging NRX1α and NL1 via Hevin. Cell *164*, 183–196.

Skaletsky, H., Kuroda-Kawaguchi, T., Minx, P.J., Cordum, H.S., Hillier, L., Brown, L.G., Repping, S., Pyntikova, T., Ali, J., Bieri, T., et al. (2003). The male-specific region of the human Y chromosome is a mosaic of discrete sequence classes. Nature *423*, 825–837.

Slomianka, L., Amrein, I., Knuesel, I., Sørensen, J.C., and Wolfer, D.P. (2011). Hippocampal pyramidal cells: the reemergence of cortical lamination. Brain Struct. Funct. *216*, 301–317.

Smith, C.M., Hayamizu, T.F., Finger, J.H., Bello, S.M., McCright, I.J., Xu, J., Baldarelli, R.M., Beal, J.S., Campbell, J., Corbani, L.E., et al. (2019). The mouse Gene Expression Database (GXD): 2019 update. Nucleic Acids Res. *47*, D774–D779.

Soltesz, I., and Losonczy, A. (2018). CA1 pyramidal cell diversity enabling parallel information processing in the hippocampus. Nat. Neurosci. *21*, 484–493.

Song, A.J., and Palmiter, R.D. (2018). Detecting and Avoiding Problems When Using the Cre–lox System. Trends Genet. *34*, 333–340.

Song, J.-Y., Ichtchenko, K., Südhof, T.C., and Brose, N. (1999). Neuroligin 1 is a postsynaptic cell-adhesion molecule of excitatory synapses. Proc. Natl. Acad. Sci. *96*, 1100–1105.

Ster, J., Steuble, M., Orlando, C., Diep, T.-M., Akhmedov, A., Raineteau, O., Pernet, V., Sonderegger, P., and Gerber, U. (2014). Calsyntenin-1 Regulates Targeting of Dendritic NMDA Receptors and Dendritic Spine Maturation in CA1 Hippocampal Pyramidal Cells during Postnatal Development. J. Neurosci. *34*, 8716–8727.

Sterky, F.H., Trotter, J.H., Lee, S.-J., Recktenwald, C.V., Du, X., Zhou, B., Zhou, P., Schwenk, J., Fakler, B., and Südhof, T.C. (2017). Carbonic anhydrase-related protein CA10 is an evolutionarily conserved pan-neurexin ligand. Proc. Natl. Acad. Sci. *114*, E1253–E1262.

Sternberg, N., and Hamilton, D. (1981). Bacteriophage P1 site-specific recombination: I. Recombination between loxP sites. J. Mol. Biol. *150*, 467–486.

Steuble, M., Diep, T.-M., Schätzle, P., Ludwig, A., Tagaya, M., Kunz, B., and Sonderegger, P. (2012). Calsyntenin-1 shelters APP from proteolytic processing during anterograde axonal transport. Biol. Open BIO20121578.

Stevens, C.F. (2003). Neurotransmitter Release at Central Synapses. Neuron *40*, 381–388.

Stuchlik, A. (2014). Dynamic learning and memory, synaptic plasticity and neurogenesis: an update. Front. Behav. Neurosci. *8*.

Südhof, T.C. (2008). Neuroligins and neurexins link synaptic function to cognitive disease. Nature *455*, 903–911.

Südhof, T.C. (2017). Synaptic Neurexin Complexes: A Molecular Code for the Logic of Neural Circuits. Cell *171*, 745–769.

Südhof, T.C. (2018). Towards an Understanding of Synapse Formation. Neuron *100*, 276–293.

Südhof, T.C., and Malenka, R.C. (2008). Understanding Synapses: Past, Present, and Future. Neuron *60*, 469–476.

Sugita, S., Saito, F., Tang, J., Satz, J., Campbell, K., and Südhof, T.C. (2001). A stoichiometric complex of neurexins and dystroglycan in brain. J Cell Biol *154*, 435–446.

Suzuki, K., Hayashi, Y., Nakahara, S., Kumazaki, H., Prox, J., Horiuchi, K., Zeng, M., Tanimura, S., Nishiyama, Y., Osawa, S., et al. (2012). Activity-dependent proteolytic cleavage of neuroligin-1. Neuron *76*, 410–422.

Tabuchi, K., and Südhof, T.C. (2002). Structure and evolution of neurexin genes: insight into the mechanism of alternative splicing. Genomics *79*, 849–859.

Tabuchi, K., Blundell, J., Etherton, M.R., Hammer, R.E., Liu, X., Powell, C.M., and Südhof, T.C. (2007). A neuroligin-3 mutation implicated in autism increases inhibitory synaptic transmission in mice. Science *318*, 71–76.

Tachibana, N., Touahri, Y., Dixit, R., David, L.A., Adnani, L., Cantrup, R., Aavani, T., Wong, R.O., Logan, C., Kurek, K.C., et al. (2018). Hamartoma-like lesions in the mouse retina: an animal model of Pten hamartoma tumour syndrome. Dis. Model. Mech. *11*.

Takács, V.T., Freund, T.F., and Nyiri, G. (2013). Neuroligin 2 Is Expressed in Synapses Established by Cholinergic Cells in the Mouse Brain. PLOS ONE *8*, e72450.

Takahashi, H., and Craig, A.M. (2013). Protein tyrosine phosphatases PTPδ, PTPσ, and LAR: presynaptic hubs for synapse organization. Trends Neurosci. *36*, 522–534.

Takahashi, H., Arstikaitis, P., Prasad, T., Bartlett, T.E., Wang, Y.T., Murphy, T.H., and Craig, A.M. (2011). Postsynaptic TrkC and presynaptic PTPσ function as a bidirectional excitatory synaptic organizing complex. Neuron *69*, 287–303.

Takahashi, H., Katayama, K.-I., Sohya, K., Miyamoto, H., Prasad, T., Matsumoto, Y., Ota, M., Yasuda, H., Tsumoto, T., Aruga, J., et al. (2012). Selective control of inhibitory synapse development by Slitrk3-PTPδ trans-synaptic interaction. Nat. Neurosci. *15*, 389–398, S1-2.

Takebayashi, H., Usui, N., Ono, K., and Ikenaka, K. (2008). Tamoxifen modulates apoptosis in multiple modes of action in CreER mice. Genes. N. Y. N 2000 *46*, 775–781.

Tanabe, Y., Naito, Y., Vasuta, C., Lee, A.K., Soumounou, Y., Linhoff, M.W., and Takahashi, H. (2017). IgSF21 promotes differentiation of inhibitory synapses via binding to neurexin2α. Nat. Commun. *8*, 408.

Taniguchi, H., He, M., Wu, P., Kim, S., Paik, R., Sugino, K., Kvitsiani, D., Kvitsani, D., Fu, Y., Lu, J., et al. (2011). A resource of Cre driver lines for genetic targeting of GABAergic neurons in cerebral cortex. Neuron *71*, 995–1013.

Terauchi, A., Gavin, E., Wilson, J., and Umemori, H. (2017). Selective Inactivation of Fibroblast Growth Factor 22 (FGF22) in CA3 Pyramidal Neurons Impairs Local Synaptogenesis and Affective Behavior Without Affecting Dentate Neurogenesis. Front. Synaptic Neurosci. *9*, 17.

Thapliyal, S., Ravindranath, S., and Babu, K. (2018a). Regulation of Glutamate Signaling in the Sensorimotor Circuit by CASY-1A/Calsyntenin in Caenorhabditis elegans. Genetics *208*, 1553–1564.

Thapliyal, S., Vasudevan, A., Dong, Y., Bai, J., Koushika, S.P., and Babu, K. (2018b). The C-terminal of CASY-1/Calsyntenin regulates GABAergic synaptic transmission at the Caenorhabditis elegans neuromuscular junction. PLOS Genet. *14*, e1007263.

Thomason, L.C., Calendar, R., and Ow, D.W. (2001). Gene insertion and replacement in Schizosaccharomyces pombe mediated by the Streptomyces bacteriophage phiC31 site-specific recombination system. Mol. Genet. Genomics MGG *265*, 1031–1038.

Tronche, F., Kellendonk, C., Kretz, O., Gass, P., Anlag, K., Orban, P.C., Bock, R., Klein, R., and Schütz, G. (1999). Disruption of the glucocorticoid receptor gene in the nervous system results in reduced anxiety. Nat. Genet. *23*, 99.

Trumpp, A., Depew, M.J., Rubenstein, J.L., Bishop, J.M., and Martin, G.R. (1999). Cre-mediated gene inactivation demonstrates that FGF8 is required for cell survival and patterning of the first branchial arch. Genes Dev. *13*, 3136–3148.

Tsai, P.T., Hull, C., Chu, Y., Greene-Colozzi, E., Sadowski, A.R., Leech, J.M., Steinberg, J., Crawley, J.N., Regehr, W.G., and Sahin, M. (2012a). Autistic-like behaviour and cerebellar dysfunction in Purkinje cell *Tsc1* mutant mice. Nature *488*, 647–651.

Tsai, P.T., Hull, C., Chu, Y., Greene-Colozzi, E., Sadowski, A.R., Leech, J.M., Steinberg, J., Crawley, J.N., Regehr, W.G., and Sahin, M. (2012b). Autistic-like behaviour and cerebellar dysfunction in Purkinje cell Tsc1 mutant mice. Nature *488*, 647–651.

Tsien, J.Z. (2018). Chapter 20 - Cre-lox Neurogenetics: History, Present, and Future. In Molecular-Genetic and Statistical Techniques for Behavioral and Neural Research, R.T. Gerlai, ed. (San Diego: Academic Press), pp. 479–490.

Tsien, J.Z., Chen, D.F., Gerber, D., Tom, C., Mercer, E.H., Anderson, D.J., Mayford, M., Kandel, E.R., and Tonegawa, S. (1996a). Subregion- and Cell Type–Restricted Gene Knockout in Mouse Brain. Cell *87*, 1317–1326.

Tsien, J.Z., Huerta, P.T., and Tonegawa, S. (1996b). The Essential Role of Hippocampal CA1 NMDA Receptor–Dependent Synaptic Plasticity in Spatial Memory. Cell *87*, 1327–1338.

Tu, R., Qian, J., Rui, M., Tao, N., Sun, M., Zhuang, Y., Lv, H., Han, J., Li, M., and Xie, W. (2017). Proteolytic cleavage is required for functional neuroligin 2 maturation and trafficking in Drosophila. J. Mol. Cell Biol. *9*, 231–242.

Twining, R.C., Vantrease, J.E., Love, S., Padival, M., and Rosenkranz, J.A. (2017). An intra-amygdala circuit specifically regulates social fear learning. Nat. Neurosci. *20*, 459–469.

Uchigashima, M., Ohtsuka, T., Kobayashi, K., and Watanabe, M. (2016). Dopamine synapse is a neuroligin-2–mediated contact between dopaminergic presynaptic and GABAergic postsynaptic structures. Proc. Natl. Acad. Sci. *113*, 4206–4211.

Uemura, T., Lee, S.-J., Yasumura, M., Takeuchi, T., Yoshida, T., Ra, M., Taguchi, R., Sakimura, K., and Mishina, M. (2010). Trans-synaptic interaction of GluRdelta2 and Neurexin through Cbln1 mediates synapse formation in the cerebellum. Cell *141*, 1068–1079.

Um, J.W., Pramanik, G., Ko, J.S., Song, M.-Y., Lee, D., Kim, H., Park, K.-S., Südhof, T.C., Tabuchi, K., and Ko, J. Calsyntenins Function as Synaptogenic Adhesion Molecules in Concert with Neurexins. Cell Rep.

Ushkaryov, Y.A., and Südhof, T.C. (1993). Neurexin III alpha: extensive alternative splicing generates membrane-bound and soluble forms. Proc. Natl. Acad. Sci. U. S. A. *90*, 6410–6414.

Ushkaryov, Y.A., Petrenko, A.G., Geppert, M., and Südhof, T.C. (1992). Neurexins: synaptic cell surface proteins related to the alpha-latrotoxin receptor and laminin. Science *257*, 50–56.

Ushkaryov, Y.A., Hata, Y., Ichtchenko, K., Moomaw, C., Afendis, S., Slaughter, C.A., and Südhof, T.C. (1994). Conserved domain structure of beta-neurexins. Unusual cleaved signal sequences in receptor-like neuronal cell-surface proteins. J. Biol. Chem. *269*, 11987–11992.

Vaags, A.K., Lionel, A.C., Sato, D., Goodenberger, M., Stein, Q.P., Curran, S., Ogilvie, C., Ahn, J.W., Drmic, I., Senman, L., et al. (2012). Rare deletions at the neurexin 3 locus in autism spectrum disorder. Am. J. Hum. Genet. *90*, 133–141.

Vagnoni, A., Rodriguez, L., Manser, C., De Vos, K.J., and Miller, C.C.J. (2011). Phosphorylation of kinesin light chain 1 at serine 460 modulates binding and trafficking of calsyntenin-1. J. Cell Sci. *124*, 1032–1042.

Vagnoni, A., Perkinton, M.S., Gray, E.H., Francis, P.T., Noble, W., and Miller, C.C.J. (2012). Calsyntenin-1 mediates axonal transport of the amyloid precursor protein and regulates Aβ production. Hum. Mol. Genet. *21*, 2845–2854.

Van Horn, M.R., and Ruthazer, E.S. (2019). Glial regulation of synapse maturation and stabilization in the developing nervous system. Curr. Opin. Neurobiol. *54*, 113–119.

Varoqueaux, F., Jamain, S., and Brose, N. (2004). Neuroligin 2 is exclusively localized to inhibitory synapses. Eur. J. Cell Biol. *83*, 449–456.

Venkatesh, H.S., Johung, T.B., Caretti, V., Noll, A., Tang, Y., Nagaraja, S., Gibson, E.M., Mount, C.W., Polepalli, J., Mitra, S.S., et al. (2015). Neuronal Activity Promotes Glioma Growth through Neuroligin-3 Secretion. Cell *161*, 803–816.

Vogt, L., Schrimpf, S.P., Meskenaite, V., Frischknecht, R., Kinter, J., Leone, D.P., Ziegler, U., and Sonderegger, P. (2001). Calsyntenin-1, a proteolytically processed postsynaptic membrane protein with a cytoplasmic calcium-binding domain. Mol. Cell. Neurosci. *17*, 151–166.

Vong, L., Ye, C., Yang, Z., Choi, B., Chua, S., and Lowell, B.B. (2011). Leptin Action on GABAergic Neurons Prevents Obesity and Reduces Inhibitory Tone to POMC Neurons. Neuron *71*, 142–154.

Walsh, T., McClellan, J.M., McCarthy, S.E., Addington, A.M., Pierce, S.B., Cooper, G.M., Nord, A.S., Kusenda, M., Malhotra, D., Bhandari, A., et al. (2008). Rare structural variants disrupt multiple genes in neurodevelopmental pathways in schizophrenia. Science *320*, 539–543.

Weng, D.Y., Zhang, Y., Hayashi, Y., Kuan, C.-Y., Liu, C.-Y., Babcock, G., Weng, W.-L., Schwemberger, S., and Kao, W.W.-Y. (2008). Promiscuous recombination of LoxP alleles during gametogenesis in cornea Cre driver mice. Mol. Vis. *14*, 562–571.

Wicksteed, B., Brissova, M., Yan, W., Opland, D.M., Plank, J.L., Reinert, R.B., Dickson, L.M., Tamarina, N.A., Philipson, L.H., Shostak, A., et al. (2010). Conditional gene targeting in mouse

pancreatic ß-Cells: analysis of ectopic Cre transgene expression in the brain. Diabetes *59*, 3090–3098.

Winkler, C.C., Yabut, O.R., Fregoso, S.P., Gomez, H.G., Dwyer, B.E., Pleasure, S.J., and Franco, S.J. (2018). The Dorsal Wave of Neocortical Oligodendrogenesis Begins Embryonically and Requires Multiple Sources of Sonic Hedgehog. J. Neurosci. *38*, 5237–5250.

Witten, I.B., Steinberg, E.E., Lee, S.Y., Davidson, T.J., Zalocusky, K.A., Brodsky, M., Yizhar, O., Cho, S.L., Gong, S., Ramakrishnan, C., et al. (2011). Recombinase-driver rat lines: tools, techniques, and optogenetic application to dopamine-mediated reinforcement. Neuron *72*, 721–733.

Wojcinski, A., Morabito, M., Lawton, A.K., Stephen, D.N., and Joyner, A.L. (2019). Genetic deletion of genes in the cerebellar rhombic lip lineage can stimulate compensation through adaptive reprogramming of ventricular zone-derived progenitors. Neural Develop. *14*, 4.

Wu, X., Morishita, W.K., Riley, A.M., Hale, W.D., Südhof, T.C., and Malenka, R.C. (2019). Neuroligin-1 Signaling Controls LTP and NMDA Receptors by Distinct Molecular Pathways. Neuron.

Yim, Y.S., Kwon, Y., Nam, J., Yoon, H.I., Lee, K., Kim, D.G., Kim, E., Kim, C.H., and Ko, J. (2013). Slitrks control excitatory and inhibitory synapse formation with LAR receptor protein tyrosine phosphatases. Proc. Natl. Acad. Sci. *110*, 4057–4062.

Zeller, A., Crestani, F., Camenisch, I., Iwasato, T., Itohara, S., Fritschy, J.M., and Rudolph, U. (2008a). Cortical glutamatergic neurons mediate the motor sedative action of diazepam. Mol. Pharmacol. *73*, 282–291.

Zeller, A., Crestani, F., Camenisch, I., Iwasato, T., Itohara, S., Fritschy, J.M., and Rudolph, U. (2008b). Cortical Glutamatergic Neurons Mediate the Motor Sedative Action of Diazepam. Mol. Pharmacol. *73*, 282–291.

Zeng, X., Ye, M., Resch, J.M., Jedrychowski, M.P., Hu, B., Lowell, B.B., Ginty, D.D., and Spiegelman, B.M. (2019). Innervation of thermogenic adipose tissue via a calsyntenin 3β–S100b axis. Nature 1.

Zerucha, T., Stühmer, T., Hatch, G., Park, B.K., Long, Q., Yu, G., Gambarotta, A., Schultz, J.R., Rubenstein, J.L.R., and Ekker, M. (2000). A Highly Conserved Enhancer in the Dlx5/Dlx6Intergenic Region is the Site of Cross-Regulatory Interactions betweenDlx Genes in the Embryonic Forebrain. J. Neurosci. *20*, 709–721.

Zhang, Z., and Lutz, B. (2002). Cre recombinase-mediated inversion using lox66 and lox71: method to introduce conditional point mutations into the CREB-binding protein. Nucleic Acids Res. *30*, e90.

Zhang, B., Chen, L.Y., Liu, X., Maxeiner, S., Lee, S.-J., Gokce, O., and Südhof, T.C. (2015). Neuroligins Sculpt Cerebellar Purkinje-Cell Circuits by Differential Control of Distinct Classes of Synapses. Neuron *87*, 781–796.

Zhang, H., Kranzler, H.R., Poling, J., Gruen, J.R., and Gelernter, J. (2009). Cognitive flexibility is associated with KIBRA variant and modulated by recent tobacco use. Neuropsychopharmacol. Off. Publ. Am. Coll. Neuropsychopharmacol. *34*, 2508–2516.

Zhang, J., Dublin, P., Griemsmann, S., Klein, A., Brehm, R., Bedner, P., Fleischmann, B.K., Steinhäuser, C., and Theis, M. (2013a). Germ-Line Recombination Activity of the Widely Used hGFAP-Cre and Nestin-Cre Transgenes. PLOS ONE *8*, e82818.

Zhang, J., Dublin, P., Griemsmann, S., Klein, A., Brehm, R., Bedner, P., Fleischmann, B.K., Steinhäuser, C., and Theis, M. (2013b). Germ-Line Recombination Activity of the Widely Used hGFAP-Cre and Nestin-Cre Transgenes. PLOS ONE *8*, e82818.

Zhang, P., Lu, H., Peixoto, R.T., Pines, M.K., Ge, Y., Oku, S., Siddiqui, T.J., Xie, Y., Wu, W., Archer-Hartmann, S., et al. (2018). Heparan Sulfate Organizes Neuronal Synapses through Neurexin Partnerships. Cell *174*, 1450-1464.e23.

Zhang, W., Rohlmann, A., Sargsyan, V., Aramuni, G., Hammer, R.E., Südhof, T.C., and Missler, M. (2005). Extracellular domains of alpha-neurexins participate in regulating synaptic transmission by selectively affecting N- and P/Q-type Ca2+ channels. J. Neurosci. Off. J. Soc. Neurosci. *25*, 4330–4342.

Zhang, Y., Chen, K., Sloan, S.A., Bennett, M.L., Scholze, A.R., O'Keeffe, S., Phatnani, H.P., Guarnieri, P., Caneda, C., Ruderisch, N., et al. (2014). An RNA-Sequencing Transcriptome and Splicing Database of Glia, Neurons, and Vascular Cells of the Cerebral Cortex. J. Neurosci. *34*, 11929–11947.

Zheng, B., Sage, M., Sheppeard, E.A., Jurecic, V., and Bradley, A. (2000). Engineering mouse chromosomes with Cre-loxP: range, efficiency, and somatic applications. Mol. Cell. Biol. *20*, 648–655.

Zhu, J., Nguyen, M.-T., Nakamura, E., Yang, J., and Mackem, S. (2012). Cre-mediated recombination can induce apoptosis in vivo by activating the p53 DNA damage-induced pathway. Genes. N. Y. N 2000 *50*, 102–111.

Zweier, C., de Jong, E.K., Zweier, M., Orrico, A., Ousager, L.B., Collins, A.L., Bijlsma, E.K., Oortveld, M.A.W., Ekici, A.B., Reis, A., et al. (2009). CNTNAP2 and NRXN1 Are Mutated in Autosomal-Recessive Pitt-Hopkins-like Mental Retardation and Determine the Level of a Common Synaptic Protein in Drosophila. Am. J. Hum. Genet. *85*, 655–666.

Appendices

Appendix A Detailed comparisons on the different Cre lines under the same driver

Common name	Cre line full name	Description	Reference	Author comments
CaMKIIα-Cre	Tg(Camk2a-cre)159Kln	**Transgene.** The expression vector for CaMKII–CRE transgenic mice consists of the 8.5 kb CaMKIIα promoter (Mayford et al., 1996) followed by a hybrid intron in front of the CRE coding region with nuclear localization sequence and a SV40 polyadenylation signal. 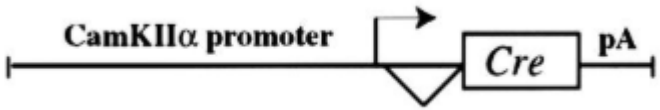	(Minichiello et al., 1999)	These three sequences are almost identical, with the 8.5kb CamKIIa promoter, the hybrid intron, Cre with nuclear localization sequence and an SV40 polyadenylation sequence. There might be a difference between the intron sequences where enhancers could locate in, resulting in different Cre
CaMKIIα-Cre	Tg(Camk2a-cre)93Kln	**Transgene.** Construct the same and generated together as above 159 line, but this is insertion 93.		
CaMKIIα-Cre	B6.Cg-Tg(Camk2a-cre)2Szi/J	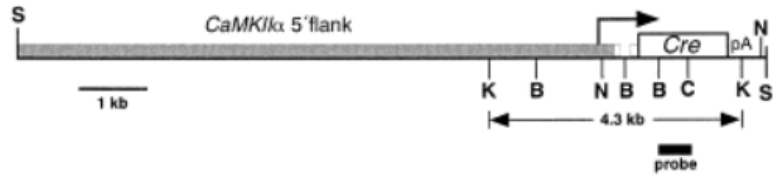 **Transgene.** The 5’-flanking sequence containing the CaMKIIa promoter (Mayford et al., 1996) and the cre coding sequence (modified with a nuclear localization signal; Guet al., 1994) are indicated with gray and white rectangles, respectively. The orientation of transcription is indicated with an arrow, and the positions of the short hybrid intron derived from an adenovirus splice donor and an immunoglobulin G splice acceptor (from pNN265;	(Dragatsis and Zeitlin, 2000)	

Common name	Cre line full name	Description	Reference	Author comments
		Choiet al., 1991) and the SV40poly(A) addition sequence from pNN265 are shown.		expression levels in ectopic regions.
CaMKIIα-Cre (T29-1)	Tg(Camk2a-cre)T29-1Stl	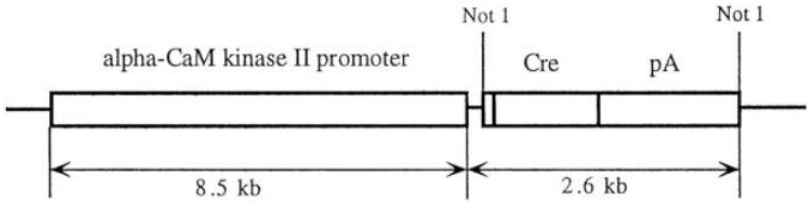 **Transgene.** For the production of Cre transgenic mice, we chose the 8.5 kb genomic DNA fragment derived from the αCaMKII gene. The Cre DNA construct contains an intron and an SV40 polyadenylation signal at the 5' and 3' sides of the Cre transgene, respectively, along with a nuclear localization signal (Kalderon et al. 1984) that may promote transport of Cre recombinase to the nucleus, the site of Cre/loxP recombination.	(Tsien et al., 1996a)	

Common name	Cre line full name	Description	Reference	Author comments
Emx1-Cre	Emx1$^{tm1(cre)Ito}$	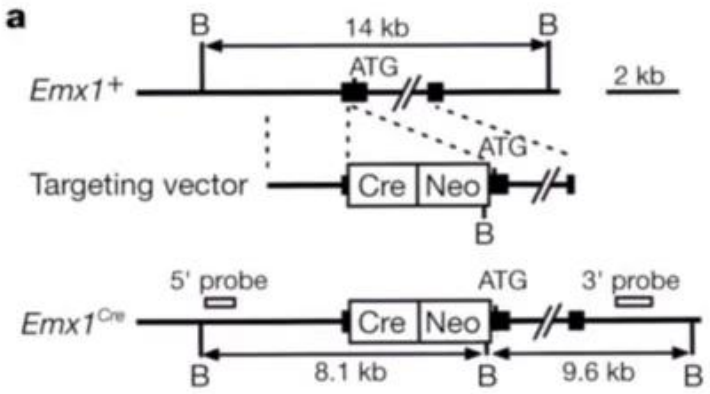 **Targeted insertion.** A 9.4-kilobase (kb) fragment of the *Emx1* gene was used to make the targeting construct. The *NLS-Cre-poly (A)* gene and the *pgk-Neo-poly (A*) gene were inserted into a *Not*I site immediately before the *Emx1*translation initiation site, in the sense orientation. The targeting construct was transfected into ES cells (E14) using a standard protocol. Homologous recombinants were identified by Southern blotting by the presence of 8.1-kb and 9.6-kb bands in *Bgl* II-digested genomic DNA hybridized with 5′ (*Eco*RI 0.9 kb) and 3′ (*Pst*I–*Eco* RI 1 kb) (not shown) probes, respectively. The ES cell clones containing the targeting event were	(Iwasato et al., 2000)	The addition of IRES may have helped to attenuate Cre expression level in ectopic regions thus reducing germline recombination, similar to Pvalb-IRES-Cre below.

Common name	Cre line full name	Description	Reference	Author comments
		injected into C57BL/6 blastocysts and chimaeras were derived. Chimeric male mice were crossed with C57BL/6 females to achieve germline transmission.		
Emx1-Cre	B6.129S2-Emx1$^{tm1(cre)Krj}$/J	 **Targeted insertion.** An Emx1 cDNA fragment (Qiu et al., 1996) was used to isolate a genomic clone containing the last Emx1 exon. An improved internal ribosomal entry site IRES *cre* gene (Gorski and Jones, 1999) followed by an FRT site-flanked PGK neo selectable marker was inserted into an *Xho*I site located 120 bp 3′ of the Emx1 stop codon. The FRT-PGKneo-FRT cassette was generated by annealing oligonucleotides containing FRT sites followed by ligation to the *Eco*RI–*Hin*dIII PGKneo fragment from pGEM7 (KJ1) (Rudnicki et al., 1992).	(Gorski et al., 2002)	
Grik4-Cre	B6-Tg(Grik4-cre)G32-4Stl/J	**Transgene.** We isolated an approximately 120-kb-long bacterial artificial chromosome (BAC) clone BAC1, that contained a part of the genomic sequence of mouse KA-1, one of the kainate receptor subunits, by screening a C57BL/6 (B6) BAC library (Genome Systems) with a probe composed of the 5' untranslated region of a mouse KA-1 cDNA clone (*S1*). The BAC1 clone contained the genomic DNA	(Nakazawa et al., 2002)	Not sufficient information for the germline recombination frequencies are

Common name	Cre line full name	Description	Reference	Author comments
		sequence of the putative promoter, exon 1 (~338 bp) and exon 2 (45 bp), but not exon 3 (105 bp) carrying the translation initiation codon. The entire BAC1-DNA fragment was coinjected into fertilized B6 mouse eggs with a DNA construct carrying both the minimal heat shock promoter (from pIND plasmid, Invitrogen), and the Cre cDNA with nuclear localization signal (pBS317, provided by B. Sauer). Out of eight founder lines in which both Cre and BAC1 sequences were cointegrated into the genome, the line referred to as G32-4 was crossed with the Rosa26 reporter line		available for comparison.
Grik4-Cre	Grik4$^{tm1(cre)Ksak}$	**Targeted insertion.** We designed a targeting vector in which Cre gene was placed just behind the translational initiation site of the GluK4 gene (*Grik4*) in frame. Therefore, two genomic DNA clones carrying the *Grik4* translational start site were isolated from a C57BL/6 genomic library (Stratagene). A 272 bp *Pst*I–*Age*I fragment was generated by two-step PCR using *GPcrik4* genomic DNA and pNCre (Tsujita et al., 1999) as templates. A knock-in vector pγ1TVCre contained a 3 kb fragment at the 5′ side, a Cre gene placed behind the *Grik4* translational start, a *Pgk*-neo-p(A) cassette, a 7.5 kb fragment at the 3′ side, and a MC1 promoter-driven diphtheria toxin gene.	(Akashi et al., 2009)	

Common name	Cre line full name	Description	Reference	Author comments
		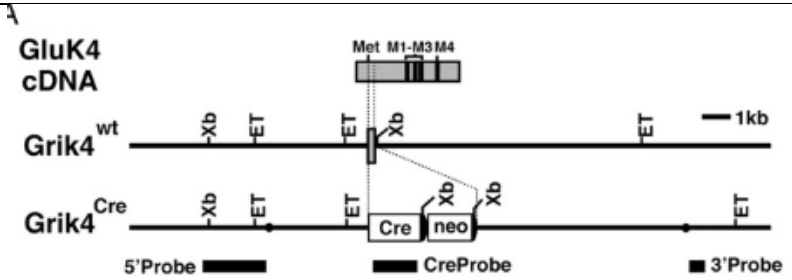 The gray boxes indicate exons. The black boxes indicate the probes for Southern blot analysis. The filled circles in the Grik4Cre allele delineate the 5' and 3' termini of the targeting vector. The semicircles indicate FRT sequences. Met, Initial methionine; Cre, Cre recombinase gene; neo, neomycin-resistant gene expression cassette; Xb, XbaI; ET, EcoT22-I.		
Nestin-Cre	Tg(Nes-cre)1Kln/J	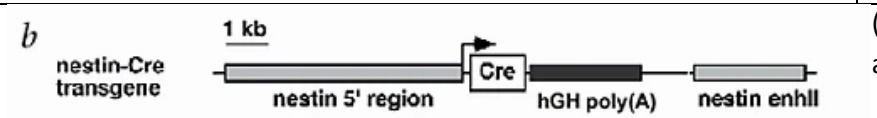 **Transgene.** Cre recombinase was expressed under the control of the promoter and the nervous system-specific enhancer present in the second intron of the rat nestin gene. hGH poly (A), human growth hormone polyadenylation signal.	(Tronche et al., 1999)	Not sufficient information for the germline recombination frequencies are available for comparison.
Nestin-Cre	Tg(Nes-cre)1Atp		(Dubois et al., 2006;	

Common name	Cre line full name	Description	Reference	Author comments
		Transgene. A modified Cre gene carrying a nuclear localization signal (NLS-Cre) and an actin polyA signal (pA) was placed in between the 5.8 kb rat nestin promoter and the rat nestin intron 2, which contains at least two enhancer elements. The grey boxes indicate short stretches of exon2 and 3.	Trumpp et al., 1999)	
Pcp2/L7-Cre	B6.129-Tg(Pcp2-cre)2Mpin/J	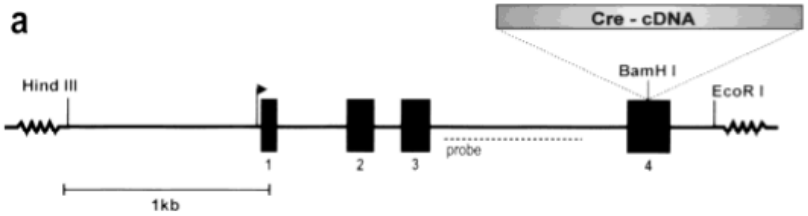 **Transgene.** The Cre cDNA was inserted into exon 4 of the L7 minigene, the construct linearized and used to electroporate R1 embryonic stem cells (Nagy et al., 1993). We have chosen a transgenic approach via embryonic stem cells as we wanted to avoid complex, potentially instable multi copy transgene arrays that are often observed after pronucleus injection.	(Barski et al., 2000)	Transgene > targeted insertion. The multi-copy caveat is avoided here by the ES cell approach, but random integration could still cause potential gene/regulatory elements disruption.

Common name	Cre line full name	Description	Reference	Author comments
Pcp2/L7-Cre	B6.129-Pcp2$^{tm1(cre)Nobs}$	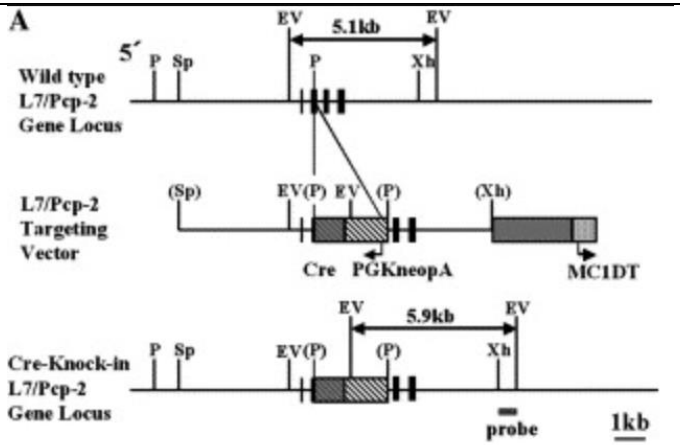 **Targeted insertion.** A knock-in-type targeting vector (Fig. 1A) was made by inserting the Cre recombinase gene with nuclear localizing signal and 1.7 kb the pgk-neo-polyA gene into the PvuI site of the second exon. The targeting vector contained SphI–PvuI 7 kb of homologous DNA upstream (left arm) of the PvuI site and PvuI–XhoI 5 kb of homologous DNA downstream (right arm) of the PvuI site. The MC1 DTA gene [11] was attached to the 3′ end of the vector for negative selection.	(Saito et al., 2005)	
Pvalb-2A-Cre	B6.Cg-Pvalb$^{tm1.1(cre)Aibs}$/J	**Targeted insertion.** The 2A-Cre sequence is inserted in frame to the 3′ end of the Pvalb coding sequence (immediately upstream of the stop codon). The resulting Cre-driver line has a similar genomic configuration as the previously reported Pvalb-IRES-Cre line, in	(Madisen et al., 2010)	The 2A-Cre is much stronger than the IRES-Cre, resulting in more widespread

Common name	Cre line full name	Description	Reference	Author comments
		which IRES-Cre is inserted by knock-in into the Pvalb 3' untranslated region. 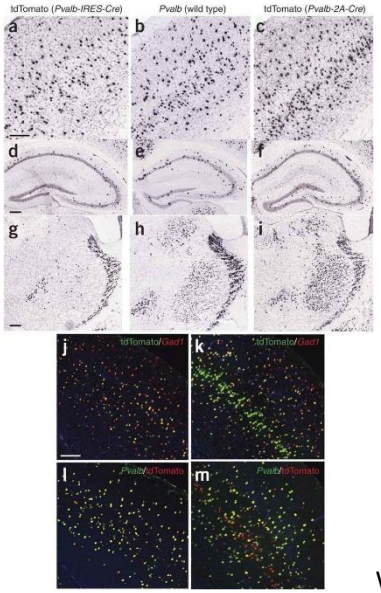 We found that, in the Pvalb-IRES-Cre mice, recombination seemed to occur only in cells with strongest Pvalb expression; that is, those large interneurons, and thus a more restricted (and perhaps more specific) pattern emerged than that of the Pvalb gene itself. By contrast, in the Pvalb-2A-Cre mice, recombination seemed to be more widespread, occurring in cells with both high and low Pvalb expression. These results indicate that different recombination patterns may be produced from different targeting methods even in the same locus. An IRES-mediated		expression in ectopic regions, including germlines.

Common name	Cre line full name	Description	Reference	Author comments
		approach may result in lower Cre protein levels and may be better used in conjunction with strong genes to increase recombination specificity. A 2A-based approach may produce more equimolar amounts of Cre relative to the targeted gene and may be better used with weakly expressing genes to increase sensitivity. Our data suggest a source of recombination variability beyond the commonly recognized positional effect as seen in the above BAC Cre lines.		
Pvalb-IRES-Cre	B6.129P2-Pvalb$^{tm1(cre)Arbr}$/J	**A** **B** 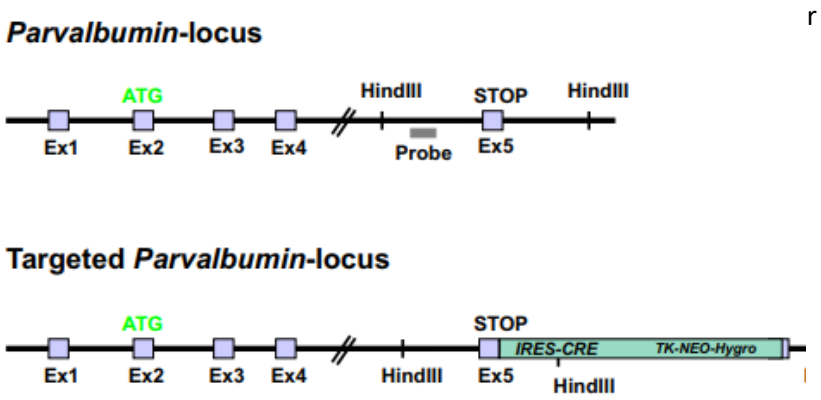 **Targeted insertion.** Probe to screen for homologous recombination is shown as grey box. Below is a schematic diagram to show the *PV* locus after the integration of an *IRES-Cre* cassette (green) 3' to the translational stop codon of *PV* using homologous recombination in ES cells.	(Hippenmeyer et al., 2005)	

Common name	Cre line full name	Description	Reference	Author comments
VGAT/VIAAT-Cre	Slc32a1$^{tm2(cre)Lowl}$/J	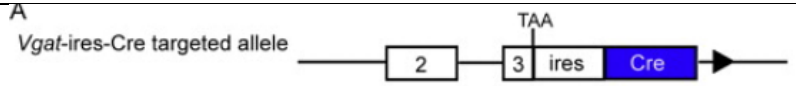 **Targeted insertion.** To ensure eutopic expression of Cre recombinase by VGAT-expressing neurons, we inserted an ires-Cre cassette by gene targeting just downstream of the endogenous Vgat stop codon.	(Vong et al., 2011)	Transgene > targeted insertion
VGAT/VIAAT-Cre	B6.FVB-Tg(Slc32a1-cre)2.1Hzo/FrkJ/	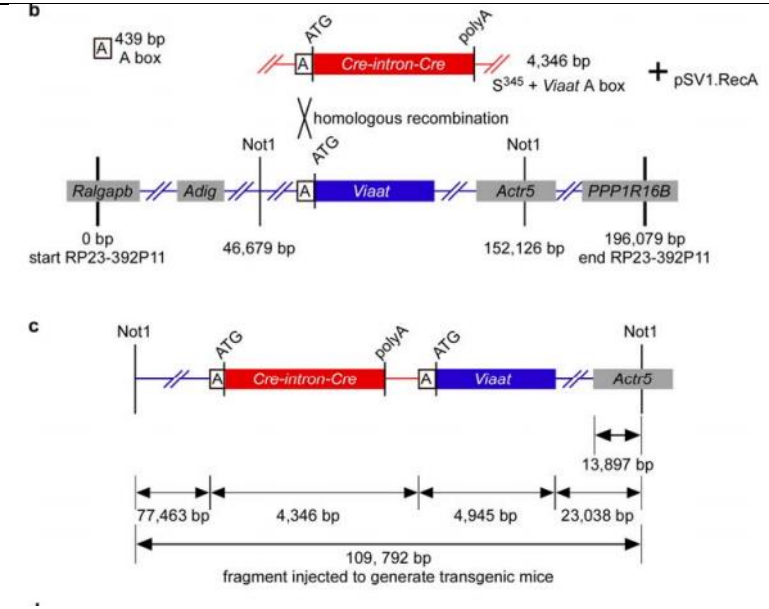 **Transgene.** Single step homologous recombination between S345 and BAC RP23-392P11 to form a co-integrate BAC with the S345 displacing Viaat coding sequence downstream of the A box	(Chao et al., 2010)	

Appendix B Detailed driver gene expression and Cre tissue activity in reproductive systems on 58 Cre lines

These data are screenshots of gene expression and Cre activity summary in different organ systems, which are either extracted from published literature or generated by Jackson Lab (MGI Direct Data Submission). The native gene expression results are from a mixture of mRNA *in situ* hybridization, immunohistochemistry, tissue specific RT-PCR, *in situ* knockin reporter expression etc., while the Cre tissue activity are mostly from recombinase reporter expression and some are from Cre antibody stainings.

Cre line common name	Full Cre line name/source	Gene expression		Cre activity		Reference (Screenshots from MGI database)	Germline recombination consistent with gene expression	Germline recombination consistent with Cre activity
		testis	ovary	testis	ovary			
799-CreER-IRES-GFP	Tg(hs799-cre/ERT2,-GFP)405Jlr						NA	NA
A2a-Cre	B6-Tg(Adora2a-Cre)KG139GSat	absent	controversial			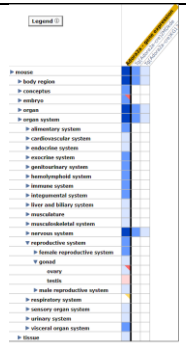	Yes?	NA
Bhlhb5-Cre	Bhlhe22$^{tm3.1(cre)Meg}$	absent	absent			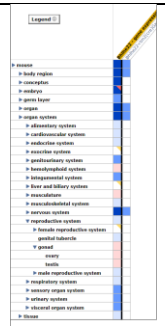	Yes	NA

Cre line common name	Full Cre line name/source	Gene expression		Cre activity		Reference (Screenshots from MGI database)	Germline recombination consistent with gene expression	Germline recombination consistent with Cre activity
		testis	ovary	testis	ovary			
Calb2-IRES-Cre	B6(Cg)-Calb2$^{tm1(cre)Zjh}$/J	present	present	Present in supporting cells, absent in spermatid	Present in supporting cells, absent in oocyte	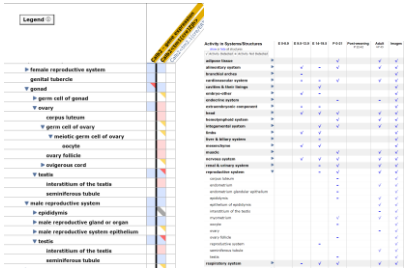	No	Yes
CaMKIIα-Cre	Tg(Camk2a-cre)159Kln	absent	present			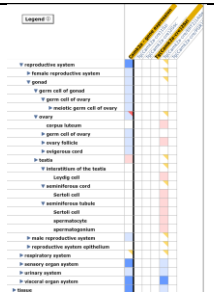	No	NA
CaMKIIα-Cre	Tg(Camk2a-cre)93Kln	absent	present			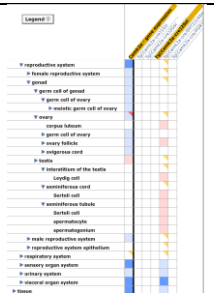	No	NA

Cre line common name	Full Cre line name/source	Gene expression		Cre activity		Reference (Screenshots from MGI database)	Germline recombination consistent with gene expression	Germline recombination consistent with Cre activity
		testis	ovary	testis	ovary			
CaMKIIα-Cre	B6.Cg-Tg(Camk2a-cre)2Szi/J	absent	present			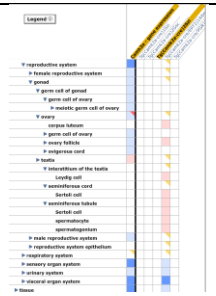	No	NA
CaMKIIα-Cre (T29-1)	Tg(Camk2a-cre)T29-1Stl	absent	present	present	absent		No	Yes
Chat-Cre	B6;129S6-Chat$^{tm2(cre)Lowl}$/J			absent	present		NA	No

Cre line common name	Full Cre line name/source	Gene expression		Cre activity		Reference (Screenshots from MGI database)	Germline recombination consistent with gene expression	Germline recombination consistent with Cre activity
		testis	ovary	testis	ovary			
Cux2-CreERT2	B6.Cg-Cux2$^{tm3.1(cre/ERT2)Mull}$/Mmmh		present			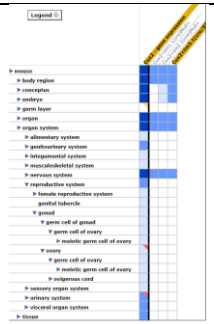	No	NA
D2-cre	Tg(Drd2-cre)44Gsat/Mmucd	present	absent			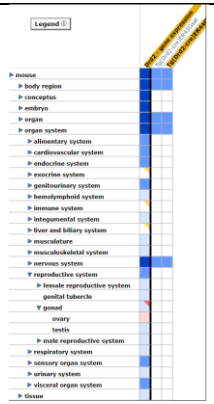	No	NA
DAT-Cre	Slc6a3$^{tm1.1(cre)Bkmn}$/J	present	absent	absent	absent		No	Yes

Cre line common name	Full Cre line name/source	Gene expression		Cre activity		Reference (Screenshots from MGI database)	Germline recombination consistent with gene expression	Germline recombination consistent with Cre activity
		testis	ovary	testis	ovary			
	B6.SJL-SLc6a3$^{tm1.1(cre)Bkm}$^{n}/J					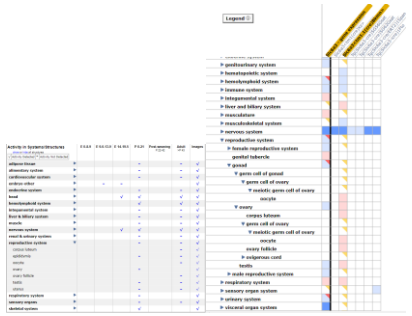		
Dlx5/6-Cre	B6-Tg(dlx5a-cre)1Mekk/J	absent	absent	Present E14-19.5, absent P0-21	Present E14-19.5, absent P0-21		No	No
DlxI12B-Cre	*Tg(I12b–cre)1Jlr*					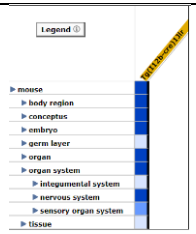	NA	NA

Cre line common name	Full Cre line name/source	Gene expression		Cre activity		Reference (Screenshots from MGI database)	Germline recombination consistent with gene expression	Germline recombination consistent with Cre activity
		testis	ovary	testis	ovary			
Drd1-Cre	B6-Tg(Drd1-Cre)EY262GSat B6.FVB(Cg)-Tg(Drd1-cre)EY262Gsat/Mmucd/GENSAT	Present	present			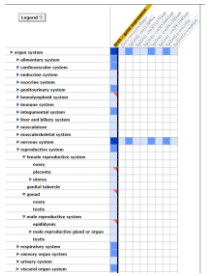	No	NA
Emx1-Cre	Emx1$^{tm1(cre)Ito}$						NA	NA
Emx1-Cre	B6.129S2-Emx1$^{tm1(cre)Krj}$/J			absent	absent	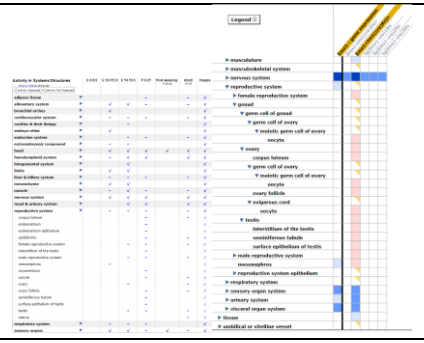	NA	No

Cre line common name	Full Cre line name/source	Gene expression		Cre activity		Reference (Screenshots from MGI database)	Germline recombination consistent with gene expression	Germline recombination consistent with Cre activity
		testis	ovary	testis	ovary			
En1-Cre	En1tm2(cre)Wrst/J	present	absent	Present in spermatocyte	absent	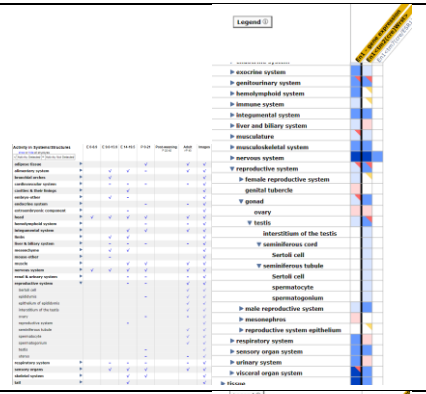	No	No
Foxd1-Cre	B6;129S4-Foxd1$^{tm1(GFP/cre)Amc}$/J	absent	absent	Present in supporting cells	Present in supporting cells		Yes	Yes

Cre line common name	Full Cre line name/source	Gene expression		Cre activity		Reference (Screenshots from MGI database)	Germline recombination consistent with gene expression	Germline recombination consistent with Cre activity
		testis	ovary	testis	ovary			
Foxg1-cre	129(Cg)-Foxg1tm1(cre)Skm/J	controversial				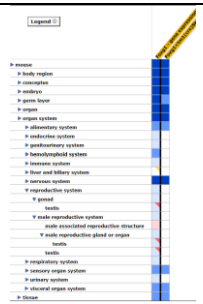	Yes?	NA
Gad2-IRES-Cre	B6.Cg-Gad2$^{tm2(cre)Zjh}$/J B6N.Cg-Gad2$^{tm2(cre)Zjh}$/J B6-GAD2$^{tm2(cre)Zjh}$/J	present	present	controversial	Absent in oocyte	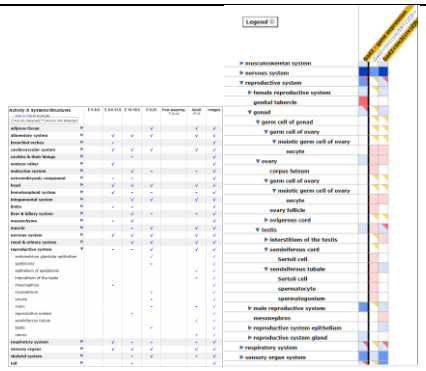	Yes?	Yes?

Cre line common name	Full Cre line name/source	Gene expression		Cre activity		Reference (Screenshots from MGI database)	Germline recombination consistent with gene expression	Germline recombination consistent with Cre activity
		testis	ovary	testis	ovary			
GFAP-cre	Tg(GFAP-cre)25Mes	absent		Present	Present	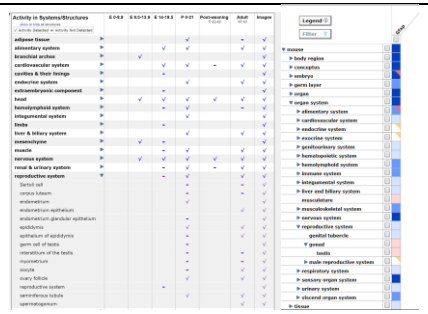	NA	Yes
Gpr26-Cre	B6-Tg(Gpr26-cre)KO250Gsat/Mmucd					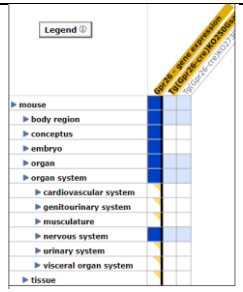	NA	NA
Grik4-Cre	B6-Tg(Grik4-cre)G32-4Stl/J			Absent in seminiferous tubule	In ovary, but not in oocyte	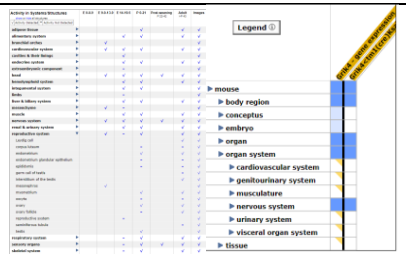	NA	No

Cre line common name	Full Cre line name/source	Gene expression		Cre activity		Reference (Screenshots from MGI database)	Germline recombination consistent with gene expression	Germline recombination consistent with Cre activity
		testis	ovary	testis	ovary			
Grik4-Cre	Grik4$^{tm1(cre)Ksak}$					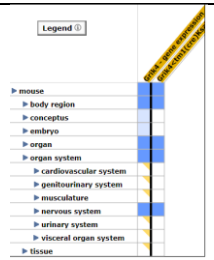	NA	NA
Htr3a-Cre	Tg(Htr3a-cre)NO152Gsat/Mmucd	present	absent			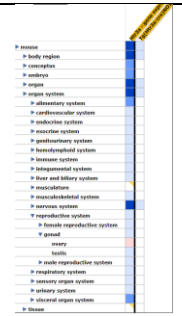	No?	NA
Isl1-Cre	Isl1$^{tm1(cre)Sev}$/J	present				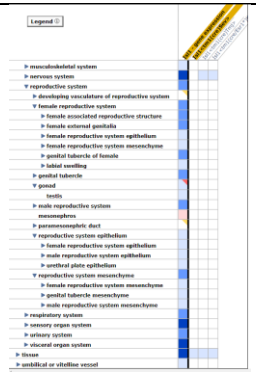	No	NA

Cre line common name	Full Cre line name/source	Gene expression		Cre activity		Reference (Screenshots from MGI database)	Germline recombination consistent with gene expression	Germline recombination consistent with Cre activity
		testis	ovary	testis	ovary			
Klf3-CreERT2	B6;129P-Klf3$^{tm1(cre/ERT2)Pzg}$/J	present	present			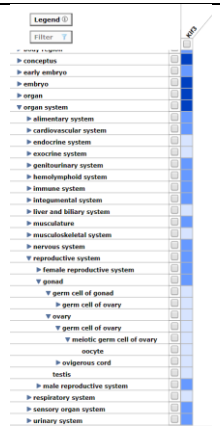	No	NA

Cre line common name	Full Cre line name/source	Gene expression		Cre activity		Reference (Screenshots from MGI database)	Germline recombination consistent with gene expression	Germline recombination consistent with Cre activity
		testis	ovary	testis	ovary			
Nestin-Cre	Tg(Nes-cre)1Kln/J			Present in spermatocyte	Present in oocyte P0-21	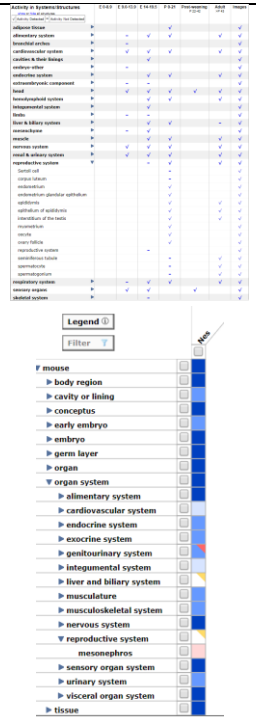	NA	Yes

Cre line common name	Full Cre line name/source	Gene expression		Cre activity		Reference (Screenshots from MGI database)	Germline recombination consistent with gene expression	Germline recombination consistent with Cre activity
		testis	ovary	testis	ovary			
Nestin-Cre	Tg(Nes-cre)1Atp					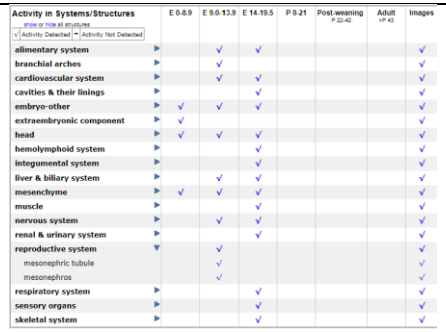	NA	NA
NEX-Cre	Neurod6$^{tm1(cre)Kan}$	present	present			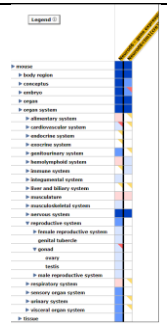	No	NA
Ngn2-CreER^{TM}	Neurog2$^{tm1(cre/Esr1)And}$						NA	NA
Nkx2.1-Cre	C57BL/6J-Tg(Nkx2-1-cre)2Sand/J			absent	absent		NA	No

Cre line common name	Full Cre line name/source	Gene expression		Cre activity		Reference (Screenshots from MGI database)	Germline recombination consistent with gene expression	Germline recombination consistent with Cre activity
		testis	ovary	testis	ovary			
	B6.CD1-Tg(Nkx2-1-cre)2Sand					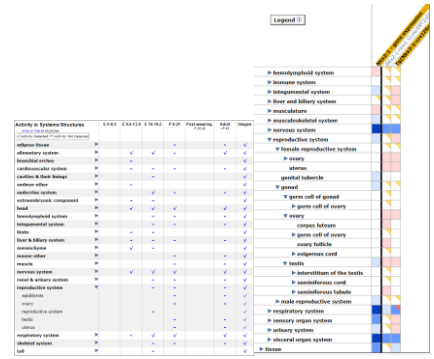		
Ntsr1-Cre	B6.Cg-Tg(Ntsr1-cre)GN220Gsat/Mmucd	present	absent			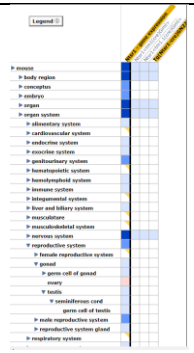	Yes	NA

Cre line common name	Full Cre line name/source	Gene expression		Cre activity		Reference (Screenshots from MGI database)	Germline recombination consistent with gene expression	Germline recombination consistent with Cre activity
		testis	ovary	testis	ovary			
Pcp2/L7-Cre	B6.129-Tg(Pcp2-cre)2Mpin/J			present	present	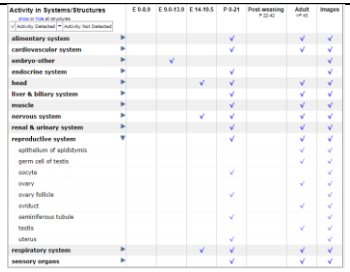	NA	No?
Pcp2/L7-Cre	B6.129-Pcp2$^{tm1(cre)Nobs}$					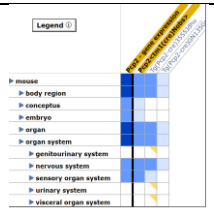	NA	NA
Pou4f2-Cre	Pou4f2$^{tm1(cre)Bnt}$/J	absent	absent			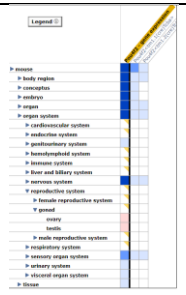	No	NA

Cre line common name	Full Cre line name/source	Gene expression		Cre activity		Reference (Screenshots from MGI database)	Germline recombination consistent with gene expression	Germline recombination consistent with Cre activity
		testis	ovary	testis	ovary			
Pvalb-2A-Cre	B6.Cg-Pvalb$^{tm1.1(cre)Aibs}$/J	present	present	present		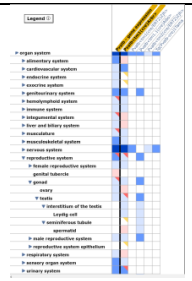	Yes	Yes?
Pvalb-IRES-Cre	B6.129P2-Pvalb$^{tm1(cre)Arbr}$/J	present	present	Present in supporting cells, absent in spermatid	absent	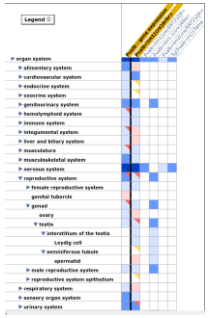	No	Yes
Rbp4-Cre	B6.Cg-Tg(Rbp4-cre)KL100Gsat/Mmucd	present					No	NA

Cre line common name	Full Cre line name/source	Gene expression		Cre activity		Reference (Screenshots from MGI database)	Germline recombination consistent with gene expression	Germline recombination consistent with Cre activity
		testis	ovary	testis	ovary			
	B6.FVB(Cg)-Tg(Rbp4-cre)KL100Gsat/Mmucd/GENSAT					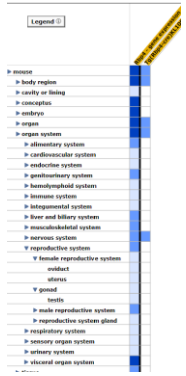		
Rgs9-cre	Rgs9$^{tm1(cre)Yql}$					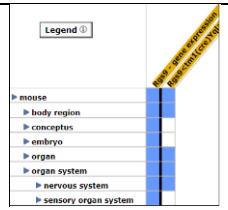	NA	NA
Rorb-Cre	B6.129S-Rorb$^{tm1.1(cre)Hze}$/J	absent	absent			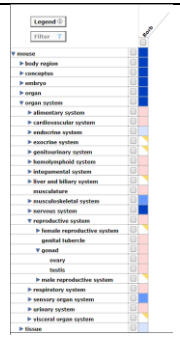	YEs	NA

Cre line common name	Full Cre line name/source	Gene expression		Cre activity		Reference (Screenshots from MGI database)	Germline recombination consistent with gene expression	Germline recombination consistent with Cre activity
		testis	ovary	testis	ovary			
Scnn1a-Cre	B6;C3-Tg(Scnn1a-cre)2Aibs/J	absent				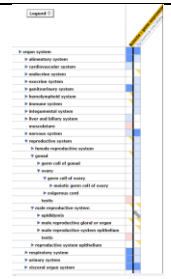	Yes	NA
Scx-Cre	Tg(Scx-GFP/cre)1Stzr	present	absent			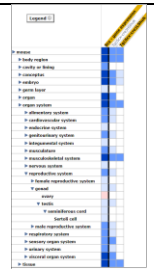	No	NA
SERT-Cre	B6.129(Cg)-*Slc6a4*$^{tm1(cre)Xz}$/J	present	absent			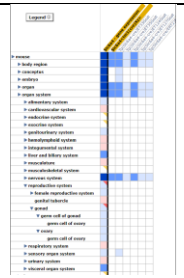	No	NA

Cre line common name	Full Cre line name/source	Gene expression		Cre activity		Reference (Screenshots from MGI database)	Germline recombination consistent with gene expression	Germline recombination consistent with Cre activity
		testis	ovary	testis	ovary			
Sim1-Cre	Tg(Sim1-cre)1Lowl/J		absent	present	absent		NA	No
Six3-Cre	Tg(Six3-cre)69Frty/GcoJ	absent	absent			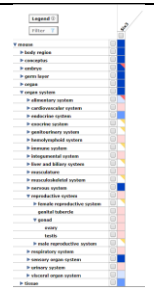	No	NA
Sst-IRES-Cre	B6-Sst$^{tm2.1(cre)Zjh}$ B6;129S4;CD1-Sst$^{tm2.1(cre)Zjh}$			absent	absent	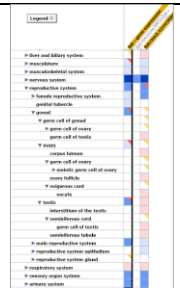	NA	Yes

Cre line common name	Full Cre line name/source	Gene expression		Cre activity		Reference (Screenshots from MGI database)	Germline recombination consistent with gene expression	Germline recombination consistent with Cre activity
		testis	ovary	testis	ovary			
Synapsin1-Cre	B6.Cg-Tg(Syn1-cre)671Jxm/J			present	present	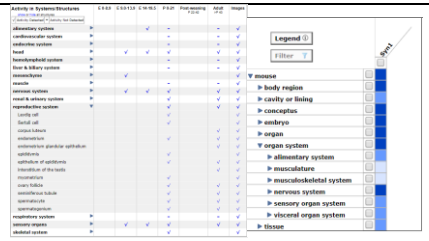	NA	No
Thy1-CreER	Tg(Thy1-cre/ERT2,-EYFP)HGfng/PyngJ					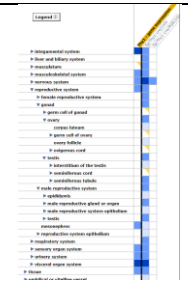	NA	NA
VAChT.Cre.Fast	B6;129-Tg(SLC18A3-cre)KMisa/0					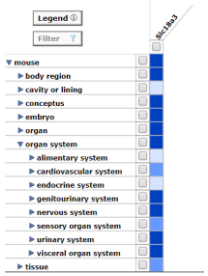	NA	NA

Cre line common name	Full Cre line name/source	Gene expression		Cre activity		Reference (Screenshots from MGI database)	Germline recombination consistent with gene expression	Germline recombination consistent with Cre activity
		testis	ovary	testis	ovary			
VGAT/VIAAT-Cre	Slc32a1$^{tm2(cre)Lowl}$/J	absent	absent			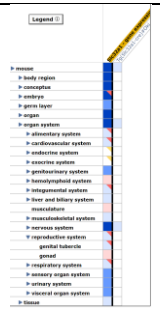	Yes	NA
VGAT/VIAAT-Cre	B6.FVB-Tg(Slc32a1-cre)2.1Hzo/FrkJ/	absent	absent			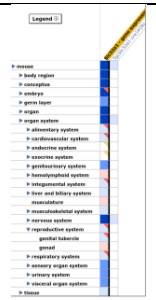	No	NA
VGluT1-IRES2-Cre-D	Slc17a7$^{tm1.1(cre)Hze}$/J					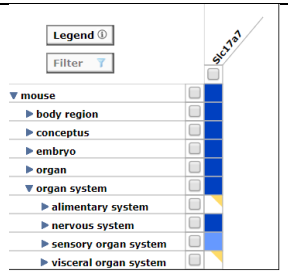	NA	NA
	B6;129S-Slc17a7$^{tm1.1(cre)Hze}$/J							

Cre line common name	Full Cre line name/source	Gene expression		Cre activity		Reference (Screenshots from MGI database)	Germline recombination consistent with gene expression	Germline recombination consistent with Cre activity
		testis	ovary	testis	ovary			
VGluT2-IRES-cre	Slc17a6$^{tm2(cre)Lowl}$/J			Present in interstitium of the testis	Present in ovary follicle	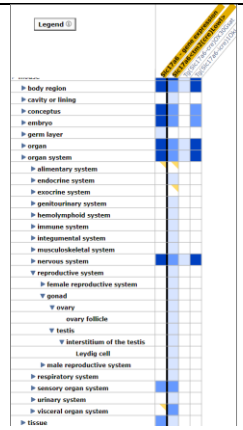	NA	No
VGluT3-Cre	Tg(Slc17a8-icre)1Edw/SealJ					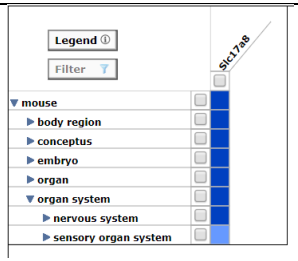	NA	NA

Cre line common name	Full Cre line name/source	Gene expression		Cre activity		Reference (Screenshots from MGI database)	Germline recombination consistent with gene expression	Germline recombination consistent with Cre activity
		testis	ovary	testis	ovary			
VIP-Cre	B6-Vip$^{tm1(cre)Zjh}$/J		absent	Present in spermatocyte	Absent in oocyte		NA	No?
Wnt1-Cre	B6.Cg-*H2afv*$^{Tg(Wnt1-cre)11Rth}$ Tg(Wnt1-GAL4)11Rth/J	absent	controversial	absent	absent	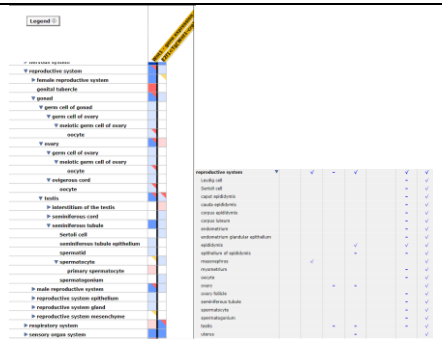	Yes	Yes